Characterizing Models to Study Cellular Composition Changes in Response to Pregnancy Hormones in the Human Mammary Gland

A dissertation presented by

Jenelys Ruiz-Ortiz

to the

School of Biological Sciences

in partial fulfillment of the requirements for the degree of

Doctor of Philosophy

in

Biological Sciences

at

Cold Spring Harbor Laboratory

April 2023

"...En mí manda mi solo corazón,
mi solo pensamiento; quien manda en mí soy yo."

-Julia de Burgos

Summary

The mammary gland is an epithelial structure composed of cells from luminal and basal lineages, all which undergo drastic changes throughout multiple postnatal developmental stages. During female puberty an interplay of Estrogen and Progesterone signaling promote the expansion of the rudimentary mammary epithelial structure into a complex ductal network. The mammary epithelium further matures during pregnancy, where an interplay of Estrogen, Progesterone and Prolactin (EPP) prepares the structure to secrete milk. Parity-associated changes to the mammary gland have been extensively described in mouse models. However, the mammary epithelial structure in mice and humans are both surrounded by different microenvironments, limiting the translational potential of studies done in intact murine mammary glands. Moreover, obtaining human mammary tissue involves invasive surgical procedures, making mammary tissue from women undergoing gestation incredibly difficult to obtain. Therefore, there is a pressing need for scalable systems that we can use to track changes to mammary gland cells in response to controlled signals, in order to advance our understanding of the molecular mechanisms underlying complex developmental stages.

Organoids are an emerging culturing system that allow for dynamic tracking of molecular and morphological changes to tissue samples in exposure to controlled developmental signals. Our lab previously demonstrated that EPP treatment can recapitulate the expression of milk associated proteins by organoids derived from murine mammary epithelial cells (MECs), as well as inducing MECs to obtain a parity-associated epigenomic signature. However, further assessment was needed to discern the extent to which hormone treatments reliably recapitulated *in vivo* developmental stages in organoids.

For this work, we used emerging single cell technologies to explore the extent to which MEC-derived organoids recapitulate *in vivo* MEC composition, providing an in-depth characterization of this system as a scalable model to study different developmental stages. We first characterized murine MECs without hormone treatment, with different doses of Estrogen to mimic hormone concentration changes during the estrous cycle, and with EPP treatment using single cell RNA-sequencing (scRNA-

seq), and found compositional and transcriptomic changes to MECs associated with hormone response and pregnancy. We further compared the resulting data to previously generated data sets from intact murine mammary tissue collected at different pregnancy stages, and found the acquisition of unique cellular states *in vitro*. Thus, the results for this portion of the thesis demonstrate the utility and limitations of using organoid systems to dissect the effects of hormones on MEC development.

To expand our characterization of models to study mammary gland development, scRNA-seq data sets were generated from mammary tissue samples from healthy women that were never pregnant and that had experienced past pregnancies. Using this approach, it would be possible to obtain a snapshot of persistent changes to the mammary gland occurring after undergoing pregnancy. Preliminary results for this portion of my thesis show MEC compositional differences between tissue from women who had never been pregnant and women who had previous pregnancies, providing a framework for subsequent studies using other human MEC-derived systems. Thus, we then cultured and sequenced organoids from human mammary tissue and treated them with EPP to mimic pregnancy-associated development. We showed human MEC-derived organoids are also able to recapitulate compositional and transcriptional changes associated with pregnancy hormones, consequently making organoids a viable system to understand hormone-induced development in human mammary tissue.

In order to truly translate our findings on murine MEC-derived organoids and determine conserved mechanisms across evolutionary timescales that contribute to tissue homeostasis during pregnancy, we next set out to compare MEC transcriptional profiles between both murine and human organoids. Similar to previous findings by our lab, we found that, at baseline, progenitor cell types were conserved across species, whereas mature cell types were species-specific. Treatment with EPP resulted in MECs segregating almost exclusively based on species of origin, alluding to MECs becoming highly specialized to species-specific functions in response to pregnancy hormones.

Altogether, we have generated a single cell map of murine and human MEC-derived organoids undergoing hormone response and pseudo-pregnancy cycles in vitro. We demonstrate the efficacy of

hormone treatments on these specific 3D culture models in recapitulating hormone-driven compositional changes to the mammary epithelial structure. These findings pave the way for future studies to further characterize dynamic changes to specific mammary epithelial sub-populations using these 3D models under different conditions to model primary tissue development.

Acknowledgements

I will begin by thanking my thesis advisor Camila dos Santos, who mentored and offered me guidance since the first day we met. I would also like to thank the dos Santos laboratory for helping me carry out my thesis project, and always being there when I needed support. I am extremely grateful for my thesis committee (Adam Siepel, Peter Koo, Molly Hammell, and Semir Beyaz), for providing vital advice for the development of my project. I appreciate my external advisor Senthil Muthuswamy for taking time to evaluate my doctoral work and contribute to its completion. I also especially have to thank my academic mentor Molly Hammell for checking-in often and lending an ear when I needed someone to talk to. Of course, I must thank the CSHLsbs program, in particular Alyson Kass-Eisler, Kim Graham, Kim Creteur, Monn Monn Myat and Alex Gann, for easing the experience of getting a PhD.

Debo agradecerle a mi familia por todo su apoyo desde siempre. Gracias a mi madre Eneida Ortiz Marrero y a mi padre Jaime R. Ruiz Otero por siempre empujarme a ser la mejor versión de mí, por creer en mí desde pequeña y por nunca ponerle freno a mis ambiciones. Gracias a mi hermano Jarel Ruiz Ortiz por convertir mis frustraciones en chistes, aunque nunca tome nada de lo que digo en serio (ni siquiera esto). Le extiendo mi agradecimiento a mis abuelos, tíos y primos por recordarme lo orgullosos que están de todo mi sacrificio cuando visito a Puerto Rico. Este doctorado es de todos ustedes.

I met amazing new friends during my time at CSHL, with whom I have shared the unique frustrations and excitements that come with being a graduate student. I am extremely grateful for my class cohort, especially for Danielle Ciren and Teri Cheng, for all of the long talking sessions and shopping therapy. I am also thankful for all of the wonderful people I met and got to work with through the Diversity Initiative for Advancement in Science (DIAS).

I am indebted forever to my friends who believed in me since day one, and pushed me to find my strength to carry out my duties. I especially thank Nailixa A. Lambert, Shakira Quintero, and Gisarrys Otero for providing the best company I could have ever asked for even in distance, and for seeing my potential ever since we were just kids. I must also thank Matthew Moss, his friends and family for always making me feel loved, and making me feel like I have a home here in the states.

Table of Contents

List of Abbreviations

AR	Androgen Receptor
ATAC-seq	Assay For Transposase-Accessible Chromatin With High Throughput Sequencing
BC	Breast Cancer
BCL11B	Baf Chromatin Remodeling Complex Subunit BCL11B
BLG	Beta Lactoglobulin
BM	Basement Membrane
BRCA1	BRCA1 Dna Repair Associated
cMYC	Myc Proto-Oncogene
DEG	Differentially Expressed Gene
DNA	Deoxyribonucleic Acid
E2	Estrogen
ECM	Extracellular Matrix
EMT	Epithelial To Mesenchymal Transition
Epcam/EPCAM	Epithelial Cell Adhesion Molecule
EPP	Estrogen, Progesterone, Prolactin
ER	Estrogen Receptor

GATA3	Globin Transcription Factor Binding Protein 3
GH	Growth Hormone
GSEA	Gene Set Enrichment Analysis
IF	Immunofluorescence
IFN-γ	Interferon Gamma
JAK2	Janus Kinase 2
Krt14/KRT14	Cytokeratin 14
Krt5/KRT5	Cytokeratin 5
Krt8/KRT8	Cytokeratin 8
P4	Progesterone
Pgr/PR	Progesterone Receptor
Prl/PRL	Prolactin
PRLR	Prolactin Receptor
Esr1/Erα	Estrogen Receptor α
MEC	Mammary Epithelial Cell
MaSC	Mammary Stem Cell
TF	Transcription Factor
Irx4	Iroquois Homeobox Protein 4
Mef2c	Myocyte-Specific Enhancer Factor 2C

Slug	Snail Family Transcriptional Repressor 2
Egr2	Early Growth Response Protein 2
Twist2	Twist-Related Protein 2
Tbx2	T-Box Transcription Factor 2
Id4	Inhibitor Of DNA Binding 4
Tp63/p63	Tumor Protein P63
Sox11	SRY-Box Transcription Factor 11
Krt16	Cytokeratin 16
Lgr6	Leucine-Rich Repeat-Containing G Protein-Coupled Receptor 6
Oxtr	Oxytocin Receptor
Osm	Oncostatin M
Lif	Leukemia Inhibitory Factor
Jag2	Jagged2
Wnt/WNT	Wingless-Type
Fzd8	Frizzled Class Receptor 8
Tcf4	Transcription Factor 4
Wif1	WNT Inhibitory Factor 1
Dkk3	Dickkopf Related Protein 3
Grk4	G Protein-Coupled Receptor Gene Family Member 4

Mafk	MAF BZIP Transcription Factor K
Sltm	SAFB Like Transcription Modulator
Dab2	Disabled Homolog 2
Ebf3	Early B-Cell Factor 3
Flt1	Fms-Related Tyrosine Kinase 1
Klf12	Kruppel-like Factor 12
Ldb2	LIM Domain Binding 2
Ogn	Osteoglycin
Samd4	Sterile Alpha Motif Domain Containing 4
Tek	TEK Receptor Tyrosine Kinase
Tfpi	Tissue Factor Pathway Inhibitor
Wscd2	WSC Domain-Containing Protein 2
9030425E11Rik	Riken cDNA 9030425E11 Gene
Procr	Protein C Receptor
Krt17	Cytokeratin 17
Cxcl14	C-X-C Motif Chemokine Ligand 14
Pdpn	Podoplanin
Acta2	Alpha 2 Smooth Muscle Actin
Sparc	Secreted Acidic Cysteine Rich Glycoprotein

Mylk/MYLK	Myosin Light Chain Kinase
Oxt/OXT	Oxytocin
RNA	Ribonucleic Acid
scRNA-seq	Single Cell Rna-Sequencing
Bptf	Bromodomain Phd Finger Transcription Factor
Lgr5	Leucine Rich Repeat Containing G Protein-Coupled Receptor 5
Nrg1	Neuregulin 1
Id4	Inhibitor Of Dna Binding 4, Hlh Protein
LP	Luminal Progenitor
Elf5/ELF5	Ets Transcription Factor 5
Cd14/CD14	Monocyte Differentiation Antigen Cd14
Stat5/STAT5	Signal Transducer And Activator Of Transcription 5
Csn/CSN	Casein
Wap/WAP	Whey Acidic Protein Gene
Lalba/LALBA	Lactalbumin Gene
VEGF	Vascular Endothelial Growth Factor
NKT	Natural Killer T-Like Immune Cell
CD1d	Cluster Of Differentiation 1D
FGF	Fibroblast Growth Factor

HOX	Homeobox Gene Family
TBX	T-Box Family
Hh	Hedgehog Pathway
Gli	Gli Family Zinc Finger
TEB	Terminal End Bud
RORγT	Rar-Related Orphan Receptor Gamma T
FoxP3	Forkhead Box P3
CD4	Cluster Of Differentiation 4
Th17 T-reg	T Helper 17 Cell-Specific Transcript Factor Rorγt
Areg/AREG	Amphiregulin
EGFR	Epidermal Growth Factor Receptor
FOXA1	Forkhead Box A Protein 1
CITED1	Cbp/P300-Interacting Transactivator With Glu/Asp-Rich Carboxy-Terminal Domain 1
WT	Wild Type
RANKL	Receptor Activator Of Nuclear Factor Kappa-B-Ligand
CCND1	Cyclin D1
CUZD1	Cub And Zona Pellucida-Like Domain-Containing Protein 1
SCRIB	Scribble
H3K27ac	Histone 3 Lysine 27 Acetylation

Flp-FRT	Flippase - Flippase Recognition Target
CyTOF	Cytometry By Time Of Flight
scATAC-seq	Single Cell Atac-Seq
fMaSC	Fetal Mammary Stem Cell
Fxyd3/FXYD3	Fxyd Domain-Containing Ion Transport Regulator 3
Cldn3/CLDN3	Claudin-3
Wfdc18	Wap Four-Disulfide Core Domain Protein 18
Muc15	Mucin-15
Birc5	Baculoviral Iap Repeat-Containing Protein 5
Hmmr	Hyaluronan Mediated Motility Receptor
Melk	Maternal Embryonic Leucine Zipper Kinase
Stmn1	Stathmin
Mki67	Marker Of Proliferation Ki-67
Ube2c	Ubiquitin Conjugating Enzyme E2 C
Top2a	Dna Topoisomerase Ii Alpha
MO	Murine Organoids
Lgals1	Galectin-1
Fbn1	Fibronectin 1
Klk8	Kallikrein-Related Peptidase 8

OIM	Organoids And Intact Mecs
Trf	Transferrin
Aldh1a3	Aldehyde Dehydrogenase 1 Family Member A3
Timp3	Tissue Inhibitor Of Metalloproteinases 3
Sat1	Spermidine/Spermine N1-Acetyltransferase 1
Gsr	Glutathione Reductase
Clu	Clusterin
Nedd9	Neural Precursor Cell Expressed, Developmentally Down-Regulated 9
Nfya	Nuclear Transcription Factor Y Subunit Alpha
Nrf1	Nuclear Respiratory Factor 1
Setdb1	Set Domain Bifurcated Histone Lysine Methyltransferase 1
Spdef	Sam Pointed Domain Containing Ets Transcription Factor
Stat1	Signal Transducer And Activator Of Transcription 1
Elk3	Ets Transcription Factor 3
OP	Organoids With Pregnancy Hormones
Myb	MYB Proto-Oncogene, Transcription Factor
Tfcp2l1	Tf Transcription Factor Cp2-Like Protein 1
Klf6	Tf Kruppel-Like Factor 6
Mefc	Myocyte Enhancer Factor 2C

Trp63	Transformation-Related Protein 63
Srebf1	Sterol Regulatory Element Binding Transcription Factor 1
Mafb	V-Maf Avian Musculoaponeurotic Fibrosarcoma Oncogene Homolog B
Foxo3	Forkhead Box O3
Pole3	Dna Polymerase Epsilon 3, Catalytic Subunit
Sap30	Sin3A-Associated Protein, 30 Kda
Rad21	Double-Strand-Break Repair Protein Rad21 Homolog
Tfcp2l1	Transcription Factor Cp2-Like 1
Foxa1	Forkhead Box Protein A1
Tead2	Tea Domain Transcription Factor 2
Usf2	Upstream Stimulatory Factor 2
Hivep1	Human Immunodeficiency Virus Type I Enhancer Binding Protein 1
Sox9	Sry-Box Transcription Factor 9
Foxj2	Forkhead Box Protein J2
Tead1	Tea Domain Transcription Factor 1
Tcf7	Transcription Factor 7
Nfatc2	Nuclear Factor Of Activated T-Cells 2
Mef2c	Myocyte Enhancer Factor 2C
Srf	Serum Response Factor

Sox10	Sry-Box Transcription Factor 10
HOP	Human Organoids With Pregnancy Hormones
RARRES1	Retinoic Acid Receptor Responder 1
WFDC2	Wap Four-Disulfide Core Domain Protein 2
BIRC3	Baculoviral Iap Repeat-Containing Protein 3
PTTG1	Pituitary Tumor-Transforming Gene 1
CCNB1	Cyclin B1
SL2A1	Solute Carrier Family 2 Member 1
NDRG1	N-Myc Downstream Regulated 1
SCD	Stearoyl-Coa Desaturase
VEGFA	Vascular Endothelial Growth Factor A
IER3	Immediate Early Response 3
INSIG1	Insulin Induced Gene 1
DDIT4	Dna Damage Inducible Transcript 4
ISG15	Interferon-Stimulated Gene 15
HMGN2	High Mobility Group Nucleosomal Binding Domain 2
LCN2	Lipocalin 2
KRT6A	Keratin 6A
FDCSP	Follicular Dendritic Cell Secreted Protein

ODAM	Odontogenic Ameloblast-Associated Protein
FKBP5	Fk506 Binding Protein 5
TSC22D3	Tsc22 Domain Family Member 3
NUPR1	Nuclear Protein 1
MHP	Murine And Human Organoids With Pregnancy Hormones
ALDOC	Aldolase, Fructose-Bisphosphate C
IGFBP5	Insulin-Like Growth Factor Binding Protein 5
APOD	Apolipoprotein D
CRISPLD2	Cysteine-Rich Secretory Protein Lccl Domain-Containing 2
GPX3	Glutathione Peroxidase 3
GLUL	Glutamate-Ammonia Ligase
GSN	Gelsolin
RGS2	Regulator Of G Protein Signaling 2
TFCP2L1	Transcription Factor Cp2-Like 1
CCNB1	Cyclin B1
PTTG1	Pituitary Tumor-Transforming 1
PLAC8	Placenta-Specific 8
H2AFZ	H2A Histone Family Member Z
CRIP1	Cysteine-Rich Protein 1

RBP1	Retinol-Binding Protein 1
TPM2	Tropomyosin 2
HMGCS1	3-Hydroxy-3-Methylglutaryl-Coa Synthase 1
IL17B	Interleukin 17B
mTOR	Mechanistic Target Of Rapamycin
INSIG1	Insulin-Induced Gene 1
SCD	Stearoyl-Coa Desaturase
HR	Hormone Responsive
qPCR	Quantitative Polymerase Chain Reaction
PCA	Principal Component Analysis
UMAP	Uniform Manifold Approximation And Projection
SCENIC	Single-Cell Regulatory Network Inference And Clustering
PBS	Phosphate Buffered Saline
BSA	Bovine Serum Albumin
EGF	Epidermal Growth Factor
ADF	Advanced Dmem/F-12 Medium
TrypLE	Trypsin
QC	Quality Control
SNN	Shared Nearest Neighbor Graph

NP	Nulliparous
MSigDB	Molecular Signatures Database
OE	Organoids with Estrogen
RSS	Regulon Specificity Score
Klf4	Krüppel-like factor 4
Ets2	TF ETS proto-oncogene 2
Relb	V-Rel Avian Reticuloendotheliosis Viral Oncogene Homolog B
Sfpq	Splicing factor proline/glutamine-rich
Zfp	Zinc Finger Protein
Gtf3c2	General Transcription Factor IIIC Subunit 2

List of Figures

List of Tables

Main Tables

Supplementary Tables

1. Introduction

The mammary gland is a unique tissue that undergoes most of its development postnatally, especially in females. Particularly during adolescence, a surge in hormones Estrogen (E2) and Progesterone (P4) transform the rudimentary mammary epithelium into a complex ductal network (Slepicka et al., 2021). Nevertheless, the most drastic postnatal developmental stages of the mammary gland occur during pregnancy. During this process, an interplay of E2, P4 and Prolactin (PRL) induce the maturation of the mammary gland into alveoli that can secrete milk (Slepicka et al., 2021). Once a pregnancy cycle ends, the mammary gland epithelial structure virtually regresses to its pre-pregnant baseline state. However, the changes that occur to the mammary gland structure during pregnancy are iterative with subsequent pregnancies, becoming increasingly efficient, thus indicating some of these changes are persistent (C. O. dos Santos et al., 2015). Moreover, it has been shown that changes to the mammary gland during pregnancy are associated with a lower risk of breast cancer (BC) (Hanasoge Somasundara et al., 2021). Therefore, understanding the molecular processes that occur during pregnancy can move us closer to utilizing these changes to help prevent neoplastic growth and increase lactation efficacy.

While mouse models have been extensively used to assess mammary gland pregnancy-associated development, they are an expensive model system with many inherent challenges including variation and time. It has also been shown that the mammary gland epithelium is surrounded by different microenvironments in mice and humans, which in part could result in species-specific cellular interactions and limit the translational potential of mouse models (Dontu & Ince, 2015). Using human mammary tissue to study development during pregnancy, however, presents an equally challenging model because obtaining tissue samples requires invasive surgical procedures. For the aforementioned reasons, finely tuned, scalable and accessible in vitro model systems for studying the effects of pregnancy hormones on MECs are vital to better understand how the mammary gland is modified during different stages of pregnancy.

Three dimensional (3D) organoid cultures are a method by which MECs are isolated from mammary tissue samples and grown in Matrigel, which serves as a basement-rich extracellular matrix (ECM) in culture thus mimicking *in vivo* conditions for MECs to organize into ductal structures (Nguyen-Ngoc et al., 2015). Previous work from our lab and others has shown that organoids are able to recapitulate MEC lineages found *in vivo*, as well as mimicking some aspects of pregnancy, such as the expression of milk-associated proteins (Ciccone et al., 2020; Gray et al., 2022; Rosenbluth et al., 2020; Sumbal et al., 2020). Further characterization of how organoid systems compare to *in vivo* mammary gland development will therefore allow us to gain insights into the effectors underlying normal and pathological mammary gland development that we can translate into clinical interventions.

For the aforementioned reasons, in this section of my thesis I will be reviewing what is known about the mammary gland epithelium and its development, the hormones that control each developmental stage and models that have been utilized to gain such understanding. This portion of my thesis will additionally involve an in-depth discussion of the known differences between mouse and human mammary glands, and the limitations and advantages of using murine-based models. I will then discuss recent studies that have begun to characterize both the murine and human mammary gland at a single cellular level, allowing for us precisely understand the developmental processes affecting different subcellular epithelial populations, and consequently allowing us to begin inferring which changes are important for lactation efficacy and BC prevention. I will subsequently introduce our current study, which involves a comprehensive analysis of the molecular mechanisms governing the different lineages found in murine and human MEC-derived organoid cultures, thus addressing gaps between mouse and human models and paving the way for a better understanding of mammary gland development during pregnancy.

1.1 Cell types that constitute the mammary gland

The mammary gland is a highly heterogeneous tissue consisting of a bi-layered epithelial structure capable of becoming a functional unit responsible for milk secretion during lactation (**Fig. 1**). The inner layer of the mammary epithelial structure consists of luminal cells that can form ducts and milk-producing alveoli, and the outer layer consists of basal cells made up primarily of myoepithelial cells that give contractile force to the structure (Cristea & Polyak, 2018). The epithelium is additionally surrounded by a microenvironment composed of a diverse array of non-epithelial cells that interact with the epithelium (Dzięgelewska & Gajewska, 2019). All of these cell types contribute to the tissue homeostasis of the mammary gland throughout its lifetime, which is why I will briefly list each of the known MEC types, how they are defined at a transcriptomic level, and cells comprising the mammary microenvironment.

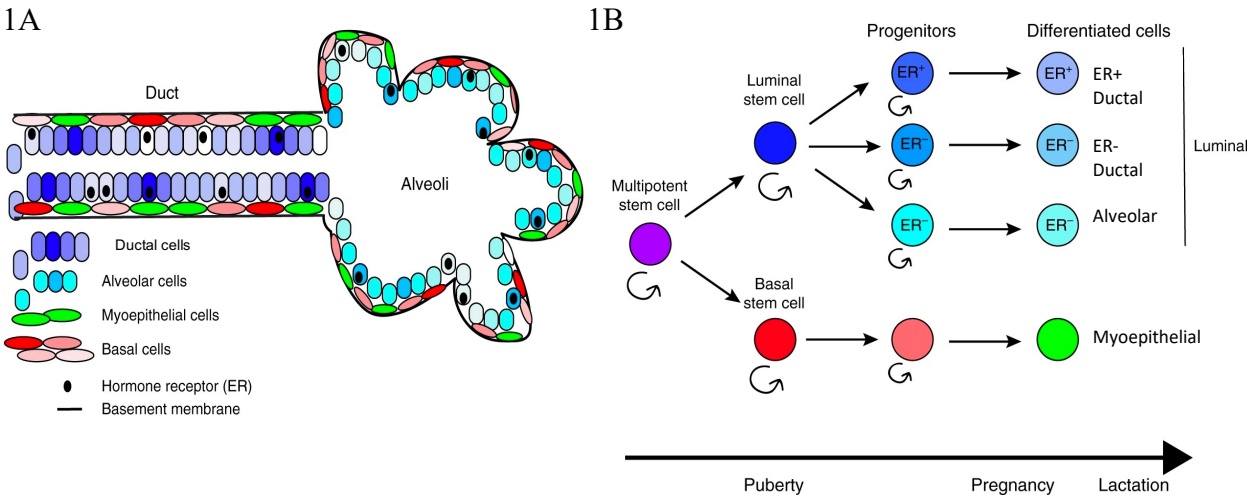

Figure 1. The mammary epithelium and cell types that constitute the structure.

(A) Schematic depiction of the bi-layered mammary epithelium. Luminal ductal (blue) and alveolar cells (turquoise) line the inner part of the structure. Ductal cells contribute to the branching of the structure and respond to a milieu of hormones throughout puberty (hormone receptor positive cells in white), while alveolar cells mature to secrete milk during pregnancy. The outer part of the mammary epithelium is lined with basal cells (red), which include different progenitors and myoepithelial cells (green), the cellular population responsible for conferring contractile force for milk ejection.

(B) Diagram showing the different luminal and basal cellular states found in the mammary gland, and when they arise throughout post-natal development. Progenitor populations for each mature luminal state (blue) and myoepithelial state (green) are maintained in the gland for renewal (blue for luminal progenitors and red for basal progenitors). The presence of a progenitor with the potential of becoming luminal or basal has likewise been described (purple). *Figures adapted from: Cristea S. & Polyak K., 2022, Nature Communications.*

1.1.1 Cell types comprising the mammary epithelium and their transcriptomic traits

MECs have been long documented to, at baseline, share certain defining characteristics by which they can be dissected from their surrounding microenvironment, such as the expression of Epithelial cell adhesion molecule gene (*Epcam*) and its protein product, as well as the expression of specific cytokeratins and their protein products (Bach et al., 2017; Shehata et al., 2012; Stingl et al., 2001). However, the adult mammary epithelial hierarchy is complex and marked by terminally differentiated cells with distinct functions, as well as lineage restricted progenitors and stem cells with different lineage potentials (Cristea & Polyak, 2018). A deep understanding of the aforementioned cellular types and states can help us characterize the effects of different perturbations on the trajectory of MECs, which is why defining markers to subset each of these populations has been a crucial task for the mammary gland biology field.

Both MECs from luminal and basal lineages can arise from multipotent mammary stem cells (MaSCs) that are maintained within the basal compartment of the mammary epithelium structure throughout its entire lifetime (Shackleton et al., 2006; Stingl et al., 2006). Gene signatures that were initially associated with MaSCs involve a series of transcription factor (TF) genes (*Irx4, Mef2c, Slug, Egr2, Twist2, Tbx2, Id4, p63,* and *Sox11*), cytokeratins (*Krt5, Krt14,* and *Krt16*), plasma membrane proteins (*Lgr6, Oxtr, Osm,* and *Lif*), genes associated with Notch signaling such as ligand *Jag2*, and genes associated with the Wnt/β-catenin pathway (*Fzd8, Tcf4, Wif1,* and *Dkk3*) (Lim et al., 2010). Over time, the techniques for isolating MaSCs have improved, enabling more in-depth transcriptomic profiling of these cells. The improvement of these methods has led to the discovery that, for example, the expression of certain genes, such as G protein-coupled receptor gene family member 4 (*Grk4*) and TF genes Mafk and Sltm, are crucial for the maintenance of MaSCs (C. O. dos Santos et al., 2013). Another larger-scale study revealed that MaSCs express genes shared with embryonic epithelial cells (*Nkain2, Mtap7* and *Mbp*) and, interestingly, embryonic mesenchymal cells (*Dab2, Ebf3, Flt1, Klf12, Ldb2, Ogn, Samd4, Tek, Tfpi, Wscd2* and the Riken ORF *9030425E11Rik*), demonstrating their epithelial-to-mesenchymal transition (EMT) potential (Soady et al., 2015). In parallel, another study

identified protein C receptor (*Procr*), a Wnt target in the mammary gland, as a unique marker for MaSCs (D. Wang et al., 2015). It is important to note that the pool of MaSCs in the adult gland appears to comprise a small percentage of MECs, and other MEC progenitors are often isolated in concert with these stem cells (Visvader, 2009). Nonetheless, efforts to identify and characterize MaSCs from the adult mammary gland, especially in humans, are ongoing, and an in-depth comprehension of how they modulate the MEC hierarchy will provide further insights into the normal and pathological development of mammary tissue.

Amongst the progenitors that are isolated unintentionally along MaSCs, it has been suggested that there are "in between" states bridging stem cells and lineage restricted progenitors, such as progenitors that are bi-potential for luminal and basal lineages (Visvader, 2009). Whether these cells are the same as MaSCs or cells with an entirely different profile is a continuing debate. Some studies suggest the mammary hierarchy is not linear, but rather accommodating to cells changing in plasticity during different normal and malignant developmental processes, resulting in luminal progenitors acquiring a basal potential, or vice versa (Bu et al., 2011; Hein et al., 2016). Overall, further research is still needed to fully understand the complexity and plasticity of the mammary hierarchy, specifically involving the characterization of transient states between progenitors with different lineage potentials.

Besides MaSCs and intermediate progenitor states, the basal compartment contains terminally differentiated myoepithelial cells, as well as a pool of lineage-restricted myoepithelial progenitors, that function to confer contractile force to the mammary gland during lactation (Sapino et al., 1993). Myoepithelial cells characteristically express *Krt5* and *Krt14, Krt17,* C-X-C Motif Chemokine Ligand 14 (*Cxcl14*), basal compartment-biased genes such as transmembrane protein podoplanin (*Pdpn*). Additionally, myoepithelial cells have been noted to express genes involved in muscle differentiation such as alpha 2 smooth muscle actin (*Acta2*), secreted acidic cysteine rich glycoprotein (*Sparc*) and Myosin light chain kinase (*Mylk*) (Abd El-Rehim et al., 2004; Allinen et al., 2004; Bresson et al., 2018; Pal et al., 2017). Terminally differentiated myoepithelial cells and their progenitors, however, share key differences in their traits that are helpful to differentiate between both cellular states. For example,

given that Oxytocin (OXT) mediates the contraction of the myoepithelium, terminally differentiated myoepithelial cells exhibit OXT receptor (Oxtr) (Bussolati et al., 1996; Sapino et al., 1993). In contrast, myoepithelial progenitors express genes that are associated with stem functions, such as Tumor protein p63 (*Tp63*), Bromodomain PHD Finger Transcription Factor (*Bptf*), Leucine Rich Repeat Containing G Protein-Coupled Receptor 5 (*Lgr5*), Neuregulin 1 (*Nrg1*) and Inhibitor of DNA Binding 4, HLH Protein (*Id4*) (de Visser et al., 2012; Dong et al., 2011; Forster et al., 2014; Frey et al., 2017; Henry et al., 2021; Kumar et al., 2020). As such, myoepithelial progenitors were initially shown to be highly similar to MaSCs, albeit displaying enough transcriptomic differences to cluster separately (C. O. dos Santos et al., 2013). Thus, the basal compartment is highly heterogeneous, containing progenitors for all MEC types and its own functional unit that promotes milk ejection during lactation, supporting the study of this compartment as key to understanding normal and pathological development during pregnancy.

Luminal cells making up the inner layer of the epithelium can be compartmentalized mainly by their two terminal states: ductal cells and secretory alveolar cells. Both terminal states share common transcriptomic traits, such as expressing *Krt8* and *Krt18* (Kendrick et al., 2008). Nevertheless, they are functionally distinct, and different pools of luminal progenitors (LPs) are maintained throughout adulthood for renewal of both terminal states. Gene signatures for LP populations have been extensively described, and include expression of genes such as proto-oncogene Kit, monocyte differentiation antigen CD14 (*Cd14*) and TF gene *Elf5* (Asselin-Labat et al., 2011; Oakes et al., 2008; Regan et al., 2012). Nonetheless, the potential of these LP populations has been primarily identified based on Estrogen Receptor (ER) expression, with ER+ LPs giving rise to ER+ ductal cells only, and ER- LPs giving rise to both ER- ductal and alveolar cells (Cristea & Polyak, 2018; Giraddi et al., 2015; C. Wang et al., 2017). Terminally differentiated ER+ ductal cells are characteristic for their hormone sensing functions (Shehata et al., 2012). Given that Estrogen modulates Progesterone Receptor gene expression (*Pgr*), which in turn upregulates PRL Receptor (*Prlr*) expression, the expression of all the aforementioned genes can be used as viable markers for hormone sensing ductal cells (Arendt & Kuperwasser, 2015; Goldhar et al., 2011). In contrast, secretory alveolar cells are known to generally

be ER-/PR-, and exist in progenitor-like states until achieving full maturation during pregnancy (Oliver et al., 2012; Rodilla et al., 2015; Watson, 2022). These cells are, after terminal differentiation, consequently marked by the expression of genes regulated by PRL and Signal transducer and activator of transcription 5 (*Stat5*), such as milk-associated protein genes like the caseins (e.g. *Csn2, Csn3,* and *Csn1s1*), Whey Acidic Protein gene (*Wap*), and lactalbumin gene (*Lalba*) along with their protein products (Long et al., 2003). In summary, cells within the main luminal terminal states involve different functionalities throughout development highly associated with milk production, and gaining knowledge on the processes that initiate these functions will give us further insights on how the mammary gland transitions from a rudimentary ductal tree to a highly complex milk secreting machine.

1.1.2 Cell types present the microenvironment surrounding the mammary epithelium

The microenvironment surrounding the mammary epithelium is composed of a diverse array of cells, which in turn communicate with MECs and regulate their development (Hovey & Aimo, 2010; Shekhar et al., 2001). Non-epithelial cells residing in the mammary gland include fibroblasts, adipocytes, endothelial and lymphatic cells, and immune cells. Having an in-depth comprehension of how each of these cell populations modulate MEC growth, expansion and function is therefore a vital part of improving our characterization of mammary gland development.

Fat-filled adipocytes are an essential component of the mammary fat pad, providing structural support to MECs. These cells have several endocrine functions, including promoting angiogenesis via the secretion of vascular endothelial growth factor (VEGF), thus proving to be integral for the regulation of non-epithelial cell types found within the mammary microenvironment (Master et al., 2002). Adipocytes have also been implicated in MEC growth and function via mechanisms such as direct cell-cell communication throughout different developmental stages (Gregor et al., 2013; Hovey & Aimo, 2010). Especially during pregnancy, these cells increase their lipogenic capacities to channel nutrients to MECs in preparation for lactation (Bartley et al., 1981). Indeed, impaired response of adipocytes to

PRL during lactation results in decreased milk production by MECs, thus demonstrating an important role for adipose tissue in the functionality of the mammary epithelium (Gregor et al., 2013).

Fibroblasts secrete the components that make up the extracellular matrix (ECM), which regulates MEC growth, survival, migration and differentiation mainly through a repertoire of transmembrane receptors, such as integrins (Fata et al., 2003). Therefore, fibroblasts modulate MEC development by the secretion of different growth factors and proteases and, additionally, via direct cell-cell contact (Howard & Lu, 2014; X. Liu et al., 2012; Makarem et al., 2013; X. Wang & Kaplan, 2012). The proportion of fibroblasts in the mammary microenvironment, and consequently the composition of ECM, varies across species. For instance, the human mammary stroma is fibroblast-rich, in contrast to the adipose-rich murine mammary microenvironment (Dontu & Ince, 2015). Differences in proportion and composition of the fibrous portion of the mammary microenvironment could, as a result, promote species-specific MEC phenotypes, which is why the characterization of fibroblasts and their effects on the epithelium has been particularly important for developing ex-vivo models that can mimic intact mammary gland composition.

Within the mammary stroma there is also a highly complex vascular and lymphatic network, which is formed during adolescence and expands during pregnancy (Matsumoto et al., 1992). The development of these endothelial cells is partly coordinated by myoepithelial and macrophages secreting pro-lymphangiogenic factors such as VEGF-C and VEGF-D, showcasing an interplay between MECs and microenvironment cells in modulating mammary tissue homeostasis (Betterman et al., 2012). During pregnancy, endothelial cells exhibit elevated numbers of mitochondria, pinocytotic vesicles and decreased cell-cell contacts, all which contribute to an increased transport of nutrients and fluids required during lactation within the vascular network (Andres & Djonov, 2010). Therefore, like the aforementioned cells comprising the mammary microenvironment, these cells are essential for the mammary gland transforming into a functional unit during lactation.

Finally, there is a wide range of immune cells present within the mammary microenvironment, which have been shown to contribute to the ductal elongation of the epithelium, as well as branching

and invasion into the mammary fat pad (Gouon-Evans et al., 2000; Lilla & Werb, 2010). These immune cells include macrophages, mast cells, eosinophils, as well as T-cells that direct lineage commitment and differentiation of MECs during pregnancy via the secretion of cytokines and other secreted factors (Chan et al., 2014; Dawson et al., 2020, p. 202; Hitchcock et al., 2020; Khaled et al., 2007; O'Brien et al., 2010; Plaks et al., 2015; Pollard & Hennighausen, 1994; Rahat et al., 2016; Stewart et al., 2019; Y. Wang et al., 2020). Moreover, our lab has shown that γδ natural killer T-like immune cells (NKTs) that infiltrate the mammary gland after lactation to promote its regression to a "pre-pregnant" state, are likely recruited by MEC expression of antigen-presenting molecule CD1d and persist in mammary tissue from post-pregnant mice, potentially contributing to oncogenesis protection (Hanasoge Somasundara et al., 2021). Therefore, there is a functional importance for immune cells present in the mammary gland, even causing persistent changes to the functionality of the gland after what appears to be transient developmental stages.

Altogether, an interplay between MECs and its surrounding microenvironment is essential for mammary tissue homeostasis, development and function. It has been reported that non-epithelial cellular proportions vary from species-to-species, which could in turn alter the conservation of developmental mechanisms across evolutionary timescales (Dontu & Ince, 2015; Hovey et al., 1999). Therefore, it has been significant to consider microenvironment variability when translating studies done in rodents to human tissue, and moreover when developing ex-vivo systems to characterize mammary development.

1.2 An outline of the processes involved in mammary gland development

In this section of my thesis, I will summarize what we know about mammary gland development, including embryonic and postnatal stages of development, the hormonal signals carrying out these stages, and a discussion of the significance of understanding mammary gland biology.

1.2.1 The developmental stages of the mammary gland

The mammary gland is unique in that its development occurs mostly postnatally, especially in females. However, the rudimentary mammary structure arises during embryonic development, and remains stalled until receiving signals to expand later in life (**Fig. 2**). Thus, in this subsection of my thesis I will give a brief description of the different developmental transitions the mammary undergoes throughout a lifetime.

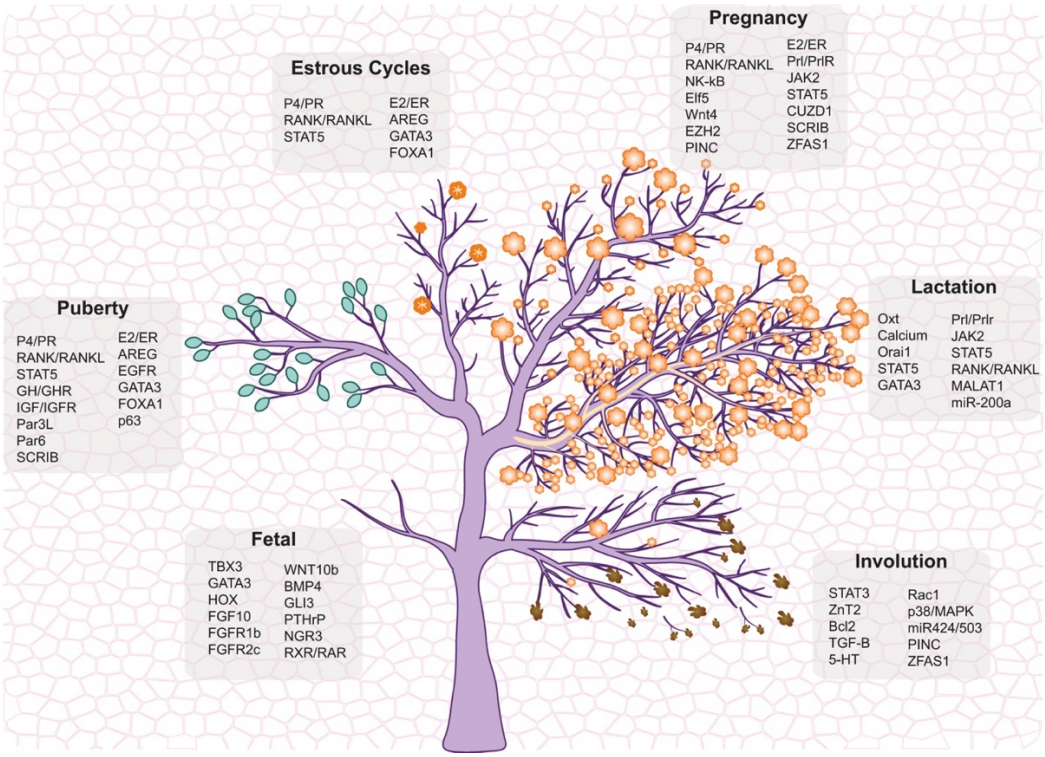

Figure 2. The developmental stages of the mammary gland.

Illustration showing the changes that occur in the mammary gland during fetal development, female puberty, estrous cycles, and a pregnancy cycle. The main molecular drivers of these developmental stages are also depicted. The background depicts the mammary fat pad, which is present throughout all developmental stages. During the embryonic stages of development, a rudimentary structure is formed. The mammary epithelium undergoes branching during female puberty, as well as the formation of terminal end buds (TEBs) in mice (green). These newly formed structures can further mature into alveoli transiently during the estrous cycle (orange flowers) and extensively during pregnancy/lactation. Milk produced during lactation is represented by yellow sap flowing from the alveoli (flowers) to the ducts (branches). The mammary structure regresses during involution (dead flowers). *Figure from: Slepicka et al., 2021, Seminars in Cell and Developmental Biology*

Embryonic development

The formation of the mammary gland during embryonic development begins during mid-gestation. The exact gestational day during which the mammary gland first arises is widely species-

dependent, and most of our knowledge from this process is based on mouse models, which have a far shorter developmental period than humans. Thus, in mice, the mammary gland first arises exactly at 10 days of gestation (E10) as a formation of mammary lines at the ventral aspect of the Wolfian ridge (Incassati et al., 2010; Macias & Hinck, 2012; Slepicka et al., 2021). At E11.25 thick bands of ectodermal cells form bilateral and vertical mammary lines, and at E11.75 clumps of ectoderm form placodes that emerge along these mammary lines (Slepicka et al., 2021; Veltmaat et al., 2004). These placodes in turn determine the number of breasts in each mammalian species. By E12.5, the placodes protrude into the mesoderm and form an early mammary bud surrounded by a basement membrane (BM) and the first traces of a mammary fat pad (Slepicka et al., 2021). The bud then gives rise to mammary bulbs with an ectodermal stalk between days E13 and E14, which will elongate into a sprout surrounded by the mammary fat pad at E15.5. Lumen formation begins at E17-18, which involves the programmed death of ectodermal cells located at the center of the mammary branches.

Signaling in mammary embryonic tissue is regulated by members of the fibroblast growth factor (FGF) and wingless-related integration site (WNT) protein families, which in turn control TFs from the Homeobox gene family (HOX), GATA binding protein 3 (GATA3), and the T-box family (TBX), all which are intermittently expressed in the endoderm and mesoderm (Asselin-Labat et al., 2007; Davenport et al., 2003; Lim et al., 2009). Another notable pathway that plays a role in mammary embryogenesis is the Hedgehog (Hh) pathway, which activates gene-specific transcription that controls bud formation via its TFs, such as Gli3 (M. Y. Lee et al., 2013; Robinson, 2007; Slepicka et al., 2021; Tickle & Jung, 2016). Additionally, Gli2 regulates ductal branching through its localization in the mammary stroma, and later becomes both stromal and epithelial during pregnancy and lactation (Hatsell & Cowin, 2006). All of these signals provide initial queues for the formation of the mammary structure and, after embryogenesis, cessation of maternal signaling reduces genesis of the mammary gland, becoming poised until female puberty (Slepicka et al., 2021).

Female adolescence

During the onset of female puberty, the development of the poised mammary structure resumes, marked by a surge of E2 and P4 triggered by an increase in gonadotropin levels that lead to the secretion of these ovarian hormones, which in turn complete mammary morphogenesis in preparation for lactation in the event of a pregnancy. During this time, in mice, terminal end buds (TEBs) composed of highly proliferative stem cells arise in response to E2, which are club-like structures that facilitate the invasion of the mammary tree through the fat pad (G. V. Dall & Britt, 2017; Smalley & Ashworth, 2003). Ducts that will contain mature alveoli at their tips during pregnancy therefore emerge during puberty as the bodies of elongating TEBs. In humans, TEBs are analogous to immature type 1 lobules arising in puberty, which later increase in complexity all the way to type 4 lobules in lactating women (G. V. Dall & Britt, 2017; Russo et al., 2009). Thus, this developmental stage is crucial to promote the eventual full maturation of the mammary gland in both mice and humans.

The exact moment at which puberty-associated development occurs varies greatly between mammalian species, with its general occurrence at ~5 weeks in mice and ~9-18 years in humans (Slepicka et al., 2021). Peak levels of E2 occur between the follicular phase and ovulation, with its synthesis being species-dependent and occurring every 2-4 days in mice and every month in humans (Fata et al., 2001). Therefore, once the surge of E2 and P4 occurs, their synthesis is cyclically maintained throughout reproductive years, transiently affecting mammary tissue homeostasis during each menstrual cycle.

Estrous cycle

During female reproductive years, the mammary gland undergoes cyclic modifications tightly correlated to the menstrual cycle, which occur every 4-5 days in mice and every 26-32 days in humans (Byers et al., 2012; Slepicka et al., 2021). The menstrual cycle occurs in two major phases in humans, which are the follicular and luteal phases. These phases are further segregated in mice, with the estrus and proestrus stages being analogous to the follicular phase, and the metestrus and diestrus stages being

analogous to the luteal phase (Byers et al., 2012; Slepicka et al., 2021). The follicular phase starts on the first day of menstruation, with P4 levels dropping as the corpus luteum degenerates and a new preovulatory folliculum is formed (Slepicka et al., 2021). During the ovulation stage of the estrous cycle (estrus in mice), E2 rises to peak levels and stimulates production of luteinizing hormone from the pituitary gland, which causes the release of the ovum from the ovary and thus marks the beginning of the luteal phase (Slepicka et al., 2021). The corpus luteum keeps up P4 production for a few days, which triggers mammary tissue expansion and lobuloalveologenesis. Consequently, the percentage of dense tissue in the female human mammary gland is reportedly amplified during the luteal phase and, analogously, increased lobuloalveologenesis and tertiary branching is observed in murine mammary tissue (Fata et al., 2001; Robinson et al., 1995; Slepicka et al., 2021). The end of the estrous cycle involves the degradation of the corpus luteum and decreasing levels of P4, which in the mammary gland results in MEC clearance through cellular death and lobuloalveolar shedding. The cycle then begins anew, preparing multiple tissues, including the mammary gland, for a possible pregnancy.

Mammary gland development during a pregnancy cycle

After puberty, the subsequent most drastic postnatal developmental stages occur during a pregnancy cycle in preparation of the mammary gland to provide nourishment to offspring of the individual. The developmental stages that occur during a pregnancy cycle include gestation, lactation and involution.

During gestation, specialized alveolar structures that will secrete milk during lactation are formed by an orchestration by P4 and PRL. Similar to pubertal development, P4 acts by promoting ductal branching during pregnancy and increasing the number of alveolar structures to promote the generation of a gland structure capable of lactating. Additionally, increasing levels of PRL play a role in maintaining the corpus luteum during this developmental stage, which in turn produces P4 (Ormandy,

Binart, et al., 1997; Ormandy, Camus, et al., 1997). The augmented levels of PRL also upregulate E2 expression, therefore coordinating mammary morphogenesis through the regulation of hormone signals.

Parturition is induced by rising levels of OXT, and marks the beginning of lactation. The aforementioned neuropeptide acts upon the mammary myoepithelium by controlling calcium uptake and contractility, and furthermore induces mechanical constriction of alveolar cells to eject milk into the mammary lumen (Moore et al., 1987). Moreover, levels of PRL increase during lactation to even more so promote alveologenesis, being expressed both by lactotrophic cells in the pituitary gland that release PRL into the bloodstream and local MECs (Slepicka et al., 2021). The presence of PRL additionally modulates the creation of tight junctions to control cell polarity, which is essential for the directionality of milk droplet secretion into the lumen (F. Liu et al., 2015; Rodriguez-Boulan & Macara, 2014). Altogether, lactation transforms the mammary gland into a functional unit that is necessary for the survival of offspring.

After lactation has ceased (and thus offspring stop providing a suckling stimulus), the mammary gland undergoes regression of the mammary structure to its "pre-pregnant" homeostatic state through involution, the last mammary developmental stage of a pregnancy cycle. As all other mammary developmental stages, the length of this developmental stage varies across mammalian species. In humans specifically, involution lasts ~24 months, while in rodents this process usually takes place for ~10-20 days. Moreover, involution takes place in two main phases, a reversible one (days ~0-2 of involution), and an irreversible one (days ~8-10 of involution) (Jindal et al., 2014; Sharp et al., 2007). During the reversible stage of involution, there is decreased milk production, milk absorption, MEC shedding, alveolar cell death, phagocytosis of apoptotic cells, leukocyte infiltration, and breakdown of tight junctions (Slepicka et al., 2021). If no suckling stimulus occurs during the reversible phase of involution, the irreversible phase of involution commences. During this part of involution, wound healing processes activate and induce the drastic remodeling of the ECM via a variety of signaling pathways. This chapter summarizes the current knowledge about the complex nature of interactions between the mammary epithelium and stroma during mammary gland development in different

mammalian species (Green & Lund, 2005). The ECM also modulates a second wave of inflammation and immune cell recruitment in the mammary gland, in order to clear cellular debris (Jena et al., 2019; Monks et al., 2005; Stein et al., 2004). Mammary involution is further modulated by a range of signaling pathways and high cell-turnover, which promote a permissive environment for immune infiltration. As such, increased numbers of RORγT+ FoxP3+ CD4+ T regulatory cells, dendritic cells, and memory Th17-Treg cells are observed in the involuting gland. At the end of involution, the immune environment is observed to mainly regress to its pre-pregnant homeostatic state (Betts et al., 2018). However, recent work from our lab has demonstrated persistent changes to the microenvironment after a pregnancy cycle, mainly involving presence of NKT-like cells recruited during involution that are linked to parity-associated onco-protection, thus demonstrating lasting effects of pregnancy developmental stages to the mammary gland (Hanasoge Somasundara et al., 2021).

Menopause

In females, menopause marks the end of the reproductive cycle and is characterized by a final menstruation period. This process is triggered by a decrease of ovarian hormones, causing the ovaries to no longer release any eggs (G. V. Dall & Britt, 2017). The age at which menopause occurs is, once more, highly variable depending on the mammalian species and the individual. In humans, the average age of menopause ranges from ~45-55 years, and is largely determined by factors such as maternal age of menopause, ethnicity, use of contraceptives, parity and certain lifestyle choices and pre-existing diseases (Gold et al., 2001; Snieder et al., 1998; van Asselt et al., 2004).

Our knowledge about the effects of menopause on the mammary gland are, moreover, widely understudied in part because mouse models do not undergo menopause. As a result, most studies about the effects of menopause in the mammary gland involve ovariectomized mice, which do not necessarily reflect how these developmental processes naturally occur (G. V. Dall & Britt, 2017). Nonetheless, a study using mouse models found that glands that were 5 weeks post-ovariectomy, and by definition of

the authors “postmenopausal”, were more responsive to E2-mediated proliferation compared to glands immediately following surgery (i.e. early menopause, also known as perimenopause) (Raafat et al., 1999). The aforementioned study also found that E2 did not increase mammary PR levels specifically during post-menopause, which is a trait of immature pubertal glands thus suggesting the aged mammary structure resembles the pre-pubertal gland the most. Furthermore, no differences in ER levels were found between early and post-menopausal glands, suggesting the existence of a mechanism beyond receptor-binding by which MECs act during this developmental stage. Therefore, menopause has drastic implications for MEC development, mammary gland hormone response at a late age and, consequently, BC risk.

In summary, the mammary gland undergoes many transformations from its formation until the end of the individual’s reproductive age, serving as an ideal system to track tissue development. Finding ways to study gland development in a controlled environment and via treatment with isolated signals has therefore been a challenge the developmental biology field has undertaken.

1.2.2 Hormone control of female mammary gland postnatal development

As briefly mentioned, some of the major regulators of mammary gland development are hormones E2, P4 and PRL. The levels of E2 and P4 first surge during female puberty to promote MEC proliferation and consequently result in ductal expansion, and then cyclically fluctuate during the estrous cycle (Arendt & Kuperwasser, 2015). Parity-associated development, which is characterized by the terminal differentiation of MECs, is also dependent on an interplay of E2, and P4, in addition to PRL to promote alveologenesis. Therefore, one of the biggest tasks of the mammary gland biology field has been to describe the effects of these hormones at both the structural and molecular level of the mammary gland throughout different female developmental processes.

Estrogen signaling

Estrogen (E2) mainly acts by binding to its receptors (ER), from which the most common is ERα. It has been shown that, during embryogenesis, MEC expression of *ERα* gene is not essential for the formation of primitive gland ducts, but it is necessary for ductal network development during pregnancy (Feng et al., 2007; Slepicka et al., 2021). Therefore, in humans, its highest expression levels of *ERα* gene have been described in immature lobule 1 during puberty (Russo et al., 1999, p. 199). In mice, ERα-expressing cells have been analogously found in the lumen within the body of TEBs that arise during adolescence (Zeps et al., 1998).

The actions of ERα can largely be seen in a paracrine manner within the mammary gland, with ERα-expressing cells stimulating surrounding ERα-deficient cells (Clarke et al., 1997, p. 1; Russo et al., 1999; Slepicka et al., 2021; Zeps et al., 1998). This paracrine effect is evidently with the fact that MECs within the tips of TEBs do not express ERα but exhibit high levels of proliferation induced by E2/ERα, thus alluding to a paracrine mechanism of action (Clarke et al., 1997; Feng et al., 2007; Mallepell et al., 2006; Mueller et al., 2002; Russo et al., 1999; Zeps et al., 1998). One major paracrine-induced signal downstream of ERα is Amphiregulin (AREG), which binds to Epidermal growth factor receptor (EGFR) in stromal cells, and is largely expressed by ERα-expressing luminal MECs. ERα ablation is sufficient to stunt AREG expression and negatively impact ductal network development, and overexpression of AREG in ERα deficient mice rescues ductal development, thus demonstrating that AREG is a crucial target of ERα for mammary gland development (Ciarloni et al., 2007; Kenney et al., 2003; Sternlicht et al., 2005). Furthermore, whilst MEC expression of AREG is sufficient to induce ductal development, stromal cells have been shown to depend on EGFR to induce ERα/AREG-associated processes, thus demonstrating the paracrine mechanism of action of ERα (Jackson-Fisher et al., 2004; Sternlicht et al., 2005; Wiesen et al., 1999).

In addition to paracrine signaling, ER exhibits highly versatile mechanisms of action and can function in a ligand-dependent and independent manner. For instance, ER can exert its effects through

its membrane localization. It has been shown that anchorage of ERα to the cellular membrane is necessary for pubertal mammary development, and for MaSCs to repopulate cleared fat pads in transplantation assays (Gagniac et al., 2020). Another mechanism of action for ER involves its function as a TF, with ER binding to open chromatin sites to activate the transcription of gene targets. This particular mechanism of action was demonstrated to be widely dependent on TF Forkhead box A protein 1 (FOXA1), which facilitates chromatin accessibility in ER-specific sites (Carroll et al., 2005; Hurtado et al., 2011; Laganière et al., 2005). ER also recruits co-regulators to aid in its function, such as glutamic acid [E] and aspartic acid [D]-rich C-terminal domain 1 (CITED1), which assist in lumen formation and ductal morphogenesis (Howlin et al., 2006). Altogether, all of the aforementioned mechanisms highlight how E2/ER can trigger extensive cascades of downstream effectors that are crucial to coordinate mammary gland development.

Besides proliferative functions during female puberty, Estrogen signaling has also been implicated as having an essential role in MEC development during a pregnancy cycle. This effect has been correlated, for instance, with an increase of ERα+ cells in early pregnancy (De Silva et al., 2015; Mastroianni et al., 2010). Moreover, the characterization of pregnancy-specific ERα+ cells in mice revealed that these cells have a limited multipotent profile and, when used in transplantation assays, can develop into structures that differentiate and lactate (Kaanta et al., 2013). Furthermore, mutations to the *ERα* gene have been shown to cause lactation defects, further providing evidence for the regulation of parity-induced MECs function via Estrogen signaling (Feng et al., 2007). However, the existence of pregnancy-induced MECs in humans is still being elucidated, making the role of E2/ERα+ in MECs during a human pregnancy unclear (Arendt & Kuperwasser, 2015). Nonetheless, it is important to note that Estrogen signaling additionally regulates Pgr and Prlr expression in MECs, making it a crucial effector for parity-induced development across species (Haslam & Shyamala, 1979; Leondires et al., 2002).

Interestingly, despite a systemic depletion of E2 during menopause, an increase of local E2 levels and an increase of ER expression in MECs has been reported, illustrating a potential mechanism

for MEC normal and pathological development during this stage (Arendt, Evans, et al., 2009; Arendt, Grafwallner-Huseth, et al., 2009; Christov et al., 1991; Cleland et al., 1985; Shoker et al., 1999). These observations coupled with empirical evidence that overall levels of E2 are highest during pregnancy but have a lower effect on proliferation compared to puberty serve to demonstrate the intricate effects of Estrogen signaling at different MEC developmental stages (Rusidzé et al., 2021).

Progesterone signaling

Similar to E2, P4 exerts its function mainly through its nuclear receptor (PR). There are two main isoforms of PR in mammals; PR-A and PR-B, both which exist at specific ratios from each other and contribute to the modulation of side-branching development and proliferation (E. Anderson, 2002; Shyamala et al., 1998). PR-A can act as a repressor for PR-B during murine puberty, but ultimately the tightly coordinated expression of both isoforms is essential for normal MEC pubertal development (Brisken et al., 1998; Conneely et al., 2001; Humphreys et al., 1997; Mulac-Jericevic et al., 2000). As an example, transplantation assays involving injections of MECs depleted of both isoforms of PR resulted in impaired lobuloalveolar development in response to E2 and P4 treatment, with WT MECs being able to rescue normal morphogenesis (Humphreys et al., 1997). Altogether, the requirement of both isoforms of PR for normal mammary development represents a unique trait for P4 signaling in comparison to other hormones.

PR is expressed in luminal MECs, which function in tissue expansion during puberty in response to a surge of P4, in both a paracrine and non-paracrine manner (Pal et al., 2013; Shehata et al., 2012). For instance, P4-induced paracrine signaling has been shown to involve the release of the Receptor activator of nuclear factor kappa-B-ligand (RANKL), which interacts with RANK in PR-negative cells and controls mammary alveologenesis (Beleut et al., 2010; Fernandez-Valdivia et al., 2009). In contrast, P4-induced non-paracrine signaling involves downstream targets to PR such as Cyclin D1 (CCND1), a mitogenic regulator that has been implicated in the proliferation of PR+ MECs

(Fernandez-Valdivia et al., 2009). Additionally, P4 mediates other genes such as those involved in Wnt4 signaling, which promote ductal expansion during puberty by enabling communication between PR+ luminal cells and PR- stem and myoepithelial cells, showcasing another indirect mode of action for P4 signaling (Rajaram et al., 2015). In the aforementioned case, one of the ways that P4 has been suggested to modulate Wnt4 signaling is through TF activity of PR, as PR has been observed to bind to Wnt4 promoter (Beleut et al., 2010; Ramamoorthy et al., 2010; Tanos et al., 2012). Overall, all of the aforementioned mechanisms of action demonstrate the complexity of P4/PR signaling in coordinating a wide array of molecular processes crucial for tissue development.

Particularly during female adolescence, surging levels of P4 serve to induce side-branching morphogenesis through the activation of quiescent ductal MECs into a multilayered epithelium (Brisken et al., 1998; Lain et al., 2013). Consequently, our lab and others have speculated that P4/PR signaling is essential for MaSC involvement in the aforementioned developmental processes, although MaSCs have not yet been demonstrated to express PR (Pal et al., 2013; Schams et al., 2003; Shehata et al., 2012; Shyamala et al., 2002; Slepicka et al., 2021). Additionally, the expression of AREG, an E2-target that heavily modulates TEB formation and expansion during puberty, is upregulated by P4 signaling, thus conferring P4 a multifaceted role in pubertal development (Aupperlee et al., 2013).

Levels of P4 are at its peak during the luteal phase in humans and the diestrus stage in mice. Rising levels of P4 consequently result in the highest rates of MEC proliferation during the estrous cycle, even in comparison with the estrus stage, when E2 levels are at its peak (Arendt & Kuperwasser, 2015; Joshi et al., 2010). The aforementioned proliferation mainly occurs by the expansion of MEC progenitors, therefore further suggesting a role for P4 signaling in stem cell maintenance and development throughout adulthood.

Like E2, serum levels of P4 are highest during pregnancy (Abbassi-Ghanavati et al., 2009). This hormone has been mainly shown to act through isoform PR-B to promote side-branching and, during the last stages of pregnancy, through isoform PR-A to promote alveologenesis (Mulac-Jericevic

et al., 2003). Nonetheless, the proportion of MECs expressing PR is overall reduced in pregnancy, suggesting a mode of P4 signaling regulation to avoid aberrant proliferation during pregnancy (Brisken & Scabia, 2020; Grimm et al., 2002). Notably, during mid-to-late pregnancy in both mice and humans, P4 inhibits milk protein production and closure of tight junctions until lactation, and temporal coordination of this process by P4 is essential to avoid reflux of accumulated milk into the mammary lumen (Loizzi, 1985; Neville et al., 2002; D. A. Nguyen et al., 2001; Obr & Edwards, 2012; Virgo & Bellward, 1974). Thus, P4 also regulates the transition from gestation to lactation, making it a necessary hormone for normal pregnancy development.

During menopause, the last stage of mammary development, there are reduced systemic levels of P4, which could be correlated to the observed decrease in proliferation of MECs at this stage (Brisken & Scabia, 2020). Moreover, expression of PR in MECs independent of P4 binding has been linked to its functions as a tumor suppressor during pregnancy, highlighting how hormone receptors such as PR also work to prevent pathological development (Obr & Edwards, 2012).

Prolactin signaling

In contrast to primarily placental E2 and P4, PRL is primarily made in the pituitary gland (Hennighausen & Robinson, 2001; Riddle et al., 1933). This pituitary hormone acts mainly by binding to its receptor (PRLR), which activates several signaling cascades, including the Janus Kinase JAK/STAT5 pathway (Rui et al., 1994; Slepicka et al., 2021; Wakao et al., 1994). Within this pathway, once PRL binds to its receptor, JAK1 and JAK2 are recruited, resulting in the phosphorylation and nuclear localization of STAT5 (Ali & Ali, 1998). Induction of STAT5 TF activity via PRL/PRLR is important in MECs for the regulation of genes associated with differentiation, proliferation and function throughout different developmental stages, such as milk-associated genes whey acidic protein (Wap) and β-casein (S. Li & Rosen, 1995; Schmitt-Ney et al., 1991). Additionally, PRL regulation of other downstream effectors of the JAK2/STAT5 pathway have further been shown to be important for MEC

development, such as activation of factor Cub and zona pellucida-like domain-containing protein 1 (CUZD1), which is involved in alveologenesis (Mapes et al., 2017). Other downstream targets of PRL/PRLR include the ETS transcription factor 5 (ELF5), which regulates alveolar cell fate and lobuloalveolar expansion during pregnancy and lactation, and RANKL, which regulates parity-associated development in MECs (Fernandez-Valdivia et al., 2009; Oakes et al., 2008; Srivastava et al., 2003; J. Zhou et al., 2005). Altogether, PRL acts as an activator for a variety of pathways involved in coordinating the development of the mammary gland, especially in the context of pregnancy.

PRL has been linked, via indirect mechanisms, to ductal side branching and TEB regression during pubertal development (Brisken et al., 1999). Nonetheless, its most notable and direct effects reportedly occur during pregnancy, where PRL coordinates lobuloalveolar development. Especially during early (5-7 days in mice) and late (11-14 days in mice) gestation, PRL acts via the JAK2/STAT5 pathway to upregulate Scribble (SCRIB) expression, which promotes alveologenesis (Baker et al., 2016). Tight junction formation is also coordinated by PRL/JAK2 signaling during late pregnancy, which is crucial for directional secretion of milk droplets into the mammary lumen (F. Liu et al., 2015; Rodriguez-Boulan & Macara, 2014). Therefore, PRL acts mainly through JAK2 signaling to ensure alveolar development and function during pregnancy cycles, making it an essential hormone for normal lactation to occur.

As expected, PRL levels first surge during early pregnancy and serve to maintain the corpus luteum and, in turn, modulate the expression of placental hormones (Ormandy, Camus, et al., 1997, 1997). Nonetheless, peak levels of PRL occur during lactation, originating from lactotrophic cells in the pituitary gland that travel through the bloodstream, and local MECs (Slepicka et al., 2021). A drop in systemic PRL levels occurs after lactation has ceased, and is partly responsible for adipogenesis to restore the mammary gland to its pre-pregnant homeostatic state (Ben-Jonathan & Hugo, 2015). Interestingly, previous studies have reported a decrease in systemic PRL levels after a first pregnancy in humans, which has been suggested as a factor that could alter BC risk after pregnancy (Ingram et al., 1990; Love et al., 1991; D. Y. Wang et al., 1988). Altogether, PRL plays a crucial role during

pregnancy, lactation and in maintaining tissue homeostasis, with regulation of PRL levels having potential implications for BC risk.

1.2.3 The mammary gland retains a memory of pregnancy

Previous epidemiological and clinical studies have extensively reported that a history of previous pregnancies is associated with decreased BC risk, suggesting a long-lasting effect of parity-associated developmental changes in the mammary gland (Rosner et al., 1994; Schedin, 2006). Both cell autonomous and non-autonomous mechanisms have been implicated in the observed parity-associated protective effect, such as hormone level changes, stromal compositional changes, and alterations to cellular states and differentiation patterns (Barton et al., 2014; Meier-Abt & Bentires-Alj, 2014; Schedin et al., 2004; Thordarson et al., 1995). For instance, PRL and growth hormone (GH) levels decrease after pregnancy, and both of these have been linked to an increase in mammary tumorigenesis incidence (Harvey, 2012). Likewise, ECM and collagen organization is altered by pregnancy, and both elements have been suggested to reduce tumor growth and invasion (Maller et al., 2013). Post-pregnancy MECs have also been observed to have decreased rates of proliferation, and increased ability to repair DNA damage, which could contribute to a decrease in aberrant development (Barton et al., 2014). Notably, altered transcriptional patterns have been observed in MEC progenitors, with pro-tumorigenic pathways being downregulated after pregnancy (Choudhury et al., 2013; Meier-Abt et al., 2013). Furthermore, pregnancy-induced terminal differentiation has been theorized to remove cells prone to malignant transformation, once more contributing to a reduced risk of BC (Meier-Abt & Bentires-Alj, 2014).

Post-pregnancy MECs have been shown to acquire a parity-induced transcriptomic signature that is retained even after pregnancy has long ended (Blakely et al., 2006). Additionally, terminally differentiated MECs that arise with pregnancy have been shown to display higher contents of heterochromatin compared to pre-pregnant MECs, demonstrating persistent parity-induced changes to the gene regulatory landscape of the mammary gland (Russo et al., 2012). One of the mechanisms by

which gene expression regulation is altered with pregnancy is by changes to the epigenetic landscape of MECs (Blakely et al., 2006; Choudhury et al., 2013). Moreover, the aforementioned epigenetic changes have been shown to be persistent in MECs, allowing for rapid re-activation of MEC function during re-exposure to pregnancy hormones (C. O. dos Santos et al., 2015). Our lab has also demonstrated that these epigenetic changes that persist after pregnancy alter *cMyc* driven oncogenesis via reduced active histone marks (H3K27ac) in the *cMyc* enhancer (Feigman et al., 2020). More recently, our lab demonstrated that another mechanism by which persistent parity-associated epigenetic changes to MECs could modulate BC risk is by alterations to the Antigen-Presenting Glycoprotein CD1d gene (*Cd1d*) locus, increasing Cd1d expression which, in turn, recruit NKTs to the mammary gland microenvironment (Hanasoge Somasundara et al., 2021). The investigation of the temporal and mechanistic aspects underlying persistent epigenetic modifications during pregnancy has therefore become a current focus in the field of mammary gland biology, with the possibility of using this knowledge in the development of preventive medical interventions.

1.3 Translational models for mammary gland development

Our knowledge of mammary gland development has stemmed from studies using a variety of models that can have been implemented in different mammalian species. Some of the primarily studied species in the context of mammary gland biology include rodent species, dairy animals and humans. However, since it has been noted that the biology of dairy animals might largely diverge from human biology, I will focus instead on models that have the most translational potential (Akers, 2017). Moreover, for this subsection of my thesis, I will be discussing the significance and limitations of these models in our attempts to reconstruct human mammary developmental processes.

1.3.1 Models for whole-mammary intact tissue development

An approach that has been long utilized to understand mammary gland development has involved observations and alterations to mammary cellular sub-populations in their original biological context. In other words, MECs, stromal cells and endocrine signals are kept intact in these models, allowing us to consider whole mammary tissue interactions when studying different developmental processes. The use of these models, however, can dampen the true influence of specific developmental signals that we might be attempting to characterize, as well as adding a layer of complexity that might not be translatable to other species. Therefore, it is crucial to acknowledge and address the tradeoffs of using these models to ensure accurate interpretation and application of their findings.

Mouse models

One of the most used systems for mammary gland development are mouse models, which are highly accessible to manipulation, in part due to our breadth of knowledge on their biology. Indeed, mice have been the pioneering system to characterize mammary development, which has long involved the engineering of these systems, transplantation assays and use of hormone pellets and other exogenous signals to re-construct developmental processes (Medina, 2010).

Transplantation assays in mice involve the surgical removal of the mammary epithelium portion of the mammary fat pad when it is still in a rudimentary state (before ~3 weeks of age) (Medina, 2010). Specific MEC sub-populations can then be re-injected into the "cleared" mammary fat pad to track their ability to re-populate the mammary gland (Kordon & Smith, 1998). Studies using this system have thus allowed for our assessment of the specific roles of MEC-subpopulations in mammary gland development. Moreover, injection of MEC sub-populations in concert with hormonal stimulation have allowed for examination of the different roles of hormonal signals in promoting sub-MEC developmental processes (Song et al., 2019). Modifications to the original transplantation assay protocol have continued to progress, with novel implementations such as intraductal transplantations allowing for recipient mice to keep their existing fat pads and undergo transplantation at any age

(Behbod et al., 2009). Moreover, coupling transplantation assays with engineered immunodeficient mice as recipients have enabled the development of xenograft models, which allow for the incorporation of MECs from other species into the mouse stromal environment without the risk of host-mediated killing. These xenograft models have provided the means to evaluate the impact of mouse stromal interactions on foreign MECs, thus enhancing the translatability of using murine models to study mammary gland development (Kuperwasser et al., 2004; Popnikolov et al., 2001).

Another widely used approach to study mammary gland development using mice has involved the creation of engineered mouse models. In the context of normal mammary gland development, this approach has involved the deletion of genes to assess their effects in impairing pubertal or parity-associated development (Miyoshi et al., 2001; Seagroves et al., 2000; Shillingford et al., 2002). In contrast, to study mammary gland malignant development, inducible systems such as those triggered by Cre-lox or FLP-FRP, are typically used to overexpress oncogenes or downregulate tumor suppressor genes and study how different mammary developmental stages affect neoplastic growths (Lewandoski, 2001; Sakamoto et al., 2015). Using engineered mouse lines have thus been widely beneficial to validate the function of different genes and developmental signals on normal and aberrant mammary gland development.

Due to the highly tractable nature of murine models, it has also been possible to introduce hormonal signals to these models in order to induce key developmental stages without the need of genetic manipulation. This approach has been possible via the implementation of subcutaneous pellets containing specific concentrations of hormones, such as 17β-estradiol (i.e. E2, the predominant form of circulating Estrogen in women), P4 and/or PRL, which result in a slow long-term release of these hormones into circulation (Atwood et al., 2000; Levin-Allerhand et al., 2003; Rudali et al., 1978; Silberstein & Daniel, 1987). Surgical implementations of pellets containing 17β-estradiol in mice have allowed, for instance, to track the effects of high doses of Estrogen on malignant development (G. Dall et al., 2015; Rudali et al., 1978). Implementation of 17β-estradiol and P4 pellets on 21-39 days old mice have also allowed assessment of the effects of both hormones on pubertal development, with pellet-

induced P4 being responsible for the formation of tertiary side branches in the mammary gland (Atwood et al., 2000). In order to tightly control the influence of ovarian hormones, many of these studies have been conducted in ovariectomized mice (Gérard, Blacher, et al., 2015; Gérard et al., 2017; Gérard, Mestdagt, et al., 2015; Mallepell et al., 2006; Péqueux et al., 2012). The removal of ovarian signals, however, might have other systemic effects that could result in artificial phenotypes. More recently, hormone pellets have been induced into intact mice in order to independently assess the effects of hormones in inducing normal mammary gland development. Using pellets containing 17β-estradiol and P4 has resulted, for instance, in the recapitulation of transcriptomic and epigenomic changes to the mammary gland typically observed with pregnancy (C. O. dos Santos et al., 2015). Our lab has also used the aforementioned pellets to assess the effects of pregnancy hormones on BC development, and found persistent epigenomic changes to the mammary gland that block malignant growths (Feigman et al., 2020). Even more recently, our lab has observed that using this approach results in epigenomic changes to MECs that could be linked to the recruitment of NKTs to the mammary gland after pregnancy (Hanasoge Somasundara et al., 2021). Overall, the use of hormone pellets in mouse models has proven to be a powerful tool for studying the effects of hormonal signals on the development of the mammary gland, providing insights into the underlying mechanisms by which these signals function.

Altogether, mouse models have propelled the mammary gland biology field forward. Nevertheless, it is important to consider the translatability of these systems as, for instance, the mammary stroma of mice and humans contains different cellular proportions of non-epithelial mammary gland resident cells that can interact with MECs, and could therefore largely affect normal developmental mechanisms (Dontu & Ince, 2015). Mouse strain-to-strain differences have also been shown to partially contribute to postnatal mammary gland developmental mechanisms, further hindering the translatability of mouse models to human mammary tissue development (Aupperlee et al., 2009). Therefore, caution should be exercised when extrapolating results obtained from mouse models to human biology.

Patient-derived mammary gland tissue samples

Patient-derived mammary tissue samples have long been used to study the development of breast tumors (Twigger & Khaled, 2021). However, recent advances in the use of patient-derived mammary gland tissues as a model to study normal mammary gland development have opened up new venues for understanding human mammary gland biology, which in turn holds great promise for translating this knowledge into preventative medical interventions. Using the aforementioned patient-derived samples to further comprehend human-specific mammary developmental mechanisms has mainly involved transcriptomic profiling of mammary tissue obtained at fixed time points during postnatal development (Twigger & Khaled, 2021). Hence, these methodologies primarily have offered a static representation of the mammary tissue during particular developmental phases rather than the kinetics of mammary gland development. Nonetheless, the knowledge we have acquired from profiling patient-derived tissue has been indispensable, and continued accessibility to these samples will continue to advance the mammary gland biology field.

Initial studies have involved transcriptomic profiling of human mammary tissue at a steady-state during adulthood, with the purpose of creating a reference atlas of the human mammary gland (Gray et al., 2022; Henry et al., 2021; Q. H. Nguyen et al., 2018). Nonetheless, some of these studies have in tandem generated transcriptomic profiles for human mammary tissue at a homeostatic state after pregnancy and during aging, providing a glimpse of the mechanisms that different mammary gland sub-populations undergo during these developmental processes (Gray et al., 2022; Murrow et al., 2020, p. 202; Pelissier Vatter et al., 2018). To circumvent the difficulty of obtaining mammary tissue from pregnant women, recent studies have profiled human milk in order to capture the transcriptomic changes that occur in different human mammary sub-populations during lactation (Martin Carli et al., 2020; Twigger et al., 2022). However, these studies do not necessarily capture the complexity of mammary gland tissue, and even more so their evolving transcriptomic profiles throughout gestation, lactation, and involution. Therefore, the extension of non-invasive methods for obtaining human mammary tissue

and its subsequent tracking and manipulation is essential to enhance our understanding of normal human mammary gland development.

1.3.2 In vitro models for mammary gland development

Although *in vivo* models have been valuable in comprehending the development of the mammary gland, examining the molecular processes in response to specific developmental cues can be challenging in these systems. Moreover, stromal interactions with the mammary epithelium might attenuate intrinsic MEC mechanisms in response to developmental signals, limiting the translatability of *in vivo* murine studies. Hence, the development of scalable and tractable models to study mammary tissue development have been a vital component of the mammary gland biology field. Consequently, techniques for isolating specific mammary sub-populations and culturing them in vitro have been extensively developed. While 2D cell line cultures were the first system used to isolate mammary sub-populations and evaluate their response to specific signals, their inability to replicate *in vivo* morphogenesis has limited their usefulness. In order to overcome these constraints, 3D cultures known as "organoids" have been developed. Mammary organoids thus present a suitable system to specifically isolate MECs from their microenvironment and dynamically track transcriptomic events controlling morphogenesis in response to controlled signals.

As briefly mentioned, in contrast to 2D cell lines, organoids are cultured in 3D gels whose composition is similar to the ECM, thus allowing cultured cells to mimic *in vivo* morphogenesis (Shamir & Ewald, 2014; Simian et al., 2001). In effect, proteomic profiling of MEC-derived organoid cultures revealed that these cultures reflect MEC lineages and cellular states found *in vivo*, as opposed to 2D cell lines which fail to separate intermediate cellular states (Rosenbluth et al., 2020). Therefore, organoids offer a more physiologically relevant approach to investigating mammary tissue development, as they can better capture the complex cellular states observed *in vivo*.

The most commonly used gels for organoid culturing are Matrigel and collagen I, which contain basement membrane (BM) matrix proteins required for MEC growth and differentiation (Kleinman & Martin, 2005; Wolf et al., 2009). Using the aforementioned gels causes MECs to organize in a bi-layered structure, which can then be treated with growth factors to induce ductal branching in vitro (Ewald et al., 2008; Florian et al., 2019; Jamieson et al., 2017). Our lab and others have further shown that treating organoids with pregnancy-associated hormones results in phenotypes observed during lactation and with involution, such as secretion of milk-associated proteins and persistent epigenomic changes that occur with parity (Ciccone et al., 2020; Feigman et al., 2020; Sumbal et al., 2020). Therefore, MEC-derived organoids can be a powerful tool for investigating the molecular mechanisms underlying mammary gland development, and can provide a physiologically relevant approach to studying these processes.

Notably, similar to 2D cell lines, organoids can be cultured from both murine and mammary gland tissue. Concurrently with murine MEC-derived organoids, specific culturing conditions have been developed for human MEC-derived organoids, incorporating distinct growth factors such as FGF-2 for mice and FGF-10 for humans, in addition to a variety of kinase inhibitors (G. Y. Lee et al., 2007; Sachs et al., 2018). Proteomics analysis using cytometry by time of flight (CyTOF) has resolved the conservation of MEC lineages in vitro, thus establishing human MEC-derived organoids as viable models to understand the molecular mechanisms driving mammary tissue morphogenesis (Gray et al., 2022; Rosenbluth et al., 2020). Moreover, patient MEC-derived organoids have been treated with E2 and P4 to assess differential responses to hormones in carriers of suppressor gene BRCA1 mutations and non-carriers (Davaadelger et al., 2019). The aforementioned study consequently establishes a possibility for further research employing hormone treatments, like those detected in subcutaneous pellets, to replicate the development of human MECs in vitro.

1.4 Single cell characterizations of mammary gland development

To address the heterogeneity of mammary tissue and the role that multiple cell types play in morphogenesis at different stages, recently developed single cell technologies have been employed to characterize mammary cellular sub-populations throughout specific developmental processes. These characterizations range all the way from embryonic development to menopause models in mice, and human mammary tissue obtained from milk extracts, as well as young and aged mammary tissue (Bach et al., 2017; Giraddi et al., 2018; Gray et al., 2022, p. 202; Henry et al., 2021; Kanaya et al., 2019; Pal et al., 2017; Pelissier Vatter et al., 2018; Twigger et al., 2022; Wuidart et al., 2018). Hence, the use of these technologies offers a valuable resource for unraveling the complex lineages of mammary cells and their contribution to mammary gland development.

As briefly mentioned, single cell technologies, in particular single cell RNA sequencing (scRNA-seq) and single cell ATAC-seq (scATAC-seq), have been used to characterize the mouse mammary gland across different life stages. For instance, one study utilized scRNA-seq to profile MECs isolated from day 14 of embryonic development (E14) and characterized the transcriptomic profiles of early multipotent progenitors, noting that they were characterized by their unique hybrid basal and luminal signature, and that these cells were additionally enriched for genes that regulate proliferation and BC-associated pathways (Wuidart et al., 2018). Another study using both scRNA-seq and scATAC-seq profiled the MEC landscape on days 16 and 18 of embryonic development (E16 and E18), and revealed that, at this point of development, fetal mammary stem cells (fMaSCs) could be categorized based on co-expression of factors with both the progenitors and mature cell states in post-natal tissue that these fMaSCs precede (Giraddi et al., 2018). Likewise, another study characterized pubertal development of mouse mammary tissue by using scRNA-seq to profile MECs obtained at 2 weeks of postnatal development (i.e., pre-puberty), 5 weeks of postnatal development (during puberty), and 10 weeks (post-puberty) (Pal et al., 2017). The aforementioned study revealed that pre-pubertal MECs exist in a basal-like program, and become restricted during puberty. Moreover, the same study investigated the proportions of different MEC sub-populations during the estrus and diestrus stages of the estrous cycle, and found that intermediate luminal cellular states are reduced in the diestrus stage, suggesting maturation of these cell types during this stage of the estrous cycle. There was also an

increase of cycling basal cells during this stage, confirming that elevated levels of P4 indeed induce proliferation. Thus, this research offered a valuable glimpse into the intricate interplay of hormones in the post-developmental dynamics of the mammary gland.

Complete single cell maps of whole-murine mammary tissue undergoing different stages of a pregnancy cycle have also been developed, allowing us to further infer the mechanisms by which the mammary gland becomes a mature functional unit (Bach et al., 2017; Han et al., 2018; Henry et al., 2021). One study obtained murine MECs for scRNA-seq from nulliparous glands and glands at 14.5 days of gestation, 6 days of lactation, and 11 days post-involution (Bach et al., 2017). This group ordered cells according to their lineage progression (i.e., pseudotime), and identified pseudo-time dependent genes that distinguish each of the terminal luminal lineages that arise with pregnancy. Our lab further examined the aforementioned data and defined lineage markers that could be transferred to our own data sets (Henry et al., 2021). The latter analysis also defined steady states for MECs at each pregnancy stage, noting how, for example, MECs undergoing gestation and lactation acquire bi-lineage traits. Another group has expanded upon the time points collected by Bach et al. to continue mapping of the entire pregnancy-associated developmental timeline, and continued efforts like the aforementioned one will provide deeper comprehension of the kinetics of parity-associated developmental stages (Pal et al., 2021).

Conversely to murine mammary tissue, obtaining patient-derived mammary samples to map human mammary gland development has proven to be a challenging task. Therefore, most patient-derived samples used for single cell studies have been obtained via reduction mammoplasty, and thus from post-pubertal tissue. The dynamics of MECs during a pregnancy cycle have relied, for example, on inferences from post-pregnancy (i.e., parous) mammary samples, as well as milk extracts. For instance, one study performed scRNA-seq on mammary tissue samples from pre-menopausal women who had not undergone previous pregnancies and who had at least one previous pregnancy, and identified transcriptional programs associated with response to pregnancy hormones and pregnancy-like processes, and which cells were associated with these programs (Murrow et al., 2022). Additionally,

Murrow et al. found reduced proportion of hormone sensing cells in parous mammary samples, suggesting a mechanism by which parous cells resist hormone-induced proliferation and potentially reduce their risk of malignant development. Another study likewise used both scRNA-seq and CyTOF to profile parous and non-parous patient-derived mammary samples, describing an increase in quiescent alveolar cells in the parous human mammary gland (Gray et al., 2022). These results support previous findings in rodent models that suggest that the parous mammary gland responds more rapidly to subsequent exposure to pregnancy hormones, thus implying a potentially evolutionary conserved mechanism across species to promote lactation efficacy (C. O. dos Santos et al., 2015).

As previously stated, attempts to understand the rapid dynamics of pregnancy-associated development in humans have led to the refinement of non-invasive procedures to obtain tissue from pregnant women, as well as using highly malleable organoid models, all which can be profiled using single cell technologies. Profiling of patient-derived milk extracts with scRNA-seq revealed these samples can recapitulate luminal lineages, as well as immune cells from the mammary microenvironment (Twigger et al., 2022). Nevertheless, CyTOF profiling of organoids has demonstrated the ability to capture MEC lineages present in primary tissues (Gray et al., 2022). These results suggest the potential of capturing molecular changes in specific MEC-subpopulations within organoid cultures treated with pregnancy hormones.

1.5 Research hypotheses

As organoid models are increasingly used to study mammary gland development, it is vital to determine how well they represent intact mammary tissue and to understand the effects of hormones on the molecular characteristics of MECs *in vitro*. In the present study, we sought to generate scRNA-seq profiles for murine MECs at steady-state and undergoing Estrogen and EPP treatment. The resulting transcriptomic profiles would then be compared with publicly available datasets from intact mammary tissue development in order to determine the advantages and limitations of these systems. We would then extend the aforementioned approach to human MEC-derived organoids. We therefore

hypothesized that, similar to the estrous cycle, varying concentrations of Estrogen would activate different pathways in MECs, especially those associated with proliferation and inflammation. We also hypothesized that we would observe changes in the plasticity of murine and human cells treated with EPP, especially by the loss of stemness in MECs that participate in lactation. We further hypothesized that MEC composition would be mostly preserved *in vitro* in accordance with previous literature (Gray et al., 2022), and that this system would be ideal to recapitulate intact pregnancy transcriptomic changes to MEC-subpopulations. Altogether, the present study will contribute to the creation of a single cell map of 3D-cultured murine and human MECs treated with different hormones, characterizing organoid systems treated as a model for post-natal development.

To translate studies characterizing murine MEC changes throughout pregnancy to human MECs, we must be able to compare MEC transcriptional profiles across species. Our lab previously utilized a pipeline to directly convert mouse to human orthologs in scRNA-seq data using a gene list curated by Zilionis et al (Zilionis et al., 2019). Using this method, our lab was able to directly compare nulliparous intact mouse MECs and intact MECs from women who had no previous pregnancies, showing for the first time the conservation of MEC composition across species. With this comparison, Henry et al. found that progenitor populations were widely similar across species, whereas differentiated cell types were more species specific. However, these MECs were not isolated from their microenvironment, and thus we do not know how MEC composition is conserved across species without species-specific stromal influences. Furthermore, we do not know how MECs from mice and humans compare in their response to similar developmental signals when isolated from their original microenvironment. Therefore, we sought to directly compare mouse and human MEC-derived organoids both at baseline and in response to pregnancy hormones. We hypothesized that, similar to what we had previously observed in intact MECs, human and mouse MECs in 3D cultures would be similar in their progenitor-like populations, and differ in mature cell states. Moreover, we hypothesized that pregnancy hormones would drive the maturation of MECs in both species, enhancing MEC compositional differences between both species. Our approaches for this portion of the present study

therefore sought to delineate transcriptional events contributing to tissue homeostasis throughout pregnancy cycles across evolutionary timescales.

Finally, our lab has obtained additional mammary gland tissue samples from healthy women that have undergone previous pregnancies (parous) and that have never been pregnant (nulliparous), which we used to generate intact scRNA-seq profiles. Transcriptomic profiling of these samples would therefore provide us with a snapshot of the transcriptomic changes that occur in whole-human mammary tissue as a result of parity associated processes. These results could be used as a baseline for comparing human mammary epithelial cell (MEC)-derived organoids with and without EPP treatment, allowing us to infer transcriptional events that may be caused by hormone exposure and that may persist in the human mammary gland. Based on several findings by our lab and others, we hypothesized that genes associated with branching, milk production, and immune recruitment would be upregulated in samples from parous women, and that we could trace back these transcriptional events to EPP treatment timepoints in organoid cultures.

With the aforementioned approaches we would thus contribute to the collaborative efforts of building a single cell map of human MECs across different gestational-like stages, laying the groundwork for future multi-omic studies to discern molecular changes to mammary sub-populations that contribute to lactation efficacy and hormone response.

2. Single cell characterization of mammary-derived organoids and comparisons with intact tissue composition

2.1 Results

2.1.1 Single cell characterization of murine MEC-derived organoids

In order to assess the cellular landscape and molecular signatures of organoids derived from murine mammary epithelial cells (MECs), we sequenced mammary organoids cells, derived from nulliparous female mice using the 10X Chromium platform.

To classify distinct populations of MECs, expression of previously defined markers for lineage commitment in intact mammary tissue were used to determine the identities of each cellular cluster (Henry et al., 2021). These markers allowed for robust classification of the cell types present in the data set. For example, Cytokeratin 8 and 18 (*Krt8/Krt18*) were used to classify luminal populations (**Fig. 3**, clusters MO1, MO2, MO3, MO5 and MO7), and Cytokeratin 5 and 14 (*Krt5/Krt14*) marking myoepithelial populations (**Fig. 3**, cluster MO4). Expression of hormone receptors such as Progesterone Receptor (*Pgr*), Prolactin Receptor (*Prlr*) and Estrogen Receptor α (*Esr1*) were used to define luminal populations of hormone sensing cells (**Fig. 3**, clusters MO2 and MO7). Alveolar cells were characterized by the expression of genes linked to a progenitor identity, such as Casein 3 (*Csn3*), and milk production, such as Lactalbumin Alpha (*Lalba*) (Cluster MO1) (Bach et al., 2017; Saeki et al., 2021) (**Fig. 3**). Additionally, since luminal clusters MO3 and MO5 did not immediately show high expression of hormone sensing, alveolar or traditional progenitor signatures, we resorted to looking at the top differentially expressed genes for these clusters to define their identities (**Table S1**). We found that cells in MO3 were characterized by expression of luminal progenitor genes FXYD domain-containing ion transport regulator 3 (*Fxyd3*), Cluster of differentiation 14 (*Cd14*) and Claudin-3 (*Cldn3*) (Asselin-Labat et al., 2011; Coradini et al., 2014; Shehata et al., 2012; H. Wang et al., 2019). MO3 cells also expressed genes associated with milk synthesis WAP four-disulfide core domain protein 18

(*Wfdc18*) and Mucin-15 (*Muc15*), suggesting MO3 is made up early alveolar progenitors (Pal et al., 2021; C. Shao et al., 2021).

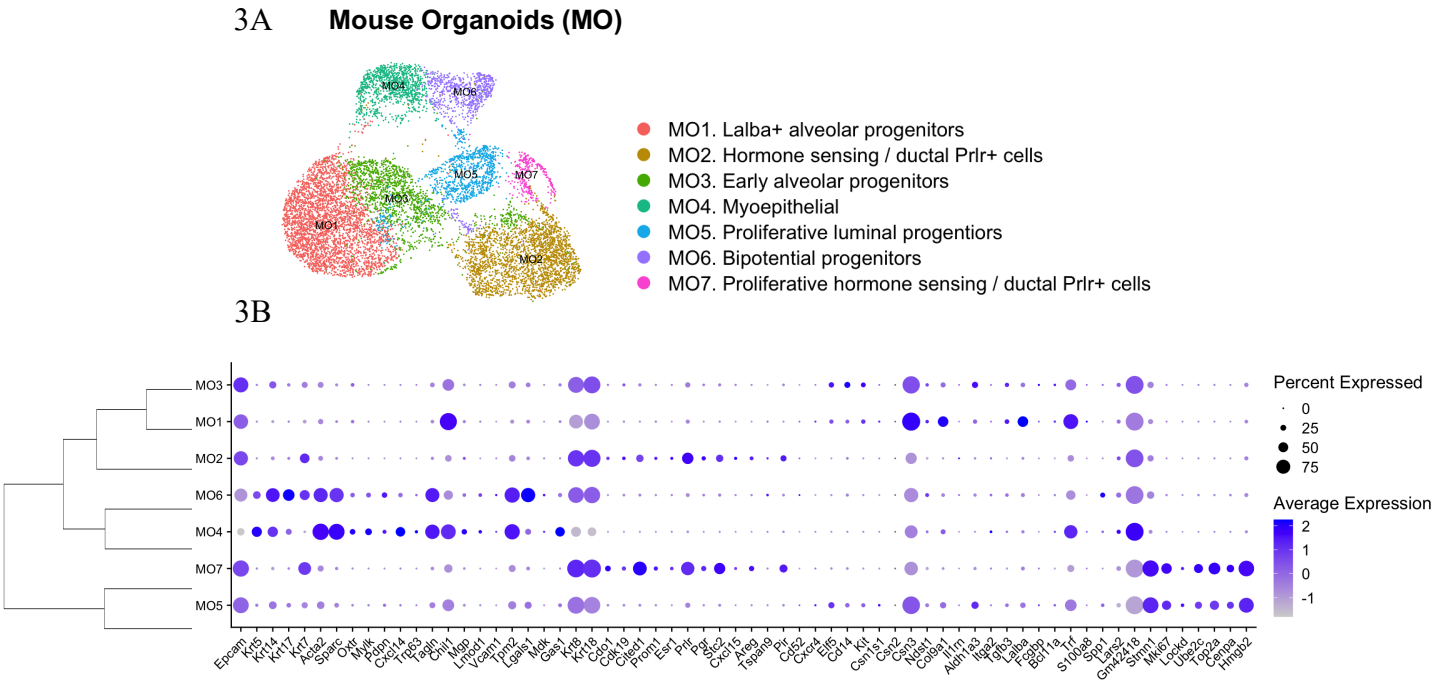

Figure 3. Single cell RNA-seq analysis of murine organoids and cluster classifications.

(A) Mouse Organoid (MO) clusters and their given identities according to gene expression from previously described MEC markers.
(B) Dotplot showing MEC markers average gene expression in each MO cluster.

Luminal cluster MO5 was characterized by the expression of genes associated with a MEC progenitor identity, such as Baculoviral IAP repeat-containing protein 5 (*Birc5*), Hyaluronan mediated motility receptor (*Hmmr*), Maternal embryonic leucine zipper kinase (*Melk*) and Stathmin (*Stmn*) (Segatto et al., 2019; Williams et al., 2009). Cellular clusters with highly proliferative gene signature were classified according to the expression of proliferative markers Marker of Proliferation Ki-67 (*Mki67*), Ubiquitin Conjugating Enzyme E2 C (*Ube2c*), DNA Topoisomerase II Alpha (*Top2a*), and according to overall cell cycle classification (**Fig. 4A**). With this analysis we defined 2 clusters of proliferating organoid cells, spanning cells that express hormone sensing signatures (MO7), and those of a less differentiated luminal progenitor state (MO5), indicating that several luminal subtypes assume a proliferative state in organoid cultures. We additionally identified one cellular cluster (MO6) with

expression of markers for both luminal and basal lineages, as well as Galectin-1 (*Lgals1*) expression, a previously identified marker for mammary stem cells (Soady et al., 2015). We therefore considered cells MO6 to have a mix/lineage/bipotential/progenitor identity. We confirmed the lineage identities of all organoid epithelial cell types with the utilization ternary plot (**Fig. 4B**). This analysis demonstrated that the distribution of cells within mix lineage/ bipotent cluster MO6 was biased towards a basal lineage, suggesting that these bipotent progenitors most likely reside in the basal compartment, as previous studies have also suggested (Stingl et al., 2001).

We next decided to investigate which molecular signatures were enriched in each one of the clusters identified on organoid cultures, using GSEA analysis (**Fig. 5A**). While clusters MO5 and MO7 were enriched with pathways associated with cell division, cells from cluster MO2 were marked by processes associated with hormone sensing, thus collectively supporting their above assigned cellular states (**Fig. 3, 4 and 5**). Accordingly, the myoepithelial state of cells from cluster MO4 were further

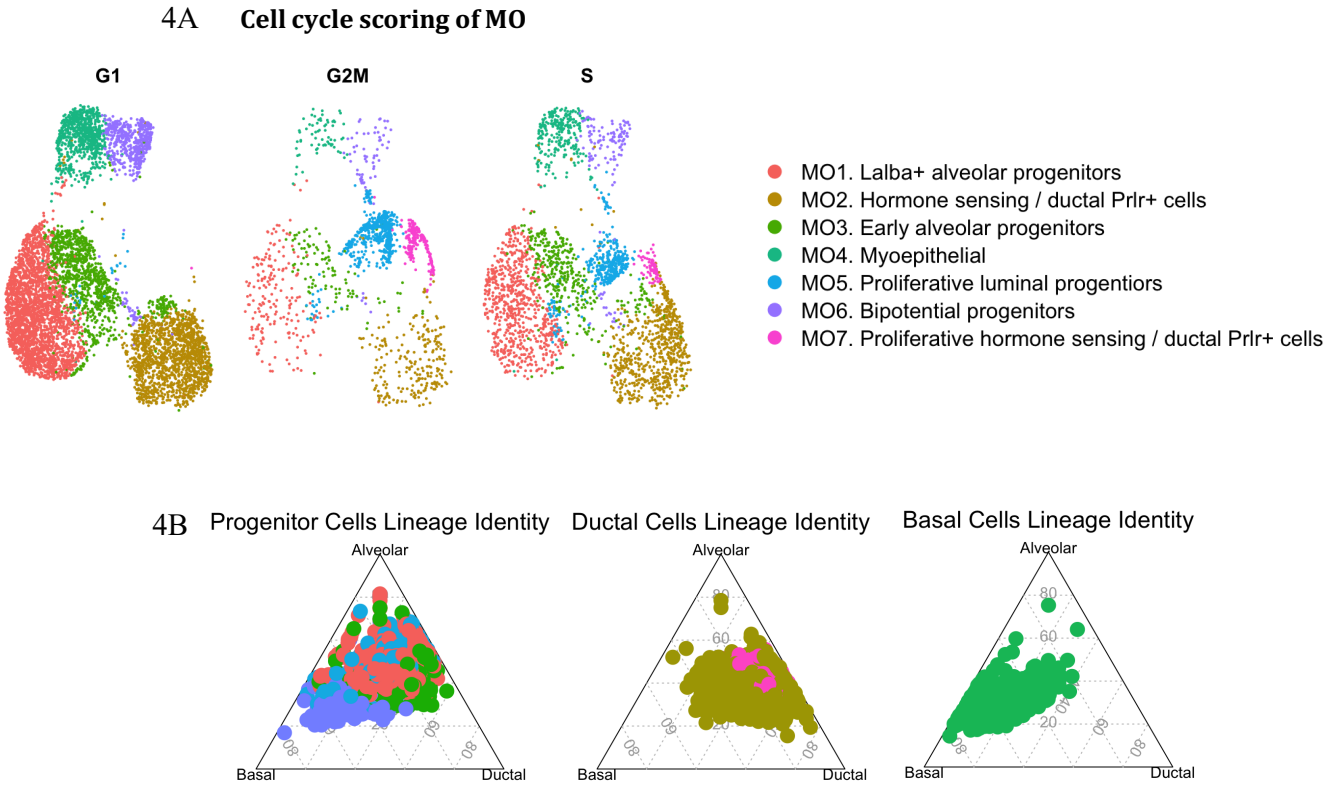

Figure 4. Approaches for MO clusters characterization.

(A) Cell cycle scoring of MO clusters.
(B) Ternary plots showing how each MO cluster scores for general lineage markers (Table 3). MO clusters are organized based on their dendrogram relationships.

supported by the enrichment of genes associated with myogenesis and EMT-like processes (Ingthorsson et al., 2015). Cells from alveolar progenitor-like cluster MO1 were significantly enriched for terms involved in hypoxia. However, when looking at the list of hypoxic genes detected in our dataset, we found that most of these were involved in milk-synthesis, such as *Lalba* and *Aldoc*, supporting an alveolar classification (**Table S2**) (Bach et al., 2017; Rudolph et al., 2007; Saeki et al., 2021). Bipotential cells in MO6 were enriched for terms similar to myoepithelial cluster MO4, as well as expressing genes involved in p53 signaling and coagulation. Adequate p53 signaling has been implicated in mammary tissue homeostasis during development (Dusek et al., 2012). Moreover, genes involved in coagulation were also implicated in EMT processes, such as Fibronectin 1 (*Fbn1*) and Kallikrein-related peptidase 8 (*Klk8*) (**Table S3**) (Bahcecioglu et al., 2021; Hua et al., 2021). Interestingly, cells from cluster MO3, classified as early alveolar progenitors did not show enrichment for specific terms in relation to all other cell types, thus suggesting an organoid cellular state that shares transcriptional signatures with all other cellular clusters. Moreover, GSEA analysis of MO3 for non-significant hallmark terms showed that these cells are downregulated for hypoxic and p53 signaling effectors, which is the opposite to what we observed in MO1 and MO6, potentially indicating a pre-pregnancy phenotype to a sub-population of alveolar cells that could depend on pregnancy hormones to switch into a hypoxic and, subsequently, a senescent state after pregnancy, as it has been previously suggested (**Fig. 5B**) (Feigman et al., 2020; Ginger & Rosen, 2003; Misra et al., 2012).

5A

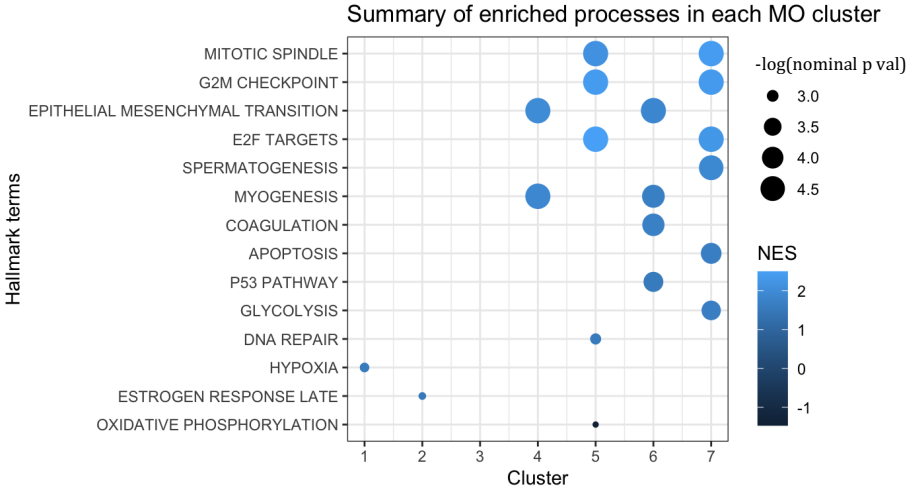

5B

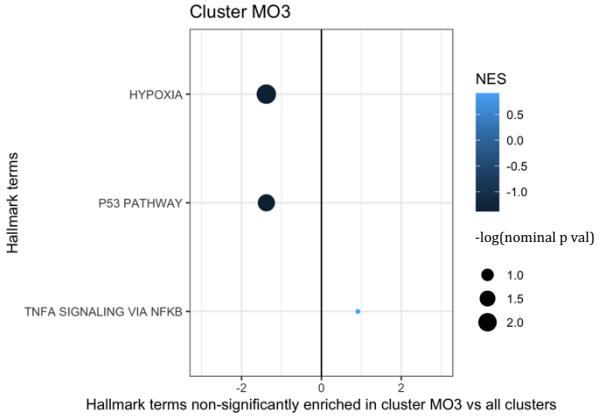

Figure 5. Summary of enriched hallmark terms in each MO cluster.

(A) Hallmark terms for each MO cluster were ordered based on each –log(nom p-val) for each term. Only terms with nom p-val < 0.05 were kept for this analysis. The color of each dot represents the NES value for each term.
(B) Hallmark terms for MO3 cluster were ordered based on each –log(nom p-val) for each term. Given that the gene signatures of MO3 were similar to the rest of the clusters, non-significant terms (p-val < 0.06) are shown. The color of each dot represents the NES value for each term.

2.2.2 Determining similarities between murine mammary organoid cultures and in vivo mammary tissue by single cell RNA sequencing

It is possible that a less defined cellular identity of organoid cells could represent changes induced by *in vitro* culturing that alters molecular signatures that define MECs cell types. In fact, transcriptional and cellular profiles of human breast organoid cultures suggest that overtime, culturing conditions can induce gene expression and lineage marker changes (Bhatia et al., 2022; Gray et al., 2022). Therefore, and in order to define the culture-induced changes to mammary organoid cultures, we integrated previously published scRNA-seq datasets to map epithelial cells from nulliparous mice mammary tissue to our analysis, to define the similarities and differences across *in vivo* and *ex vivo* MECs (Bach et al., 2017; Henry et al., 2021) (**Fig 6**).

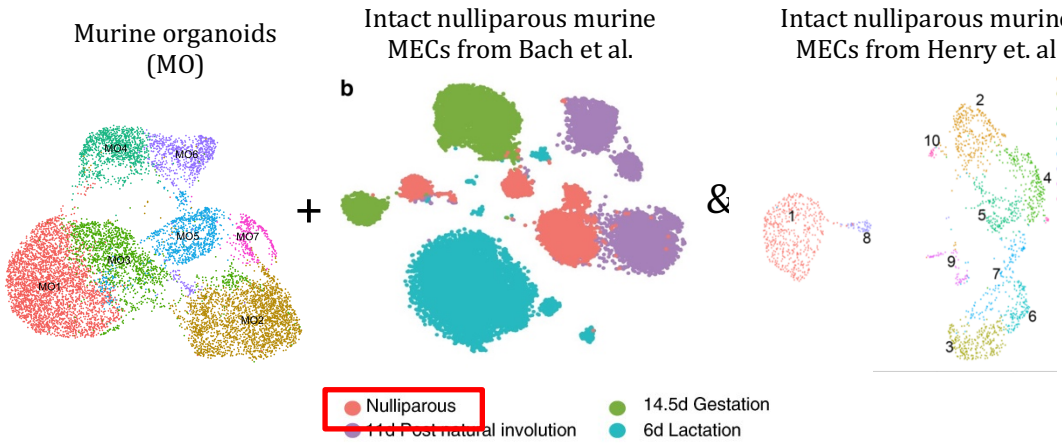

Figure 6. Integration strategy for comparisons with intact MECs.

Our murine organoids data set was integrated with mammary samples from nulliparous mice from Bach et al. (n=2) and Henry et al. (n=1). This approach was used in order to match the number of cells in the MO data set.

This analysis yielded several epithelial clusters, including those of luminal fate (OIM1, OIM2, OIM3, OIM5 and OIM6) or myoepithelial lineage (OIM4) (**Fig. 7A-B**). Overall, the majority of clusters defined on organoid cultures were also represented in intact mammary tissue, with the exception of cluster OIM6, which was markedly expanded in libraries prepared from organoid conditions (**Fig. 7C**).

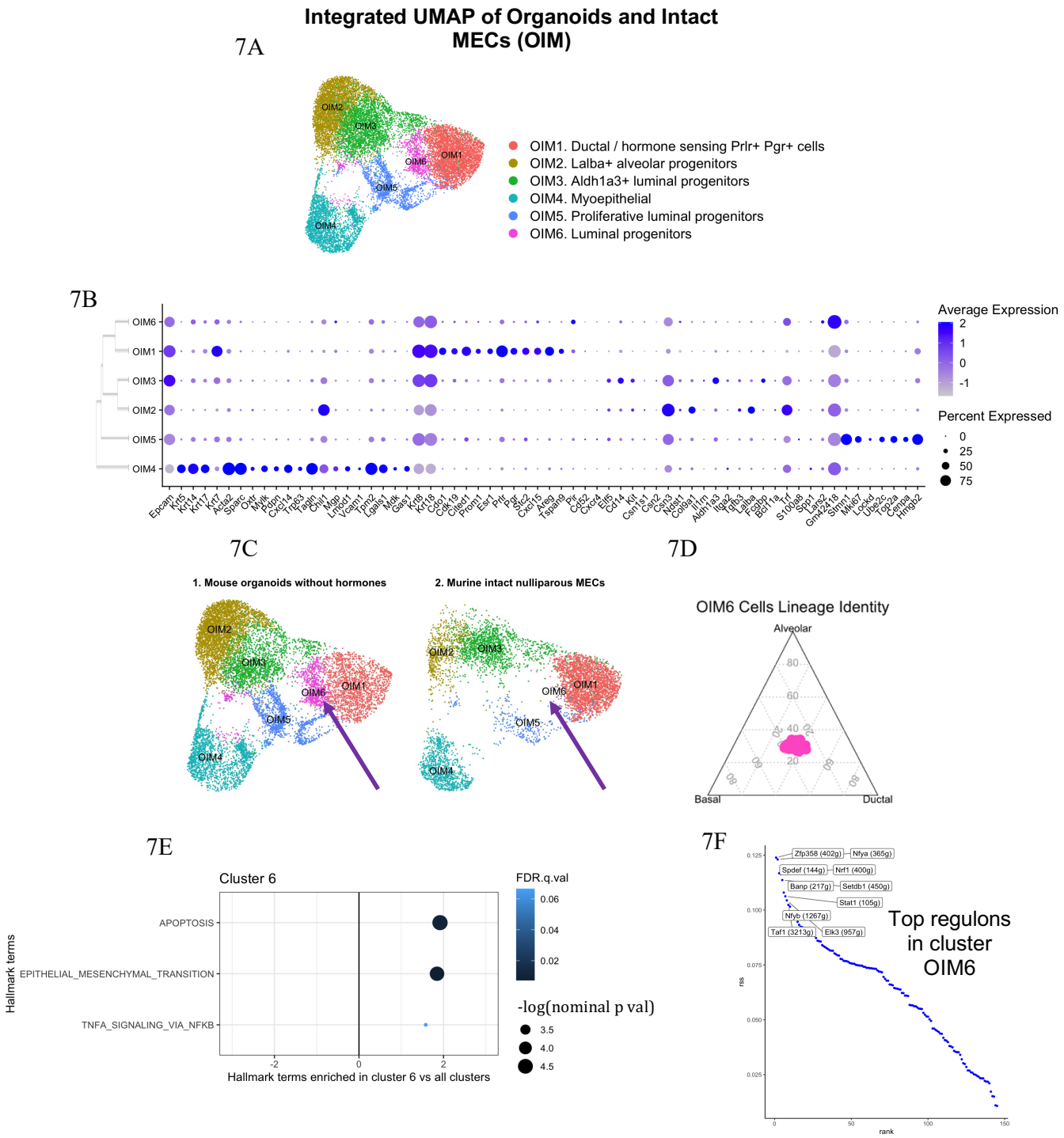

Figure 7. Integrated analysis of organoids and intact MECs (OIM) scRNA-seq data sets.

(A) Resulting clusters for the integration of murine organoids and intact MECs (OIM), and their assigned identities according to gene expression from previously described MEC markers.
(B) Dotplot for MEC marker expression from OIM clusters. OIM clusters are organized based on dendrogram relationships.
(C) OIM clusters split by condition (cells originating from organoids or from intact tissue). The purple arrow is highlighting OIM6, a cluster of luminal progenitors that appears to be enriched in organoid cultures.
(D) Ternary plot showing how OIM6 scores for general lineage markers (Table 3).
(E) GSEA for hallmark terms enriched in cluster OIM6. Hallmark terms are ordered based on the –log of nominal p-values for each term. Only terms with a nominal p-value (nom p-val) < 0.05 were kept for this analysis, in order to only show significantly enriched terms. The dots are colored based on their false discovery rate (FDR q-value), and the x-axis represents normalized enrichment scores (NES).
(F) Top 10 regulons with the highest regulon specificity scores (RSS) for cluster OIM6 vs all other clusters.

Interestingly, global expression hierarchical relationship across all clusters (dendrogram),

indicated a closer relationship between cluster OIM1 (ductal/hormone sensing cells) and OIM6, which lacks the expression signature of hormone-responsive cells (**Fig. 7B**). Conversely, OIM6 expressed elevate levels of alveolar-like cellular states such as *Csn3*, *Trf*, and *Gm42418*, in comparison to cells from OIM1 cluster, suggesting an expression signature of a not fully defined luminal state (**Fig. 7B**). In fact, our analysis indicated that OIM6 cells are positioned in an intermediary state, right in between luminal ductal/hormone sensing cluster (OIM1), and luminal alveolar-like clusters (*Lalba*+ OIM2, and *Aldh1a3*+ OIM3), further suggesting a luminal progenitor state (**Fig. 7D**). GSEA for hallmark terms revealed that organoid-exclusive cluster OIM6 was significantly enriched for terms involving apoptosis and EMT, both terms associated with undifferentiated process in mammary epithelial cells, further suggesting the presence of organoid cells with early progenitor phenotypes in culture (**Fig. 7E**) (C.-W. Li et al., 2012).

These observations were supported by the analysis of regulatory networks (regulon core) enriched in cluster OIM6, which indicated expression of signatures regulated by transcription factors such as Nuclear Transcription Factor Y Subunit Alpha (Nfya), Nuclear Respiratory Factor 1 (Nrf1), SET Domain Bifurcated Histone Lysine Methyltransferase 1 (Setdb1), SAM Pointed Domain Containing ETS Transcription Factor (Spdef), Signal Transducer and Activator Of Transcription 1 (Stat1) and ETS Transcription Factor (Elk3), which have all been associated with gene regulation in luminal lineages of the breast (**Fig. 7F**) (Das et al., 2018; Huang & Esteller, 2010; Kim et al., 2018; Raven et al., 2011; Ye et al., 2020; Yoh et al., 2016).

Overall, our initial mapping of molecular and cellular makeup of mammary-derived organoid cultures illustrates aspects of *ex vivo* models that resemble intact mammary tissue, while highlighting those that are induced by several of the stimuli of a culturing system.

3. Characterizing the effects of Estrogen treatment on mammary-derived organoid cultures

3.1 Results

Puberty represents the first key signal post-birth that drives mammary tissue expansion and MEC lineage differentiation, with increased levels of estrogen regulating cell-to-cell signaling, immune modulation, and transcription regulation (C. O. dos Santos et al., 2015; Hanasoge Somasundara et al., 2021; Rusidzé et al., 2021; Tower et al., 2022; Vasquez, 2018). Once developed, physiological levels of estrogen sustain mammary tissue homeostasis, with cyclical cellular dynamics throughout the estrous cycle further influencing MEC differentiation and proliferation (Pal et al., 2017). Yet, the necessity and effects of estrogen supplementation for the growth of mammary organoid cultures has not been fully characterized (Lacouture et al., 2021; Rosenbluth et al., 2020; L. Zhang et al., 2017).

With the purpose of determining the effects of estrogen on gene expression, growth, and cellular heterogeneity, we set out to characterize mammary organoids treated with two concentrations of 17-β-Estradiol (referred hereafter as OE), define the effects of lower levels of estrogen (33.3 ng/mL, low estrogen), and those with higher concentrations of estrogen (66.6 ng/mL high estrogen) (**Fig. 8**). Our analysis identified several clusters in all conditions, spanning myoepithelial fates (OE4), luminal ductal/hormone sensing states (OE6 and OE8), luminal alveolar/secretory subtypes (OE1, OE2, OE8), general progenitor-like luminal cells (OE3), and cells expressing both luminal and basal cells lineage markers, referred hereafter as bipotent/mixed lineages subtypes (OE7) (**Fig. 8A-B**). We also identified

cellular clusters marked by the expression of proliferation markers, encompassing ductal/hormone sensing (OE9), and alveolar/secretory (OE5) luminal states (**Fig. 8C**).

Further analysis of cell population distribution across organoid conditions, indicated a few cellular clusters biased to specific datasets (**Fig. 9A-B**).This analysis indicated a subtle decrease on the abundance of general luminal progenitor subtypes (cluster OE3) in organoid conditions supplemented

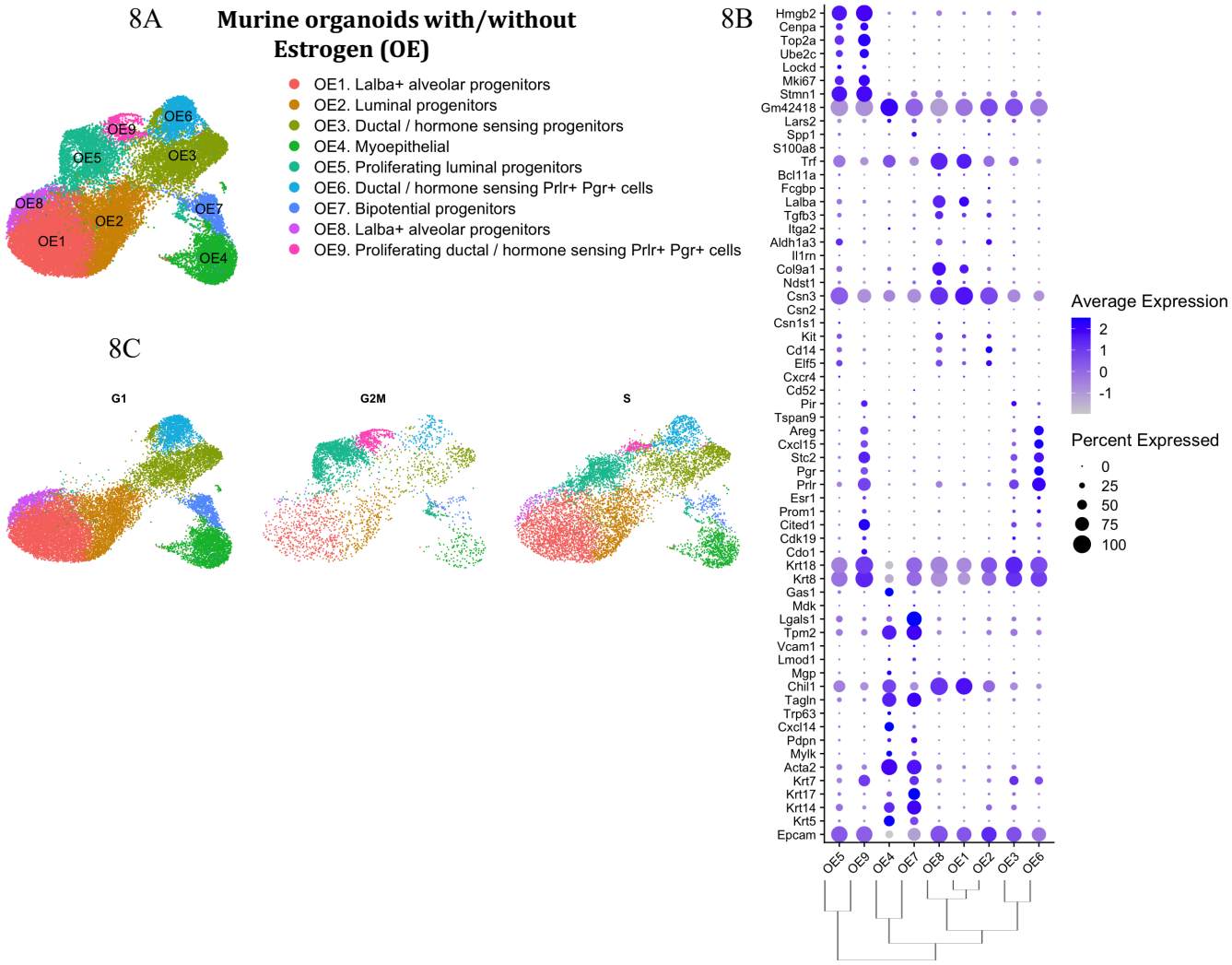

Figure 8. Single cell RNA-seq analysis of murine organoids treated with Estrogen (OE) and approaches for cluster characterization

(A) Resulting clusters for murine organoids with and without Estrogen (OE), with cluster identities based on intact MEC marker expression.
(B) Dotplot for OE clusters expression of intact MEC gene markers. OE clusters are organized based on dendrogram relationships.
(C) Cell cycle scoring or OE clusters.

with estrogen, perhaps suggesting that luminal progenitor differentiation in response to increased levels of estrogen can also be observed in organoid cultures (Basak et al., 2015) (**Fig. 9A-B**). Depletion of

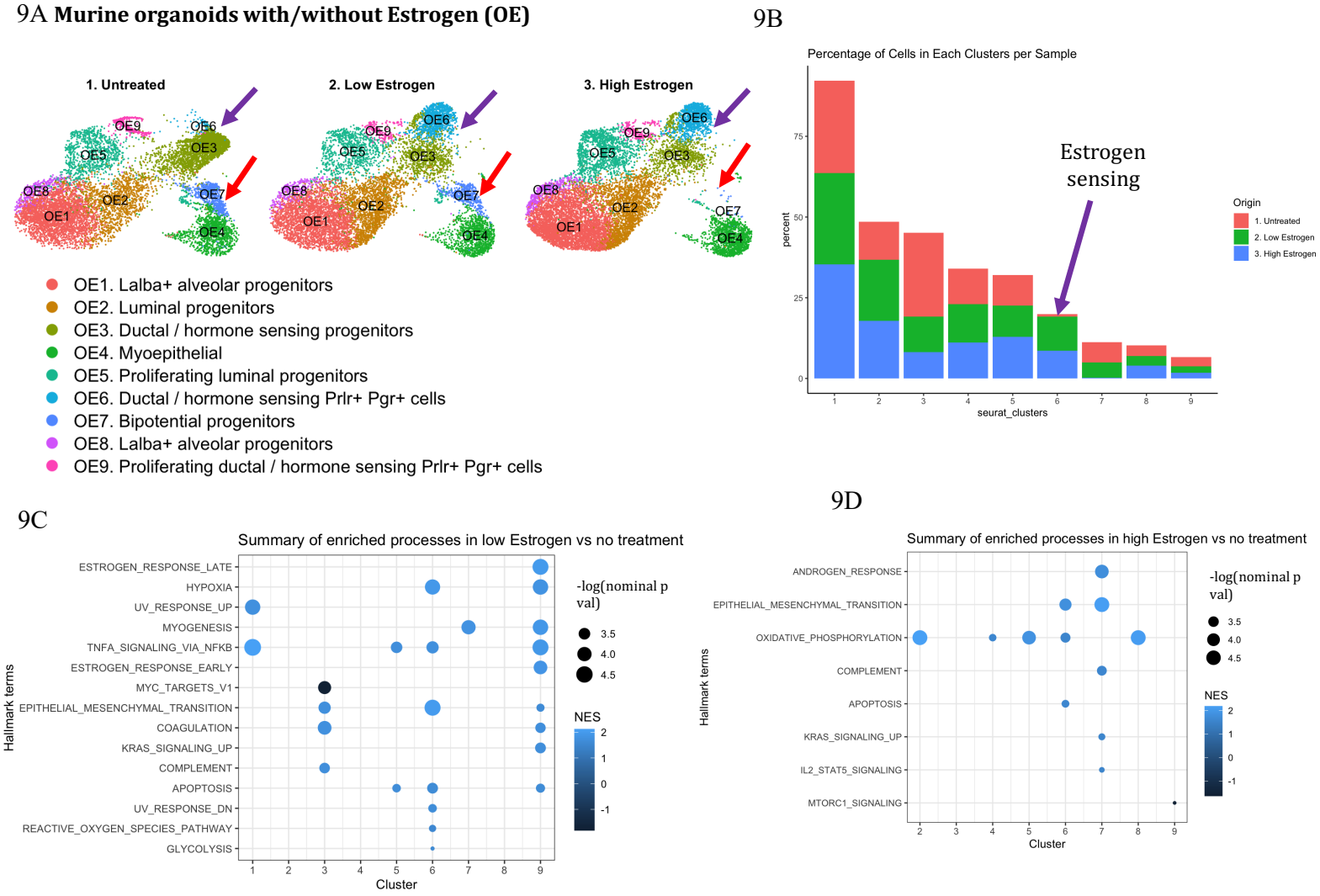

bipotent/mixed lineage cells (cluster OE7) was also observed in organoid cultures treated with estrogen,

Figure 9. Transcriptomic differences between organoids with no treatment and organoids with Estrogen treatments (OE).

(A) OE clusters split by condition, highlighting Estrogen-specific cluster OE6 (purple arrow) and OE7 (red arrow), which is depleted only at a high Estrogen dose.
(B) Bar plot showing percentage of cells per condition in each cellular cluster. The purple arrow highlights OE6, an Estrogen-exclusive cellular cluster.
(C) GSEA for hallmark terms differentially enriched in low Estrogen compared to no treatment. Terms were ordered decreasingly based on their–log(nom p-value). Only terms with nom p-val <0.05 were kept for these analyses. The color of each dot represents the NES for each term.
(D) GSEA for hallmark terms differentially enriched in high Estrogen compared to no treatment.

supporting the suggestion that estrogen supplementation may be inducing the differentiation of more immature cell types, as it is observed *in vivo* (Simões & Vivanco, 2011). Interestingly, none of these cell types express hormone genes, thus suggesting a possible indirect effect of estrogen on their homeostasis/differentiation (**Fig. 8B and 9A**) (Sleeman et al., 2006). We also identified alterations to cluster of ductal/hormone responsive cells (OE6), thus validating that expression of hormone responsive genes in subtypes of organoid cells are linked with cellular expansion in response to increased estrogen levels (**Fig. 8B and 9A**) (Feng et al., 2007).

Given that our observations above indicated that estrogen supplementation of organoid cultures can influence cellular populations independently of the expression of hormone-associated genes, we next decided to investigate global gene expression alterations across all organoid clusters. For this, we opted to focus on gene expression alterations across untreated organoids and those treated with low levels of estrogen, given that all identified clusters are represented in both conditions (**Fig. 9C**). Our analysis identified that clusters defined to have a duct/hormone sensing identity where the ones with the most alterations to enriched pathways in response to estrogen treatment, with proliferative duct/hormone sensing cells (OE9) demonstrating selective enrichment for processes associated with Estrogen response (early and late) and K-ras signaling, a pathway previously associated with estrogen receptor signaling (Dischinger et al., 2018) (**Fig. 9C**). Conversely, the population of hormone sensing cells expanded in response to estrogen levels (OE6) was selectively enriched for pathways associated with reactive oxygen response and genes that downregulate UV responses, both potential antioxidant pathways also described to be regulated by estrogen (Caldon, 2014; Halliday, 2010), in marked contrast to subtypes of secretory-like cells (OE1), which increased expression of UV responses was linked with estrogen treatment. Both OE6 and OE9 clusters were also enriched for pathways related to hypoxia, thus suggesting the diverse gene regulation modules regulated by estrogen on hormone sensing cells (**Fig. 9C**).

In addition to pathways that were shared with cell types defined as hormone responsive, estrogen treatment of organoids induced enrichment to specific pathways in a hormone expression independent manner. For example, enrichment for TNF-α signaling via NF-κB pathways was observed in both secretory luminal cells (OE1, OE5) and hormone sensing cells (OE6, OE9), a pathway linked with increased mitogenic activity in response to Estrogen, which here we show to be associated with highly proliferative clusters in general (OE5 and OE9) (**Fig. 9C**) (Rubio et al., 2006). In addition, cluster of bipotent/mixed lineage cells (cluster OE7) and those of proliferating hormone sensing cells (OE9) were exclusively enriched with genes associated with myogenesis, a process that can either be suppressed or activated by estrogen levels on cellular contact dependent fashion, thus suggesting a deeper level of estrogen related signals, that can be recapitulated in *ex vivo* organoid cultures (**Fig. 9C**)

(Mallepell et al., 2006; Ogawa et al., 2011; Strum, 1978). Another controversial signal pathway regulated by estrogen, EMT, was also observed on luminal fate clusters mostly affected by estrogen supplementation, including general luminal progenitor subtypes (cluster OE3), ductal/hormone responsive cells (OE6), and proliferative duct/hormone sensing cells (OE9), an observation that may link EMT with loss of cell plasticity, and estrogen-induced differentiation (**Fig. 9C**) (Guttilla et al., 2012; Wahl & Spike, 2017). In fact, the only statistical significantly enriched pathway downregulated by estrogen was associated with cMYC regulated processes in general luminal progenitor subtypes (cluster OE3), a signal that is essential to keep immature properties of mammary epithelial cells (**Fig. 9C**) (Poli et al., 2018). Yet, and despite of the findings above described, low levels of estrogen did not result on the significant enrichment of pathways in clusters of cells with myoepithelial fate (OE4), or Lalba+ secretory cell types, suggesting that subtypes of MECs that lack the expression of hormone genes are less affected by female hormones.

To assess how the regulatory networks modulating processes in each cellular sub-type might be affected by Estrogen, we calculated the regulons with the highest specificity scores (RSS) for each of the OE clusters and segregated them by condition (i.e. no treatment, low Estrogen treatment and High Estrogen treatment) (**Fig. 10**). We found that hormone sensing clusters OE3, OE6 and OE9 were modulated by similar regulons which were not significantly active in other cellular clusters. These regulons included ER-modulated programs, such as those controlled by effector of Estrogen/ER signaling TF MYB proto-oncogene (Myb) (Drabsch et al., 2007), GATA binding protein 3 (Gata3), which is known to participate in a cross-regulatory loop with ERα (Eeckhoute et al., 2007), the protein product of Krüppel-like factor 4 (Klf4), which is stabilized by ER to promote cellular growth (Hu et al., 2012), and TF ETS proto-oncogene 2 (Ets2), which has been shown to recruit Nuclear Receptor Coactivators to estrogen responsive genes (Kalet et al., 2013).

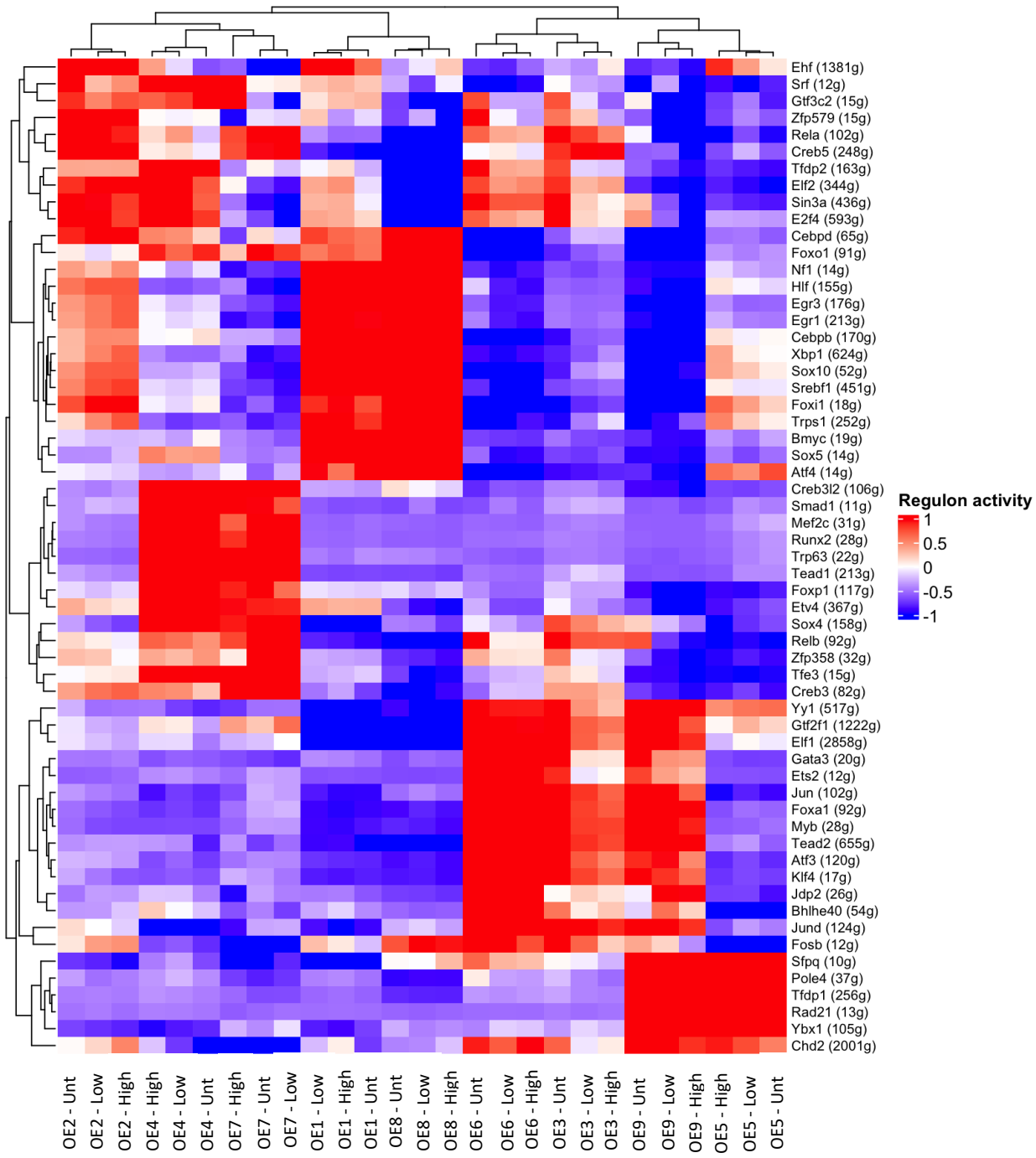

Figure 10. Regulons governing each OE cellular state.

The scaled activities of regulons with the highest specificity score (RSS) for cells in each OE cluster and condition (Low for 20ng/mL of Estrogen, High for 40ng/mL of Estrogen, and Unt for no treatment) are shown. Red indicates that the regulons are significantly active in the corresponding clusters and conditions, while blue indicates inactivity. Cells in OE clusters from each condition are organized based on dendrogram relations, and therefore based on their regulatory network similarities.

Since Estrogen has been noted to participate in a negative feedback loop with its own receptor (Hatsumi & Yamamuro, 2006), the activities of the aforementioned regulons appeared to decrease with incremental doses of Estrogen specifically in clusters OE3 and OE9. Estrogen-exclusive Seurat cluster OE6 virtually maintained high activity levels for the aforementioned ER-associated regulons, regardless

of Estrogen presence. Nonetheless, we found Estrogen-modulated regulons that had OE6-specific tendencies in OE6. One such regulon involved v-rel avian reticuloendotheliosis viral oncogene homolog B (Relb), which is known to downregulate ERα in the mammary gland (X. Wang et al., 2009).

We found that, in OE6 cells, RelB decreased in activity with Estrogen treatment. Another regulon displaying a decrease in activity with Estrogen treatment in OE6 involved Splicing factor proline/glutamine-rich (Sfpq). Interestingly, Sfpq has been noted to be downregulated in the mammary gland of parous rats treated with Estrogen, suggesting a complex interplay between this regulon and Estrogen signaling in modulating hormone sensing cells (de Assis et al., 2013). Other regulons that displayed a decrease in activity in all hormone sensing cells (OE3, OE6 and OE9) involved Zfp579, which has not previously been studied in the context of mammary development or hormone response, underscoring the need for further investigation into its potential roles in hormone sensing mammary cells.

In OE7 bipotential progenitors we also observed regulons with patterned responses to Estrogen, although with an opposite tendency to hormone sensing clusters. Two of these regulons involved Gtf3c2 and Zfp729b, which are decreased with Estrogen in OE6 but exclusively active in OE7 cells treated with high Estrogen. Gtf3c2 in particular has been characterized in ductal carcinomas but, similar to Zfp729b, its role in Estrogen signaling and normal development is still largely unknown (J. Zhang et al., 2022). A regulon that displayed a specific tendency for OE7 cells involved FOXO gene is Forkhead box O (Foxo1), which had decreased activity levels in high Estrogen. Foxo1 in particular has been shown to be anti-proliferative and to cooperate with tamoxifen to repress ER+ breast cancers (Vaziri-Gohar et al., 2017). These findings indicate, once more, that further investigation is needed to fully understand the roles of these regulons in modulating bipotential progenitor processes in response to Estrogen signaling.

4. Pregnancy hormones exposure, cellular states, and gene expression

4.1 Results

4.1.1 Single cell characterization of cellular and molecular changes induced by pregnancy hormones

Mammary organoid systems have been previously optimized to mimic aspects of pregnancy-induced development of the gland, such as branching and production of milk-associated proteins, involution-like processes, and mechano-regulated actions of lactation (Ciccone et al., 2020; Stewart et al., 2021; Sumbal et al., 2020). Yet, it is unclear whether mimicking pregnancy-induced changes *ex vivo* drives cellular and transcription alterations such as those that take place *in vivo*. Therefore, we set out to characterize mammary organoid cultures, grown with a combination of Estrogen, Progesterone, and Prolactin hormones (referred hereafter as OP) using scRNA-seq approaches. Our analysis identified clusters present in both conditions, representing cellular states of luminal secretory fate (OP1, OP3, and OP6), and myoepithelial lineage (OP5) (**Fig. 11**). We also observed that populations of duct/hormone sensing and bipotential/mixed lineage identities had a condition biased distribution, with cluster OP4, OP9 (hormone sensing), and OP7 (mixed lineage) been more abundant in untreated organoid samples, while clusters OP2, OP8 (hormone sensing), and OP10 (mixed lineage) defining samples grown with pregnancy hormones (**Fig. 11C-D**). Amongst these clusters, we identified highly proliferative cells in both conditions (OP6), and as well those biased towards untreated conditions (OP9), and hormone treated organoids (OP8) (**Fig. 11B-C**).

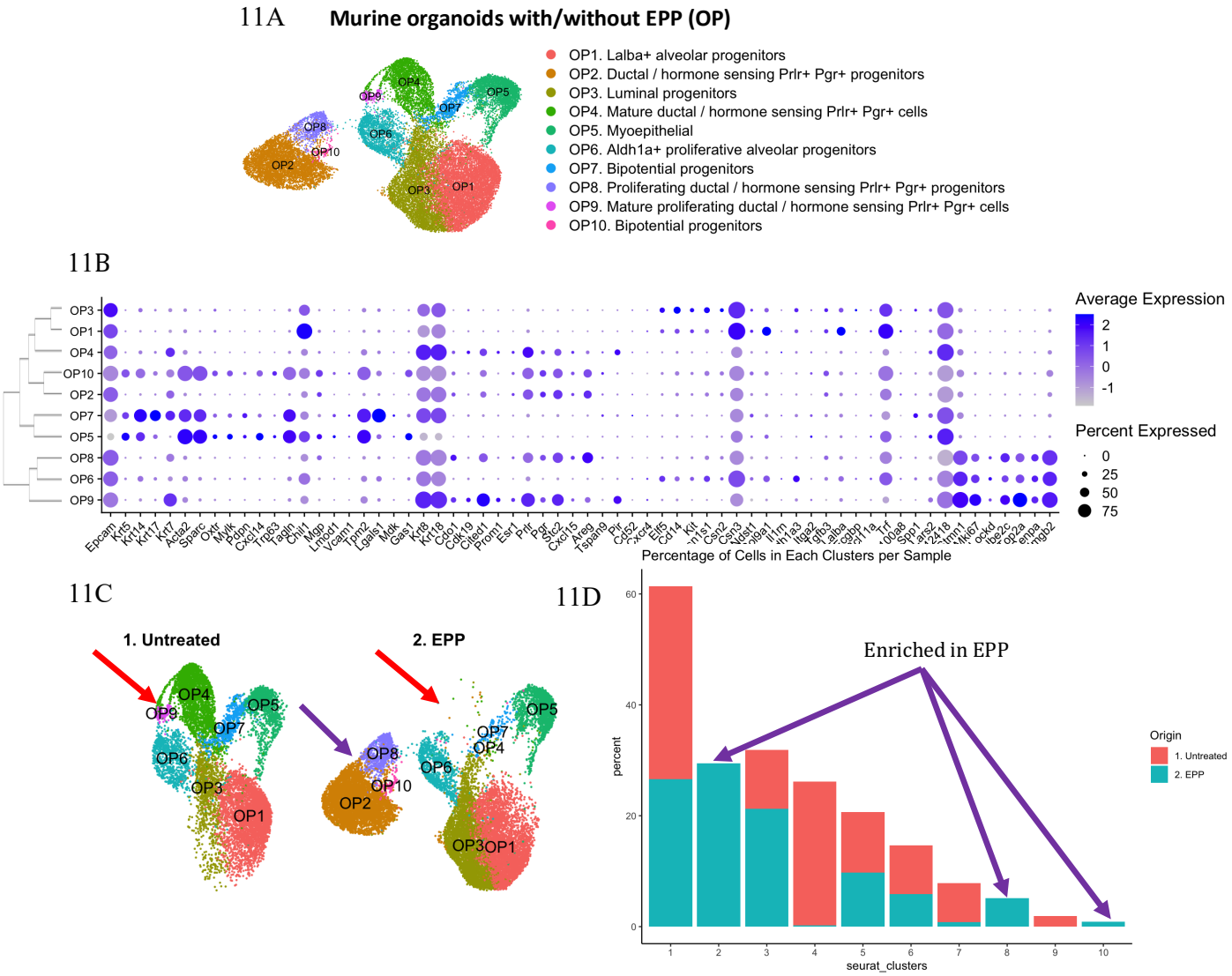

Figure 11. Single cell RNA-seq analysis of murine organoids treated with pregnancy hormones (OP) and cluster classifications.

(A) Resulting clusters for organoids with/without EPP treatment (OP), and their given identities according to gene expression from previously described MEC markers.
(B) Dotplot showing MEC markers average gene expression in each OP cluster.
(C) OP clusters split by treatment condition (no treatment or EPP treatment). The purple arrow highlights EPP-enriched cellular clusters OP2, OP8 and OP10. The red arrow highlights cellular clusters depleted with EPP treatment, clusters OP4, OP7 and OP9.
(D) Bar plot showing percentage of cells per condition in each OP cluster. The purple arrows highlight clusters enriched in EPP samples.

We next defined the pathways differentially expressed in each of the identified cellular clusters in response to pregnancy hormone treatment. Across the cellular clusters that were present in both untreated and pregnancy hormone treated conditions, which encompassed hormone negative cell types (OP1, OP3, OP5, and OP6), we found clusters with no statistically significant enrichment for specific

terms (OP1, and OP3, luminal secretory identity), indicating cellular stages that were minimally affected by the supplemented amounts of pregnancy hormone (**Fig. 12A**). Conversely, clusters identified as myoepithelial lineage (OP5) and proliferating luminal cells (OP6) were enriched for term that were related to their lineage specific developmental state (such as myogenesis and EMT for OP5) (Mallepell et al., 2006; Ogawa et al., 2011; Strum, 1978), or cellular state (mitotic spindle and G2M checkpoint for OP6), suggesting that similarly like estrogen alone, pregnancy hormones can induce indirect transcription changes in hormone negative cells (**Fig. 12A**).

12A

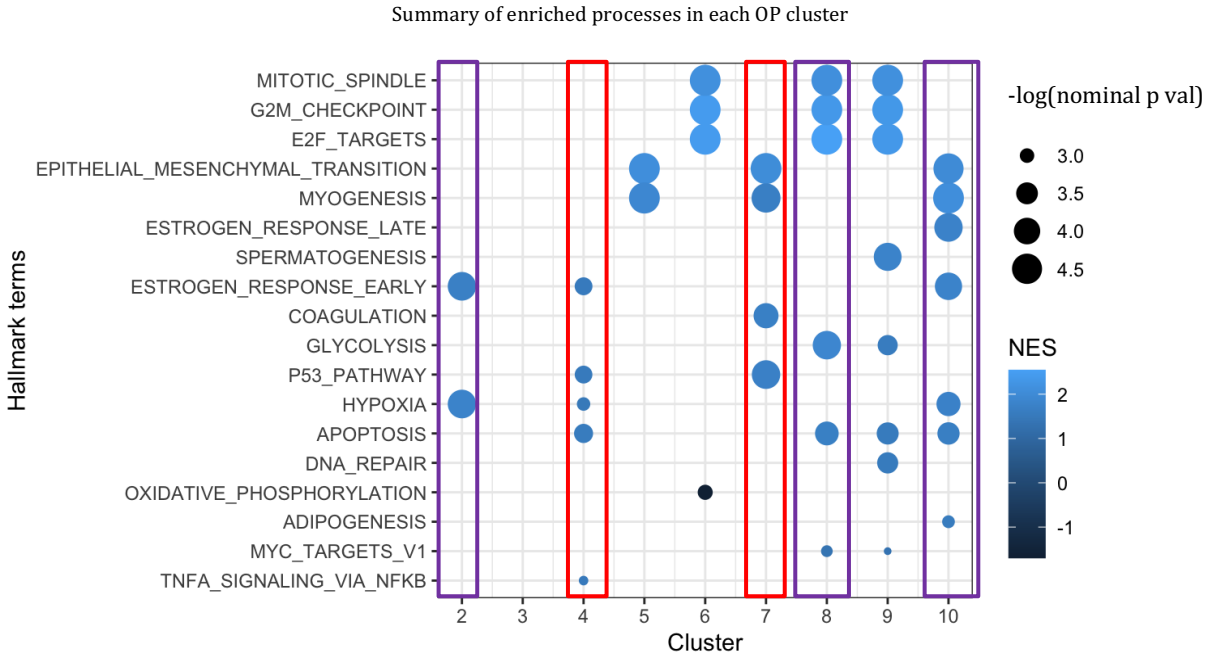

12B

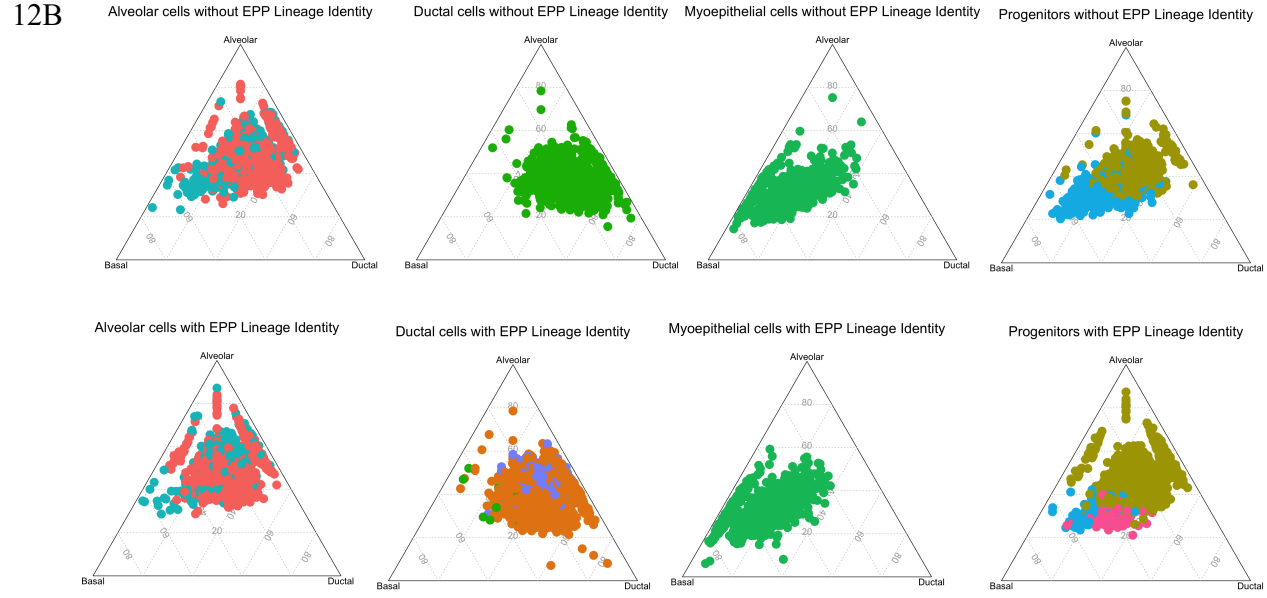

Figure 12. Approaches to characterize pregnancy-induced changes in OP clusters.

(A) GSEA for hallmark terms enriched in each OP cluster. Terms are ordered from highest –log(nom p-value). Only hallmark terms with a normalized p-val < 0.05 were kept for this analysis. The color of each dot represents the NES for each term. The red boxes mark clusters depleted with EPP treatment, and the purple boxes mark clusters enriched with EPP.

(B) Ternary plots showing how each OP cluster scores for general lineage markers (Table 3). OP clusters are organized based on their dendrogram relationships.

Interestingly, clusters biased towards untreated samples (OP4, OP7, OP9) and those more abundant in pregnancy hormone treated samples (OP2, OP8, OP10), represented very similar cellular identities, with hormone sensing cells (OP4, OP9, OP2, OP8) and bipotential/mixed lineage fate (OP7, OP10), suggesting that pregnancy hormones act on cellular states fully present in untreated conditions

(**Fig. 12B**). In fact, hormone sensing clusters OP4 (untreated condition), and OP2 (pregnancy hormone condition) where enrichment for similar pathways such as estrogen response and hypoxia, with the exception of untreated cluster OP4, that was also enriched for pathways regulated by p53 (**Fig. 12A**). Interestingly p53 pathways have been associated with acquisition of a senescent-like state, which can be modulated by pregnancy hormones (Feigman et al., 2020). Additional hormone sensing clusters OP9 (untreated condition) and OP8 (pregnancy hormone condition) were enriched with terms associated with cell division function, thus validating our initial classification of these clusters as proliferative (**Fig. 12A**).

Moreover, pathways associated with myogenesis and EMT were both enriched in bipotential/mixed clusters OP7 (untreated condition) and OP10 (pregnancy hormone condition), with the specific enrichment of p53 pathways in cells from untreated conditions, supporting the suggestion that pregnancy hormones may suppress similar pathway in different cellular states. The hormone expression on cells from OP10 cluster was linked with the enrichment of estrogen response and hypoxia, a pathway also associated with pregnancy signals, thus suggesting that hormone regulated pathways are also synchronized in more immature cell types (**Fig. 12A**) (Y. Shao & Zhao, 2014).

To more specifically understand the effects of pregnancy hormone treatment on organoids, we further analyzed the enrichment for regulons on clusters biased to such conditions, focusing on hormone sensing state (OP2), and bipotential/mixed lineage identities (OP10) (**Fig. 13**). Our analysis found that both clusters, despite their different fate identity, were enriched for regulatory networks controlled by Myb, Tfcp2l1, and Stat5, all transcription factors that have been reported to modulate gene expression in MECs in response to pregnancy (**Fig. 13**) (Liu et al., 1997; Otto et al., 2013; Quintana et al., 2011). We also found regulons with high specificity biased towards one cluster, with hormone sensing cells (OP2) showing enrichment for transcriptional programs regulated by Pgr and Klf6, both previously described to be downstream programs operated by estrogen (**Fig. 13**) (Arendt & Kuperwasser, 2015; Cicatiello et al., 2010). Moreover, bipotential/mixed lineage cells (OP10) were marked by networks

regulated Mef2c and Trp63, both implicated on stem-cell like activity of MECs and pregnancy-induced development of the gland (**Fig. 13**) (Lim et al., 2010; Pellacani et al., 2019).

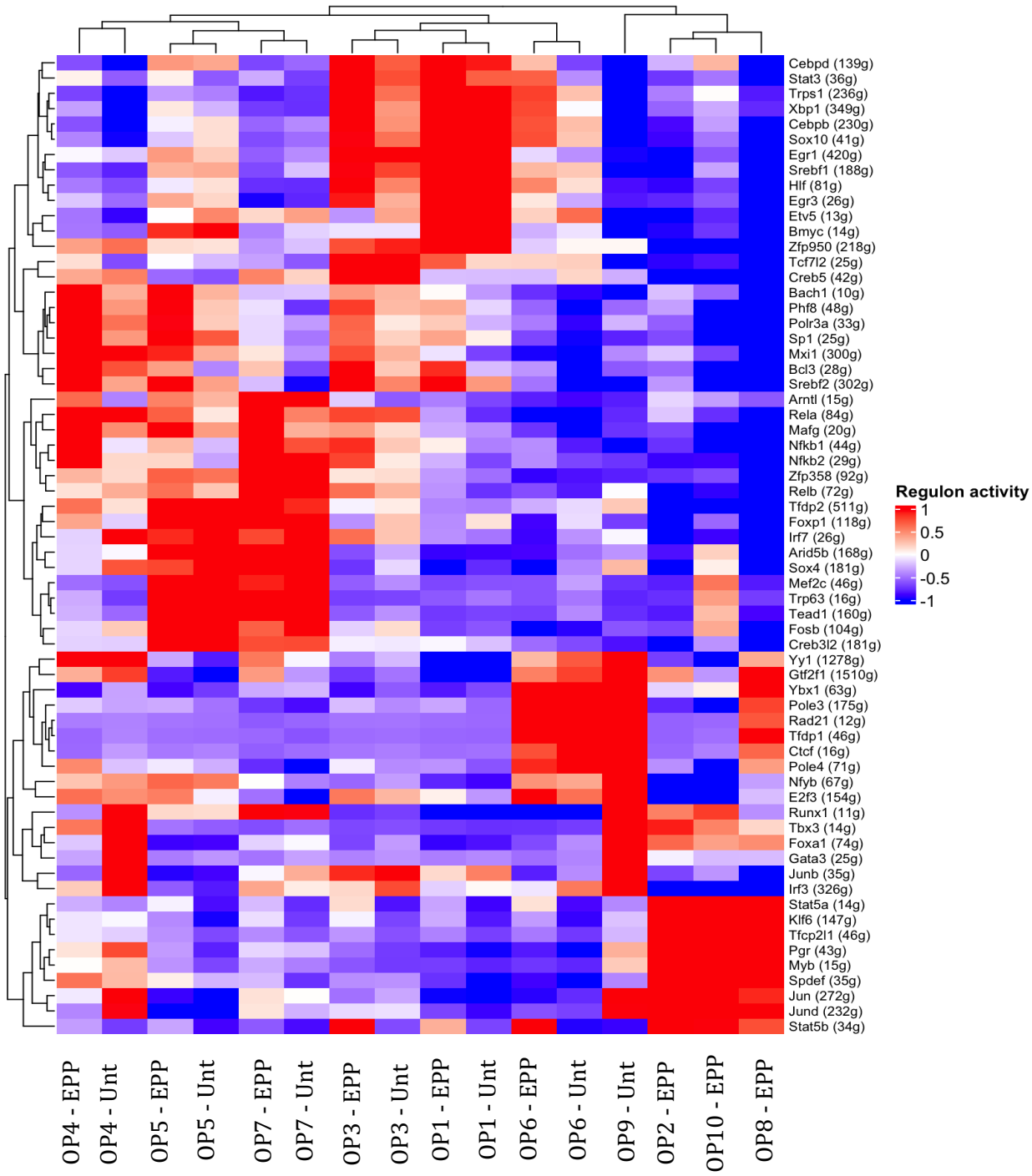

Figure 13. Regulons governing each OP cellular state.

The scaled activities of regulons with the highest specificity score (RSS) for cells in each OP cluster and condition (EPP vs no treatment, or "Unt" for "untreated") are shown. Red indicates that the regulons are significantly active in the corresponding clusters and conditions, while blue indicates inactivity. Cells in OP clusters from each condition are organized based on dendrogram relations, and therefore based on their regulatory network similarities.

4.1.2 Comparisons with an intact pregnancy cycle

As demonstrated, our differential gene expression analysis and regulon enrichment identified many pathways that are activated both in pregnancy hormone treated organoid cultures and in mammary tissue from pregnant female mice (**Fig. 12A and 13**). Our initial analysis indicated that untreated organoids bear similar cell types and transcriptional output than MECs directly extracted from mammary tissue (**Fig. 7**). Therefore, in order to assess whether clusters identified in our culturing system were also represented during pregnancy in mice, we performed a scRNAseq data integration between organoid datasets, and publicly available scRNA profiles generated from mammary tissue during distinct stages of pregnancy (gestation, lactation, and involution) (Bach et al., 2017).

This analysis identified a total of 7 clusters, spanning 5 luminal cell fate clusters, and 2 myoepithelial cell clusters (referred hereafter as OIP), with variated distribution across all datasets (**Fig. 14**). We found several clusters with similar representation in all datasets, including those make up of alveolar/secretory cell types (OIP1), and two populations of myoepithelial cells which demonstrated slightly less abundance in samples from mammary tissue during involution (OIP3), and those with more abundance during lactation (OIP4) (**Fig. 14C**). Cluster OIP6, identified as a population of ductal/hormone sensing cells, was exclusively detected in organoids without treatment, while OIP7 of proliferative ductal/hormone sensing cells was exclusively detected in EPP-treated organoids, potentially indicating a cellular phenotype exclusive to organoids that is modulated by EPP (**Fig. 14C**). Collectively, this analysis also suggests an array of cellular states, not necessarily hormone positive, that are sustained in the mammary tissue across the pregnancy cycle, and present in organoid cultures. For example, clusters OIP1 of alveolar progenitors and OIP3 of myoepithelial cells were sustained

before and throughout pregnancy, and also present in both our organoid conditions, indicating hormone-independent cellular states (**Fig. 14C**).

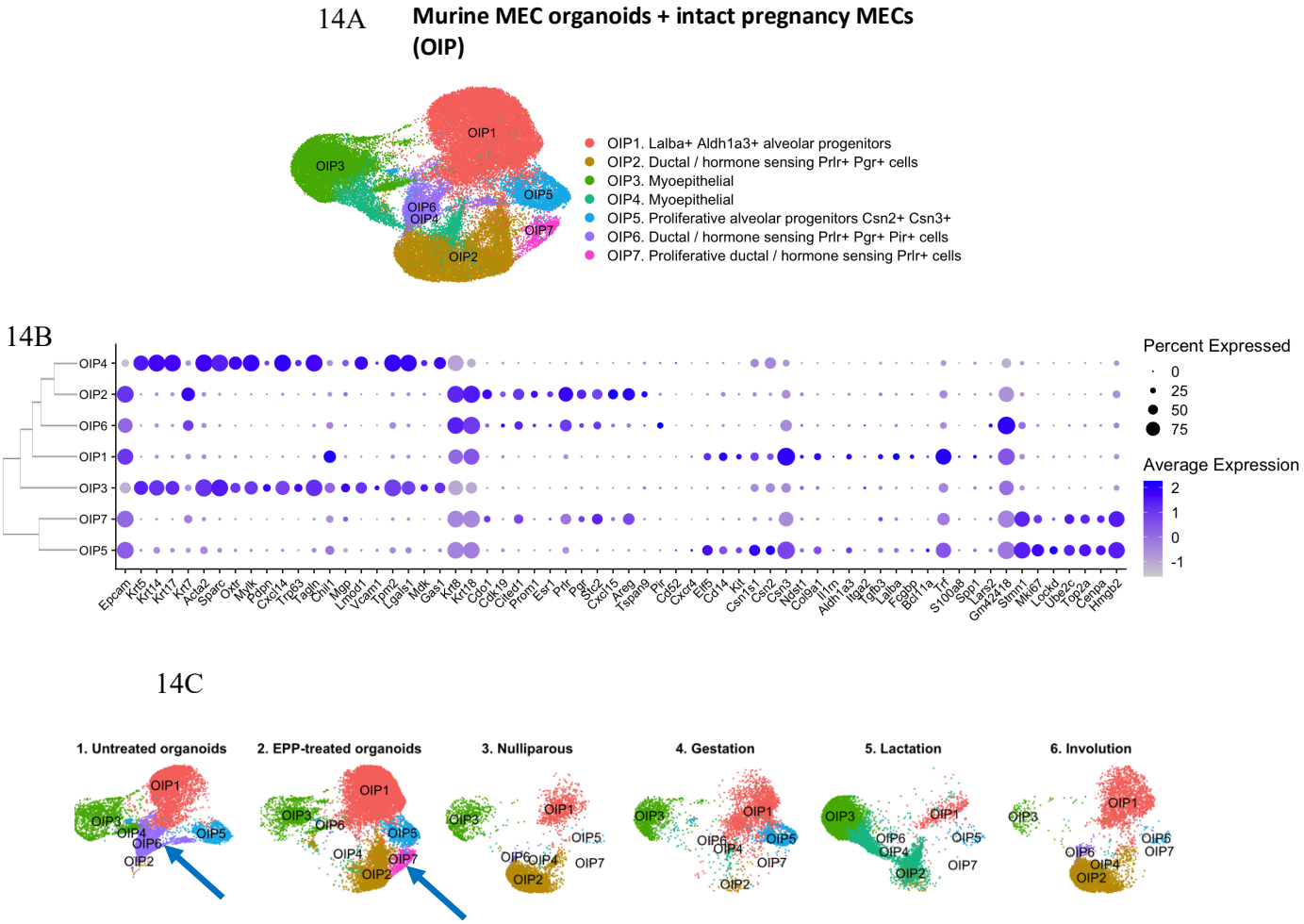

Figure 14. Integration of OP with MECs from an intact pregnancy cycle (OIP).

(A) Resulting clusters for integration of OP data set with intact MECs obtained at different pregnancy stages from Bach et al. (organoids and intact pregnancy - OIP). The identities of each OIP cluster was determined according to their gene expression of previously described MEC markers.
(B) Bar plot showing percentage of cells per condition in each OIP cluster. The blue arrow highlights cluster OIP7, which is enriched in EPP-treated organoids.
(C) OIP clusters split by condition, highlighting cellular states enriched in organoids with and without EPP (blue arrow).

We identified a population of proliferating alveolar luminal cells (cluster OIP5), which were abundant in organoid cultures with and without EPP treatment, and in mammary tissue during gestation, suggesting a general proliferative state that is independent of hormone responsiveness (**Fig. 14C**). Interestingly, our analysis has identified proliferating secretory cell states in untreated organoids (MO4), and as well in those treated with estrogen levels (OE5), and pregnancy hormones (OP6),

suggesting that organoid culturing conditions may in general provide the signals for active proliferation of cell types (**Fig. 3A, 8A, 11A and 14C**). However, specific populations of proliferative hormone sensing cells were detected in response to pregnancy hormone treatment (OIP7), thus suggesting an additional level of cell proliferation activation in response to specific stimuli (**Fig. 14C**).

5. Defining the molecular alterations induced by pregnancy hormones in human MEC-derived organoids

5.1 Results

5.1.1 Single cell characterization of human MEC-derived organoids in response to pregnancy hormones

The current understanding of tissue alterations in response to pregnancy signals is largely biased towards the investigation of molecular and cellular dynamics in rodent models. Our above-mentioned findings suggest that the utilization of organoid cultures represent a suitable system to model, in part, the response of MECs to female and pregnancy hormones. Given that normal, human breast tissue has been utilized for the development of organoid systems (Bhatia et al., 2022; Gray et al., 2022; Rosenbluth et al., 2020; Sachs et al., 2018), we next decided to test their response to supplementation with pregnancy hormones. In doing so, we utilized an already established and characterized normal breast organoid culture, generated from breast specimens from women undergoing cosmetic reduction mammoplasty (Bhatia et al., 2022).

At first, and to define the overall response to pregnancy hormone treatment, we treated organoid cultures with same conditions utilized for the treatment of murine mammary organoids, given that human MECs, injected into the fat pad of mice, following pregnancy, have been show to engage on pregnancy-induced development (Kuperwasser et al., 2004). qPCR analysis indicated increased levels of *CSN2* mRNA, previously described to increase in response to pregnancy hormones (Maningat et al., 2009; Rijnkels et al., 2013), starting on day 10 after pregnancy hormone treatment, a response that was sustained up to 21 days of culturing, thus supporting that such approach promotes pregnancy-associated changes to gene expression (**Fig. 15**). Therefore, we utilized the same conditions for the generation of scRNAseq profiles of untreated and pregnancy-hormone treated human mammary organoids.

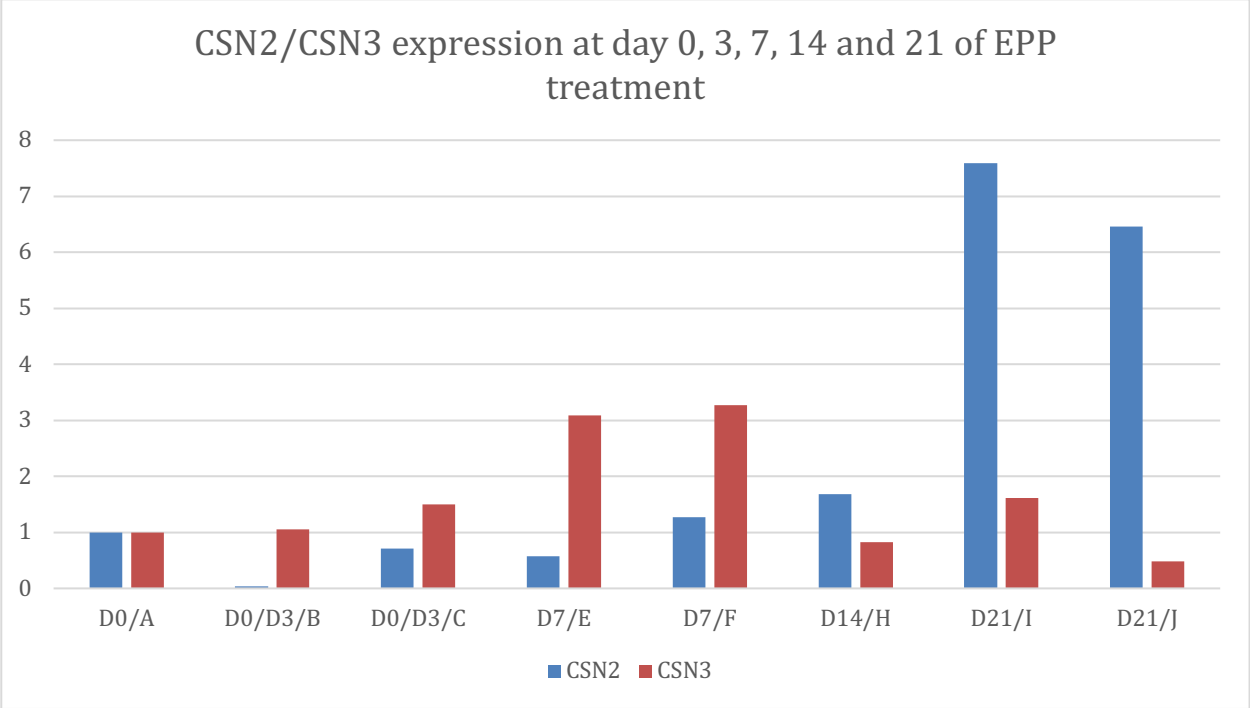

Figure 15. qPCR results for CSN2/CSN3 expression in human MEC-derived organoids treated with EPP for 21 days.

Human MEC-derived organoids were treated with EPP until maximal CSN2 expression, and were collected for CSN3/CSN2 qPCRs at day 0 (D0), day 3 (D3), day 7 (D7), day 14 (D14) and day 21 (D21). Blue represents CSN2 expression and orange represents CSN3 expression.

Characterization of lineage identity, utilizing previously described gene signatures of human MECs (Henry et al., 2021), indicated that the majority of cells from untreated and treated organoid cultures bear both luminal and basal traits, defined by the expression of *KRT8*, *KRT8*, *KRT5* and *KRT14*, suggesting that independently of treatment, established human breast organoid system have a more generalized mix-lineage signature (**Fig. 16B**). This observation is in agreement with previous studies

describing that human breast organoid systems assume a more basal-like cellular phenotype after several culture passages, with consecutive loss of hormone receptor expression, thus suggesting the

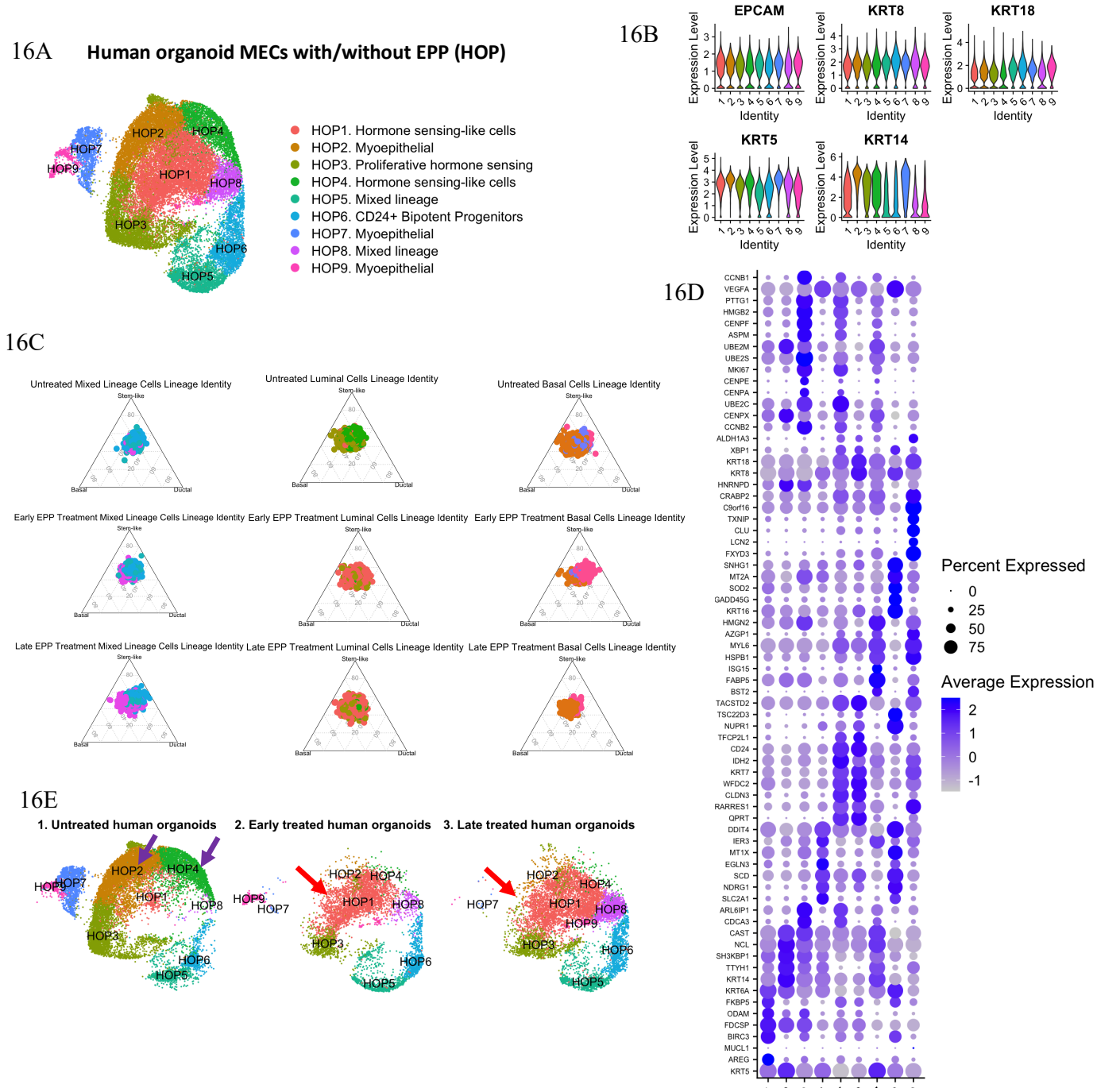

Figure 16. Analysis of scRNA-seq data from human organoid MECs treated with EPP (HOP).

(A) Resulting clusters for human organoid MECs with and without EPP treatment (HOP), along with cluster identities based on expression of previously described markers from intact human MECs and top 10 differentially expressed genes (DEGs) per cluster.
(B) Violin Plots showing the expression of cytokeratins used to classify luminal and basal populations within each HOP cluster.
(C) Ternary plots for broad human MEC lineage marker scores from HOP clusters at each EPP timepoint.
(D) Dotplot for top 10 DEGs per HOP cluster. Clusters are organized based on dendrogram relationships.
(E) HOP clusters split by condition. The purple arrows highlight clusters enriched in organoids without treatment, and red arrows highlight clusters enriched with EPP, independent of the amount of time with EPP treatment.

need of specific signatures to define cellular states of established human breast organoid cultures (Bhatia et al., 2022).

In doing so, we proceeded with cellular identity characterization based on the top differentially expressed genes across all clusters, and their behavior in relation to the culturing with pregnancy hormones (**Fig. 16D**). This approached identified cell types largely represented in all culturing conditions, spanning luminal secretory-like fates defined by the combined expression of pregnancy/lactation associated genes *RARRES1, WFDC2* (clusters HP5 and HP6) (Bhat-Nakshatri et al., 2021; Watt et al., 2012) and proliferating luminal cells characterized by the expression of the pregnancy hormone associated genes *BIRC3, PTTG1* and *CCNB1* (cluster HP3, hormone-sensing like) (LaMarca & Rosen, 2007; Neubauer et al., 2011; Wei et al., 2013) (**Fig. 16D-E**). In addition, we identified clusters with cellular abundance that was suppressed by treatment with pregnancy hormones, including hormone sensing-like cells marked by the expression of pregnancy-associated *NDRG1, SCD, VEGFA, IER3, INSIG1* and *DDIT4* (HP4) (Anderson et al., 2007; Bambhroliya et al., 2018; Deroo et al., 2009; Fan et al., 2020; Meng et al., 2019; Qiu et al., 2008; Sato et al., 2013), myoepithelial cells (HP2), and mixed lineage cell states marked by the expression of pregnancy/lactation genes *ISG15* and *HMGN2* (Schauwecker et al., 2017; Yang et al., 2010), and genes associated with myoepithelial cells contractibility *MYL6* and *FXYD3* (cluster HP7) (**Fig. 16D-E**).

Additionally, one cluster of mixed lineage cells (HP9) was exclusively depleted at 21 days of EPP treatment, which was characterized by expression of myoepithelial contractibility-associated *FXYD3* (Schauwecker et al., 2017), and pregnancy-associated genes *RARRES1* and *LCN2* (Pellacani et al., 2016; Stein et al., 2004) (**Fig. 16D-E**). We also identified two pregnancy hormone-induced cellular clusters of luminal-like lineage, one which bears the expression of progenitor-associated *KRT6A* and *FDCSP* (Holloway et al., 2015; McMullen & Soto, 2022), pregnancy hormone associated *AREG*, *BIRC3, ODAM* and myoepithelial cells contractibility *FKBP5* (Cai et al., 2020; Jaswal et al., 2021; Kang et al., 2014; Yamamoto et al., 2019) (cluster HP1), and one which bears the expression of lactation-associated genes *TSC22D3, NUPR1, NDRG1* and *VEGFA* (Meng et al., 2019; Qiu et al., 2008;

Sornapudi et al., 2018; Zhou et al., 2014), in addition to multipotent-associated *KRT16* (Henry et al., 2021) (cluster HP8) (**Fig. 16D-E**). Cluster HP8 in particular appears to gradually increase in abundance with the time course of EPP treatment. Collectively, this analysis identifies distinct cellular states, based on alterations to gene expression and organoid treatment response, thus illustrating the complex cellular dynamics induced by pregnancy hormones.

To further complement the molecular characterization of untreated and pregnancy hormone treated human breast organoid cultures, we employed a more general gene expression analysis, to indicate potential pathways enriched in each state (**Fig. 17**). We found that pregnancy hormone treatment for 10 days had selective effects across all organoid clusters. For example, while some clusters that remained relatively unchanged across conditions did not show enrichment for particular pathways (HP2, myoepithelial), clusters of hormone-sensing like cells were enriched with pathways associated with hormone response, such as TNF-α signaling via NF-κB pathways, a pathway linked with increased mitogenic activity in response to estrogen (see HP1), and mTOR signaling, which promotes proliferation in response to Estrogen (see HP4) (**Fig. 17B**) (Ketterer et al., 2020; Morrison et al., 2015; Rubio et al., 2006). A similar effect was found in the transcriptional networks of HP3, HP4, HP6, HP7 and HP8 for organoid cultures grown for 21 days with pregnancy hormones (**Fig. 17C-D**). Cells from clusters that virtually shrink with pregnancy (HP7) showed, however, an enrichment of genes associated with Oxidative phosphorylation process at 21 days of EPP treatment, suggesting that in these hormone negative cell types, pregnancy hormones may influence mitochondrial functions (Klinge, 2020) (**Fig. 17D**). These cells also showed an enrichment for genes involved in responses to Interferon gamma, thus collectively suggesting a potential decrease in the proliferative state of such cells than the one observed in untreated and short term treatment conditions (**Fig. 17A-B/D**) (Bracken et al., 2004; Khalkhali-Ellis et al., 2008). Likewise, cluster HP9, which is depleted with EPP treatment at 21 days, showed similar pathway enrichments (**Fig. 17D**). Cells from cluster HP9 were additionally overall enriched with genes associated with p53 pathway, Androgen response, and Apoptosis, known processes regulated by pregnancy hormones (**Fig. 17A**) (Carsol et al., 2002; Dunphy et al., 2008). Interestingly, cluster HP8 of mixed lineage cells that proliferate with pregnancy were also enriched for genes associated with

Oxidative phosphorylation at day 21 of EPP treatment, suggesting a complex interplay between metabolic processes and pregnancy development (**Fig. 17D**). Collectively, these findings suggest a pregnancy hormone modulates molecular signature that accompanies fluctuating cellular dynamics of specific cellular subtypes in response to hormone treatment.

17A

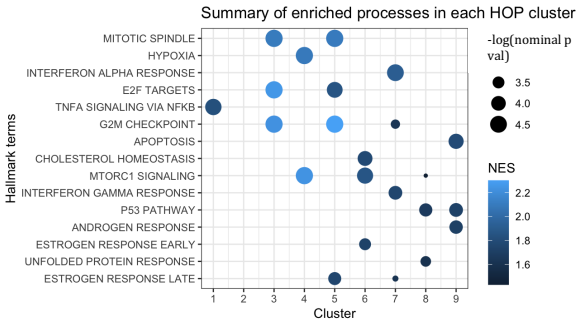

17B

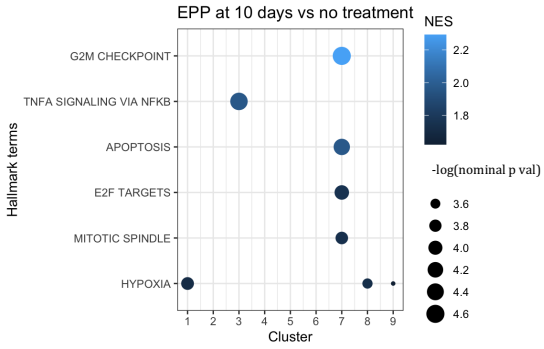

17C

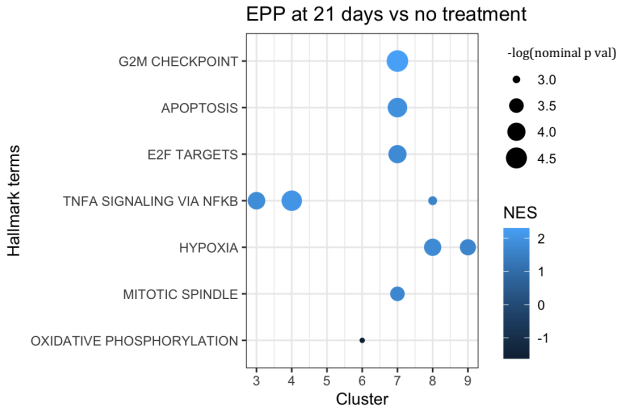

17D

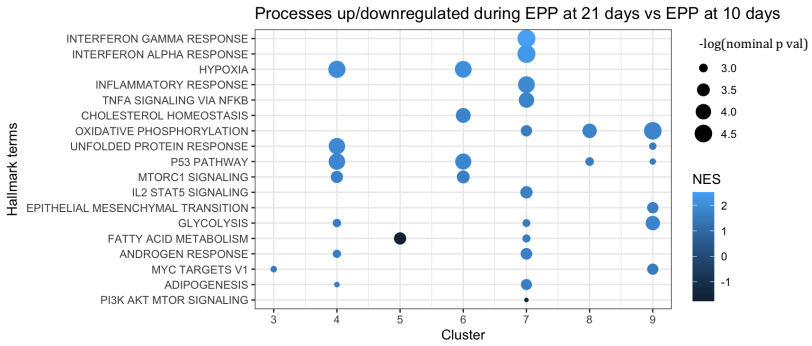

Figure 17. Summary of enriched hallmark terms in each HOP cluster, per EPP treatment timepoint.

(A) GSEA for enriched hallmark terms in each HOP cluster. Terms are ordered based on–log(nom p-value). Only hallmark terms with a normalized p-val < 0.05 were kept for this analysis. The color of the dots represents NES.
(B) GSEA for hallmark terms differentially enriched in each HOP cluster at 10 days of EPP treatment.
(C) GSEA for hallmark terms differentially enriched in each HOP cluster at 21 days of EPP treatment.
(D) GSEA for hallmark terms differentially enriched in each HOP cluster at 21 days of EPP treatment compared to 10 days.

Conversely, since pregnancy hormone regulated growth pathways were detected in these cellular clusters after 21 days of treatment, such as TNF-α signaling via NF-κB pathways (cluster HP3, HP4 and HP7), and IL2-STAT5 signaling (HP7), this could suggest possible cellular states transitions that, after adaptation to pregnancy hormones, may be inducing differentiation/specialization of cells with less specified lineages identities, into more defined cellular states (Liu et al., 1997) (**Fig. 17C-D**).

Cohesively, we also found that, in mixed lineage cluster HP5, pregnancy hormone treatment was accompanied by increased levels of luminal biased lineage genes (CLDN3, and WFDC2), with concomitant decrease on the expression of basal lineage genes (KRT14, MYL6), potentially suggesting that this cluster assumes a more luminal-like identity after exposure to pregnancy hormones (**Fig. 16D**).

Moreover, gene expression analysis of pregnancy-induced cluster HP1 indicated that these cells were enriched for hypoxia during early (10 days) EPP treatment, and no significant enrichment of other pathways at 21 days of EPP treatment (**Fig. 17C-D**). Given that hypoxia has a bi-directional effect on the cell cycle, it is possible that cells from HP1 cluster could be rapidly responding to signals from exposure to pregnancy hormones, and the developmental snapshots captured at 10 and 21 days represent a more stable and less dynamic cellular state.

5.1.2 Evolutionary conservation of MEC responses to pregnancy hormones

Despite the fact that both murine and human mammary organoids treated with pregnancy hormones recapitulated some of the previously described changes that take place *in vivo*, not all cellular pathways and states were identified in these two model systems, suggesting that pregnancy signals may activate pathways that are both evolutionary conserved and species specific. Therefore, we assessed the evolutionary conservation of responses to pregnancy hormones between human and murine organoids, by integrating pregnancy hormone treated, murine and human organoids datasets (referred hereafter as MHP clusters). Such an approach identified a total of 9 clusters with varied distribution across species (**Fig. 18A**). To avoid lineage classification issues, biased by the state of human organoid cultures, we utilized once again the top differentially expressed genes to determine the identities of each MHP cluster (**Fig. 18B**).

This approach identified six clusters of luminal-like cellular lineages (MHP1, MHP3, MHP4, MHP6, MHP8, and MHP9), from which two clusters (MHP6 and MHP8) bore high expression of

proliferative markers, confirmed by cell cycle scoring, and three clusters (MHP2, MHP5, and MHP7) expressed mixed lineage markers (**Fig. 18B-C**). The distribution of these clusters also varied according to species, with clusters exclusive to murine samples (luminal MHP1, MHP3, MHP8, MHP9 and mixed lineage MHP7), those more abundant in human samples (luminal cluster MHP4 and mixed lineage MHP2 and MHP5), and those with cells representative from both species datasets (MHP4 and MHP6) (**Fig. 19A-B**).

Molecular characterization of luminal MHP revealed gene signatures that indicated their sub-specialization (**Fig. 18B**). We found mouse-biased MHP1 displayed a wide array of alveolar/secretory features, including expression of *LALBA*, casein genes *CSN1S1* and *CSN3*, milk-synthesis associated *ALDOC*, and *IGFBP5*, which has been linked to a lactogenic environment (Allan et al., 2004; Chen et al., 2010; Rudolph et al., 2007). Cells in MHP3, MHP4, MHP6, MHP8 and MHP9 all expressed

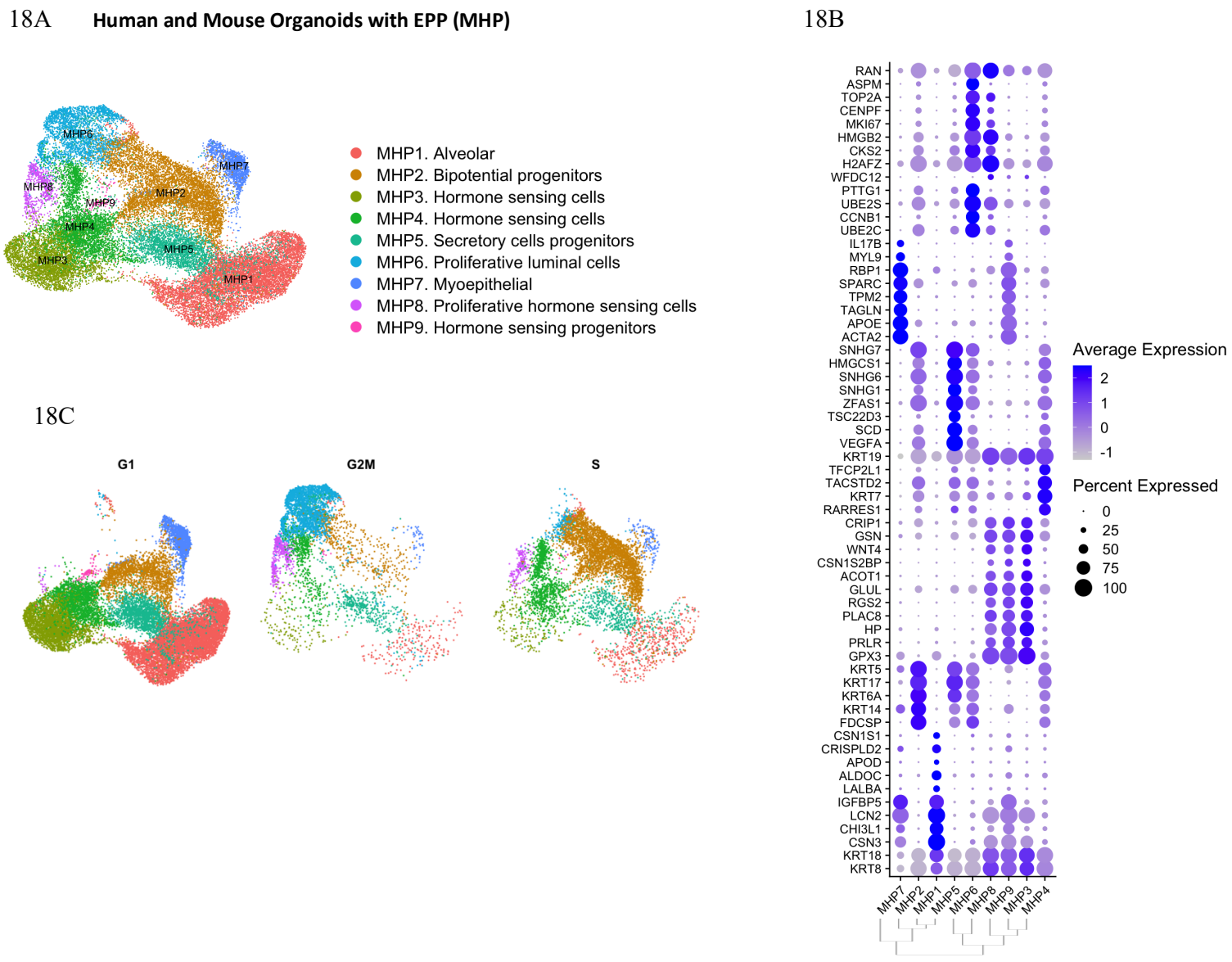

Figure 18. Evolutionary comparisons between EPP-treated murine and human organoid MECs (MHP), and approaches for MHP clusters characterization.

(A) Resulting clusters of human and mouse organoids with EPP (MHP). MHP clusters were assigned their respective identities based on previously described human MEC markers gene expression and their top DEGs.
(B) Dotplot showing expression of the top 10 DEGs per MHP cluster. Clusters are organized based on their dendrogram relationships.
(C) Cell cycle scoring of MHP clusters.

hormone sensing features, with signature differences that suggest a role for these cells in pregnancy (**Fig. 18B**). Hormone sensing mouse-biased cluster MHP3, for instance, characteristically expressed progestin-associated *GPX3, GLUL* and *WNT4* (Rajaram et al., 2015; S. J. Santos et al., 2009; Zhong et al., 2018), as well as *RGS2*, which has been described as a progestin-modulated gene in organoid cultures (S. J. Santos et al., 2010).

Cluster MHP4, present in both human and murine systems, expressed higher levels of *KRT7* as well as *TFCP2L1* mRNAs, which are found in fully differentiated cells during the follicular phase, thus suggesting a more differentiated cellular state (Pardo et al., 2014). Cells in MHP6 were mostly characterized by their expression of proliferative markers, although they also expressed pregnancy-associated *CCNB1* and *PTTG1*, thus suggesting an actively growing cell state present in mammary organoids from mouse and humans (Hatcher et al., 2014; Pellacani et al., 2019). Mouse-biased MHP8 also expressed proliferative markers and, additionally, hormone sensing-associated PLAC8 (S. J. Santos et al., 2010), and lactation-associated GPX3 (Lu et al., 2008), indicating a more mature and proliferative cell stage. Cluster MHP9 expressed *PRLR*, as well as *PLAC8* (S. J. Santos et al., 2009) and *CRIP1* (Deroo et al., 2009), indicating their hormone sensing identity. Likewise, these cells expressed *GPX3* (Lu et al., 2008; S. J. Santos et al., 2009) and hormone-induced *RBP1* (Lu et al., 2008), further indicating their hormone responsiveness. Interestingly, these cells also expressed basal features *ACTA2* (Haaksma et al., 2011; C. M.-C. Li et al., 2020), *SPARC* (Twigger & Khaled, 2021), *TAGLN* (Nguyen et al., 2018) and *TPM2* (Twigger et al., 2022), suggesting these cells reside in the basal compartment.

Taking a closer look at mixed lineage and basal clusters MHP2, MHP5 and MHP7 likewise allowed us to better profile these cells based on their transcriptomic characteristics (**Fig. 18B**). Human-biased MHP2 cells expressed both luminal progenitor marker *FDCSP* (McMullen & Soto, 2022), as well as myoepithelial *KRT5*, *KRT14* and *KRT17*. Nonetheless, these cells also expressed *KRT6A*, a marker for bipotential progenitors, which indicates that these cells are not just mixed lineage, but have a multipotential progenitor identity. This description matches the identity of cluster HOP6, confirming that with integration of other data sets, this cluster maintains its identity (**Fig. 16A and 18B**). Likewise,

cells in human-biased cluster MHP5 expressed *KRT6*, another marker of bipotential cells (Bu et al., 2011), although these cells also expressed genes related to lactation and milk secretion, such as *VEGFA* (Rossiter et al., 2007), SCD (Anderson et al., 2007; Rudolph et al., 2007) and HMGCS1 (Laporta et al., 2015), suggesting these cells may represent early progenitors of secretory cells. Therefore, MHP5 cells could correspond to cells in clusters HP5 or HP8, and integration of the human with the mouse data set could allow for a more discrete classification of human MECs (**Fig 16A and Fig. 18B**).

Cluster MHP7 displayed a strong basal signature, with these cells expressing *ACTA2, TAGLN, TPM2, SPARC* and *IL17B* (Haaksma et al., 2011; C. M.-C. Li et al., 2020; Twigger et al., 2022; Twigger & Khaled, 2021; Wei et al., 2013). These cells also expressed *MYL9*, a myoepithelial marker (Pal et al., 2021), in addition to low levels of *KRT14*, indicating these cells are myoepithelial.

We then performed analysis of the pathways enriched in each MHP cluster, in order to assess the gene expression signatures of mouse-biased and human-biased clusters (**Fig. 19C-D**). We first assessed which hallmark terms were enriched in human cells in relation to mouse cells within each MHP cluster (**Fig. 19C**). Notably, we were unable to perform GSEA on human MECs in mouse-biased clusters MHP3, MHP6, MHP8 and MHP9 because they could not be detected at sufficiently high levels. Nonetheless, with this analysis, we found an enrichment of terms linked to pregnancy processes (hypoxia and p53 signaling both in MHP1, MHP4, MHP5, and MHP7, cholesterol homeostasis in MHP1, MHP4 and MHP5, oxidative phosphorylation in MHP2, EMT in MHP4 and MHP5, and mTOR signaling in MHP5) and hormone response (TNF-α signaling via NF-κB in MHP5 and MHP7) in human organoid MECs across the rest of the MHP clusters, suggesting that human MECs are highly dynamic in response to EPP compared to mouse MECs (Ketterer et al., 2020; C.-W. Li et al., 2012; Morrison et al., 2015; Rubio et al., 2006; Y. Shao & Zhao, 2014; Sivaraman et al., 2001; Smith et al., 1998; C.-C. Wang, 2021). Interestingly, human cells in clusters MHP1, MHP4 and MHP5 displayed an enrichment for androgen response terms compared to mouse cells, which has been linked to impairment of lactation (Raths et al., 2023). However, when taking a closer look at the genes found to be associated with androgen response in human organoid MECs, we found that many of these overlapped with genes associated with response to pregnancy hormones, such as *INSIG1* (Fan et al., 2020) and *SCD* (Anderson

et al., 2007) (**Table S4**). Nevertheless, these results could indicate that human MECs are overall more responsive to hormones that simultaneously enhance pregnancy-associated processes (EPP), and that

19A

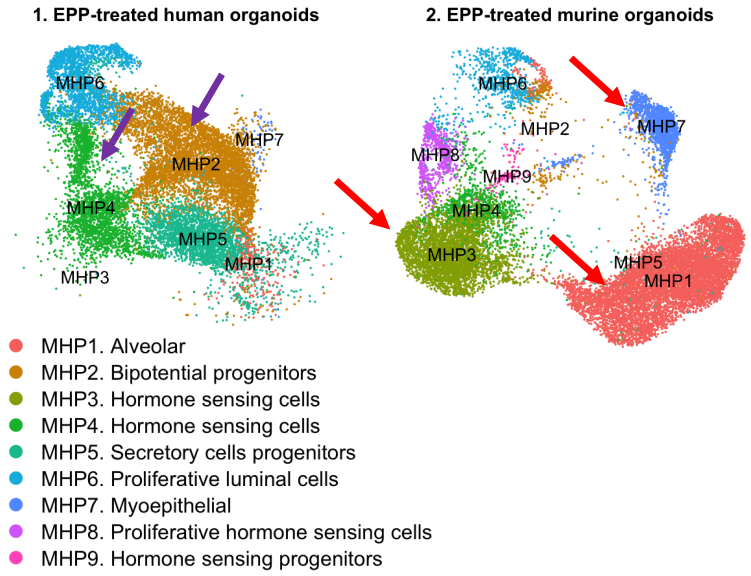

19B

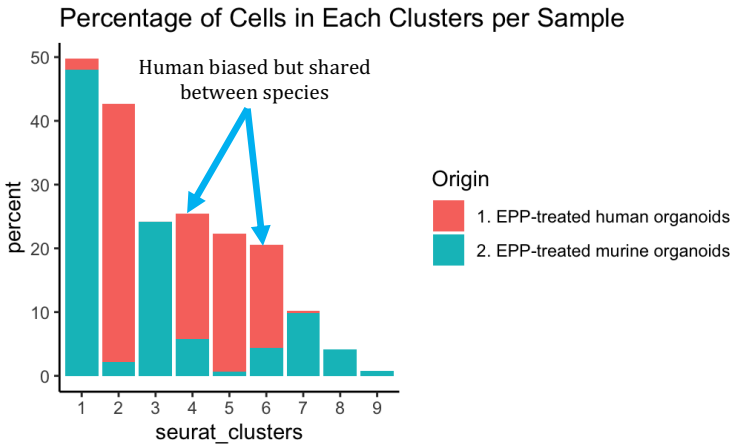

19C

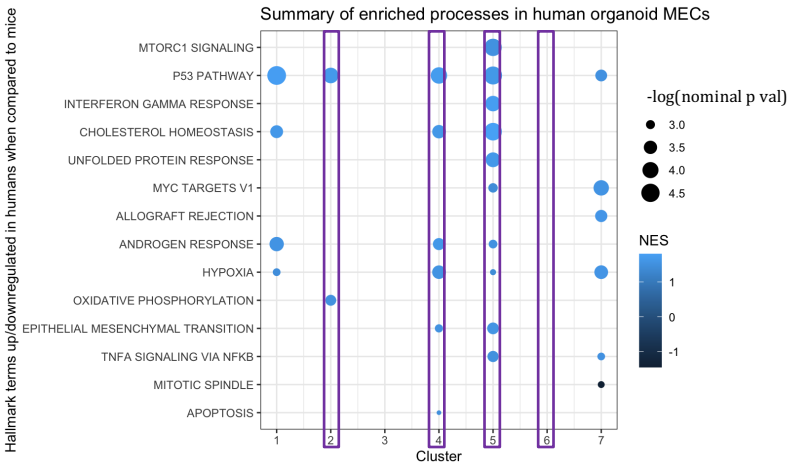

19D

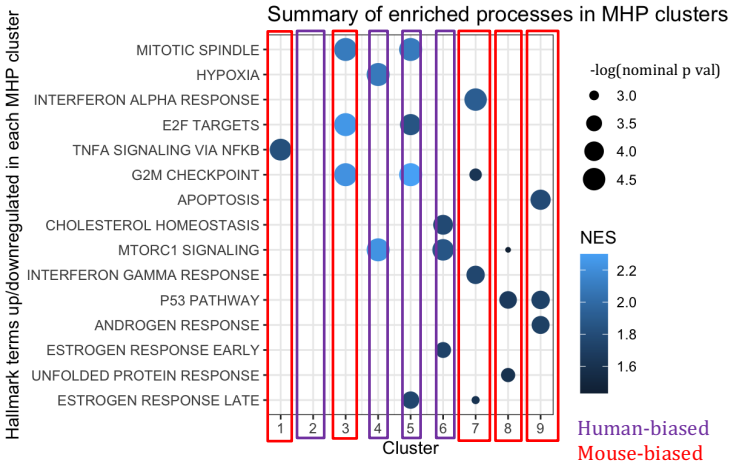

Figure 19. Transcriptomic differences between human and murine MEC organoids (MHP).

(A) MHP clusters split by species of origin. The purple arrows highlight clusters enriched in human samples and red arrows highlight clusters enriched in mouse samples.
(B) Bar plot showing percentage of cells per condition in each MHP cluster. Clusters enriched in both species (blue arrow) are highlighted.
(C) GSEA for enriched hallmark terms in human organoid MECs vs mouse organoid MECs. Terms are ordered based on–log(nom p-value). Only values with a norm p-val <0.05 were kept for these analyses. The color of each dot represents the NES value for each term.
(D) GSEA for hallmark terms enriched in each HOEPP cluster. Terms were ordered based on –log(nominal p-value). Only terms with nom p-val <0.05 were kept for these analyses. The color of each dots represents the NES value for each term.

impair pregnancy-associated development (such as Androgen), potentially making human MECs more susceptible to hormonal imbalances.

We then looked at the hallmark terms enriched in each cellular cluster, despite species of origin (i.e. mixed human and mouse cells) (**Fig. 19D**). With this analysis, we would determine the processes overall governing each mouse-biased and human-biased MHP cluster. We found that mouse-biased clusters MHP3 and MHP7 were enriched with proliferative terms and, likewise, clusters MHP1 and MHP7 were enriched for Estrogen-associated terms (MHP1 for TNF-α signaling pathway via NF-κB, and MHP7 for Interferon Gamma response), suggesting these cells are highly responsive specifically to Estrogen (Karpuzoglu-Sahin et al., 2001; Rubio et al., 2006). The results are in line with the notion that murine MECs exhibit a more pronounced branching response to Estrogen compared to their human counterparts (Ewan et al., 2005; Feng et al., 2007). Meanwhile, we could only detect differentially enriched terms in three of the four human-biased clusters. Given that the cluster that did not contain significantly enriched terms was cluster MHP2 of bipotential progenitors, we concluded that these results support the classification of this cluster, as it contains traits from the rest of the cell types present in the mammary gland. Moreover, two of the human-biased clusters MHP4 and MHP6 displayed an enrichment for terms associated with pregnancy-associated processes (hypoxia in MHP4, mTOR signaling in MHP4 and MHP6, and cholesterol homeostasis in MHP6), suggesting that the high dynamism of human MECs in response to EPP results in the activation of processes preparing the mammary gland for milk synthesis, in comparison to highly proliferative mouse-biased clusters (Ketterer et al., 2020; Morrison et al., 2015; Y. Shao & Zhao, 2014; Smith et al., 1998). Nonetheless, there was one human-biased cluster (MHP5 of secretory progenitors) that were highly proliferative and were particularly responsive to Estrogen, therefore sharing similarities with murine MECs in terms of their hormonal response mechanisms. Moreover, although cluster 4 was biased towards human samples, it still contained murine MECs, suggesting differences between MEC response to hormones across evolutionary timescales are subtle. Likewise, human-biased cluster MHP6, which was also shared with murine cells, appeared to be responsive to Estrogen, further supporting similarities between human and murine MECs in their response to hormones.

20A

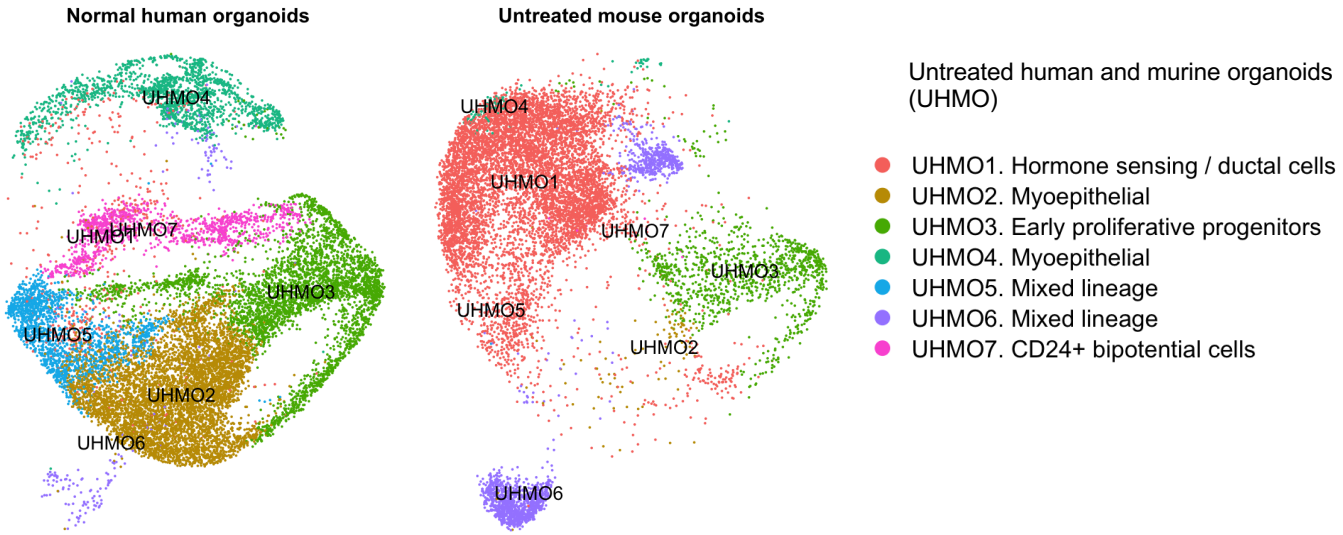

20B

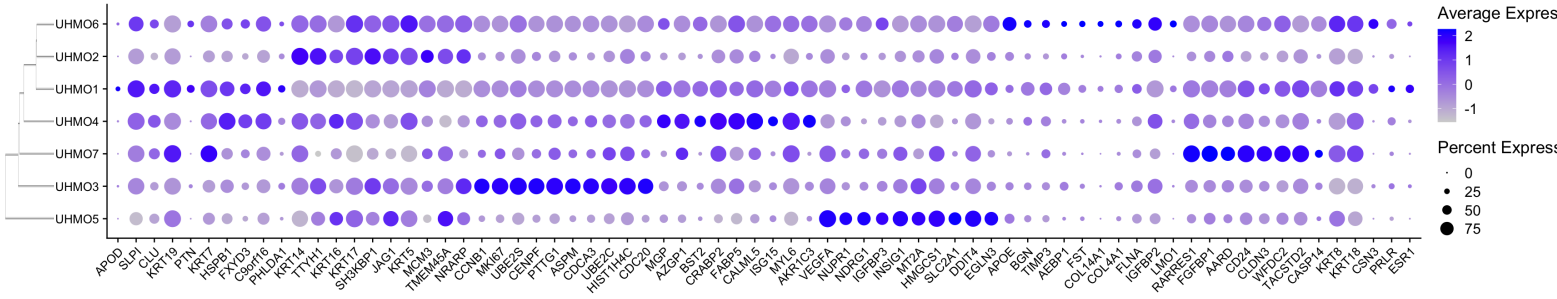

20C

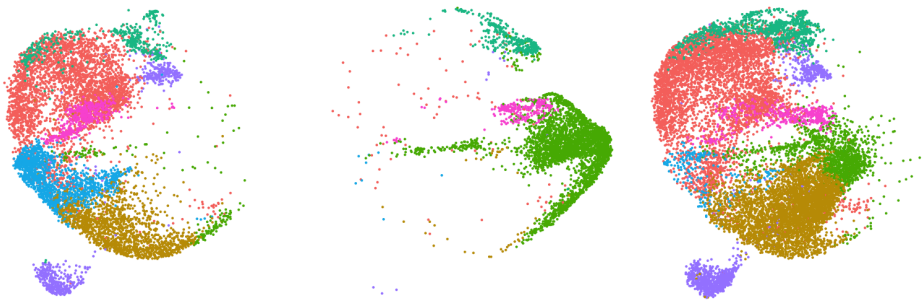

Figure 20. Integrated analysis of human and murine organoids with no treatment (UHMO).

(A) Integration of data sets from murine and human organoid MECs without treatment (Untreated and Human MEC organoids – UHMO). Cluster identities were assigned based on previously described human MEC markers and top DEGs per cluster.
(B) Dotplot showing expression of the top 10 DEGs per UHMO cluster. Clusters are organized based on their dendrogram relationships.
(C) Cell cycle scoring of UHMO clusters.

To further confirm our findings and verify whether the differences in cellular states between murine and human MECs were maintained without EPP treatment, our untreated murine organoids data set were merged with our human organoids without treatment (from now on called UHMO clusters) (**Fig. 20**). We found that the majority of UHMO clusters were species-specific, with the exception of cluster

UHMO4, which appeared to be shared across species. We classified each cellular cluster using a similar strategy as the one employed for HP and MHP clusters, and found that UHMO4 expressed similar markers as shared mouse and human cluster MHP6 (**Fig. 18B and 20B-C**). Nonetheless, UHMO4 cells did not appear to be proliferative, in contrast to MHP6 (**Fig. 18C and 20C**). Therefore, UHMO4 and MHP6 cells could represent a highly conserved cell type across evolutionary timescales that is, in tandem, highly responsive to pregnancy hormones.

6. Determining transcriptional and cellular composition changes in intact human mammary tissue after pregnancy

6.1 Results

We obtained samples for single cell RNA-sequencing from women that had no previous pregnancies, and women who had at least one previous pregnancy (parous), with the purpose of investigating the changes that occur in the human mammary gland during terminal differentiation caused by pregnancy. In doing so, we aimed to capture a snapshot of how the postnatal developmental stages modify the gland, with intact microenvironmental queues. We could then compare our results with our previously gained knowledge of the dynamics of pregnancy hormone response in murine and human organoids.

Previous studies have shown that the age of a first full term pregnancy can alter lactation efficacy and BC risk (Chie et al., 2000; Dewey et al., 1986) potentially making the parity-associated transcriptomic and epigenomic signature that the mammary gland obtains age-dependent. Therefore, for subsequent analyses, age at first pregnancy was factored into consideration, dividing samples into an early age of first pregnancy (<25 years of age) and late age of first pregnancy (>35 years of age). Given that assessing the effects of age of first pregnancy is out of the scope of my thesis project, this aim became a collaboration with graduate student Sam Henry. She is therefore leading the analysis of these data sets as part of her thesis work.

We preliminarily analyzed new data sets together without integration of our previously published data sets. Quality control (QC) steps were performed on the data, which involved eliminating cells with less than 200 features and over 5,000 features, and eliminating cells with over 25% mitochondrial content (**Table 1**).

Table 1. Quality Control (QC) metrics for scRNA-seq data from intact human mammary tissue.

			Before QC		QC Parameters		After QC	
Sample Name	Location	Description	features	cells	nFeatures_RNA	percent.mt	features	Cells
NP2	JR01_S4	Never pregnant	22765	12093	200-5000	25	22765	11030
NEP7	JR01_S8	Early pregnancy	22318	8929	200-5000	25	22318	8807
NEP8	JR01_S1	Early pregnancy	20574	3505	200-5000	25	20574	3321
NEP9	JR01_S6	Early pregnancy	22853	15617	200-5000	25	23853	14352
NLP5	JR01_S2	Late pregnancy	22132	11821	200-5000	25	22132	11581
NLP7	JR01_S3	Late pregnancy	23283	8762	200-5000	25	23283	8231

The mitochondrial content threshold was higher for these cells than what we usually use (~10% mitochondrial content or less), given that accumulation of mitochondrial content has been observed with age (Yadava et al., 2013). Initial clustering by Sam Henry resolved 24 clusters, showing compositional changes across conditions, with cluster 6 being significantly enriched in nulliparous mammary tissue (**Fig. 21A-B**). MECs were then identified based on *EPCAM* expression and *KRT8, KRT18, KRT5,* or *KRT14* expression, and isolated for re-clustering. Upon re-clustering, the resulting 14 clusters were classified based on the curated list of human gene markers by Henry et al. (Henry et al., 2021). Overall, clusters could be divided into myoepithelial cells, bipotential hormone responsive (HR+) progenitors, HR+ luminal cells, bipotential HR- progenitors, and HR- luminal cells (**Fig. 21C**). Splitting MEC clusters by condition reveals visual differences in composition between nulliparous, early parous and late parous clusters (**Fig. 21D**). In particular, myoepithelial, luminal HR+ and HR- progenitor populations were depleted in parous samples overall, whereas a population of bipotential progenitors was enriched in samples from women who were never pregnant, suggesting that pregnancy permanently decreases the plasticity of human MECs. These findings may enhance our understanding of the mechanisms through which pregnancy helps prevent malignant transformation, as well as how post-partum human MECs, similar to their murine counterparts, can rapidly respond to hormone signals upon re-exposure.

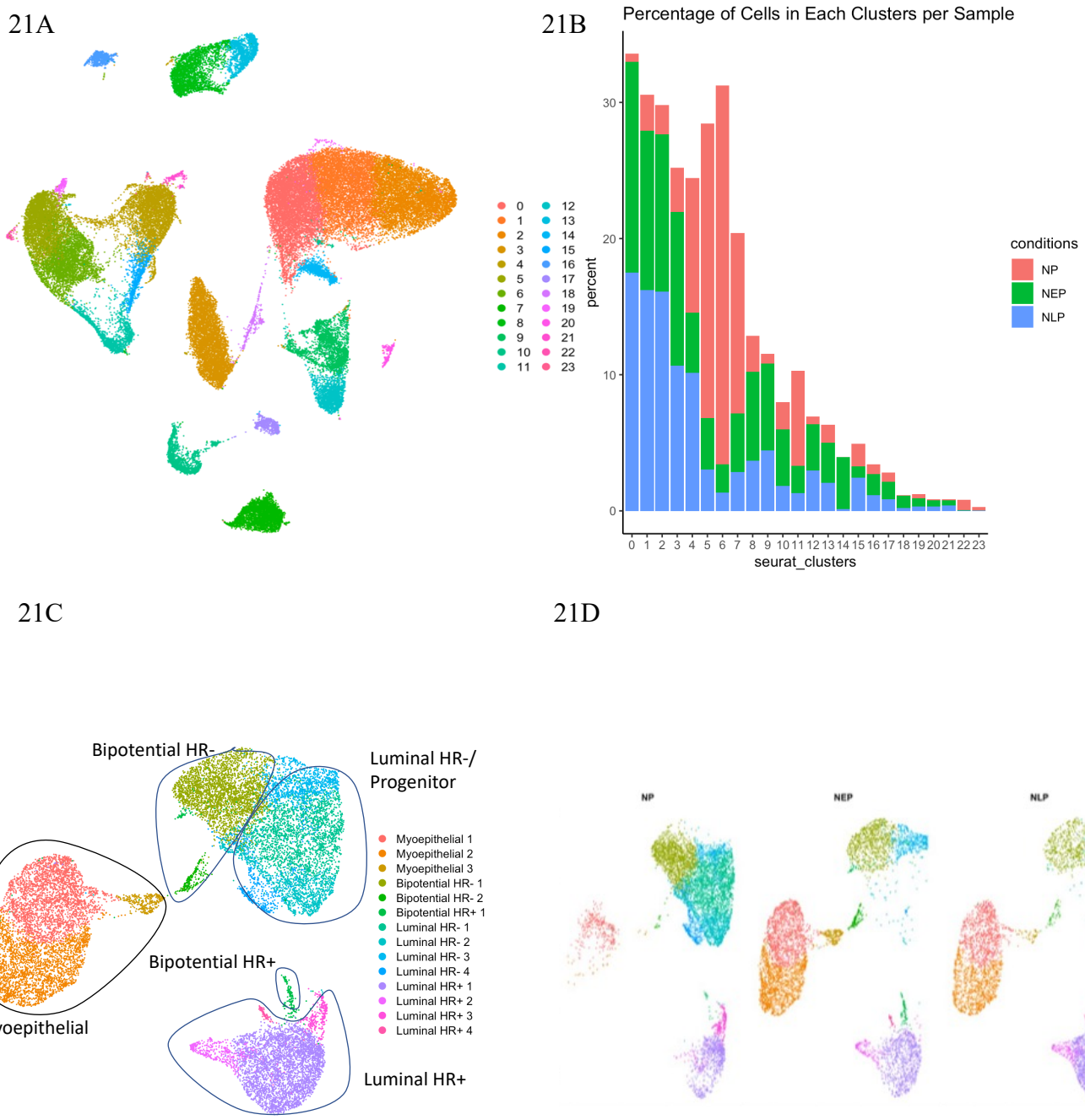

Figure 21. Clustering of scRNA-seq data from intact human mammary tissue reveals differences across conditions.

(A) Initial clustering resulted in 24 clusters of mammary epithelial cells (MECs) and non-ECs.

(B) Statistical analyses by Sam Henry revealed cluster 6 is significantly enriched (pval < 0.05) in mammary tissue from women who have never been pregnant.

(C) Re-clustering of MECs was performed in order to classify each cellular population and determine specific changes to the MEC and/or nEC compartment.

(D) Using the split.by( ) parameter allows for appreciation of visual MEC composition differences across conditions.

7. Discussion

Our characterization of MEC-derived organoids at a single cell level has allowed us to carry out a comprehensive assessment of organoid systems to model mammary gland development. Our initial analysis of murine MEC-derived organoids scRNA-seq data confirmed conservation of *in vivo* lineage signatures, as well as representation of a diverse array of MEC lineages *in vitro*. These results complement a previous proteomics study that made use of Cytometry by time of flight (CyTOF) to confirm that MEC lineages found *in vivo* are present in patient MEC-derived organoid cultures (Gray et al., 2022). We further confirmed lineage fidelity between *in vivo* and 3D *in vitro* systems by comparing scRNA-seq data from intact murine mammary tissue to data we generated from murine MEC-derived organoids. This particular analysis resulted in the appearance of a luminal progenitor population that is organoid exclusive, suggesting that certain cells in culture exist in a stem-like state, perhaps responsible for maintaining the growth of organoids *ex vivo*.

The induction of MECs into an immature cellular state in organoid cultures could have resulted from a lack of microenvironment queues that are crucial for mammary development. For example, it has been shown that the mammary epithelium readily interacts with the surrounding stroma to give rise to the mature mammary structure (Howard & Lu, 2014). Moreover, signals that are not necessarily produced by surrounding non-epithelial cells in the mammary gland but that can result from paracrine signaling from other tissues are also vital for the maturation of specific MECs, such as OT, which promotes the differentiation of myoepithelial cells (Sapino et al., 1993). Furthermore, media composition has been shown to affect organoid culture composition (Gray et al., 2022), which could also have contributed to the observed phenotype. Nonetheless, SCENIC analysis revealed that regulons with a high RSS for each system overall contributed to the needs of each system to survive and reach a homeostatic state in their respective microenvironments. Thus, MEC-derived organoids are a suitable system to assess the effect of controlled developmental signals, but should be used with the previously discussed considerations. Future studies involving the addition of signals that contribute to endogenous

mammary gland development and maintenance, along with co-culturing with essential cells from the mammary microenvironment will further improve the fidelity of this system.

Single cell characterization of murine MEC-derived organoids treated with different concentrations of Estrogen enabled us to begin to isolate the effects of individual hormones on MEC development, especially during distinct biological processes involving an interplay of varying hormone doses (e.g. the estrus cycle). This analysis revealed the emergence of an Estrogen-exclusive ductal population independent of dosage, as well as a depletion of bipotential progenitors exclusively at a high dose of Estrogen (66.6 ng/mL). Our results suggest that ductal cells in our estrogen-exclusive cluster are potentially cells that were already present in organoids without treatment, in a cellular state triggered by hormone treatment. This is evidenced by the simultaneous depletion of a cellular cluster of ductal cells enriched in no treatment. Further comparison of both ductal clusters revealed that Estrogen-exclusive ductal cells highly express *Areg* and *Pgr*, both which have been previously described to be upregulated by Estrogen (Kanaya et al., 2019). Moreover, our findings that Estrogen-exclusive ductal cells are highly differentiated compared to ductal cells with no treatment indicate that hormone treatment could be promoting cellular maturation, in accordance with previous studies indicating that a ductal cell mature state is correlated with expression of hormone receptors (Bach et al., 2017).

A lack of hormone signals at base state could further explain why we observe an enrichment of bipotential progenitors in organoids without treatment and a stark depletion in organoids treated with a high dose of Estrogen. This interpretation is complementary to a previous study that delineates a quiescent state for bipotential progenitors in the adult mammary gland, which become active in the presence of hormones (Fu et al., 2017). Therefore, these results can additionally be interpreted as organoid culturing conditions at baseline resembling developmental stages occurring in a microenvironment depleted of hormones, such as pre-pubescent development and menopause. Given that an aged extracellular matrix alone can drive MECs into neoplastic and invasive cellular states (Bahcecioglu et al., 2021), it will be important to identify what stages of development the composition of Matrigel and organoid media resembles most. Thus, our analysis paves the way to future studies that

will involve comparing organoid MECs with intact MECs from pre-pubescent and post-menopausal mice, as well as more studies involving dissecting the individual effects of hormones on MEC development and maintenance.

Previous work using a combination of Prolactin, hydrocortisone, OT, and growth factors showed mouse MEC-derived organoids are able to mimic lactation and involution (Sumbal et al., 2020). Additional studies further introduced the idea of using Estrogen, Progesterone, and Prolactin (EPP) cocktail without growth factors to simulate a pseudo-lactation state, which resulted in the incremental expression of *Csn2* and changes to the epigenome previously associated with pregnancy (Ciccone et al., 2020). Our current study extends upon these studies by demonstrating compositional and transcriptomic changes to mammary organoids as a direct effect of EPP treatment. We show a depletion and emergence of similar cell types with EPP treatment, suggesting that the observed compositional differences between organoids without treatment and with EPP are likely due to subtle changes in cellular states. Moreover, cellular clusters that emerge with EPP treatment are enriched for processes that have been previously associated with lactation, such as adipogenesis and hypoxia (Colleluori et al., 2021; Y. Shao & Zhao, 2014). Therefore, these results indicate specific cell types obtain a parity-associated gene expression signature with exposure to hormones during pregnancy. We further compared scRNA-seq data from MECs obtained at intact pregnancy stages (Bach et al., 2017) with our EPP-treated organoids, and found our organoid cultures recapitulate lineages from all pregnancy stages.

We also found that our organoids with and without EPP treatment both have cellular populations present in a cellular state only found in MECs undergoing gestation, thus suggesting that the proliferative and stem-like state of organoid MECs is most similar to this stage of pregnancy. Additionally, the emergence of a cellular state exclusive to EPP-treated organoid cultures once more suggests that certain phenotypes are exclusive to our culturing conditions, even in the presence of hormones. Therefore, we conclude that organoids can recapitulate drastic cellular changes that occur with pregnancy, particularly by mimicking the gene signature of MECs during pregnancy. However, since organoid MECs at baseline resemble MECs from gestation more than those from a nulliparous

gland, this model must be used with caution to understand other aspects of pregnancy-associated development.

In fact, analysis comparing untreated and treated organoid cultures identified a population of hormone sensing MECs largely exclusive to conditions supplemented with pregnancy hormones, thus supporting a possible cellular expansion in response to pregnancy signals. Interestingly, the existence of pregnancy-induced MECs (PI-MECs) has already been suggested in intact mammary tissue, although its true lineage identity and function remain very controversial (Chang et al., 2014). Such pregnancy-induced, stably sustained cellular state, could also represent populations that bear pregnancy-induced epigenetic changes, and therefore the cellular basis for a robust response to consecutive exposures to pregnancy signals (Ciccone et al., 2020; C. O. dos Santos et al., 2015; Feigman et al., 2020).

We were able to uncover the translational potential of MEC-derived organoids by further showing that patient MEC-derived organoids respond to EPP by inducing transcriptomic changes to organoid MECs associated with pregnancy. We however found that most human organoid MECs exist in a luminal-basal state. The phenomenon of organoids becoming more basal-like after long term culturing had already previously been reported (Bhatia et al., 2022), thus potentially confirming that the phenotype we observed could be a result of the number of passages prior and during the course of the experiment. Altogether, we have developed an atlas of normal MEC-derived organoids from mouse and human tissue, which can be incorporated with other single cell methods to understand the molecular mechanisms governing MEC development *in vitro*. We characterize the effects of feminizing hormones on these 3D cultures at a single cell level, supporting hormone treatment of organoids as a system to understand developmental processes associated with adolescence, pregnancy and menopause. Our findings support the implementation of this procedure as a non-invasive method to understand how the human mammary gland is modified during a pregnancy cycle. This system can also be extended to other species, in order to assess the evolutionary basis of MEC response to hormones across other mammalian species.

8. Conclusion and perspectives

Our analysis has shown that organoids are capable of replicating the heterogeneity of primary tissue, which has been previously reported in the context of malignant and homeostatic states (Bhatia et al., 2022; Gray et al., 2022; Rosenbluth et al., 2020). However, we have also discovered exclusive organoid states in both non-stimulated and hormone-stimulated organoids, indicating that discrepancies between the systems could be causing these phenotypes to emerge in culture.

It is important to note that there are missing microenvironmental cues that contribute to the homeostasis of the mammary epithelium. Prior research has highlighted the significance of various fibroblast types in MEC development and homeostasis, as well as the potential role of adipocytes in regulating MEC growth and function stages (Gregor et al., 2013; Hovey & Aimo, 2010; Howard & Lu, 2014; Liu et al., 2012; Makarem et al., 2013; Wang & Kaplan, 2012). Therefore, in the absence of key signals for cell maturation originating from the microenvironment, organoid MECs could potentially obtain an immature phenotype that is uncontrollably proliferative given the absence of regulatory signals. One approach that could lead to a better understanding of key components in the mammary microenvironment for MEC maintenance would be culturing organoid MECs with different stromal components. We could then assess secreted factors by these stromal cells and estimate direct cell-cell communication dynamics. We could also add other signals that are known to promote MEC maintenance and development. For example, Oxytocin addition to cultures could potentially promote pseudo-lactation rather than a pseudo-gestation heterogeneity in culture (Sumbal et al., 2020).

Our results also show that hormone treatments affect the heterogeneity of MECs in culture, demonstrating that these systems are hormone responsive. These findings confirm previous observations in the global effects of EPP treatment in organoids (Ciccone et al., 2020). Moreover, we have shown that individual doses of estrogen can induce compositional changes in MECs. By establishing that our system is able to mimic the heterogeneous response of primary tissue to different hormone signals, we have created a valuable tool for assessing the molecular and genomic mechanisms

by which hormones interact with the mammary gland. This is particularly important because hormones control mammary gland changes throughout puberty, cyclically during the estrous cycle, and during pregnancy. Our system can therefore help us better understand how cellular dynamics change throughout hormone-driven developmental processes, and how they modify the risk of certain MEC types in, for example, initiating different types of breast cancer.

Examination of the global gene signature changes induced by hormones in cells that were both changed in composition by hormone treatments and those which seemed invariable between conditions demonstrated a plethora of activated pathways. Estrogen activated pathways associated with proliferation and inflammation, as noted by previous literature (Maharjan et al., 2021). In bipotential progenitors depleted at a high concentration of Estrogen, an activation of genes associated with Androgen response was observed. Androgen receptors can block the pro-proliferative role of Estrogen, suggesting a mechanism by which these cells are depleted in the presence of a certain Estrogen dose (Bleach & McIlroy, 2018). EPP had alternative effects on MECs, where bipotential progenitors were not totally depleted, but moved to a different cellular cluster with global gene signatures associated with pregnancy. The same effect was observed for ductal cells. Surprisingly, hypoxia was one of the pathways continuously enriched in EPP-exclusive clusters compared to those depleted by EPP. This enrichment was also observed in human MEC-derived organoids treated with EPP. Hypoxia has been implicated in pregnancy, where the mammary gland increases its metabolic rate to support mammary growth and lactogenesis, resulting in hypoxic genes being activated (Shao & Zhao, 2014). Hypoxia stabilizes HIF-1α from the HIF complex, which upregulates glucose intake in the mammary gland. Interestingly, we observed a coupled enrichment of glycolysis-associated genes in EPP-treated human organoids, potentially indicating a striking role of hypoxia in preparing mammary organoids for pseudo-lactation.

The study found that although the human organoids were responsive to EPP, they displayed minimal lineage fidelity. This lack of fidelity may be due to the passing of the organoids prior to the experiments, which could have been selected for stem-like cells. To address this issue, one approach

that could be implemented is to grow the cells and sequence them right before the next passaging, allowing cells to differentiate in culture prior to sequencing. However, there are other factors that could affect the observed phenotypes in culture, such as the inability to remove growth factors from culture due to the developmental timeline of human organoid MECs compared to murine organoids.

Keeping the potential limitations of experiments involving human organoids in consideration, it is important to optimize these cultures given the opportunity they present. Human-derived organoids provide a non-invasive method to investigate pregnancy-associated processes and offer potential for developing personalized medicines for breast cancer prevention and treatment. Additionally, breast cancers that occur during pregnancy are among the most aggressive types, and using organoids to study them can help develop better treatments. These systems can be genetically manipulated and accelerate the developmental timeline of studies that would otherwise take months to complete. Therefore, with careful consideration of the limitations, human organoids have significant potential to advance our understanding and treatment of pregnancy-related diseases. Molecular characterization of these organoid systems, like the one we present in this study, will be key to pushing the development of organoid systems forward, and will enable us to fully realize their potential for improving our understanding of pregnancy-related processes in human mammary tissue.

9. Author contributions

I acknowledge the following people who assisted with this project. Camila dos Santos oversaw the project, and participated in experimental design and data analyses. Steven Lewis and Michael Ciccone cultured the organoids and prepared cells for single cell RNA-seq libraries. The Single Cell Sequencing core at CSHL provided the sequencing files. I performed quality control steps on the resulting files, as well as subsequent analysis steps including classification of clusters, differential gene expression analysis, pseudo-time estimation and gene set enrichment analysis. Sam Henry provided code for data integration, which I then applied to directly compare data sets sequenced in different batches. Deeptiman Chatterjee set up the SCENIC runs and provided code for subsequent analyses, which I used as a basis for my code to perform analysis of specific regulons coordinating transcriptional programs in each condition and cellular cluster.

For experiments mentioned in chapter 5, David Spector generously provided normal human organoids for culturing and the protocols for doing so. Asma Kaleem cultured the aforementioned human MEC-derived organoids and prepared cells for single cell RNA-seq libraries. Yixin Zhao from the Siepel lab provided code for the conversion of mouse gene names to their human orthologs, which I then further modified to achieve direct integration of murine and human organoid data sets.

In case of the experiments mentioned in chapter 6, the tissue banks utilized for the analyses were obtained via the Northwell Health Tissue Donation Program (TDP). Samples were first prepared for single cell RNA-seq libraries by Camila dos Santos. The Single Cell Sequencing core at CSHL provided the sequencing files. I performed initial quality control steps and analyses to identify differences in mammary gland composition and gene expression between women who had never been pregnant and whom had previously been pregnant. However, given that one of the factors included in the data collection was age at first pregnancy, this project became a collaboration with Sam Henry, who is now analyzing the samples in the context of age of parity to include in her own dissertation.

10. Experimental Procedures

10.1 Experimental Model and Subject details

Animal studies

Nulliparous female C57BL/6 mice were purchased from Jackson Laboratory. All animals were housed in a 12 hour light-dark cycle with controlled temperature and humidity at 72ºF and 40-60%, respectively, with access to dry food and water ad libitum. All animal experiments were performed in accordance with the CSHL Institutional Animal Care and Use Committee.

Human samples

Patient-derived normal mammary tissues were collected during reduction mammoplasties via partners from Northwell Health, in compliance with Institutional Review Board protocol IRB-03–012 and IRB 20–0150 and with written informed consent from the patients. Samples for organoid culturing were obtained by Spector et al. and frozen vials of MEC-derived organoids were shared with our lab (Bhatia et al., 2022).

10.2 Method details

Murine Organoid Derivation and Culture

Mammary-derived organoid cultures were cultured as previously described (Ciccone et al., 2020), within matrigel (Corning) domes, submerged in Advanced DMEM/F12+++ media c supplemented with 1X ITS (Insulin/Transferrin/Sodium Selenite, Gibco #41400-045) and FGF-2 at 5 nm (PeproTech, Cat# 450-33): essential medium. Organoid culture media was changed every 2 days. FGF-2 was then withdrawn from the organoid cultures for 24 hours after which the treatment regimen was initiated. Organoid conditions with “low” levels of estrogen were grown with media supplemented with 33.3 ng/mL of 17-β-Estradiol (Sigma #E2758), and those with “high” levels of estrogen were grown in the presence of 66.6 ng/mL of 17-β-Estradiol. Mouse organoid conditions to mimic pregnancy were cultured with media supplemented with 66.6 ng/mL of 17-β-Estradiol, 200 ng/mL of progesterone

(Sigma #P8783) and 200 ng/mL of prolactin (Sigma #L4021). In all conditions, hormone treatment was carried out for 48 hours. For the preparation of scRNAseq, organoid cultures were dissociated with 500 µL of Cell Recovery Solution (Corning® # 354253) for 30 minutes, followed by incubation with 500 µL of cold Tryp-LE (Thermo Fisher Scientific #12604-013) at 37 °C for 10 minutes. Dissociated organoids were resuspended with 1 mL , transferred to a 15 mL BSA pre-coated Falcon tube, and spun at 300 G for 5 minutes. Dissociated organoid cells were then resuspended in 1 mL of media and submitted for library preparation and sequencing.

Human Organoids

Established patient-derived normal breast organoid cultures (Bhatia et al., 2022) were cultured as previously described, within matrigel (Corning) domes, submerged in media containing 10% R-Spondin1 conditioned medium, 5 nmol/L Neuregulin 1 (Peprotech, 100–03), 5 ng/mL FGF7 (Peprotech, 100–19), 20 ng/mL FGF10 (Peprotech, 100–26), 5 ng/mL EGF (Peprotech, AF-100–15), 100 ng/mL Noggin (Peprotech, 120–10C), 500 nmol/L A83–01 (Tocris, 2939), 5 µmol/L Y-27632 (Abmole, Y-27632), 500 nmol/L SB202190 (Sigma, S7067), 1× B27 supplement (Gibco, 17504–44), 1.25 mmol/L N-acetylcysteine (Sigma, A9165), 5 mmol/L nicotinamide (Sigma, N0636), and 50 µg/mL Primocin (Invitrogen, ant-pm-1) in ADF+++. Organoid culture media was changed every 3 days, and organoids were passed every 5-8 days to avoid confluency. Human MEC derived organoids were treated with pregnancy hormone concentrations similar to those utilized for the growth of murine organoids. We confirmed with qPCR analyses that these growth conditions induced the expression of casein genes, and utilized such analysis to define the collection time points for scRNAseq (untreated cultures, and 10 and 21 after supplementation of media with pregnancy hormones). Cultured human organoids were processed similarly to mouse organoids prior submission for library preparation and sequencing.

Human Casein primer sequence - See **Table 2** for qPCR primer sequences. Human b-actin was used for normalization, so this sequence is included as well.

Table 2. Primer sequences for CSN2/CSN3

Name	Primer sequence
Human b-actin	FWD 5'AGA GCT ACG AGC TGC CTG AC 3'
	REV 5'AGC ACT GTG TTG GCG TAC AG
Human Csn2 (SET 11)	FWD 5'CCC ACC CAC CAG ATC TAC C 3'
	REV 5' CAT CAT ATT TCC AGT CTC AGT CAA 3'
Human Csn3 (SET 10)	FWD 5'GTT GCA GTT ACT CCA CCT ACG3'
	REV 5'AGG AGA GTG TGA AGT AGT AAT TTG G5'

scRNAseq library preparation and data analysis of murine and human organoids.

Libraries were prepared with the 10X Chromium platform for single cell libraries. The libraries were run with 3' chemistry single end sequencing and indexing using the Illumina NextSeq 550 high output platform. Libraries from mouse samples were aligned to the mm10 genome using CellRanger v3, and human libraries were aligned to the GRCh38-2020 genome using CellRanger v6. All further data processing and analysis was completed in the Seurat package in R version 4.0.0. Initial quality control involved removing any cells with mitochondrial RNA expression over 15%, removing clusters with high ribosomal RNA expression and removing clusters with >5,000 and <200 features. For batch effect correction and normalization, anchors were discovered between the datasets using the FindIntegrationAnchors() function before integrating with the IntegrateData() function. Throughout the analysis and re-clustering, repeated quality control through evaluation of clusters with a large proportion of cells expressing low features or high mitochondrial RNA content were removed. This ensured the removal of low quality clusters at each stage of the processing and analysis. Uniform manifold approximation and projection (UMAP) clustering using a shared nearest neighbor graph (SNN) was performed. The resolution of each clustering step with the help of Clustree (Zappia & Oshlack, 2018), and all of the analysis presented here were run with a resolution of 0.3, with the exception to data analysis shown on Figure 14, which due to the large number of samples, was performed with a resolution of 0.2. Differences in cell numbers between datasets were analyzed with the Propeller package, which uses a robust and flexible method that leverages biological replication to find

statistically significant differences in cell type proportions between groups (Phipson et al., 2022). Regulon analysis for each culturing condition and species was performed using SCENIC (Single-Cell rEgulatory Network Inference and Clustering) version 1.2.0 in R (Aibar et al., 2017).

Identity assignment of epithelial cell clusters were assigned using module scores based on known lineage markers (Henry et al., 2021) (**Tables 3 and 4**), assigned to each cluster in each Sobj in order to generate ternary plots, to further assess cluster identities. To evaluate differentially expressed genes (DEGs) within our data, we utilized the FindMarkers() function, which completes a Wilcoxon rank-sum test to identify DEGs between clusters. For visualizing DEGs and particular genes of interest within the data, we utilized the following functions: DotPlot(), FeaturePlot(), VlnPlot() and HeatMap(). For a dendrogram analysis of the relative relatedness of the clusters, we utilized the BuildClusterTree() function using default parameters. In order to ensure our analysis only involved epithelial cells, those that expressed low epithelial features (low *Epcam* and low cytokeratin expression) were eliminated from our analyses.

Table 3. Murine MEC lineage markers

Broad lineage	Cellular state	Genes
Myoepithelial	Progenitor	Epcam, Lgals1, Bptf, Krt17, Ppic, Mdk, Krt14, Krt5, Acta2, Mgp, Lmod, Lhfp, Cxcl14, Serpina3n, Cnn1, Vcam1, Nrg1, Col7a1, Nexn, Il17b, Mylk, Sparc, Lgr5, Jag1, Scn7a, Trp63, Lbp, Tagln, Bmpr2, Fgf1, Lipg, Arc, Id4, Mme, Mmp2, Igfbp3
	Differentiated	Epcam, Lgals1, Krt17, Krt14, Krt5, Acta2, Mgp, Lmod, Oxtr, Cxcl14, Cnn1, Mylk, Sparc, Tagln, Bmpr2, Igfbp3
Luminal Ductal	Ductal Rcan1+ differentiated	Epcam, Krt8, Krt18, Prlr, Armcx2, Ak3, Cdk19, Cited1, Areg, Stc2, Rcan1, Prom1, Esr1, Pgr, Pak6, Cdo1, Wnt5, Cxcl15, Ly6a, Tspan9, Pir, Fgb, Cd14, Fam83g, Dusp4, Tph1, Notch3, Il6ra, Itpripl2, Calca, Ptbp2
	Ductal Fxyd2+ differentiated	Epcam, Krt8, Krt18, Prlr, Prrg2, Ak3, Cdk19, Fxyd2, Areg, Stc2, Prom1, Esr1, Pgr, Cdo1, Gstm2, Wnt5, Cxcl15, Ly6a, Tspan9, Gltp, Cd14, Ppme1, Adck5, Dusp4, Tph1, Notch3, Itpripl1, Calca
Luminal Alveolar	Progenitor	Epcam, Krt8, Krt18, Col9a1, Aldh1a3, Il1rn, Itga2, Csn1s1, Car2, Csn2, Ceacam1, Bptf, Kit, Armcx2, Csf3, Cxcl1, Ndst1, Ezh2, Ap1g1, Areg, Cd14, Snx27, Lbp, Bmpr2, Egln3, Erf, Ptbp2

	Differentiated	Epcam, Krt8, Krt18, Col9a1, Il1rn, Itga2, Csn1s1, Car2, Csn2, Bptf, Lalba, Kit, Armcx2, Trf, Cxcl1, Ndst1, Ezh2, Ap1g1, Areg, Spp, Sfxn3, Cd14, Snx27, Mfsd5, S100a8, Lbp, Gjb2, Notch3, Il6ra, Kctd20, Erf, Ptbp2, Ireb2
	Proliferating	Epcam, Krt8, Krt18, Col9a1, Il1m, Itga2, Csn1s1, Car2, Lgals1, Stmn1, Csn2, Tgfb3, Mki67, Lalba, Lockd, Kit, Armcx2, Cxcl1, Ndst1, H2afz, Ezh2, Ap1g1, Ube2c, Prrg2, Ak3, Cdk19, Areg, Sfxn3, Mdk, Ly6a, Krt14, Cd14, Snx27, Mfsd5, Top2, Lbp, Gjb2, Tagln, Cenpa, Bmpr2, Fam83g, Rangrf, Ppme1, Notch3, Hmgb2, Il6ra, Itpripl2, Kctd20, Erf, Setd7, Cwc22, Ptbp2, Ireb2, Parp1, Sms, Sp110, Cxcr4

Table 4. Human MEC lineage markers

Broad lineage	Specific cell type	Genes
Luminal ductal	Differentiated	KRT8, ANKRD30A, DNAJC12, TMC5, TBX3, AFF3, TMEM45B, EFHD1, SYTL2, SFMBT2, TSPAN5, PRLR, GALNT6, GSTM3, PTHLH, ITGAV, EREG, ERBB2, AREG, AR, FBP1, KRT18, MLPH, FOXA1, ELOVL5, CD164, MUC1, RUNX1, KDM5B, KRT19, GATA3, CLDN4, CLDN7, ITGA2, ITGB6, SERPINA1, NPY1R, GFRA1, ESR1, PIEZO2, NEK10, PREX1, PGR, CITED1, TSPAN13, FOXP1, ARMCX3, ITGA6, KRT7
Myoepithelial	Progenitor	CXCL14, TP63, EGR2, FBXO32, HAS3, ANO1, ETV1, CLDN11, BRD2, PER2, MME, ACTG2, MYLK, ACTA2, DKK3, GLT8D2, KRT17, KRT5, KRT14, TAGLN, MYH11, LAMB3, OXTR, ZNF503, APOE, STMN1, ITGB4, CITED2

	Differentiated	WIF1, GRP, CD200, NTF3, CLMP, ACTG2, KRT17, TRNP1, PTPRZ1, NGFR, LGR4, KRT14, KRT5, MYLK, ACTA2, ERG, DKK3, GLT8D2, LMOD1, ITGB1, APOE, SEMA5A, SPRY2, MYO1E, CAV1, TAGLN, LAMB3, ZNF503, ITGB4, OXTR
Progenitors / stem cells	Bipotential	GABRP, PTN, NCALD, BBOX1, RGS2, KIT, MUC15, ANPEP, PROM1, KRT16, NFATC2, S100A6, LY6E, CD14, KRT19, CLDN4, CLDN7, KRT15, IGF2BP2, SLPI, CHI3L1, LIF, PIGR, ELF5, ALDH1A3, SOX9, FGFBP1, KLF5, CRYAB, ANXA1, FOLR1, SAA1, NACA, FTH1, GAS5, ITGB6, KRT7, MMP7, LAMB3
	Luminal	CYP24A1, CCL20, SLC6A14, CXCL5, CXCL1, SAA2, TNIP3, CALML5, KRT15, IGF2BP2, SLPI, CHI3L1, LIF, PIGR, ALDH1A3, FGFBP1, ANXA1, ELF5, FOLR1, SAA1, CAV1, TPT1, GNB2L1, NACA, FTH1, ITGB6, KRT7, ITGA6, MMP7, MYO1E

For data presented on Figure 3, organoids derived from MECs of 3 never pregnant, nulliparous female mice were utilized on the generation of scRNA-seq libraries, using the 10X Chromium platform, yielding a total 10,508 Mouse Organoid (MO) cells. For data presented on Figure 7, only epithelial cells (Epcam+, Krt5+, Krt14+, Krt8+, and Krt18+) were selected from publicly available, intact mammary tissue scRNAseq datasets (Bach et al., 2017; Henry et al., 2021). After integration with mammary organoids scRNAseq (Fig. 1A), a total of 6 Organoid-MECs Integrated with Mouse-MECs (OIM) clusters, composed of 10,502 cells from organoid cultures and 6,011 cells from intact mammary tissue. Batch effect correction was performed to account for the different number of cells in both organoids and intact tissue samples and any technical variability due to sequencing samples on different days.

For data presented on Figure 8, organoid cultures treated with estrogen concentrations for 48 were prepared for scRNA-seq with the 10X Chromium platform. Quality control filtering steps and clustering alongside the untreated murine MEC-derived organoids, yielded a total of 9 clusters containing 31,802 Organoid-MECs with Estrogen (OE). From these, 10,508 cells were from untreated samples, 9,695 cells were from samples treated with a low dose of Estrogen (33.3 ng/mL), and 11,599 cells were from samples treated with a high dose of Estrogen (66.6 ng/mL). Each of the cell cluster identities were determined once more using previously described lineage commitment markers in intact mammary tissue (Henry et al., 2021).

For data presented on Figure 11, quality control steps and clustering of datasets from organoids without treatment, and those treated with EPP, resulted in 10 Organoids with/without EPP (OP) clusters, with a total of 26,971 cells, 10,508 from our no treatment samples and 16,463 from our samples treated with EPP. Untreated organoids and those treated with EPP were also merged with publicly available datasets from murine mammary tissue collected at different pregnancy stages (Bach et al., 2017). This included, pre-QC, 4,376 cells from NP mammary glands, 6,021 cells from gestation, 9,603 cells from lactation and 5,806 cells from post-involution. After QC filtering, we obtained a total of 7 clusters, with a total of 4,004 cells from NP MECs, 5,216 MECs from mice during gestation, 8,222 from mice during lactation, 5,607 from mice during involution, 10,497 untreated organoid cells, and 16,449 pregnancy hormone treated organoid cells.

For data presented on Figure 17, scRNAseq profiles of untreated human organoids, and pregnancy hormone treated ones (10 days and 21 days of EPP treatment), were removed from low quality cells, yielding a total of 14,621 cells from organoids without treatment, 5,888 cells from organoids at 10 days of EPP treatment, and 8,167 cells from organoids at 21 days of EPP treatment, respectively, which were utilized on further analysis.

For data investigating similarities across species, murine genes were converted into their human orthologs before scRNAseq data integration (Zilionis et al., 2019). Clusters with low levels of *EPCAM*

and cytokeratin expression were considered as low-quality cells and removed them from further analysis. This approach yielded a total of 5 clusters of Murine and Human Organoids with EPP (MHP) objects, with 14,055 cells from humans and 16,463 cells from murine MEC organoids

Pathway analysis

Pathway analysis was performed using Gene Set Enrichment Analysis (GSEA) v3.0 and with the Molecular Signatures Database (MSigDB) Hallmark Terms (Liberzon et al., 2015; Mootha et al., 2003; Subramanian et al., 2005). This database was selected with the purpose of obtaining an overview of the processes each cellular cluster was undergoing. The resulting hallmark terms were further filtered based on their nominal (nom) p-value (<0.05), with the purpose of only showing significant terms per cluster and/or condition. The -log(nom p-value) for each hallmark term was calculated so that these could be visualized based on significance.

On Figure 5, given that most MO clusters had similar signature gene modules, differentially expressed pathways with an adjusted p-value of <0.06 were kept for further analysis.

Collection of intact human mammary samples for scRNA-seq

Processing of mammary tissue from never pregnant and post-partum women consisted of mincing the tissue and digesting it with 1 x Collagenase /Hyaluronidase (10 × solution) at 37C (with constant agitation) in RPMI 1640 GlutaMAX supplemented with 5% FBS. After 4-6 hours, the tissue was washed with cold HBSS supplemented with 5% FBS, incubated with TrypLE Express, and washed again with HBSS. This was followed by incubation with Dispase supplemented with 80U DNaseI, and filtering through a 100um Cell Strainer (see methods section in Henry et al. 2021). Digested tissue was resuspended in freezing media and kept frozen in a liquid nitrogen tank for future sequencing and organoid culturing.

scRNAseq library preparation and data analysis of intact human mammary tissue

Libraries were prepared with the 10X Chromium platform for single cell libraries. The libraries were run with 3' chemistry single end sequencing and indexing using the Illumina NextSeq 550 high output platform. Libraries were aligned to the GRCh38-2020 genome using CellRanger v6. All further data processing and analysis was completed in the Seurat package in R version 4.0.0. Initial QC steps involved eliminating cells with less than 200 features and over 5,000 features, and eliminating cells with over 25% mitochondrial content.

10.3 Data availability

The resulting data sets from this project will be deposited on the Gene Expression Omnibus (GEO) once it is published. Code will also be made available, accordingly.

11. References

Abbassi-Ghanavati, M., Greer, L. G., & Cunningham, F. G. (2009). Pregnancy and Laboratory Studies: A Reference Table for Clinicians. *Obstetrics & Gynecology*, *114*(6), 1326. https://doi.org/10.1097/AOG.0b013e3181c2bde8

Abd El-Rehim, D. M., Pinder, S. E., Paish, C. E., Bell, J., Blamey, R., Robertson, J. F., Nicholson, R. I., & Ellis, I. O. (2004). Expression of luminal and basal cytokeratins in human breast carcinoma. *The Journal of Pathology*, *203*(2), 661–671. https://doi.org/10.1002/path.1559

Aibar, S., González-Blas, C. B., Moerman, T., Huynh-Thu, V. A., Imrichova, H., Hulselmans, G., Rambow, F., Marine, J.-C., Geurts, P., Aerts, J., van den Oord, J., Atak, Z. K., Wouters, J., & Aerts, S. (2017). SCENIC: Single-cell regulatory network inference and clustering. *Nature Methods*, *14*(11), Article 11. https://doi.org/10.1038/nmeth.4463

Akers, R. M. (2017). A 100-Year Review: Mammary development and lactation. *Journal of Dairy Science*, *100*(12), 10332–10352. https://doi.org/10.3168/jds.2017-12983

Ali, S., & Ali, S. (1998). Prolactin Receptor Regulates Stat5 Tyrosine Phosphorylation and Nuclear Translocation by Two Separate Pathways *. *Journal of Biological Chemistry*, *273*(13), 7709–7716. https://doi.org/10.1074/jbc.273.13.7709

Allan, G. J., Beattie, J., & Flint, D. J. (2004). The role of IGFBP-5 in mammary gland development and involution. *Domestic Animal Endocrinology*, *27*(3), 257–266. https://doi.org/10.1016/j.domaniend.2004.06.009

Allinen, M., Beroukhim, R., Cai, L., Brennan, C., Lahti-Domenici, J., Huang, H., Porter, D., Hu, M., Chin, L., Richardson, A., Schnitt, S., Sellers, W. R., & Polyak, K. (2004). Molecular characterization of the tumor microenvironment in breast cancer. *Cancer Cell*, *6*(1), 17–32. https://doi.org/10.1016/j.ccr.2004.06.010

Anderson, E. (2002). The role of oestrogen and progesterone receptors in human mammary development and tumorigenesis. *Breast Cancer Research: BCR*, *4*(5), 197–201. https://doi.org/10.1186/bcr452

Anderson, S. M., Rudolph, M. C., McManaman, J. L., & Neville, M. C. (2007). Key stages in mammary gland development. Secretory activation in the mammary gland: It's not just about milk protein synthesis! *Breast Cancer Research*, *9*(1), 204. https://doi.org/10.1186/bcr1653

Andres, A.-C., & Djonov, V. (2010). The Mammary Gland Vasculature Revisited. *Journal of Mammary Gland Biology and Neoplasia*, *15*(3), 319–328. https://doi.org/10.1007/s10911-010-9186-9

Arendt, L. M., Evans, L. C., Rugowski, D. E., Garcia-Barchino, M. J., Rui, H., & Schuler, L. A. (2009). Ovarian Hormones Are Not Required for PRL-induced Mammary Tumorigenesis, But Estrogen Enhances Neoplastic Processes. *The Journal of Endocrinology*, *203*(1), 99–110. https://doi.org/10.1677/JOE-09-0221

Arendt, L. M., Grafwallner-Huseth, T. L., & Schuler, L. A. (2009). Prolactin–Growth Factor Crosstalk Reduces Mammary Estrogen Responsiveness Despite Elevated ERα Expression. *The American Journal of Pathology*, *174*(3), 1065–1074. https://doi.org/10.2353/ajpath.2009.080719

Arendt, L. M., & Kuperwasser, C. (2015). Form and function: How estrogen and progesterone regulate the mammary epithelial hierarchy. *Journal of Mammary Gland Biology and Neoplasia*, *20*(0), 9. https://doi.org/10.1007/s10911-015-9337-0

Asselin-Labat, M.-L., Sutherland, K. D., Barker, H., Thomas, R., Shackleton, M., Forrest, N. C., Hartley, L., Robb, L., Grosveld, F. G., van der Wees, J., Lindeman, G. J., & Visvader, J. E. (2007). Gata-3 is an essential regulator of mammary-gland morphogenesis and luminal-cell differentiation. *Nature Cell Biology*, *9*(2), 201–209. https://doi.org/10.1038/ncb1530

Asselin-Labat, M.-L., Sutherland, K. D., Vaillant, F., Gyorki, D. E., Wu, D., Holroyd, S., Breslin, K., Ward, T., Shi, W., Bath, M. L., Deb, S., Fox, S. B., Smyth, G. K., Lindeman, G. J., & Visvader, J. E. (2011). Gata-3 negatively regulates the tumor-initiating capacity of mammary luminal progenitor cells and targets the putative tumor suppressor caspase-14. *Molecular and Cellular Biology*, *31*(22), 4609–4622. https://doi.org/10.1128/MCB.05766-11

Atwood, C. S., Hovey, R. C., Glover, J. P., Chepko, G., Ginsburg, E., Robison, W. G., & Vonderhaar, B. K. (2000). Progesterone induces side-branching of the ductal epithelium in the mammary glands of peripubertal mice. *The Journal of Endocrinology*, *167*(1), 39–52. https://doi.org/10.1677/joe.0.1670039

Aupperlee, M. D., Drolet, A. A., Durairaj, S., Wang, W., Schwartz, R. C., & Haslam, S. Z. (2009). Strain-Specific Differences in the Mechanisms of Progesterone Regulation of Murine Mammary Gland Development. *Endocrinology*, *150*(3), 1485–1494. https://doi.org/10.1210/en.2008-1459

Aupperlee, M. D., Leipprandt, J. R., Bennett, J. M., Schwartz, R. C., & Haslam, S. Z. (2013). Amphiregulin mediates progesterone-induced mammary ductal development during puberty. *Breast Cancer Research*, *15*(3), R44. https://doi.org/10.1186/bcr3431

Bach, K., Pensa, S., Grzelak, M., Hadfield, J., Adams, D. J., Marioni, J. C., & Khaled, W. T. (2017). Differentiation dynamics of mammary epithelial cells revealed by single-cell RNA sequencing. *Nature Communications*, *8*(1), 2128. https://doi.org/10.1038/s41467-017-02001-5

Bahcecioglu, G., Yue, X., Howe, E., Guldner, I., Stack, M. S., Nakshatri, H., Zhang, S., & Zorlutuna, P. (2021). Aged Breast Extracellular Matrix Drives Mammary Epithelial Cells to an Invasive and Cancer-Like Phenotype.

Advanced Science (Weinheim, Baden-Wurttemberg, Germany), *8*(22), e2100128. https://doi.org/10.1002/advs.202100128

Baker, L., BeGora, M., Au Yeung, F., Feigin, M. E., Rosenberg, A. Z., Lowe, S. W., Kislinger, T., & Muthuswamy, S. K. (2016). Scribble is required for pregnancy-induced alveologenesis in the adult mammary gland. *Journal of Cell Science*, *129*(12), 2307–2315. https://doi.org/10.1242/jcs.185413

Bambhroliya, A., Van Wyhe, R. D., Kumar, S., Debeb, B. G., Reddy, J. P., Van Laere, S., El-Zein, R., Rao, A., & Woodward, W. A. (2018). Gene set analysis of post-lactational mammary gland involution gene signatures in inflammatory and triple-negative breast cancer. *PLoS ONE*, *13*(4), e0192689. https://doi.org/10.1371/journal.pone.0192689

Bartley, J. C., Emerman, J. T., & Bissell, M. J. (1981). Metabolic cooperativity between epithelial cells and adipocytes of mice. *American Journal of Physiology-Cell Physiology*, *241*(5), C204–C208. https://doi.org/10.1152/ajpcell.1981.241.5.C204

Barton, M., Santucci-Pereira, J., & Russo, J. (2014). Molecular Pathways Involved in Pregnancy-Induced Prevention Against Breast Cancer. *Frontiers in Endocrinology*, *5*. https://www.frontiersin.org/articles/10.3389/fendo.2014.00213

Basak, P., Chatterjee, S., Weger, S., Bruce, M. C., Murphy, L. C., & Raouf, A. (2015). Estrogen regulates luminal progenitor cell differentiation through H19 gene expression. *Endocrine-Related Cancer*, *22*(4), 505–517. https://doi.org/10.1530/ERC-15-0105

Behbod, F., Kittrell, F. S., LaMarca, H., Edwards, D., Kerbawy, S., Heestand, J. C., Young, E., Mukhopadhyay, P., Yeh, H.-W., Allred, D. C., Hu, M., Polyak, K., Rosen, J. M., & Medina, D. (2009). An intraductal human-in-mouse transplantation model mimics the subtypes of ductal carcinoma in situ. *Breast Cancer Research: BCR*, *11*(5), R66. https://doi.org/10.1186/bcr2358

Beleut, M., Rajaram, R. D., Caikovski, M., Ayyanan, A., Germano, D., Choi, Y., Schneider, P., & Brisken, C. (2010). Two distinct mechanisms underlie progesterone-induced proliferation in the mammary gland. *Proceedings of the National Academy of Sciences of the United States of America*, *107*(7), 2989–2994. https://doi.org/10.1073/pnas.0915148107

Ben-Jonathan, N., & Hugo, E. (2015). Prolactin (PRL) in Adipose Tissue: Regulation and Functions. In P. Diakonova Maria (Ed.), *Recent Advances in Prolactin Research* (pp. 1–35). Springer International Publishing. https://doi.org/10.1007/978-3-319-12114-7_1

Betterman, K. L., Paquet-Fifield, S., Asselin-Labat, M.-L., Visvader, J. E., Butler, L. M., Stacker, S. A., Achen, M. G., & Harvey, N. L. (2012). Remodeling of the lymphatic vasculature during mouse mammary gland morphogenesis is mediated via epithelial-derived lymphangiogenic stimuli. *The American Journal of Pathology*, *181*(6), 2225–2238. https://doi.org/10.1016/j.ajpath.2012.08.035

Betts, C. B., Pennock, N. D., Caruso, B. P., Ruffell, B., Borges, V. F., & Schedin, P. (2018). Mucosal Immunity in the Female Murine Mammary Gland. *Journal of Immunology (Baltimore, Md.: 1950)*, *201*(2), 734–746. https://doi.org/10.4049/jimmunol.1800023

Bhatia, S., Kramer, M., Russo, S., Naik, P., Arun, G., Brophy, K., Andrews, P., Fan, C., Perou, C. M., Preall, J., Ha, T., Plenker, D., Tuveson, D. A., Rishi, A., Wilkinson, J. E., McCombie, W. R., Kostroff, K., & Spector, D. L. (2022). Patient-Derived Triple-Negative Breast Cancer Organoids Provide Robust Model Systems That Recapitulate Tumor Intrinsic Characteristics. *Cancer Research*, *82*(7), 1174–1192. https://doi.org/10.1158/0008-5472.CAN-21-2807

Bhat-Nakshatri, P., Gao, H., Sheng, L., McGuire, P. C., Xuei, X., Wan, J., Liu, Y., Althouse, S. K., Colter, A., Sandusky, G., Storniolo, A. M., & Nakshatri, H. (2021). A single-cell atlas of the healthy breast tissues reveals clinically relevant clusters of breast epithelial cells. *Cell Reports Medicine*, *2*(3), 100219. https://doi.org/10.1016/j.xcrm.2021.100219

Blakely, C. M., Stoddard, A. J., Belka, G. K., Dugan, K. D., Notarfrancesco, K. L., Moody, S. E., D'Cruz, C. M., & Chodosh, L. A. (2006). Hormone-Induced Protection against Mammary Tumorigenesis Is Conserved in Multiple Rat Strains and Identifies a Core Gene Expression Signature Induced by Pregnancy. *Cancer Research*, *66*(12), 6421–6431. https://doi.org/10.1158/0008-5472.CAN-05-4235

Bleach, R., & McIlroy, M. (2018). The Divergent Function of Androgen Receptor in Breast Cancer; Analysis of Steroid Mediators and Tumor Intracrinology. *Frontiers in Endocrinology*, *9*, 594. https://doi.org/10.3389/fendo.2018.00594

Bracken, A. P., Ciro, M., Cocito, A., & Helin, K. (2004). E2F target genes: Unraveling the biology. *Trends in Biochemical Sciences*, *29*(8), 409–417. https://doi.org/10.1016/j.tibs.2004.06.006

Bresson, L., Faraldo, M. M., Di-Cicco, A., Quintanilla, M., Glukhova, M. A., & Deugnier, M.-A. (2018). Podoplanin regulates mammary stem cell function and tumorigenesis by potentiating Wnt/β-catenin signaling. *Development*, *145*(4), dev160382. https://doi.org/10.1242/dev.160382

Brisken, C., Kaur, S., Chavarria, T. E., Binart, N., Sutherland, R. L., Weinberg, R. A., Kelly, P. A., & Ormandy, C. J. (1999). Prolactin Controls Mammary Gland Development via Direct and Indirect Mechanisms. *Developmental Biology*, *210*(1), 96–106. https://doi.org/10.1006/dbio.1999.9271

Brisken, C., Park, S., Vass, T., Lydon, J. P., O'Malley, B. W., & Weinberg, R. A. (1998). A paracrine role for the epithelial progesterone receptor in mammary gland development. *Proceedings of the National Academy of Sciences*, *95*(9), 5076–5081. https://doi.org/10.1073/pnas.95.9.5076

Brisken, C., & Scabia, V. (2020). 90 YEARS OF PROGESTERONE: Progesterone receptor signaling in the normal breast and its implications for cancer. *Journal of Molecular Endocrinology*, *65*(1), T81–T94. https://doi.org/10.1530/JME-20-0091

Bu, W., Chen, J., Morrison, G. D., Huang, S., Creighton, C. J., Huang, J., Chamness, G. C., Hilsenbeck, S. G., Roop, D. R., Leavitt, A. D., & Li, Y. (2011a). Keratin 6a marks mammary bipotential progenitor cells that can give rise to a unique tumor model resembling human normal-like breast cancer. *Oncogene*, *30*(43), 4399–4409. https://doi.org/10.1038/onc.2011.147

Bu, W., Chen, J., Morrison, G. D., Huang, S., Creighton, C. J., Huang, J., Chamness, G. C., Hilsenbeck, S. G., Roop, D. R., Leavitt, A. D., & Li, Y. (2011b). Keratin 6a marks mammary bipotential progenitor cells that can give rise to a unique tumor model resembling human normal-like breast cancer. *Oncogene*, *30*(43), Article 43. https://doi.org/10.1038/onc.2011.147

Bussolati, G., Cassoni, P., Ghisolfi, G., Negro, F., & Sapino, A. (1996). Immunolocalization and gene expression of oxytocin receptors in carcinomas and non-neoplastic tissues of the breast. *The American Journal of Pathology*, *148*(6), 1895–1903.

Byers, S. L., Wiles, M. V., Dunn, S. L., & Taft, R. A. (2012). Mouse Estrous Cycle Identification Tool and Images. *PLoS ONE*, *7*(4), e35538. https://doi.org/10.1371/journal.pone.0035538

Cai, C., Geng, A., Wang, M., Yang, L., Yu, Q. C., & Zeng, Y. A. (2020). Amphiregulin mediates the hormonal regulation on Rspondin-1 expression in the mammary gland. *Developmental Biology*, *458*(1), 43–51. https://doi.org/10.1016/j.ydbio.2019.10.006

Caldon, C. E. (2014). Estrogen Signaling and the DNA Damage Response in Hormone Dependent Breast Cancers. *Frontiers in Oncology*, *4*, 106. https://doi.org/10.3389/fonc.2014.00106

Carroll, J. S., Liu, X. S., Brodsky, A. S., Li, W., Meyer, C. A., Szary, A. J., Eeckhoute, J., Shao, W., Hestermann, E. V., Geistlinger, T. R., Fox, E. A., Silver, P. A., & Brown, M. (2005). Chromosome-Wide Mapping of Estrogen

Receptor Binding Reveals Long-Range Regulation Requiring the Forkhead Protein FoxA1. *Cell*, *122*(1), 33–43. https://doi.org/10.1016/j.cell.2005.05.008

Carsol, J.-L., Gingras, S., & Simard, J. (2002). Synergistic Action of Prolactin (PRL) and Androgen on PRL-Inducible Protein Gene Expression in Human Breast Cancer Cells: A Unique Model for Functional Cooperation between Signal Transducer and Activator of Transcription-5 and Androgen Receptor. *Molecular Endocrinology*, *16*(7), 1696–1710. https://doi.org/10.1210/mend.16.7.0875

Chan, S. R., Rickert, C. G., Vermi, W., Sheehan, K. C. F., Arthur, C., Allen, J. A., White, J. M., Archambault, J., Lonardi, S., McDevitt, T. M., Bhattacharya, D., Lorenzi, M. V., Allred, D. C., & Schreiber, R. D. (2014). Dysregulated STAT1-SOCS1 control of JAK2 promotes mammary luminal progenitor cell survival and drives ERα+ tumorigenesis. *Cell Death and Differentiation*, *21*(2), 234–246. https://doi.org/10.1038/cdd.2013.116

Chang, T. H.-T., Kunasegaran, K., Tarulli, G. A., De Silva, D., Voorhoeve, P. M., & Pietersen, A. M. (2014). New insights into lineage restriction of mammary gland epithelium using parity-identified mammary epithelial cells. *Breast Cancer Research: BCR*, *16*(1), R1. https://doi.org/10.1186/bcr3593

Chen, C.-C., Boxer, R. B., Stairs, D. B., Portocarrero, C. P., Horton, R. H., Alvarez, J. V., Birnbaum, M. J., & Chodosh, L. A. (2010). Akt is required for Stat5 activation and mammary differentiation. *Breast Cancer Research : BCR*, *12*(5), R72. https://doi.org/10.1186/bcr2640

Chie, W. C., Hsieh, C., Newcomb, P. A., Longnecker, M. P., Mittendorf, R., Greenberg, E. R., Clapp, R. W., Burke, K. P., Titus-Ernstoff, L., Trentham-Dietz, A., & MacMahon, B. (2000). Age at any full-term pregnancy and breast cancer risk. *American Journal of Epidemiology*, *151*(7), 715–722. https://doi.org/10.1093/oxfordjournals.aje.a010266

Choudhury, S., Almendro, V., Merino, V. F., Wu, Z., Maruyama, R., Su, Y., Martins, F. C., Fackler, M. J., Bessarabova, M., Kowalczyk, A., Conway, T., Beresford-Smith, B., Macintyre, G., Cheng, Y.-K., Lopez-Bujanda, Z., Kaspi, A., Hu, R., Robens, J., Nikolskaya, T., … Polyak, K. (2013). Molecular profiling of human mammary gland links breast cancer risk to a p27(+) cell population with progenitor characteristics. *Cell Stem Cell*, *13*(1), 117–130. https://doi.org/10.1016/j.stem.2013.05.004

Christov, K., Chew, K. L., Ljung, B. M., Waldman, F. M., Duarte, L. A., Goodson, W. H., Smith, H. S., & Mayall, B. H. (1991). Proliferation of normal breast epithelial cells as shown by in vivo labeling with bromodeoxyuridine. *The American Journal of Pathology*, *138*(6), 1371–1377.

Ciarloni, L., Mallepell, S., & Brisken, C. (2007). Amphiregulin is an essential mediator of estrogen receptor α function in mammary gland development. *Proceedings of the National Academy of Sciences*, *104*(13), 5455–5460. https://doi.org/10.1073/pnas.0611647104

Cicatiello, L., Mutarelli, M., Grober, O. M. V., Paris, O., Ferraro, L., Ravo, M., Tarallo, R., Luo, S., Schroth, G. P., Seifert, M., Zinser, C., Luisa Chiusano, M., Traini, A., De Bortoli, M., & Weisz, A. (2010). Estrogen Receptor α Controls a Gene Network in Luminal-Like Breast Cancer Cells Comprising Multiple Transcription Factors and MicroRNAs. *The American Journal of Pathology*, *176*(5), 2113–2130. https://doi.org/10.2353/ajpath.2010.090837

Ciccone, M. F., Trousdell, M. C., & dos Santos, C. O. (2020). Characterization of Organoid Cultures to Study the Effects of Pregnancy Hormones on the Epigenome and Transcriptional Output of Mammary Epithelial Cells. *Journal of Mammary Gland Biology and Neoplasia*, *25*(4), 351–366. https://doi.org/10.1007/s10911-020-09465-0

Clarke, R. B., Howell, A., Potten, C. S., & Anderson, E. (1997). Dissociation between Steroid Receptor Expression and Cell Proliferation in the Human Breast1. *Cancer Research*, *57*(22), 4987–4991.

CLELAND, W. H., MENDELSON, C. R., & SIMPSON, E. R. (1985). Effects of Aging and Obesity on Aromatase Activity of Human Adipose Cells *. *The Journal of Clinical Endocrinology & Metabolism*, *60*(1), 174–177. https://doi.org/10.1210/jcem-60-1-174

Colleluori, G., Perugini, J., Barbatelli, G., & Cinti, S. (2021). Mammary gland adipocytes in lactation cycle, obesity and breast cancer. *Reviews in Endocrine and Metabolic Disorders*, *22*(2), 241–255. https://doi.org/10.1007/s11154-021-09633-5

Conneely, O. M., Mulac-Jericevic, B., Lydon, J. P., & De Mayo, F. J. (2001). Reproductive functions of the progesterone receptor isoforms: Lessons from knock-out mice. *Molecular and Cellular Endocrinology*, *179*(1), 97–103. https://doi.org/10.1016/S0303-7207(01)00465-8

Coradini, D., Boracchi, P., Oriana, S., Biganzoli, E., & Ambrogi, F. (2014). Differential expression of genes involved in the epigenetic regulation of cell identity in normal human mammary cell commitment and differentiation. *Chinese Journal of Cancer*, *33*(10), 501–510. https://doi.org/10.5732/cjc.014.10066

Cristea, S., & Polyak, K. (2018). Dissecting the mammary gland one cell at a time. *Nature Communications*, *9*(1), 2473. https://doi.org/10.1038/s41467-018-04905-2

Dall, G. V., & Britt, K. L. (2017). Estrogen Effects on the Mammary Gland in Early and Late Life and Breast Cancer Risk. *Frontiers in Oncology*, *7*, 110. https://doi.org/10.3389/fonc.2017.00110

Dall, G., Vieusseux, J., Unsworth, A., Anderson, R., & Britt, K. (2015). Low Dose, Low Cost Estradiol Pellets Can Support MCF-7 Tumour Growth in Nude Mice without Bladder Symptoms. *Journal of Cancer*, *6*(12), 1331–1336. https://doi.org/10.7150/jca.10890

Das, J. K., Felty, Q., Poppiti, R., Jackson, R. M., & Roy, D. (2018). Nuclear Respiratory Factor 1 Acting as an Oncoprotein Drives Estrogen-Induced Breast Carcinogenesis. *Cells*, *7*(12). https://doi.org/10.3390/cells7120234

Davaadelger, B., Choi, M.-R., Singhal, H., Clare, S. E., Khan, S. A., & Kim, J. J. (2019). BRCA1 mutation influences progesterone response in human benign mammary organoids. *Breast Cancer Research*, *21*(1), 124. https://doi.org/10.1186/s13058-019-1214-0

Davenport, T. G., Jerome-Majewska, L. A., & Papaioannou, V. E. (2003). Mammary gland, limb and yolk sac defects in mice lacking Tbx3, the gene mutated in human ulnar mammary syndrome. *Development (Cambridge, England)*, *130*(10), 2263–2273. https://doi.org/10.1242/dev.00431

Dawson, C. A., Pal, B., Vaillant, F., Gandolfo, L. C., Liu, Z., Bleriot, C., Ginhoux, F., Smyth, G. K., Lindeman, G. J., Mueller, S. N., Rios, A. C., & Visvader, J. E. (2020). Tissue-resident ductal macrophages survey the mammary epithelium and facilitate tissue remodelling. *Nature Cell Biology*, *22*(5), 546–558. https://doi.org/10.1038/s41556-020-0505-0

de Assis, S., Wang, M., Jin, L., Bouker, K. B., & Hilakivi-Clarke, L. A. (2013). Exposure to excess estradiol or leptin during pregnancy increases mammary cancer risk and prevents parity-induced protective genomic changes in rats. *Cancer Prevention Research (Philadelphia, Pa.)*, *6*(11), 1194–1211. https://doi.org/10.1158/1940-6207.CAPR-13-0207

De Silva, D., Kunasegaran, K., Ghosh, S., & Pietersen, A. M. (2015). Transcriptome analysis of the hormone-sensing cells in mammary epithelial reveals dynamic changes in early pregnancy. *BMC Developmental Biology*, *15*, 7. https://doi.org/10.1186/s12861-015-0058-9

de Visser, K. E., Ciampricotti, M., Michalak, E. M., Tan, D. W.-M., Speksnijder, E. N., Hau, C.-S., Clevers, H., Barker, N., & Jonkers, J. (2012). Developmental stage-specific contribution of LGR5+ cells to basal and luminal epithelial lineages in the postnatal mammary gland. *The Journal of Pathology*, *228*(3), 300–309. https://doi.org/10.1002/path.4096

Deroo, B. J., Hewitt, S. C., Collins, J. B., Grissom, S. F., Hamilton, K. J., & Korach, K. S. (2009). Profile of estrogen-responsive genes in an estrogen-specific mammary gland outgrowth model. *Molecular Reproduction and Development*, *76*(8), 733–750. https://doi.org/10.1002/mrd.21041

Dewey, K. G., Finley, D. A., Strode, M. A., & Lönnerdal, B. (1986). Relationship of Maternal Age to Breast Milk Volume and Composition. In M. Hamosh & A. S. Goldman (Eds.), *Human Lactation 2: Maternal and Environmental Factors* (pp. 263–273). Springer US. https://doi.org/10.1007/978-1-4615-7207-7_23

Dischinger, P. S., Tovar, E. A., Essenburg, C. J., Madaj, Z. B., Gardner, E. E., Callaghan, M. E., Turner, A. N., Challa, A. K., Kempston, T., Eagleson, B., Kesterson, R. A., Bronson, R. T., Bowman, M. J., Graveel, C. R., & Steensma, M. R. (2018). NF1 deficiency correlates with estrogen receptor signaling and diminished survival in breast cancer. *NPJ Breast Cancer*, *4*. https://doi.org/10.1038/s41523-018-0080-8

Dong, J., Huang, S., Caikovski, M., Ji, S., McGrath, A., Custorio, M. G., Creighton, C. J., Maliakkal, P., Bogoslovskaia, E., Du, Z., Zhang, X., Lewis, M. T., Sablitzky, F., Brisken, C., & Li, Y. (2011). ID4 regulates mammary gland development by suppressing p38MAPK activity. *Development*, *138*(23), 5247–5256. https://doi.org/10.1242/dev.069203

Dontu, G., & Ince, T. A. (2015). Of Mice and Women: A Comparative Tissue Biology Perspective of Breast Stem Cells and Differentiation. *Journal of Mammary Gland Biology and Neoplasia*, *20*(1–2), 51–62. https://doi.org/10.1007/s10911-015-9341-4

dos Santos, C. O., Dolzhenko, E., Hodges, E., Smith, A. D., & Hannon, G. J. (2015). An Epigenetic Memory of Pregnancy in the Mouse Mammary Gland. *Cell Reports*, *11*(7), 1102–1109. https://doi.org/10.1016/j.celrep.2015.04.015

dos Santos, C. O., Rebbeck, C., Rozhkova, E., Valentine, A., Samuels, A., Kadiri, L. R., Osten, P., Harris, E. Y., Uren, P. J., Smith, A. D., & Hannon, G. J. (2013). Molecular hierarchy of mammary differentiation yields refined markers of mammary stem cells. *Proceedings of the National Academy of Sciences*, *110*(18), 7123–7130. https://doi.org/10.1073/pnas.1303919110

Drabsch, Y., Hugo, H., Zhang, R., Dowhan, D. H., Miao, Y. R., Gewirtz, A. M., Barry, S. C., Ramsay, R. G., & Gonda, T. J. (2007). Mechanism of and requirement for estrogen-regulated MYB expression in estrogen-receptor-positive breast cancer cells. *Proceedings of the National Academy of Sciences*, *104*(34), 13762–13767. https://doi.org/10.1073/pnas.0700104104

Dunphy, K. A., Blackburn, A. C., Yan, H., O'Connell, L. R., & Jerry, D. J. (2008). Estrogen and progesterone induce persistent increases in p53-dependent apoptosis and suppress mammary tumors in BALB/c-Trp53+/-mice. *Breast Cancer Research*, *10*(3), R43. https://doi.org/10.1186/bcr2094

Dusek, R. L., Bascom, J. L., Vogel, H., Baron, S., Borowsky, A. D., Bissell, M. J., & Attardi, L. D. (2012). Deficiency of the p53/p63 target Perp alters mammary gland homeostasis and promotes cancer. *Breast Cancer Research : BCR*, *14*(2), R65. https://doi.org/10.1186/bcr3171

Dzięgelewska, Ż., & Gajewska, M. (2019). *Stromal-Epithelial Interactions during Mammary Gland Development*. https://doi.org/10.5772/intechopen.80405

Eeckhoute, J., Keeton, E. K., Lupien, M., Krum, S. A., Carroll, J. S., & Brown, M. (2007). Positive cross-regulatory loop ties GATA-3 to estrogen receptor alpha expression in breast cancer. *Cancer Research*, *67*(13), 6477–6483. https://doi.org/10.1158/0008-5472.CAN-07-0746

Ewald, A. J., Brenot, A., Duong, M., Chan, B. S., & Werb, Z. (2008). Collective Epithelial Migration and Cell Rearrangements Drive Mammary Branching Morphogenesis. *Developmental Cell*, *14*(4), 570–581. https://doi.org/10.1016/j.devcel.2008.03.003

Ewan, K. B. R., Oketch-Rabah, H. A., Ravani, S. A., Shyamala, G., Moses, H. L., & Barcellos-Hoff, M. H. (2005). Proliferation of Estrogen Receptor-α-Positive Mammary Epithelial Cells Is Restrained by Transforming Growth Factor-β1 in Adult Mice. *The American Journal of Pathology*, *167*(2), 409–417.

Fan, X., Qiu, L., Teng, X., Zhang, Y., & Miao, Y. (2020). Effect of INSIG1 on the milk fat synthesis of buffalo mammary epithelial cells. *The Journal of Dairy Research*, *87*(3), 349–355. https://doi.org/10.1017/S0022029920000710

Fata, J. E., Chaudhary, V., & Khokha, R. (2001). Cellular Turnover in the Mammary Gland Is Correlated with Systemic Levels of Progesterone and Not 17β-Estradiol During the Estrous Cycle1. *Biology of Reproduction*, *65*(3), 680–688. https://doi.org/10.1095/biolreprod65.3.680

Fata, J. E., Werb, Z., & Bissell, M. J. (2003). Regulation of mammary gland branching morphogenesis by the extracellular matrix and its remodeling enzymes. *Breast Cancer Research*, *6*(1), 1. https://doi.org/10.1186/bcr634

Feigman, M. J., Moss, M. A., Chen, C., Cyrill, S. L., Ciccone, M. F., Trousdell, M. C., Yang, S.-T., Frey, W. D., Wilkinson, J. E., & dos Santos, C. O. (2020). Pregnancy reprograms the epigenome of mammary epithelial cells and blocks the development of premalignant lesions. *Nature Communications*, *11*(1), 2649. https://doi.org/10.1038/s41467-020-16479-z

Feng, Y., Manka, D., Wagner, K.-U., & Khan, S. A. (2007). Estrogen receptor-α expression in the mammary epithelium is required for ductal and alveolar morphogenesis in mice. *Proceedings of the National Academy of Sciences*, *104*(37), 14718–14723. https://doi.org/10.1073/pnas.0706933104

Fernandez-Valdivia, R., Mukherjee, A., Ying, Y., Li, J., Paquet, M., DeMayo, F. J., & Lydon, J. P. (2009). The RANKL signaling axis is sufficient to elicit ductal side-branching and alveologenesis in the mammary gland of the virgin mouse. *Developmental Biology*, *328*(1), 127–139. https://doi.org/10.1016/j.ydbio.2009.01.019

Florian, S., Iwamoto, Y., Coughlin, M., Weissleder, R., & Mitchison, T. J. (2019). A human organoid system that self-organizes to recapitulate growth and differentiation of a benign mammary tumor. *Proceedings of the National Academy of Sciences of the United States of America*, *116*(23), 11444–11453. https://doi.org/10.1073/pnas.1702372116

Forster, N., Saladi, S. V., van Bragt, M., Sfondouris, M. E., Jones, F. E., Li, Z., & Ellisen, L. W. (2014). Basal cell signaling by p63 controls luminal progenitor function and lactation via NRG1. *Developmental Cell*, *28*(2), 147–160. https://doi.org/10.1016/j.devcel.2013.11.019

Frey, W. D., Chaudhry, A., Slepicka, P. F., Ouellette, A. M., Kirberger, S. E., Pomerantz, W. C. K., Hannon, G. J., & Santos, C. O. dos. (2017). BPTF Maintains Chromatin Accessibility and the Self-Renewal Capacity of Mammary Gland Stem Cells. *Stem Cell Reports*, *9*(1), 23–31. https://doi.org/10.1016/j.stemcr.2017.04.031

Fu, N. Y., Rios, A. C., Pal, B., Law, C. W., Jamieson, P., Liu, R., Vaillant, F., Jackling, F., Liu, K. H., Smyth, G. K., Lindeman, G. J., Ritchie, M. E., & Visvader, J. E. (2017). Identification of quiescent and spatially restricted mammary stem cells that are hormone responsive. *Nature Cell Biology*, *19*(3), Article 3. https://doi.org/10.1038/ncb3471

Gagniac, L., Rusidzé, M., Boudou, F., Cagnet, S., Adlanmerini, M., Jeannot, P., Gaide, N., Giton, F., Besson, A., Weyl, A., Gourdy, P., Raymond-Letron, I., Arnal, J.-F., Brisken, C., & Lenfant, F. (2020). Membrane expression of the estrogen receptor ERα is required for intercellular communications in the mammary epithelium. *Development*, *147*(5), dev182303. https://doi.org/10.1242/dev.182303

Gérard, C., Blacher, S., Communal, L., Courtin, A., Tskitishvili, E., Mestdagt, M., Munaut, C., Noel, A., Gompel, A., Péqueux, C., & Foidart, J. M. (2015). Estetrol is a weak estrogen antagonizing estradiol-dependent mammary gland proliferation. *The Journal of Endocrinology*, *224*(1), 85–95. https://doi.org/10.1530/JOE-14-0549

Gérard, C., Gallez, A., Dubois, C., Drion, P., Delahaut, P., Quertemont, E., Noël, A., & Pequeux, C. (2017). Accurate Control of 17β-Estradiol Long-Term Release Increases Reliability and Reproducibility of Preclinical Animal Studies. *Journal of Mammary Gland Biology and Neoplasia*, *22*(1), 1–11. https://doi.org/10.1007/s10911-016-9368-1

Gérard, C., Mestdagt, M., Tskitishvili, E., Communal, L., Gompel, A., Silva, E., Arnal, J.-F., Lenfant, F., Noel, A., Foidart, J.-M., & Péqueux, C. (2015). Combined estrogenic and anti-estrogenic properties of estetrol on breast

cancer may provide a safe therapeutic window for the treatment of menopausal symptoms. *Oncotarget*, *6*(19), 17621–17636.

Ginger, M. R., & Rosen, J. M. (2003). Pregnancy-induced changes in cell-fate in the mammary gland. *Breast Cancer Research*, *5*(4), 192–197. https://doi.org/10.1186/bcr603

Giraddi, R. R., Chung, C.-Y., Heinz, R. E., Balcioglu, O., Novotny, M., Trejo, C. L., Dravis, C., Hagos, B. M., Mehrabad, E. M., Rodewald, L. W., Hwang, J. Y., Fan, C., Lasken, R., Varley, K. E., Perou, C. M., Wahl, G. M., & Spike, B. T. (2018). Single-Cell Transcriptomes Distinguish Stem Cell State Changes and Lineage Specification Programs in Early Mammary Gland Development. *Cell Reports*, *24*(6), 1653-1666.e7. https://doi.org/10.1016/j.celrep.2018.07.025

Giraddi, R. R., Shehata, M., Gallardo, M., Blasco, M. A., Simons, B. D., & Stingl, J. (2015). Stem and progenitor cell division kinetics during postnatal mouse mammary gland development. *Nature Communications*, *6*(1), Article 1. https://doi.org/10.1038/ncomms9487

Gold, E. B., Bromberger, J., Crawford, S., Samuels, S., Greendale, G. A., Harlow, S. D., & Skurnick, J. (2001). Factors Associated with Age at Natural Menopause in a Multiethnic Sample of Midlife Women. *American Journal of Epidemiology*, *153*(9), 865–874. https://doi.org/10.1093/aje/153.9.865

Goldhar, A. S., Duan, R., Ginsburg, E., & Vonderhaar, B. K. (2011). Progesterone induces expression of the prolactin receptor gene through cooperative action of Sp1 and C/EBP. *Molecular and Cellular Endocrinology*, *335*(2), 148–157. https://doi.org/10.1016/j.mce.2011.01.004

Gouon-Evans, V., Rothenberg, M. E., & Pollard, J. W. (2000). Postnatal mammary gland development requires macrophages and eosinophils. *Development (Cambridge, England)*, *127*(11), 2269–2282. https://doi.org/10.1242/dev.127.11.2269

Gray, G. K., Li, C. M.-C., Rosenbluth, J. M., Selfors, L. M., Girnius, N., Lin, J.-R., Schackmann, R. C. J., Goh, W. L., Moore, K., Shapiro, H. K., Mei, S., D'Andrea, K., Nathanson, K. L., Sorger, P. K., Santagata, S., Regev, A., Garber, J. E., Dillon, D. A., & Brugge, J. S. (2022). A human breast atlas integrating single-cell proteomics and transcriptomics. *Developmental Cell*, *57*(11), 1400-1420.e7. https://doi.org/10.1016/j.devcel.2022.05.003

Green, K. A., & Lund, L. R. (2005). ECM degrading proteases and tissue remodelling in the mammary gland. *BioEssays: News and Reviews in Molecular, Cellular and Developmental Biology*, *27*(9), 894–903. https://doi.org/10.1002/bies.20281

Gregor, M. F., Misch, E. S., Yang, L., Hummasti, S., Inouye, K. E., Lee, A.-H., Bierie, B., & Hotamisligil, G. S. (2013). The Role of Adipocyte XBP1 in Metabolic Regulation during Lactation. *Cell Reports*, *3*(5), 1430–1439. https://doi.org/10.1016/j.celrep.2013.03.042

Grimm, S. L., Seagroves, T. N., Kabotyanski, E. B., Hovey, R. C., Vonderhaar, B. K., Lydon, J. P., Miyoshi, K., Hennighausen, L., Ormandy, C. J., Lee, A. V., Stull, M. A., Wood, T. L., & Rosen, J. M. (2002). Disruption of Steroid and Prolactin Receptor Patterning in the Mammary Gland Correlates with a Block in Lobuloalveolar Development. *Molecular Endocrinology*, *16*(12), 2675–2691. https://doi.org/10.1210/me.2002-0239

Guttilla, I. K., Adams, B. D., & White, B. A. (2012). ERα, microRNAs, and the epithelial-mesenchymal transition in breast cancer. *Trends in Endocrinology and Metabolism: TEM*, *23*(2), 73–82. https://doi.org/10.1016/j.tem.2011.12.001

Haaksma, C. J., Schwartz, R. J., & Tomasek, J. J. (2011). Myoepithelial Cell Contraction and Milk Ejection Are Impaired in Mammary Glands of Mice Lacking Smooth Muscle Alpha-Actin. *Biology of Reproduction*, *85*(1), 13. https://doi.org/10.1095/biolreprod.110.090639

Halliday, G. M. (2010). Common Links among the Pathways Leading to UV-Induced Immunosuppression. *Journal of Investigative Dermatology*, *130*(5), 1209–1212. https://doi.org/10.1038/jid.2009.374

Han, X., Wang, R., Zhou, Y., Fei, L., Sun, H., Lai, S., Saadatpour, A., Zhou, Z., Chen, H., Ye, F., Huang, D., Xu, Y., Huang, W., Jiang, M., Jiang, X., Mao, J., Chen, Y., Lu, C., Xie, J., … Guo, G. (2018). Mapping the Mouse Cell Atlas by Microwell-Seq. *Cell*, *172*(5), 1091-1107.e17. https://doi.org/10.1016/j.cell.2018.02.001

Hanasoge Somasundara, A. V., Moss, M. A., Feigman, M. J., Chen, C., Cyrill, S. L., Ciccone, M. F., Trousdell, M. C., Vollbrecht, M., Li, S., Kendall, J., Beyaz, S., Wilkinson, J. E., & dos Santos, C. O. (2021). Parity-induced changes to mammary epithelial cells control NKT cell expansion and mammary oncogenesis. *Cell Reports*, *37*(10), 110099. https://doi.org/10.1016/j.celrep.2021.110099

Harvey, P. W. (2012). Hypothesis: Prolactin is tumorigenic to human breast: dispelling the myth that prolactin-induced mammary tumors are rodent-specific. *Journal of Applied Toxicology: JAT*, *32*(1), 1–9. https://doi.org/10.1002/jat.1772

HASLAM, S. Z., & SHYAMALA, G. (1979). Progesterone Receptors in Normal Mammary Glands of Mice: Characterization and Relationship to Development*. *Endocrinology*, *105*(3), 786–795. https://doi.org/10.1210/endo-105-3-786

Hatcher, R. J., Dong, J., Liu, S., Bian, G., Contreras, A., Wang, T., Hilsenbeck, S. G., Li, Y., & Zhang, P. (2014). Pttg1/securin is required for the branching morphogenesis of the mammary gland and suppresses mammary

tumorigenesis. *Proceedings of the National Academy of Sciences of the United States of America*, *111*(3), 1008–1013. https://doi.org/10.1073/pnas.1318124111

Hatsell, S. J., & Cowin, P. (2006). Gli3-mediated repression of Hedgehog targets is required for normal mammary development. *Development (Cambridge, England)*, *133*(18), 3661–3670. https://doi.org/10.1242/dev.02542

Hatsumi, T., & Yamamuro, Y. (2006). Downregulation of estrogen receptor gene expression by exogenous 17beta-estradiol in the mammary glands of lactating mice. *Experimental Biology and Medicine (Maywood, N.J.)*, *231*(3), 311–316. https://doi.org/10.1177/153537020623100311

Hein, S. M., Haricharan, S., Johnston, A. N., Toneff, M. J., Reddy, J. P., Dong, J., Bu, W., & Li, Y. (2016). Luminal Epithelial Cells within the Mammary Gland Can Produce Basal Cells upon Oncogenic Stress. *Oncogene*, *35*(11), 1461–1467. https://doi.org/10.1038/onc.2015.206

Hennighausen, L., & Robinson, G. W. (2001). Signaling Pathways in Mammary Gland Development. *Developmental Cell*, *1*(4), 467–475. https://doi.org/10.1016/S1534-5807(01)00064-8

Henry, S., Trousdell, M. C., Cyrill, S. L., Zhao, Y., Feigman, Mary. J., Bouhuis, J. M., Aylard, D. A., Siepel, A., & dos Santos, C. O. (2021). Characterization of Gene Expression Signatures for the Identification of Cellular Heterogeneity in the Developing Mammary Gland. *Journal of Mammary Gland Biology and Neoplasia*, *26*(1), 43–66. https://doi.org/10.1007/s10911-021-09486-3

Hitchcock, J. R., Hughes, K., Harris, O. B., & Watson, C. J. (2020). Dynamic architectural interplay between leucocytes and mammary epithelial cells. *The FEBS Journal*, *287*(2), 250–266. https://doi.org/10.1111/febs.15126

Holloway, K. R., Sinha, V. C., Toneff, M. J., Bu, W., Hilsenbeck, S. G., & Li, Y. (2015). Krt6a-Positive Mammary Epithelial Progenitors Are Not at Increased Vulnerability to Tumorigenesis Initiated by ErbB2. *PLoS ONE*, *10*(1), e0117239. https://doi.org/10.1371/journal.pone.0117239

Hovey, R. C., & Aimo, L. (2010). Diverse and Active Roles for Adipocytes During Mammary Gland Growth and Function. *Journal of Mammary Gland Biology and Neoplasia*, *15*(3), 279–290. https://doi.org/10.1007/s10911-010-9187-8

Hovey, R. C., Mcfadden, T. B., & Akers, R. M. (1999). Regulation of Mammary Gland Growth and Morphogenesis by the Mammary Fat Pad: A Species Comparison. *Journal of Mammary Gland Biology and Neoplasia*, *4*(1), 53–68. https://doi.org/10.1023/A:1018704603426

Howard, B. A., & Lu, P. (2014). Stromal regulation of embryonic and postnatal mammary epithelial development and differentiation. *Seminars in Cell & Developmental Biology*, *25–26*, 43–51. https://doi.org/10.1016/j.semcdb.2014.01.004

Howlin, J., McBryan, J., Napoletano, S., Lambe, T., McArdle, E., Shioda, T., & Martin, F. (2006). CITED1 homozygous null mice display aberrant pubertal mammary ductal morphogenesis. *Oncogene*, *25*(10), Article 10. https://doi.org/10.1038/sj.onc.1209183

Hu, D., Zhou, Z., Davidson, N. E., Huang, Y., & Wan, Y. (2012). Novel Insight into KLF4 Proteolytic Regulation in Estrogen Receptor Signaling and Breast Carcinogenesis. *The Journal of Biological Chemistry*, *287*(17), 13584–13597. https://doi.org/10.1074/jbc.M112.343566

Hua, Q., Sun, Z., Liu, Y., Shen, X., Zhao, W., Zhu, X., & Xu, P. (2021). KLK8 promotes the proliferation and metastasis of colorectal cancer via the activation of EMT associated with PAR1. *Cell Death & Disease*, *12*(10), 860. https://doi.org/10.1038/s41419-021-04149-x

Huang, T. H.-M., & Esteller, M. (2010). Chromatin Remodeling in Mammary Gland Differentiation and Breast Tumorigenesis. *Cold Spring Harbor Perspectives in Biology*, *2*(9), a004515. https://doi.org/10.1101/cshperspect.a004515

Humphreys, R. C., Lydon, J. P., O'Malley, B. W., & Rosen, J. M. (1997). Use of PRKO Mice to Study the Role of Progesterone in Mammary Gland Development. *Journal of Mammary Gland Biology and Neoplasia*, *2*(4), 343–354. https://doi.org/10.1023/A:1026343212187

Hurtado, A., Holmes, K. A., Ross-Innes, C. S., Schmidt, D., & Carroll, J. S. (2011). FOXA1 is a key determinant of estrogen receptor function and endocrine response. *Nature Genetics*, *43*(1), Article 1. https://doi.org/10.1038/ng.730

Incassati, A., Chandramouli, A., Eelkema, R., & Cowin, P. (2010). Key signaling nodes in mammary gland development and cancer: β-catenin. *Breast Cancer Research*, *12*(6), 213. https://doi.org/10.1186/bcr2723

Ingram, D. M., Nottage, E. M., & Roberts, A. N. (1990). Prolactin and breast cancer risk. *Medical Journal of Australia*, *153*(8), 469–473. https://doi.org/10.5694/j.1326-5377.1990.tb126153.x

Ingthorsson, S., Hilmarsdottir, B., Kricker, J., Magnusson, M. K., & Gudjonsson, T. (2015). Context-Dependent Function of Myoepithelial Cells in Breast Morphogenesis and Neoplasia. *Current Molecular Biology Reports*, *1*(4), 168–174. https://doi.org/10.1007/s40610-015-0027-x

Jackson-Fisher, A. J., Bellinger, G., Ramabhadran, R., Morris, J. K., Lee, K.-F., & Stern, D. F. (2004). ErbB2 is required for ductal morphogenesis of the mammary gland. *Proceedings of the National Academy of Sciences of the United States of America*, *101*(49), 17138–17143. https://doi.org/10.1073/pnas.0407057101

Jamieson, P. R., Dekkers, J. F., Rios, A. C., Fu, N. Y., Lindeman, G. J., & Visvader, J. E. (2017). Derivation of a robust mouse mammary organoid system for studying tissue dynamics. *Development (Cambridge, England)*, *144*(6), 1065–1071. https://doi.org/10.1242/dev.145045

Jaswal, S., Anand, V., Ali, S. A., Jena, M. K., Kumar, S., Kaushik, J. K., & Mohanty, A. K. (2021). TMT based deep proteome analysis of buffalo mammary epithelial cells and identification of novel protein signatures during lactogenic differentiation. *FASEB Journal: Official Publication of the Federation of American Societies for Experimental Biology*, *35*(6), e21621. https://doi.org/10.1096/fj.202002476RR

Jena, M. K., Jaswal, S., Kumar, S., & Mohanty, A. K. (2019). Molecular mechanism of mammary gland involution: An update. *Developmental Biology*, *445*(2), 145–155. https://doi.org/10.1016/j.ydbio.2018.11.002

Jindal, S., Gao, D., Bell, P., Albrektsen, G., Edgerton, S. M., Ambrosone, C. B., Thor, A. D., Borges, V. F., & Schedin, P. (2014). Postpartum breast involution reveals regression of secretory lobules mediated by tissue-remodeling. *Breast Cancer Research: BCR*, *16*(2), R31. https://doi.org/10.1186/bcr3633

Joshi, P. A., Jackson, H. W., Beristain, A. G., Di Grappa, M. A., Mote, P. A., Clarke, C. L., Stingl, J., Waterhouse, P. D., & Khokha, R. (2010). Progesterone induces adult mammary stem cell expansion. *Nature*, *465*(7299), 803–807. https://doi.org/10.1038/nature09091

Kaanta, A. S., Virtanen, C., Selfors, L. M., Brugge, J. S., & Neel, B. G. (2013). Evidence for a multipotent mammary progenitor with pregnancy-specific activity. *Breast Cancer Research : BCR*, *15*(4), R65. https://doi.org/10.1186/bcr3459

Kalet, B. T., Anglin, S. R., Handschy, A., O'Donoghue, L. E., Halsey, C., Chubb, L., Korch, C., & Duval, D. L. (2013). Transcription Factor Ets1 Cooperates with Estrogen Receptor α to Stimulate Estradiol-Dependent Growth in Breast Cancer Cells and Tumors. *PLoS ONE*, *8*(7), e68815. https://doi.org/10.1371/journal.pone.0068815

Kanaya, N., Chang, G., Wu, X., Saeki, K., Bernal, L., Shim, H.-J., Wang, J., Warden, C., Yamamoto, T., Li, J., Park, J.-S., Synold, T., Vonderfecht, S., Rakoff, M., Neuhausen, S. L., & Chen, S. (2019). Single-cell RNA-sequencing analysis of estrogen- and endocrine-disrupting chemical-induced reorganization of mouse mammary gland. *Communications Biology*, *2*, 406. https://doi.org/10.1038/s42003-019-0618-9

Kang, K., Yamaji, D., Yoo, K. H., Robinson, G. W., & Hennighausen, L. (2014). Mammary-Specific Gene Activation Is Defined by Progressive Recruitment of STAT5 during Pregnancy and the Establishment of H3K4me3 Marks. *Molecular and Cellular Biology*, *34*(3), 464–473. https://doi.org/10.1128/MCB.00988-13

Karpuzoglu-Sahin, E., Hissong, B. D., & Ansar Ahmed, S. (2001). Interferon-gamma levels are upregulated by 17-beta-estradiol and diethylstilbestrol. *Journal of Reproductive Immunology*, *52*(1–2), 113–127. https://doi.org/10.1016/s0165-0378(01)00117-6

Kendrick, H., Regan, J. L., Magnay, F.-A., Grigoriadis, A., Mitsopoulos, C., Zvelebil, M., & Smalley, M. J. (2008). Transcriptome analysis of mammary epithelial subpopulations identifies novel determinants of lineage commitment and cell fate. *BMC Genomics*, *9*, 591. https://doi.org/10.1186/1471-2164-9-591

Kenney, N. J., Bowman, A., Korach, K. S., Carl Barrett, J., & Salomon, D. S. (2003). Effect of Exogenous Epidermal-Like Growth Factors on Mammary Gland Development and Differentiation in the Estrogen Receptor-Alpha Knockout (ERKO) Mouse. *Breast Cancer Research and Treatment*, *79*(2), 161–173. https://doi.org/10.1023/A:1023938510508

Ketterer, S., Mitschke, J., Ketscher, A., Schlimpert, M., Reichardt, W., Baeuerle, N., Hess, M. E., Metzger, P., Boerries, M., Peters, C., Kammerer, B., Brummer, T., Steinberg, F., & Reinheckel, T. (2020). Cathepsin D deficiency in mammary epithelium transiently stalls breast cancer by interference with mTORC1 signaling. *Nature Communications*, *11*(1), Article 1. https://doi.org/10.1038/s41467-020-18935-2

Khaled, W. T., Read, E. K. C., Nicholson, S. E., Baxter, F. O., Brennan, A. J., Came, P. J., Sprigg, N., McKenzie, A. N. J., & Watson, C. J. (2007). The IL-4/IL-13/Stat6 signalling pathway promotes luminal mammary epithelial cell development. *Development (Cambridge, England)*, *134*(15), 2739–2750. https://doi.org/10.1242/dev.003194

Khalkhali-Ellis, Z., Abbott, D. E., Bailey, C. M., Goossens, W., Margaryan, N. V., Gluck, S. L., Reuveni, M., & Hendrix, M. J. C. (2008). IFN-γ regulation of vacuolar pH, cathepsin D processing and autophagy in mammary epithelial cells. *Journal of Cellular Biochemistry*, *105*(1), 208–218. https://doi.org/10.1002/jcb.21814

Kim, K.-S., Kim, J., Oh, N., Kim, M.-Y., & Park, K.-S. (2018). ELK3-GATA3 axis modulates MDA-MB-231 metastasis by regulating cell-cell adhesion-related genes. *Biochemical and Biophysical Research Communications*, *498*(3), 509–515. https://doi.org/10.1016/j.bbrc.2018.03.011

Kleinman, H. K., & Martin, G. R. (2005). Matrigel: Basement membrane matrix with biological activity. *Seminars in Cancer Biology*, *15*(5), 378–386. https://doi.org/10.1016/j.semcancer.2005.05.004

Klinge, C. M. (2020). Estrogenic control of mitochondrial function. *Redox Biology*, *31*. https://doi.org/10.1016/j.redox.2020.101435

Kordon, E. C., & Smith, G. H. (1998). An entire functional mammary gland may comprise the progeny from a single cell. *Development*, *125*(10), 1921–1930. https://doi.org/10.1242/dev.125.10.1921

Kumar, S., Nandi, A., Mahesh, A., Sinha, S., Flores, E., & Chakrabarti, R. (2020). Inducible knockout of ΔNp63 alters cell polarity and metabolism during pubertal mammary gland development. *FEBS Letters*, *594*(6), 973–985. https://doi.org/10.1002/1873-3468.13703

Kuperwasser, C., Chavarria, T., Wu, M., Magrane, G., Gray, J. W., Carey, L., Richardson, A., & Weinberg, R. A. (2004). Reconstruction of functionally normal and malignant human breast tissues in mice. *Proceedings of the National Academy of Sciences*, *101*(14), 4966–4971. https://doi.org/10.1073/pnas.0401064101

Lacouture, A., Jobin, C., Weidmann, C., Berthiaume, L., Bastien, D., Laverdière, I., Pelletier, M., & Audet-Walsh, É. (2021). A FACS-Free Purification Method to Study Estrogen Signaling, Organoid Formation, and Metabolic Reprogramming in Mammary Epithelial Cells. *Frontiers in Endocrinology*, *12*. https://www.frontiersin.org/articles/10.3389/fendo.2021.672466

Laganière, J., Deblois, G., Lefebvre, C., Bataille, A. R., Robert, F., & Giguère, V. (2005). Location analysis of estrogen receptor α target promoters reveals that FOXA1 defines a domain of the estrogen response. *Proceedings of the National Academy of Sciences*, *102*(33), 11651–11656. https://doi.org/10.1073/pnas.0505575102

Lain, A. R., Creighton, C. J., & Conneely, O. M. (2013). Research Resource: Progesterone Receptor Targetome Underlying Mammary Gland Branching Morphogenesis. *Molecular Endocrinology*, *27*(10), 1743–1761. https://doi.org/10.1210/me.2013-1144

LaMarca, H. L., & Rosen, J. M. (2007). Estrogen regulation of mammary gland development and breast cancer: Amphiregulin takes center stage. *Breast Cancer Research : BCR*, *9*(4), 304. https://doi.org/10.1186/bcr1740

Laporta, J., Peñagaricano, F., & Hernandez, L. L. (2015). Transcriptomic Analysis of the Mouse Mammary Gland Reveals New Insights for the Role of Serotonin in Lactation. *PLOS ONE*, *10*(10), e0140425. https://doi.org/10.1371/journal.pone.0140425

Lee, G. Y., Kenny, P. A., Lee, E. H., & Bissell, M. J. (2007). Three-dimensional culture models of normal and malignant breast epithelial cells. *Nature Methods*, *4*(4), Article 4. https://doi.org/10.1038/nmeth1015

Lee, M. Y., Sun, L., & Veltmaat, J. M. (2013). Hedgehog and Gli Signaling in Embryonic Mammary Gland Development. *Journal of Mammary Gland Biology and Neoplasia*, *18*(2), 133–138. https://doi.org/10.1007/s10911-013-9291-7

Leondires, M. P., Hu, Z.-Z., Dong, J., Tsai-Morris, C.-H., & Dufau, M. L. (2002). Estradiol stimulates expression of two human prolactin receptor isoforms with alternative exons-1 in T47D breast cancer cells. *The Journal of Steroid Biochemistry and Molecular Biology*, *82*(2), 263–268. https://doi.org/10.1016/S0960-0760(02)00184-X

Levin-Allerhand, J. A., Sokol, K., & Smith, J. D. (2003). Safe and Effective Method for Chronic 17□-Estradiol Administration to Mice. *Journal of the American Association for Laboratory Animal Science*, *42*(6), 33–35.

Lewandoski, M. (2001). Conditional control of gene expression in the mouse. *Nature Reviews. Genetics*, *2*(10), 743–755. https://doi.org/10.1038/35093537

Li, C. M.-C., Shapiro, H., Tsiobikas, C., Selfors, L. M., Chen, H., Rosenbluth, J., Moore, K., Gupta, K. P., Gray, G. K., Oren, Y., Steinbaugh, M. J., Guerriero, J. L., Pinello, L., Regev, A., & Brugge, J. S. (2020). Aging-Associated Alterations in Mammary Epithelia and Stroma Revealed by Single-Cell RNA Sequencing. *Cell Reports*, *33*(13), 108566. https://doi.org/10.1016/j.celrep.2020.108566

Li, C.-W., Xia, W., Huo, L., Lim, S.-O., Wu, Y., Hsu, J. L., Chao, C.-H., Yamaguchi, H., Yang, N.-K., Ding, Q., Wang, Y., Lai, Y.-J., LaBaff, A. M., Wu, T.-J., Lin, B.-R., Yang, M.-H., Hortobagyi, G. N., & Hung, M.-C. (2012). Epithelial-mesenchymal transition induced by TNF-α requires NF-κB-mediated transcriptional upregulation of Twist1. *Cancer Research*, *72*(5), 1290–1300. https://doi.org/10.1158/0008-5472.CAN-11-3123

Li, S., & Rosen, J. M. (1995). Nuclear factor I and mammary gland factor (STAT5) play a critical role in regulating rat whey acidic protein gene expression in transgenic mice. *Molecular and Cellular Biology*, *15*(4), 2063–2070. https://doi.org/10.1128/MCB.15.4.2063

Liberzon, A., Birger, C., Thorvaldsdóttir, H., Ghandi, M., Mesirov, J. P., & Tamayo, P. (2015). The Molecular Signatures Database (MSigDB) hallmark gene set collection. *Cell Systems*, *1*(6), 417–425. https://doi.org/10.1016/j.cels.2015.12.004

Lilla, J. N., & Werb, Z. (2010). Mast cells contribute to the stromal microenvironment in mammary gland branching morphogenesis. *Developmental Biology*, *337*(1), 124–133. https://doi.org/10.1016/j.ydbio.2009.10.021

Lim, E., Vaillant, F., Wu, D., Forrest, N. C., Pal, B., Hart, A. H., Asselin-Labat, M.-L., Gyorki, D. E., Ward, T., Partanen, A., Feleppa, F., Huschtscha, L. I., Thorne, H. J., kConFab, Fox, S. B., Yan, M., French, J. D., Brown, M. A., Smyth, G. K., … Lindeman, G. J. (2009). Aberrant luminal progenitors as the candidate target population for basal tumor development in BRCA1 mutation carriers. *Nature Medicine*, *15*(8), 907–913. https://doi.org/10.1038/nm.2000

Lim, E., Wu, D., Pal, B., Bouras, T., Asselin-Labat, M.-L., Vaillant, F., Yagita, H., Lindeman, G. J., Smyth, G. K., & Visvader, J. E. (2010). Transcriptome analyses of mouse and human mammary cell subpopulations reveal multiple conserved genes and pathways. *Breast Cancer Research*, *12*(2), R21. https://doi.org/10.1186/bcr2560

Liu, F., Pawliwec, A., Feng, Z., Yasruel, Z., Lebrun, J.-J., & Ali, S. (2015). Prolactin/Jak2 directs apical/basal polarization and luminal linage maturation of mammary epithelial cells through regulation of the Erk1/2 pathway. *Stem Cell Research*, *15*(2), 376–383. https://doi.org/10.1016/j.scr.2015.08.001

Liu, X., Ory, V., Chapman, S., Yuan, H., Albanese, C., Kallakury, B., Timofeeva, O. A., Nealon, C., Dakic, A., Simic, V., Haddad, B. R., Rhim, J. S., Dritschilo, A., Riegel, A., McBride, A., & Schlegel, R. (2012). ROCK inhibitor and feeder cells induce the conditional reprogramming of epithelial cells. *The American Journal of Pathology*, *180*(2), 599–607. https://doi.org/10.1016/j.ajpath.2011.10.036

Liu, X., Robinson, G. W., Wagner, K. U., Garrett, L., Wynshaw-Boris, A., & Hennighausen, L. (1997). Stat5a is mandatory for adult mammary gland development and lactogenesis. *Genes & Development*, *11*(2), 179–186. https://doi.org/10.1101/gad.11.2.179

Loizzi, R. F. (1985). Progesterone withdrawal stimulates mammary gland tubulin polymerization in pregnant rats. *Endocrinology*, *116*(6), 2543–2547. https://doi.org/10.1210/endo-116-6-2543

Long, W., Wagner, K.-U., Lloyd, K. C. K., Binart, N., Shillingford, J. M., Hennighausen, L., & Jones, F. E. (2003). Impaired differentiation and lactational failure of Erbb4-deficient mammary glands identify ERBB4 as an obligate mediator of STAT5. *Development*, *130*(21), 5257–5268. https://doi.org/10.1242/dev.00715

Love, R. R., Rose, D. R., Surawicz, T. S., & Newcomb, P. A. (1991). Prolactin and growth hormone levels in premenopausal women with breast cancer and healthy women with a strong family history of breast cancer. *Cancer*, *68*(6), 1401–1405. https://doi.org/10.1002/1097-0142(19910915)68:6<1401::AID-CNCR2820680637>3.0.CO;2-K

Lu, S., Becker, K. A., Hagen, M. J., Yan, H., Roberts, A. L., Mathews, L. A., Schneider, S. S., Siegelmann, H. T., MacBeth, K. J., Tirrell, S. M., Blanchard, J. L., & Jerry, D. J. (2008). Transcriptional Responses to Estrogen and Progesterone in Mammary Gland Identify Networks Regulating p53 Activity. *Endocrinology*, *149*(10), 4809–4820. https://doi.org/10.1210/en.2008-0035

Macias, H., & Hinck, L. (2012). Mammary Gland Development. *Wiley Interdisciplinary Reviews. Developmental Biology*, *1*(4), 533–557. https://doi.org/10.1002/wdev.35

Maharjan, C. K., Mo, J., Wang, L., Kim, M.-C., Wang, S., Borcherding, N., Vikas, P., & Zhang, W. (2021). Natural and Synthetic Estrogens in Chronic Inflammation and Breast Cancer. *Cancers*, *14*(1), 206. https://doi.org/10.3390/cancers14010206

Makarem, M., Kannan, N., Nguyen, L. V., Knapp, D. J. H. F., Balani, S., Prater, M. D., Stingl, J., Raouf, A., Nemirovsky, O., Eirew, P., & Eaves, C. J. (2013). Developmental changes in the in vitro activated regenerative

activity of primitive mammary epithelial cells. *PLoS Biology*, *11*(8), e1001630. https://doi.org/10.1371/journal.pbio.1001630

Mallepell, S., Krust, A., Chambon, P., & Brisken, C. (2006). Paracrine signaling through the epithelial estrogen receptor α is required for proliferation and morphogenesis in the mammary gland. *Proceedings of the National Academy of Sciences*, *103*(7), 2196–2201. https://doi.org/10.1073/pnas.0510974103

Maller, O., Hansen, K. C., Lyons, T. R., Acerbi, I., Weaver, V. M., Prekeris, R., Tan, A.-C., & Schedin, P. (2013). Collagen architecture in pregnancy-induced protection from breast cancer. *Journal of Cell Science*, *126*(18), 4108. https://doi.org/10.1242/jcs.121590

Maningat, P. D., Sen, P., Rijnkels, M., Sunehag, A. L., Hadsell, D. L., Bray, M., & Haymond, M. W. (2009). Gene expression in the human mammary epithelium during lactation: The milk fat globule transcriptome. *Physiological Genomics*, *37*(1), 12. https://doi.org/10.1152/physiolgenomics.90341.2008

Mapes, J., Li, Q., Kannan, A., Anandan, L., Laws, M., Lydon, J. P., Bagchi, I. C., & Bagchi, M. K. (2017). CUZD1 is a critical mediator of the JAK/STAT5 signaling pathway that controls mammary gland development during pregnancy. *PLOS Genetics*, *13*(3), e1006654. https://doi.org/10.1371/journal.pgen.1006654

Martin Carli, J. F., Trahan, G. D., Jones, K. L., Hirsch, N., Rolloff, K. P., Dunn, E. Z., Friedman, J. E., Barbour, L. A., Hernandez, T. L., MacLean, P. S., Monks, J., McManaman, J. L., & Rudolph, M. C. (2020). Single Cell RNA Sequencing of Human Milk-Derived Cells Reveals Sub-Populations of Mammary Epithelial Cells with Molecular Signatures of Progenitor and Mature States: A Novel, Non-invasive Framework for Investigating Human Lactation Physiology. *Journal of Mammary Gland Biology and Neoplasia*, *25*(4), 367–387. https://doi.org/10.1007/s10911-020-09466-z

Master, S. R., Hartman, J. L., D'Cruz, C. M., Moody, S. E., Keiper, E. A., Ha, S. I., Cox, J. D., Belka, G. K., & Chodosh, L. A. (2002). Functional Microarray Analysis of Mammary Organogenesis Reveals a Developmental Role in Adaptive Thermogenesis. *Molecular Endocrinology*, *16*(6), 1185–1203. https://doi.org/10.1210/mend.16.6.0865

Mastroianni, M., Kim, S., Kim, Y. C., Esch, A., Wagner, C., & Alexander, C. M. (2010). Wnt Signaling can Substitute for Estrogen to Induce Division of ERα-positive Cells in a Mouse Mammary Tumor Model. *Cancer Letters*, *289*(1), 23–31. https://doi.org/10.1016/j.canlet.2009.07.012

Matsumoto, M., Nishinakagawa, H., Kurohmaru, M., Hayashi, Y., & Otsuka, J. (1992). Pregnancy and lactation affect the microvasculature of the mammary gland in mice. *The Journal of Veterinary Medical Science*, *54*(5), 937–943. https://doi.org/10.1292/jvms.54.937

McMullen, J. R. W., & Soto, U. (2022). Newly identified breast luminal progenitor and gestational stem cell populations likely give rise to HER2-overexpressing and basal-like breast cancers. *Discover. Oncology*, *13*, 38. https://doi.org/10.1007/s12672-022-00500-6

Medina, D. (2010). Of Mice and Women: A Short History of Mouse Mammary Cancer Research with an Emphasis on the Paradigms Inspired by the Transplantation Method. *Cold Spring Harbor Perspectives in Biology*, *2*(10), a004523. https://doi.org/10.1101/cshperspect.a004523

Meier-Abt, F., & Bentires-Alj, M. (2014). How pregnancy at early age protects against breast cancer. *Trends in Molecular Medicine*, *20*(3), 143–153. https://doi.org/10.1016/j.molmed.2013.11.002

Meier-Abt, F., Milani, E., Roloff, T., Brinkhaus, H., Duss, S., Meyer, D. S., Klebba, I., Balwierz, P. J., van Nimwegen, E., & Bentires-Alj, M. (2013). Parity induces differentiation and reduces Wnt/Notch signaling ratio and proliferation potential of basal stem/progenitor cells isolated from mouse mammary epithelium. *Breast Cancer Research*, *15*(2), R36. https://doi.org/10.1186/bcr3419

Meng, N., Yang, Q., He, Y., Gu, W.-W., Gu, Y., Zhen, X.-X., Wang, J., Zhang, X., Sun, Z.-G., & Wang, J. (2019). Decreased NDRG1 expression is associated with pregnancy loss in mice and attenuates the in vitro decidualization of endometrial stromal cells. *Molecular Reproduction and Development*, *86*(9), 1210–1223. https://doi.org/10.1002/mrd.23238

Misra, Y., Bentley, P. A., Bond, J. P., Tighe, S., Hunter, T., & Zhao, F.-Q. (2012). Mammary gland morphological and gene expression changes underlying pregnancy protection of breast cancer tumorigenesis. *Physiological Genomics*, *44*(1), 76–88. https://doi.org/10.1152/physiolgenomics.00056.2011

Miyoshi, K., Shillingford, J. M., Smith, G. H., Grimm, S. L., Wagner, K.-U., Oka, T., Rosen, J. M., Robinson, G. W., & Hennighausen, L. (2001). Signal transducer and activator of transcription (Stat) 5 controls the proliferation and differentiation of mammary alveolar epithelium. *Journal of Cell Biology*, *155*(4), 531–542. https://doi.org/10.1083/jcb.200107065

Monks, J., Rosner, D., Geske, F. J., Lehman, L., Hanson, L., Neville, M. C., & Fadok, V. A. (2005). Epithelial cells as phagocytes: Apoptotic epithelial cells are engulfed by mammary alveolar epithelial cells and repress inflammatory mediator release. *Cell Death and Differentiation*, *12*(2), 107–114. https://doi.org/10.1038/sj.cdd.4401517

Moore, D. M., Vogl, A. W., Baimbridge, K., & Emerman, J. T. (1987). Effect of calcium on oxytocin-induced contraction of mammary gland myoepithelium as visualized by NBD-phallacidin. *Journal of Cell Science*, *88 (Pt 5)*, 563–569. https://doi.org/10.1242/jcs.88.5.563

Mootha, V. K., Lindgren, C. M., Eriksson, K.-F., Subramanian, A., Sihag, S., Lehar, J., Puigserver, P., Carlsson, E., Ridderstråle, M., Laurila, E., Houstis, N., Daly, M. J., Patterson, N., Mesirov, J. P., Golub, T. R., Tamayo, P., Spiegelman, B., Lander, E. S., Hirschhorn, J. N., … Groop, L. C. (2003). PGC-1α-responsive genes involved in oxidative phosphorylation are coordinately downregulated in human diabetes. *Nature Genetics*, *34*(3), Article 3. https://doi.org/10.1038/ng1180

Morrison, M. M., Young, C. D., Wang, S., Sobolik, T., Sanchez, V. M., Hicks, D. J., Cook, R. S., & Brantley-Sieders, D. M. (2015). MTOR Directs Breast Morphogenesis through the PKC-alpha-Rac1 Signaling Axis. *PLoS Genetics*, *11*(7), e1005291. https://doi.org/10.1371/journal.pgen.1005291

Mueller, S. O., Clark, J. A., Myers, P. H., & Korach, K. S. (2002). Mammary Gland Development in Adult Mice Requires Epithelial and Stromal Estrogen Receptor α. *Endocrinology*, *143*(6), 2357–2365. https://doi.org/10.1210/endo.143.6.8836

Mulac-Jericevic, B., Lydon, J. P., DeMayo, F. J., & Conneely, O. M. (2003). Defective mammary gland morphogenesis in mice lacking the progesterone receptor B isoform. *Proceedings of the National Academy of Sciences*, *100*(17), 9744–9749. https://doi.org/10.1073/pnas.1732707100

Mulac-Jericevic, B., Mullinax, R. A., DeMayo, F. J., Lydon, J. P., & Conneely, O. M. (2000). Subgroup of Reproductive Functions of Progesterone Mediated by Progesterone Receptor-B Isoform. *Science*, *289*(5485), 1751–1754. https://doi.org/10.1126/science.289.5485.1751

Murrow, L. M., Weber, R. J., Caruso, J. A., McGinnis, C. S., Phong, K., Gascard, P., Borowsky, A. D., Desai, T. A., Thomson, M., Tlsty, T., & Gartner, Z. J. (2020). *Changes in epithelial proportions and transcriptional state underlie major premenopausal breast cancer risks* (p. 430611). https://doi.org/10.1101/430611

Murrow, L. M., Weber, R. J., Caruso, J. A., McGinnis, C. S., Phong, K., Gascard, P., Rabadam, G., Borowsky, A. D., Desai, T. A., Thomson, M., Tlsty, T., & Gartner, Z. J. (2022). Mapping hormone-regulated cell-cell interaction networks in the human breast at single-cell resolution. *Cell Systems*, *13*(8), 644-664.e8. https://doi.org/10.1016/j.cels.2022.06.005

Neubauer, N. L., Ward, E. C., Patel, P., Lu, Z., Lee, I., Blok, L. J., Hanifi-Moghaddam, P., Schink, J., & Kim, J. J. (2011). Progesterone Receptor-B Induction of BIRC3 Protects Endometrial Cancer Cells from AP1-59-Mediated Apoptosis. *Hormones & Cancer*, *2*(3), 170–181. https://doi.org/10.1007/s12672-011-0065-7

Neville, M. C., McFadden, T. B., & Forsyth, I. (2002). Hormonal regulation of mammary differentiation and milk secretion. *Journal of Mammary Gland Biology and Neoplasia*, *7*(1), 49–66. https://doi.org/10.1023/a:1015770423167

Nguyen, D. A., Parlow, A. F., & Neville, M. C. (2001). Hormonal regulation of tight junction closure in the mouse mammary epithelium during the transition from pregnancy to lactation. *The Journal of Endocrinology*, *170*(2), 347–356. https://doi.org/10.1677/joe.0.1700347

Nguyen, Q. H., Pervolarakis, N., Blake, K., Ma, D., Davis, R. T., James, N., Phung, A. T., Willey, E., Kumar, R., Jabart, E., Driver, I., Rock, J., Goga, A., Khan, S. A., Lawson, D. A., Werb, Z., & Kessenbrock, K. (2018). Profiling human breast epithelial cells using single cell RNA sequencing identifies cell diversity. *Nature Communications*, *9*(1), 2028. https://doi.org/10.1038/s41467-018-04334-1

Nguyen-Ngoc, K.-V., Shamir, E. R., Huebner, R. J., Beck, J. N., Cheung, K. J., & Ewald, A. J. (2015). 3D Culture Assays of Murine Mammary Branching Morphogenesis and Epithelial Invasion. In C. M. Nelson (Ed.), *Tissue Morphogenesis: Methods and Protocols* (pp. 135–162). Springer. https://doi.org/10.1007/978-1-4939-1164-6_10

Oakes, S. R., Naylor, M. J., Asselin-Labat, M.-L., Blazek, K. D., Gardiner-Garden, M., Hilton, H. N., Kazlauskas, M., Pritchard, M. A., Chodosh, L. A., Pfeffer, P. L., Lindeman, G. J., Visvader, J. E., & Ormandy, C. J. (2008). The Ets transcription factor Elf5 specifies mammary alveolar cell fate. *Genes & Development*, *22*(5), 581–586. https://doi.org/10.1101/gad.1614608

Obr, A., & Edwards, D. P. (2012). The Biology of Progesterone Receptor in the Normal Mammary gland and in Breast Cancer. *Molecular and Cellular Endocrinology*, *357*(1–2), 4–17. https://doi.org/10.1016/j.mce.2011.10.030

O'Brien, J., Lyons, T., Monks, J., Lucia, M. S., Wilson, R. S., Hines, L., Man, Y., Borges, V., & Schedin, P. (2010). Alternatively Activated Macrophages and Collagen Remodeling Characterize the Postpartum Involuting Mammary Gland across Species. *The American Journal of Pathology*, *176*(3), 1241–1255. https://doi.org/10.2353/ajpath.2010.090735

Ogawa, M., Yamaji, R., Higashimura, Y., Harada, N., Ashida, H., Nakano, Y., & Inui, H. (2011). 17β-Estradiol Represses Myogenic Differentiation by Increasing Ubiquitin-specific Peptidase 19 through Estrogen Receptor α. *The Journal of Biological Chemistry*, *286*(48), 41455–41465. https://doi.org/10.1074/jbc.M111.276824

Oliver, C. H., Khaled, W. T., Frend, H., Nichols, J., & Watson, C. J. (2012). The Stat6-regulated KRAB domain zinc finger protein Zfp157 regulates the balance of lineages in mammary glands and compensates for loss of Gata-3. *Genes & Development*, *26*(10), 1086–1097. https://doi.org/10.1101/gad.184051.111

Ormandy, C. J., Binart, N., & Kelly, P. A. (1997). Mammary Gland Development in Prolactin Receptor Knockout Mice. *Journal of Mammary Gland Biology and Neoplasia*, *2*(4), 355–364. https://doi.org/10.1023/A:1026395229025

Ormandy, C. J., Camus, A., Barra, J., Damotte, D., Lucas, B., Buteau, H., Edery, M., Brousse, N., Babinet, C., Binart, N., & Kelly, P. A. (1997). Null mutation of the prolactin receptor gene produces multiple reproductive defects in the mouse. *Genes & Development*, *11*(2), 167–178. https://doi.org/10.1101/gad.11.2.167

Otto, B., Streichert, T., Wegwitz, F., Gevensleben, H., Klätschke, K., Wagener, C., Deppert, W., & Tolstonog, G. V. (2013). Transcription factors link mouse WAP-T mammary tumors with human breast cancer. *International Journal of Cancer*, *132*(6), 1311–1322. https://doi.org/10.1002/ijc.27941

Pal, B., Bouras, T., Shi, W., Vaillant, F., Sheridan, J. M., Fu, N., Breslin, K., Jiang, K., Ritchie, M. E., Young, M., Lindeman, G. J., Smyth, G. K., & Visvader, J. E. (2013). Global Changes in the Mammary Epigenome Are Induced by Hormonal Cues and Coordinated by Ezh2. *Cell Reports*, *3*(2), 411–426. https://doi.org/10.1016/j.celrep.2012.12.020

Pal, B., Chen, Y., Milevskiy, M. J. G., Vaillant, F., Prokopuk, L., Dawson, C. A., Capaldo, B. D., Song, X., Jackling, F., Timpson, P., Lindeman, G. J., Smyth, G. K., & Visvader, J. E. (2021). Single cell transcriptome atlas of mouse mammary epithelial cells across development. *Breast Cancer Research*, *23*(1), 69. https://doi.org/10.1186/s13058-021-01445-4

Pal, B., Chen, Y., Vaillant, F., Jamieson, P., Gordon, L., Rios, A. C., Wilcox, S., Fu, N., Liu, K. H., Jackling, F. C., Davis, M. J., Lindeman, G. J., Smyth, G. K., & Visvader, J. E. (2017). Construction of developmental lineage relationships in the mouse mammary gland by single-cell RNA profiling. *Nature Communications*, *8*(1), Article 1. https://doi.org/10.1038/s41467-017-01560-x

Pardo, I., Lillemoe, H. A., Blosser, R. J., Choi, M., Sauder, C. A. M., Doxey, D. K., Mathieson, T., Hancock, B. A., Baptiste, D., Atale, R., Hickenbotham, M., Zhu, J., Glasscock, J., Storniolo, A. M. V., Zheng, F., Doerge, R., Liu, Y., Badve, S., Radovich, M., & Clare, S. E. (2014). Next-generation transcriptome sequencing of the premenopausal breast epithelium using specimens from a normal human breast tissue bank. *Breast Cancer Research : BCR*, *16*(2), R26. https://doi.org/10.1186/bcr3627

Pelissier Vatter, F. A., Schapiro, D., Chang, H., Borowsky, A. D., Lee, J. K., Parvin, B., Stampfer, M. R., LaBarge, M. A., Bodenmiller, B., & Lorens, J. B. (2018). High-Dimensional Phenotyping Identifies Age-Emergent Cells in Human Mammary Epithelia. *Cell Reports*, *23*(4), 1205–1219. https://doi.org/10.1016/j.celrep.2018.03.114

Pellacani, D., Bilenky, M., Kannan, N., Heravi-Moussavi, A., Knapp, D. J. H. F., Gakkhar, S., Moksa, M., Carles, A., Moore, R., Mungall, A. J., Marra, M. A., Jones, S. J. M., Aparicio, S., Hirst, M., & Eaves, C. J. (2016). Analysis of Normal Human Mammary Epigenomes Reveals Cell-Specific Active Enhancer States and Associated Transcription Factor Networks. *Cell Reports*, *17*(8), 2060–2074. https://doi.org/10.1016/j.celrep.2016.10.058

Pellacani, D., Tan, S., Lefort, S., & Eaves, C. J. (2019). Transcriptional regulation of normal human mammary cell heterogeneity and its perturbation in breast cancer. *The EMBO Journal*, *38*(14), e100330. https://doi.org/10.15252/embj.2018100330

Péqueux, C., Raymond-Letron, I., Blacher, S., Boudou, F., Adlanmerini, M., Fouque, M.-J., Rochaix, P., Noël, A., Foidart, J.-M., Krust, A., Chambon, P., Brouchet, L., Arnal, J.-F., & Lenfant, F. (2012). Stromal Estrogen Receptor-α Promotes Tumor Growth by Normalizing an Increased Angiogenesis. *Cancer Research*, *72*(12), 3010–3019. https://doi.org/10.1158/0008-5472.CAN-11-3768

Phipson, B., Sim, C. B., Porrello, E. R., Hewitt, A. W., Powell, J., & Oshlack, A. (2022). propeller: Testing for differences in cell type proportions in single cell data. *Bioinformatics*, *38*(20), 4720–4726. https://doi.org/10.1093/bioinformatics/btac582

Plaks, V., Boldajipour, B., Linnemann, J. R., Nguyen, N. H., Kersten, K., Wolf, Y., Casbon, A.-J., Kong, N., van den Bijgaart, R. J. E., Sheppard, D., Melton, A. C., Krummel, M. F., & Werb, Z. (2015). Adaptive Immune Regulation of Mammary Postnatal Organogenesis. *Developmental Cell*, *34*(5), 493–504. https://doi.org/10.1016/j.devcel.2015.07.015

Poli, V., Fagnocchi, L., Fasciani, A., Cherubini, A., Mazzoleni, S., Ferrillo, S., Miluzio, A., Gaudioso, G., Vaira, V., Turdo, A., Gaggianesi, M., Chinnici, A., Lipari, E., Bicciato, S., Bosari, S., Todaro, M., & Zippo, A. (2018). MYC-driven epigenetic reprogramming favors the onset of tumorigenesis by inducing a stem cell-like state. *Nature Communications*, *9*(1), Article 1. https://doi.org/10.1038/s41467-018-03264-2

Pollard, J. W., & Hennighausen, L. (1994). Colony stimulating factor 1 is required for mammary gland development during pregnancy. *Proceedings of the National Academy of Sciences of the United States of America*, *91*(20), 9312–9316.

Popnikolov, N., Yang, J., Liu, A., Guzman, R., & Nandi, S. (2001). Reconstituted normal human breast in nude mice: Effect of host pregnancy environment and human chorionic gonadotropin on proliferation. *Journal of Endocrinology*, *168*(3), 487–496. https://doi.org/10.1677/joe.0.1680487

Qiu, Y., Bevan, H., Weeraperuma, S., Wratting, D., Murphy, D., Neal, C. R., Bates, D. O., & Harper, S. J. (2008). Mammary alveolar development during lactation is inhibited by the endogenous antiangiogenic growth factor isoform, VEGF165b. *FASEB Journal: Official Publication of the Federation of American Societies for Experimental Biology*, *22*(4), 1104–1112. https://doi.org/10.1096/fj.07-9718com

Quintana, A. M., Liu, F., O'Rourke, J. P., & Ness, S. A. (2011). Identification and Regulation of c-Myb Target Genes in MCF-7 Cells. *BMC Cancer*, *11*(1), 30. https://doi.org/10.1186/1471-2407-11-30

Raafat, A. M., Hofseth, L. J., Li, S., Bennett, J. M., & Haslam, S. Z. (1999). A Mouse Model to Study the Effects of Hormone Replacement Therapy on Normal Mammary Gland during Menopause: Enhanced Proliferative Response to Estrogen in Late Postmenopausal Mice*. *Endocrinology*, *140*(6), 2570–2580. https://doi.org/10.1210/endo.140.6.6634

Rahat, M. A., Coffelt, S. B., Granot, Z., Muthana, M., & Amedei, A. (2016). Macrophages and Neutrophils: Regulation of the Inflammatory Microenvironment in Autoimmunity and Cancer. *Mediators of Inflammation*, *2016*, 5894347. https://doi.org/10.1155/2016/5894347

Rajaram, R. D., Buric, D., Caikovski, M., Ayyanan, A., Rougemont, J., Shan, J., Vainio, S. J., Yalcin-Ozuysal, O., & Brisken, C. (2015). Progesterone and Wnt4 control mammary stem cells via myoepithelial crosstalk. *The EMBO Journal*, *34*(5), 641–652. https://doi.org/10.15252/embj.201490434

Ramamoorthy, S., Dhananjayan, S. C., Demayo, F. J., & Nawaz, Z. (2010). Isoform-specific degradation of PR-B by E6-AP is critical for normal mammary gland development. *Molecular Endocrinology (Baltimore, Md.)*, *24*(11), 2099–2113. https://doi.org/10.1210/me.2010-0116

Raths, F., Karimzadeh, M., Ing, N., Martinez, A., Yang, Y., Qu, Y., Lee, T.-Y., Mulligan, B., Devkota, S., Tilley, W. T., Hickey, T. E., Wang, B., Giuliano, A. E., Bose, S., Goodarzi, H., Ray, E. C., Cui, X., & Knott, S. R. V. (2023). The molecular consequences of androgen activity in the human breast. *Cell Genomics*, *3*(3), 100272. https://doi.org/10.1016/j.xgen.2023.100272

Raven, J. F., Williams, V., Wang, S., Tremblay, M. L., Muller, W. J., Durbin, J. E., & Koromilas, A. E. (2011). Stat1 is a suppressor of ErbB2/Neu-mediated cellular transformation and mouse mammary gland tumor formation. *Cell Cycle*, *10*(5), 794–804. https://doi.org/10.4161/cc.10.5.14956

Regan, J. L., Kendrick, H., Magnay, F.-A., Vafaizadeh, V., Groner, B., & Smalley, M. J. (2012). C-Kit is required for growth and survival of the cells of origin of Brca1-mutation-associated breast cancer. *Oncogene*, *31*(7), Article 7. https://doi.org/10.1038/onc.2011.289

Riddle, O., Bates, R. W., & Dykshorn, S. W. (1933). THE PREPARATION, IDENTIFICATION AND ASSAY OF PROLACTIN—A HORMONE OF THE ANTERIOR PITUITARY. *American Journal of Physiology-Legacy Content*, *105*(1), 191–216. https://doi.org/10.1152/ajplegacy.1933.105.1.191

Rijnkels, M., Freeman-Zadrowski, C., Hernandez, J., Potluri, V., Wang, L., Li, W., & Lemay, D. G. (2013). Epigenetic Modifications Unlock the Milk Protein Gene Loci during Mouse Mammary Gland Development and Differentiation. *PLOS ONE*, *8*(1), e53270. https://doi.org/10.1371/journal.pone.0053270

Robinson, G. W. (2007). Cooperation of signalling pathways in embryonic mammary gland development. *Nature Reviews. Genetics*, *8*(12), 963–972. https://doi.org/10.1038/nrg2227

Robinson, G. W., McKnight, R. A., Smith, G. H., & Hennighausen, L. (1995). Mammary epithelial cells undergo secretory differentiation in cycling virgins but require pregnancy for the establishment of terminal differentiation. *Development*, *121*(7), 2079–2090. https://doi.org/10.1242/dev.121.7.2079

Rodilla, V., Dasti, A., Huyghe, M., Lafkas, D., Laurent, C., Reyal, F., & Fre, S. (2015). Luminal Progenitors Restrict Their Lineage Potential during Mammary Gland Development. *PLoS Biology*, *13*(2), e1002069. https://doi.org/10.1371/journal.pbio.1002069

Rodriguez-Boulan, E., & Macara, I. G. (2014). Organization and execution of the epithelial polarity programme. *Nature Reviews Molecular Cell Biology*, *15*(4), Article 4. https://doi.org/10.1038/nrm3775

Rosenbluth, J. M., Schackmann, R. C. J., Gray, G. K., Selfors, L. M., Li, C. M.-C., Boedicker, M., Kuiken, H. J., Richardson, A., Brock, J., Garber, J., Dillon, D., Sachs, N., Clevers, H., & Brugge, J. S. (2020). Organoid cultures from normal and cancer-prone human breast tissues preserve complex epithelial lineages. *Nature Communications*, *11*(1), 1711. https://doi.org/10.1038/s41467-020-15548-7

Rosner, B., Colditz, G. A., & Willett, W. C. (1994). Reproductive risk factors in a prospective study of breast cancer: The Nurses' Health Study. *American Journal of Epidemiology*, *139*(8), 819–835. https://doi.org/10.1093/oxfordjournals.aje.a117079

Rossiter, H., Barresi, C., Ghannadan, M., Gruber, F., Mildner, M., Födinger, D., & Tschachler, E. (2007). Inactivation of VEGF in mammary gland epithelium severely compromises mammary gland development and function. *FASEB Journal: Official Publication of the Federation of American Societies for Experimental Biology*, *21*(14), 3994–4004. https://doi.org/10.1096/fj.07-8720com

Rubio, M. F., Werbajh, S., Cafferata, E. G. A., Quaglino, A., Coló, G. P., Nojek, I. M., Kordon, E. C., Nahmod, V. E., & Costas, M. A. (2006). TNF-α enhances estrogen-induced cell proliferation of estrogen-dependent breast tumor cells through a complex containing nuclear factor-kappa B. *Oncogene*, *25*(9), Article 9. https://doi.org/10.1038/sj.onc.1209176

Rudali, G., Julien, P., Vives, C., & Apiou, F. (1978). Dose-effect studies on estrogen induced mammary cancers in mice. *Biomedicine / [Publiee Pour l'A.A.I.C.I.G.]*, *29*(2), 45–46.

Rudolph, M. C., McManaman, J. L., Phang, T., Russell, T., Kominsky, D. J., Serkova, N. J., Stein, T., Anderson, S. M., & Neville, M. C. (2007). Metabolic regulation in the lactating mammary gland: A lipid synthesizing machine. *Physiological Genomics*, *28*(3), 323–336. https://doi.org/10.1152/physiolgenomics.00020.2006

Rui, H., Kirken, R. A., & Farrar, W. L. (1994). Activation of receptor-associated tyrosine kinase JAK2 by prolactin. *Journal of Biological Chemistry*, *269*(7), 5364–5368. https://doi.org/10.1016/S0021-9258(17)37695-0

Rusidzé, M., Adlanmérini, M., Chantalat, E., Raymond-Letron, I., Cayre, S., Arnal, J.-F., Deugnier, M.-A., & Lenfant, F. (2021). Estrogen receptor-α signaling in post-natal mammary development and breast cancers. *Cellular and Molecular Life Sciences*, *78*(15), 5681–5705. https://doi.org/10.1007/s00018-021-03860-4

Russo, J., Ao, X., Grill, C., & Russo, I. H. (1999). Pattern of distribution of cells positive for estrogen receptor α and progesterone receptor in relation to proliferating cells in the mammary gland. *Breast Cancer Research and Treatment*, *53*(3), 217–227. https://doi.org/10.1023/A:1006186719322

Russo, J., Mailo, D., Hu, Y.-F., Balogh, G., Sheriff, F., & Russo, I. H. (2009). Breast Differentiation and Its Implication in Cancer Prevention. *Clinical Cancer Research*, *11*(2), 931s–936s. https://doi.org/10.1158/1078-0432.931s.11.2

Russo, J., Santucci-Pereira, J., de Cicco, R. L., Sheriff, F., Russo, P. A., Peri, S., Slifker, M., Ross, E., Mello, M. L. S., Vidal, B. C., Belitskaya-Lévy, I., Arslan, A., Zeleniuch-Jacquotte, A., Bordas, P., Lenner, P., Ahman, J., Afanasyeva, Y., Hallmans, G., Toniolo, P., & Russo, I. H. (2012). Pregnancy-induced chromatin remodeling in the breast of postmenopausal women. *International Journal of Cancer. Journal International Du Cancer*, *131*(5), 1059–1070. https://doi.org/10.1002/ijc.27323

Sachs, N., de Ligt, J., Kopper, O., Gogola, E., Bounova, G., Weeber, F., Balgobind, A. V., Wind, K., Gracanin, A., Begthel, H., Korving, J., van Boxtel, R., Duarte, A. A., Lelieveld, D., van Hoeck, A., Ernst, R. F., Blokzijl, F., Nijman, I. J., Hoogstraat, M., … Clevers, H. (2018). A Living Biobank of Breast Cancer Organoids Captures Disease Heterogeneity. *Cell*, *172*(1), 373-386.e10. https://doi.org/10.1016/j.cell.2017.11.010

Saeki, K., Chang, G., Kanaya, N., Wu, X., Wang, J., Bernal, L., Ha, D., Neuhausen, S. L., & Chen, S. (2021). Mammary cell gene expression atlas links epithelial cell remodeling events to breast carcinogenesis. *Communications Biology*, *4*(1), Article 1. https://doi.org/10.1038/s42003-021-02201-2

Sakamoto, K., Schmidt, J. W., & Wagner, K.-U. (2015). Mouse Models of Breast Cancer. *Methods in Molecular Biology (Clifton, N.J.)*, *1267*, 47–71. https://doi.org/10.1007/978-1-4939-2297-0_3

Santos, S. J., Aupperlee, M. D., Xie, J., Durairaj, S., Miksicek, R., Conrad, S. E., Leipprandt, J. R., Tan, Y. S., Schwartz, R. C., & Haslam, S. Z. (2009). Progesterone receptor A-regulated gene expression in mammary organoid cultures. *The Journal of Steroid Biochemistry and Molecular Biology*, *115*(3–5), 161–172. https://doi.org/10.1016/j.jsbmb.2009.04.001

Santos, S. J., Haslam, S. Z., & Conrad, S. E. (2010). Signal transducer and activator of transcription 5a mediates mammary ductal branching and proliferation in the nulliparous mouse. *Endocrinology*, *151*(6), 2876–2885. https://doi.org/10.1210/en.2009-1282

Sapino, A., Macrì, L., Tonda, L., & Bussolati, G. (1993). Oxytocin enhances myoepithelial cell differentiation and proliferation in the mouse mammary gland. *Endocrinology*, *133*(2), 838–842. https://doi.org/10.1210/endo.133.2.8344220

Sato, T., Tran, T. H., Peck, A. R., Liu, C., Ertel, A., Lin, J., Neilson, L. M., & Rui, H. (2013). Global profiling of prolactin-modulated transcripts in breast cancer in vivo. *Molecular Cancer*, *12*(1), 59. https://doi.org/10.1186/1476-4598-12-59

Schams, D., Kohlenberg, S., Amselgruber, W., Berisha, B., Pfaffl, M., & Sinowatz, F. (2003). Expression and localisation of oestrogen and progesterone receptors in the bovine mammary gland during development, function and involution. *Journal of Endocrinology*, *177*(2), 305–317. https://doi.org/10.1677/joe.0.1770305

Schauwecker, S. M., Kim, J. J., Licht, J. D., & Clevenger, C. V. (2017). Histone H1 and Chromosomal Protein HMGN2 Regulate Prolactin-induced STAT5 Transcription Factor Recruitment and Function in Breast Cancer Cells. *The Journal of Biological Chemistry*, *292*(6), 2237–2254. https://doi.org/10.1074/jbc.M116.764233

Schedin, P. (2006). Pregnancy-associated breast cancer and metastasis. *Nature Reviews. Cancer*, *6*(4), 281–291. https://doi.org/10.1038/nrc1839

Schedin, P., Mitrenga, T., McDaniel, S., & Kaeck, M. (2004). Mammary ECM composition and function are altered by reproductive state. *Molecular Carcinogenesis*, *41*(4), 207–220. https://doi.org/10.1002/mc.20058

Schmitt-Ney, M., Doppler, W., Ball, R. K., & Groner, B. (1991). Beta-casein gene promoter activity is regulated by the hormone-mediated relief of transcriptional repression and a mammary-gland-specific nuclear factor. *Molecular and Cellular Biology*, *11*(7), 3745–3755. https://doi.org/10.1128/mcb.11.7.3745-3755.1991

Seagroves, T. N., Lydon, J. P., Hovey, R. C., Vonderhaar, B. K., & Rosen, J. M. (2000). C/EBPβ (CCAAT/Enhancer Binding Protein) Controls Cell Fate Determination during Mammary Gland Development. *Molecular Endocrinology*, *14*(3), 359–368. https://doi.org/10.1210/mend.14.3.0434

Segatto, I., Zompit, M. D. M., Citron, F., D'Andrea, S., Vinciguerra, G. L. R., Perin, T., Berton, S., Mungo, G., Schiappacassi, M., Marchini, C., Amici, A., Vecchione, A., Baldassarre, G., & Belletti, B. (2019). Stathmin Is Required for Normal Mouse Mammary Gland Development and Δ16HER2-Driven Tumorigenesis. *Cancer Research*, *79*(2), 397–409. https://doi.org/10.1158/0008-5472.CAN-18-2488

Shackleton, M., Vaillant, F., Simpson, K. J., Stingl, J., Smyth, G. K., Asselin-Labat, M.-L., Wu, L., Lindeman, G. J., & Visvader, J. E. (2006). Generation of a functional mammary gland from a single stem cell. *Nature*, *439*(7072), Article 7072. https://doi.org/10.1038/nature04372

Shamir, E. R., & Ewald, A. J. (2014). Three-dimensional organotypic culture: Experimental models of mammalian biology and disease. *Nature Reviews Molecular Cell Biology*, *15*(10), Article 10. https://doi.org/10.1038/nrm3873

Shao, C., Lou, P., Liu, R., Bi, X., Li, G., Yang, X., Sheng, X., Xu, J., Lv, C., & Yu, Z. (2021). Hormone-Responsive BMP Signaling Expands Myoepithelial Cell Lineages and Prevents Alveolar Precocity in Mammary Gland. *Frontiers in Cell and Developmental Biology*, *9*, 691050. https://doi.org/10.3389/fcell.2021.691050

Shao, Y., & Zhao, F.-Q. (2014). Emerging evidence of the physiological role of hypoxia in mammary development and lactation. *Journal of Animal Science and Biotechnology*, *5*(1), 9. https://doi.org/10.1186/2049-1891-5-9

Sharp, J. A., Lefevre, C., Brennan, A. J., & Nicholas, K. R. (2007). The Fur Seal—A Model Lactation Phenotype to Explore Molecular Factors Involved in the Initiation of Apoptosis at Involution. *Journal of Mammary Gland Biology and Neoplasia*, *12*(1), 47–58. https://doi.org/10.1007/s10911-007-9037-5

Shehata, M., Teschendorff, A., Sharp, G., Novcic, N., Russell, I. A., Avril, S., Prater, M., Eirew, P., Caldas, C., Watson, C. J., & Stingl, J. (2012). Phenotypic and functional characterisation of the luminal cell hierarchy of the mammary gland. *Breast Cancer Research*, *14*(5), R134. https://doi.org/10.1186/bcr3334

Shekhar, M. P., Werdell, J., Santner, S. J., Pauley, R. J., & Tait, L. (2001). Breast stroma plays a dominant regulatory role in breast epithelial growth and differentiation: Implications for tumor development and progression. *Cancer Research*, *61*(4), 1320–1326.

Shillingford, J. M., Miyoshi, K., Flagella, M., Shull, G. E., & Hennighausen, L. (2002). Mouse mammary epithelial cells express the Na-K-Cl cotransporter, NKCC1: Characterization, localization, and involvement in ductal development and morphogenesis. *Molecular Endocrinology (Baltimore, Md.)*, *16*(6), 1309–1321. https://doi.org/10.1210/mend.16.6.0857

Shoker, B. S., Jarvis, C., Sibson, D. R., Walker, C., & Sloane, J. P. (1999). Oestrogen receptor expression in the normal and pre-cancerous breast. *The Journal of Pathology*, *188*(3), 237–244. https://doi.org/10.1002/(SICI)1096-9896(199907)188:3<237::AID-PATH343>3.0.CO;2-8

Shyamala, G., Chou, Y.-C., Louie, S. G., Guzman, R. C., Smith, G. H., & Nandi, S. (2002). Cellular expression of estrogen and progesterone receptors in mammary glands: Regulation by hormones, development and aging. *The*

Journal of Steroid Biochemistry and Molecular Biology, *80*(2), 137–148. https://doi.org/10.1016/S0960-0760(01)00182-0

Shyamala, G., Yang, X., Silberstein, G., Barcellos-Hoff, M. H., & Dale, E. (1998). Transgenic mice carrying an imbalance in the native ratio of A to B forms of progesterone receptor exhibit developmental abnormalities in mammary glands. *Proceedings of the National Academy of Sciences*, *95*(2), 696–701. https://doi.org/10.1073/pnas.95.2.696

Silberstein, G. B., & Daniel, C. W. (1987). Investigation of Mouse Mammary Ductal Growth Regulation Using Slow-Release Plastic Implants. *Journal of Dairy Science*, *70*(9), 1981–1990. https://doi.org/10.3168/jds.S0022-0302(87)80240-0

Simian, M., Hirai, Y., Navre, M., Werb, Z., Lochter, A., & Bissell, M. J. (2001). The interplay of matrix metalloproteinases, morphogens and growth factors is necessary for branching of mammary epithelial cells. *Development (Cambridge, England)*, *128*(16), 3117–3131. https://doi.org/10.1242/dev.128.16.3117

Simões, B. M., & Vivanco, M. dM. (2011). Cancer stem cells in the human mammary gland and regulation of their differentiation by estrogen. *Future Oncology*, *7*(8), 995–1006. https://doi.org/10.2217/fon.11.80

Sivaraman, L., Conneely, O. M., Medina, D., & O'Malley, B. W. (2001). P53 is a potential mediator of pregnancy and hormone-induced resistance to mammary carcinogenesis. *Proceedings of the National Academy of Sciences of the United States of America*, *98*(22), 12379–12384. https://doi.org/10.1073/pnas.221459098

Sleeman, K. E., Kendrick, H., Robertson, D., Isacke, C. M., Ashworth, A., & Smalley, M. J. (2006). Dissociation of estrogen receptor expression and in vivo stem cell activity in the mammary gland. *Journal of Cell Biology*, *176*(1), 19–26. https://doi.org/10.1083/jcb.200604065

Slepicka, P. F., Somasundara, A. V. H., & dos Santos, C. O. (2021). The molecular basis of mammary gland development and epithelial differentiation. *Seminars in Cell & Developmental Biology*, *114*, 93–112. https://doi.org/10.1016/j.semcdb.2020.09.014

Smalley, M., & Ashworth, A. (2003). Stem cells and breast cancer: A field in transit. *Nature Reviews Cancer*, *3*(11), Article 11. https://doi.org/10.1038/nrc1212

Smith, J. L., Lear, S. R., Forte, T. M., Ko, W., Massimi, M., & Erickson, S. K. (1998). Effect of pregnancy and lactation on lipoprotein and cholesterol metabolism in the rat. *Journal of Lipid Research*, *39*(11), 2237–2249. https://doi.org/10.1016/S0022-2275(20)32479-2

Snieder, H., MacGregor, A. J., & Spector, T. D. (1998). Genes Control the Cessation of a Woman's Reproductive Life: A Twin Study of Hysterectomy and Age at Menopause1. *The Journal of Clinical Endocrinology & Metabolism*, *83*(6), 1875–1880. https://doi.org/10.1210/jcem.83.6.4890

Soady, K. J., Kendrick, H., Gao, Q., Tutt, A., Zvelebil, M., Ordonez, L. D., Quist, J., Tan, D. W.-M., Isacke, C. M., Grigoriadis, A., & Smalley, M. J. (2015). Mouse mammary stem cells express prognostic markers for triple-negative breast cancer. *Breast Cancer Research*, *17*(1), 31. https://doi.org/10.1186/s13058-015-0539-6

Song, W., Wang, R., Jiang, W., Yin, Q., Peng, G., Yang, R., Yu, Q. C., Chen, J., Li, J., Cheung, T. H., Jing, N., & Zeng, Y. A. (2019). Hormones induce the formation of luminal-derived basal cells in the mammary gland. *Cell Research*, *29*(3), 206–220. https://doi.org/10.1038/s41422-018-0137-0

Sornapudi, T. R., Nayak, R., Guthikonda, P. K., Pasupulati, A. K., Kethavath, S., Uppada, V., Mondal, S., Yellaboina, S., & Kurukuti, S. (2018). Comprehensive profiling of transcriptional networks specific for lactogenic differentiation of HC11 mammary epithelial stem-like cells. *Scientific Reports*, *8*, 11777. https://doi.org/10.1038/s41598-018-30122-4

Srivastava, S., Matsuda, M., Hou, Z., Bailey, J. P., Kitazawa, R., Herbst, M. P., & Horseman, N. D. (2003). Receptor Activator of NF-κB Ligand Induction via Jak2 and Stat5a in Mammary Epithelial Cells *. *Journal of Biological Chemistry*, *278*(46), 46171–46178. https://doi.org/10.1074/jbc.M308545200

Stein, T., Morris, J. S., Davies, C. R., Weber-Hall, S. J., Duffy, M.-A., Heath, V. J., Bell, A. K., Ferrier, R. K., Sandilands, G. P., & Gusterson, B. A. (2004). Involution of the mouse mammary gland is associated with an immune cascade and an acute-phase response, involving LBP, CD14 and STAT3. *Breast Cancer Research*, *6*(2), R75. https://doi.org/10.1186/bcr753

Sternlicht, M. D., Sunnarborg, S. W., Kouros-Mehr, H., Yu, Y., Lee, D. C., & Werb, Z. (2005). Mammary ductal morphogenesis requires paracrine activation of stromal EGFR via ADAM17-dependent shedding of epithelial amphiregulin. *Development*, *132*(17), 3923–3933. https://doi.org/10.1242/dev.01966

Stewart, T. A., Hughes, K., Hume, D. A., & Davis, F. M. (2019). Developmental Stage-Specific Distribution of Macrophages in Mouse Mammary Gland. *Frontiers in Cell and Developmental Biology*, *7*. https://www.frontiersin.org/articles/10.3389/fcell.2019.00250

Stewart, T. A., Hughes, K., Stevenson, A. J., Marino, N., Ju, A. L., Morehead, M., & Davis, F. M. (2021). Mammary mechanobiology – investigating roles for mechanically activated ion channels in lactation and involution. *Journal of Cell Science*, *134*(1), jcs248849. https://doi.org/10.1242/jcs.248849

Stingl, J., Eaves, C. J., Zandieh, I., & Emerman, J. T. (2001). Characterization of bipotent mammary epithelial progenitor cells in normal adult human breast tissue. *Breast Cancer Research and Treatment*, *67*(2), 93–109. https://doi.org/10.1023/a:1010615124301

Stingl, J., Eirew, P., Ricketson, I., Shackleton, M., Vaillant, F., Choi, D., Li, H. I., & Eaves, C. J. (2006). Purification and unique properties of mammary epithelial stem cells. *Nature*, *439*(7079), Article 7079. https://doi.org/10.1038/nature04496

Strum, J. M. (1978). Estrogen-induced alterations in the myoepithelial cells of the rat mammary gland. *Cell and Tissue Research*, *193*(1), 155–161. https://doi.org/10.1007/BF00221608

Subramanian, A., Tamayo, P., Mootha, V. K., Mukherjee, S., Ebert, B. L., Gillette, M. A., Paulovich, A., Pomeroy, S. L., Golub, T. R., Lander, E. S., & Mesirov, J. P. (2005). Gene set enrichment analysis: A knowledge-based approach for interpreting genome-wide expression profiles. *Proceedings of the National Academy of Sciences*, *102*(43), 15545–15550. https://doi.org/10.1073/pnas.0506580102

Sumbal, J., Chiche, A., Charifou, E., Koledova, Z., & Li, H. (2020). Primary Mammary Organoid Model of Lactation and Involution. *Frontiers in Cell and Developmental Biology*, *8*. https://doi.org/10.3389/fcell.2020.00068

Tanos, T., Rojo, L. J., Echeverria, P., & Brisken, C. (2012). ER and PR signaling nodes during mammary gland development. *Breast Cancer Research*, *14*(4), 210. https://doi.org/10.1186/bcr3166

Thordarson, G., Jin, E., Guzman, R. C., Swanson, S. M., Nandi, S., & Talamantes, F. (1995). Refractoriness to mammary tumorigenesis in parous rats: Is it caused by persistent changes in the hormonal environment or permanent biochemical alterations in the mammary epithelia? *Carcinogenesis*, *16*(11), 2847–2853. https://doi.org/10.1093/carcin/16.11.2847

Tickle, C., & Jung, H.-S. (2016). Embryonic Mammary Gland Development. In *Encyclopedia of Life Sciences* (pp. 1–10). John Wiley & Sons, Ltd. https://doi.org/10.1002/9780470015902.a0026057

Tower, H., Dall, G., Davey, A., Stewart, M., Lanteri, P., Ruppert, M., Lambouras, M., Nasir, I., Yeow, S., Darcy, P. K., Ingman, W. V., Parker, B., Haynes, N. M., & Britt, K. L. (2022). Estrogen-induced immune changes within the normal mammary gland. *Scientific Reports*, *12*(1), 18986. https://doi.org/10.1038/s41598-022-21871-4

Twigger, A.-J., Engelbrecht, L. K., Bach, K., Schultz-Pernice, I., Pensa, S., Stenning, J., Petricca, S., Scheel, C. H., & Khaled, W. T. (2022). Transcriptional changes in the mammary gland during lactation revealed by single cell sequencing of cells from human milk. *Nature Communications*, *13*, 562. https://doi.org/10.1038/s41467-021-27895-0

Twigger, A.-J., & Khaled, W. T. (2021). Mammary gland development from a single cell ‘omics view. *Seminars in Cell & Developmental Biology*, *114*, 171–185. https://doi.org/10.1016/j.semcdb.2021.03.013

van Asselt, K. M., Kok, H. S., Pearson, P. L., Dubas, J. S., Peeters, P. H. M., te Velde, E. R., & van Noord, P. A. H. (2004). Heritability of menopausal age in mothers and daughters. *Fertility and Sterility*, *82*(5), 1348–1351. https://doi.org/10.1016/j.fertnstert.2004.04.047

Vasquez, Y. M. (2018). Estrogen-regulated transcription: Mammary gland and uterus. *Steroids*, *133*, 82–86. https://doi.org/10.1016/j.steroids.2017.12.014

Vaziri-Gohar, A., Zheng, Y., & Houston, K. D. (2017). IGF-1 Receptor Modulates FoxO1-mediated Tamoxifen Response in Breast Cancer Cells. *Molecular Cancer Research : MCR*, *15*(4), 489–497. https://doi.org/10.1158/1541-7786.MCR-16-0176

Veltmaat, J. M., Van Veelen, W., Thiery, J. P., & Bellusci, S. (2004). Identification of the mammary line in mouse by Wnt10b expression. *Developmental Dynamics*, *229*(2), 349–356. https://doi.org/10.1002/dvdy.10441

Virgo, B. B., & Bellward, G. D. (1974). Serum progesterone levels in the pregnant and postpartum laboratory mouse. *Endocrinology*, *95*(5), 1486–1490. https://doi.org/10.1210/endo-95-5-1486

Visvader, J. E. (2009). Keeping abreast of the mammary epithelial hierarchy and breast tumorigenesis. *Genes & Development*, *23*(22), 2563–2577. https://doi.org/10.1101/gad.1849509

Wahl, G. M., & Spike, B. T. (2017). Cell state plasticity, stem cells, EMT, and the generation of intra-tumoral heterogeneity. *NPJ Breast Cancer*, *3*, 14. https://doi.org/10.1038/s41523-017-0012-z

Wakao, H., Gouilleux, F., & Groner, B. (1994). Mammary gland factor (MGF) is a novel member of the cytokine regulated transcription factor gene family and confers the prolactin response. *The EMBO Journal*, *13*(9), 2182–2191. https://doi.org/10.1002/j.1460-2075.1994.tb06495.x

Wang, C., Christin, J. R., Oktay, M. H., & Guo, W. (2017). Lineage-Biased Stem Cells Maintain Estrogen-Receptor-Positive and -Negative Mouse Mammary Luminal Lineages. *Cell Reports*, *18*(12), 2825–2835. https://doi.org/10.1016/j.celrep.2017.02.071

Wang, C.-C. (2021). Metabolic Stress Adaptations Underlie Mammary Gland Morphogenesis and Breast Cancer Progression. *Cells*, *10*(10), 2641. https://doi.org/10.3390/cells10102641

Wang, D., Cai, C., Dong, X., Yu, Q. C., Zhang, X.-O., Yang, L., & Zeng, Y. A. (2015). Identification of multipotent mammary stem cells by protein C receptor expression. *Nature*, *517*(7532), Article 7532. https://doi.org/10.1038/nature13851

Wang, D. Y., De Stavola, B. L., Bulbrook, R. D., Allen, D. S., Kwa, H. G., Verstraeten, A. A., Moore, J. W., Fentiman, I. S., Hayward, J. L., & Gravelle, I. H. (1988). The permanent effect of reproductive events on blood prolactin levels and its relation to breast cancer risk: A population study of postmenopausal women. *European Journal of Cancer and Clinical Oncology*, *24*(7), 1225–1231. https://doi.org/10.1016/0277-5379(88)90132-0

Wang, H., Xiang, D., Liu, B., He, A., Randle, H. J., Zhang, K. X., Dongre, A., Sachs, N., Clark, A. P., Tao, L., Chen, Q., Botchkarev, V. V., Xie, Y., Dai, N., Clevers, H., Li, Z., & Livingston, D. M. (2019). Inadequate DNA damage repair promotes mammary transdifferentiation leading to BRCA1 breast cancer. *Cell*, *178*(1), 135-151.e19. https://doi.org/10.1016/j.cell.2019.06.002

Wang, X., Belguise, K., O'Neill, C. F., Sánchez-Morgan, N., Romagnoli, M., Eddy, S. F., Mineva, N. D., Yu, Z., Min, C., Trinkaus-Randall, V., Chalbos, D., & Sonenshein, G. E. (2009). RelB NF-κB Represses Estrogen Receptor α Expression via Induction of the Zinc Finger Protein Blimp1. *Molecular and Cellular Biology*, *29*(14), 3832–3844. https://doi.org/10.1128/MCB.00032-09

Wang, X., & Kaplan, D. L. (2012). Hormone-responsive 3D multicellular culture model of human breast tissue. *Biomaterials*, *33*(12), 3411–3420. https://doi.org/10.1016/j.biomaterials.2012.01.011

Wang, Y., Chaffee, T. S., LaRue, R. S., Huggins, D. N., Witschen, P. M., Ibrahim, A. M., Nelson, A. C., Machado, H. L., & Schwertfeger, K. L. (2020). Tissue-resident macrophages promote extracellular matrix homeostasis in the mammary gland stroma of nulliparous mice. *ELife*, *9*. https://doi.org/10.7554/eLife.57438

Watson, C. J. (2022). Alveolar cells in the mammary gland: Lineage commitment and cell death. *Biochemical Journal*, *479*(9), 995–1006. https://doi.org/10.1042/BCJ20210734

Watt, A. P., Sharp, J. A., Lefevre, C., & Nicholas, K. R. (2012). WFDC2 is differentially expressed in the mammary gland of the tammar wallaby and provides immune protection to the mammary gland and the developing pouch young. *Developmental and Comparative Immunology*, *36*(3), 584–590. https://doi.org/10.1016/j.dci.2011.10.001

Wei, J., Ramanathan, P., Martin, I. C., Moran, C., Taylor, R. M., & Williamson, P. (2013). Identification of gene sets and pathways associated with lactation performance in mice. *Physiological Genomics*, *45*(5), 171–181. https://doi.org/10.1152/physiolgenomics.00139.2011

Wiesen, J. F., Young, P., Werb, Z., & Cunha, G. R. (1999). Signaling through the stromal epidermal growth factor receptor is necessary for mammary ductal development. *Development*, *126*(2), 335–344. https://doi.org/10.1242/dev.126.2.335

Williams, C., Helguero, L., Edvardsson, K., Haldosén, L.-A., & Gustafsson, J.-Å. (2009). Gene expression in murine mammary epithelial stem cell-like cells shows similarities to human breast cancer gene expression. *Breast Cancer Research : BCR*, *11*(3), R26. https://doi.org/10.1186/bcr2256

Wolf, K., Alexander, S., Schacht, V., Coussens, L. M., von Andrian, U. H., van Rheenen, J., Deryugina, E., & Friedl, P. (2009). Collagen-based cell migration models in vitro and in vivo. *Seminars in Cell & Developmental Biology*, *20*(8), 931–941. https://doi.org/10.1016/j.semcdb.2009.08.005

Wuidart, A., Sifrim, A., Fioramonti, M., Matsumura, S., Brisebarre, A., Brown, D., Centonze, A., Dannau, A., Dubois, C., Van Keymeulen, A., Voet, T., & Blanpain, C. (2018). Early lineage segregation of multipotent embryonic mammary gland progenitors. *Nature Cell Biology*, *20*(6), 666–676. https://doi.org/10.1038/s41556-018-0095-2

Yadava, N., Schneider, S. S., Jerry, D. J., & Kim, C. (2013). Impaired mitochondrial metabolism and mammary carcinogenesis. *Journal of Mammary Gland Biology and Neoplasia*, *18*(1), 75–87. https://doi.org/10.1007/s10911-012-9271-3

Yamamoto, M., Abe, C., Wakinaga, S., Sakane, K., Yumiketa, Y., Taguchi, Y., Matsumura, T., Ishikawa, K., Fujimoto, J., Semba, K., Miyauchi, M., Akiyama, T., & Inoue, J. (2019). TRAF6 maintains mammary stem cells and promotes pregnancy-induced mammary epithelial cell expansion. *Communications Biology*, *2*(1), Article 1. https://doi.org/10.1038/s42003-019-0547-7

Yang, L., Wang, X. L., Wan, P. C., Zhang, L. Y., Wu, Y., Tang, D. W., & Zeng, S. M. (2010). Up-regulation of expression of interferon-stimulated gene 15 in the bovine corpus luteum during early pregnancy. *Journal of Dairy Science*, *93*(3), 1000–1011. https://doi.org/10.3168/jds.2009-2529

Ye, T., Feng, J., Wan, X., Xie, D., & Liu, J. (2020). Double Agent: SPDEF Gene with Both Oncogenic and Tumor-Suppressor Functions in Breast Cancer. *Cancer Management and Research*, *12*, 3891–3902. https://doi.org/10.2147/CMAR.S243748

Yoh, K. E., Regunath, K., Guzman, A., Lee, S.-M., Pfister, N. T., Akanni, O., Kaufman, L. J., Prives, C., & Prywes, R. (2016). Repression of p63 and induction of EMT by mutant Ras in mammary epithelial cells. *Proceedings of the National Academy of Sciences*, *113*(41), E6107–E6116. https://doi.org/10.1073/pnas.1613417113

Zappia, L., & Oshlack, A. (2018). Clustering trees: A visualization for evaluating clusterings at multiple resolutions. *GigaScience*, *7*(7), giy083. https://doi.org/10.1093/gigascience/giy083

Zeps, N., Bentel, J. M., Papadimitriou, J. M., D'Antuono, M. F., & Dawkins, H. J. S. (1998). Estrogen receptor-negative epithelial cells in mouse mammary gland development and growth. *Differentiation*, *62*(5), 221–226. https://doi.org/10.1046/j.1432-0436.1998.6250221.x

Zhang, J., Lin, H., Hou, L., Xiao, H., Gong, X., Guo, X., Cao, X., & Liu, Z. (2022). Exploration of the breast ductal carcinoma in situ signature and its prognostic implications. *Cancer Medicine*, *12*(3), 3758–3772. https://doi.org/10.1002/cam4.5071

Zhang, L., Adileh, M., Martin, M. L., Klingler, S., White, J., Ma, X., Howe, L. R., Brown, A. M. C., & Kolesnick, R. (2017). Establishing estrogen-responsive mouse mammary organoids from single Lgr5+ cells,,. *Cellular Signalling*, *29*, 41–51. https://doi.org/10.1016/j.cellsig.2016.08.001

Zhong, H., Wang, P., Song, Y., Zhang, X., Che, L., Feng, B., Lin, Y., Xu, S., Li, J., Wu, D., Wu, Q., & Fang, Z. (2018). Mammary cell proliferation and catabolism of adipose tissues in nutrition-restricted lactating sows were associated with extracellular high glutamate levels. *Journal of Animal Science and Biotechnology*, *9*(1), 78. https://doi.org/10.1186/s40104-018-0293-6

Zhou, J., Chehab, R., Tkalcevic, J., Naylor, M. J., Harris, J., Wilson, T. J., Tsao, S., Tellis, I., Zavarsek, S., Xu, D., Lapinskas, E. J., Visvader, J., Lindeman, G. J., Thomas, R., Ormandy, C. J., Hertzog, P. J., Kola, I., & Pritchard, M. A. (2005). Elf5 is essential for early embryogenesis and mammary gland development during pregnancy and lactation. *The EMBO Journal*, *24*(3), 635–644. https://doi.org/10.1038/sj.emboj.7600538

Zhou, Y., Gong, W., Xiao, J., Wu, J., Pan, L., Li, X., Wang, X., Wang, W., Hu, S., & Yu, J. (2014). Transcriptomic analysis reveals key regulators of mammogenesis and the pregnancy-lactation cycle. *Science China Life Sciences*, *57*(3), 340–355. https://doi.org/10.1007/s11427-013-4579-9

Zilionis, R., Engblom, C., Pfirschke, C., Savova, V., Zemmour, D., Saatcioglu, H. D., Krishnan, I., Maroni, G., Meyerovitz, C. V., Kerwin, C. M., Choi, S., Richards, W. G., Rienzo, A. D., Tenen, D. G., Bueno, R., Levantini, E., Pittet, M. J., & Klein, A. M. (2019). Single-Cell Transcriptomics of Human and Mouse Lung Cancers Reveals Conserved Myeloid Populations across Individuals and Species. *Immunity*, *50*(5), 1317-1334.e10. https://doi.org/10.1016/j.immuni.2019.03.009

12. Appendix – Tables

Table S 1. Top DEGs in cluster MO3

Gene	p_val	avg_log2FC	pct.1	pct.2	p_val_adj	cluster
Wfdc18	0	2.61635813	0.91	0.473	0	3
Snorc	3.11E-153	1.59507454	0.363	0.116	6.16E-149	3
Itm2b1	4.80E-137	0.97430352	0.893	0.737	9.51E-133	3
Cytip	1.56E-127	1.30782957	0.201	0.042	3.08E-123	3
Kcne3	8.45E-91	1.09566948	0.206	0.058	1.67E-86	3
Fxyd3	1.75E-84	0.83701522	0.732	0.531	3.47E-80	3
Muc15l	2.84E-84	1.16853712	0.283	0.109	5.63E-80	3
Cd14	1.92E-81	1.15201161	0.261	0.096	3.80E-77	3
Cldn3	1.90E-74	0.74940455	0.71	0.521	3.77E-70	3
Slc5a8	2.24E-69	0.74006536	0.115	0.024	4.43E-65	3
Cited4l	4.43E-66	0.90246207	0.413	0.224	8.77E-62	3
Dbi1	7.25E-65	0.58954336	0.84	0.689	1.44E-60	3
Atp6v1b1l	2.04E-64	1.00836901	0.254	0.106	4.04E-60	3
Aldh1a3	2.99E-62	1.04327722	0.274	0.123	5.93E-58	3
Krt18l	4.83E-57	0.43960189	0.924	0.843	9.57E-53	3
Ly6e	3.24E-56	0.47600691	0.906	0.85	6.42E-52	3
Ltbp1	2.10E-55	0.74169599	0.131	0.037	4.17E-51	3
Atp2b1	2.08E-54	0.91070777	0.354	0.194	4.11E-50	3
Mme	2.36E-52	0.88887815	0.21	0.087	4.67E-48	3
Ehf	1.35E-51	0.91401045	0.269	0.129	2.68E-47	3
Elf5l	3.07E-50	0.8534225	0.223	0.097	6.08E-46	3
Plb1	1.14E-49	0.74534378	0.127	0.038	2.27E-45	3
Pla2g4a	1.54E-47	0.82011909	0.222	0.099	3.04E-43	3
Wwp2	2.43E-47	0.9645787	0.302	0.159	4.82E-43	3
Hspb1	3.99E-46	0.82156697	0.548	0.391	7.90E-42	3
Ptx3	9.21E-45	0.84044616	0.177	0.072	1.82E-40	3
Plet1l	5.28E-44	0.81912712	0.34	0.194	1.05E-39	3
Snta1	1.36E-42	0.68829505	0.127	0.043	2.69E-38	3
Osgin2	1.38E-40	0.68650379	0.1	0.029	2.74E-36	3
Ogfrl1l	1.42E-39	0.7849143	0.286	0.155	2.81E-35	3
Cryab	1.02E-38	0.69814013	0.327	0.188	2.02E-34	3
Tspan8l	1.60E-37	0.67802405	0.502	0.351	3.17E-33	3
Kit1	1.63E-36	0.74825441	0.189	0.087	3.22E-32	3
Epcam1	3.73E-36	0.42950663	0.814	0.732	7.39E-32	3
Mgst1	7.67E-36	0.54894153	0.676	0.557	1.52E-31	3
Phlda1l	3.45E-32	0.6065831	0.47	0.332	6.83E-28	3

Igfbp51	3.44E-31	0.54534364	0.78	0.653	6.82E-27	3
Anxa21	2.39E-30	0.5241698	0.597	0.477	4.74E-26	3
Anxa11	8.01E-30	0.63222776	0.409	0.28	1.59E-25	3
Cdc42ep31	3.01E-29	0.68322711	0.261	0.152	5.96E-25	3
Cck	6.46E-29	0.6928011	0.103	0.039	1.28E-24	3
Cst3	3.42E-28	1.03745994	0.501	0.39	6.78E-24	3
Krt81	1.03E-26	0.2910835	0.868	0.791	2.04E-22	3
Trps11	1.43E-26	0.55411903	0.503	0.385	2.83E-22	3
Tacstd21	2.40E-26	0.52610909	0.249	0.143	4.76E-22	3
Slc15a2	3.19E-26	0.60535034	0.145	0.069	6.32E-22	3
Gadd45b1	1.15E-24	0.63716978	0.21	0.119	2.28E-20	3
Cldn71	1.28E-24	0.47018606	0.534	0.41	2.54E-20	3
Jund1	1.31E-24	0.47726508	0.553	0.439	2.60E-20	3
Cp	1.49E-24	0.52964578	0.425	0.305	2.95E-20	3
Lmo41	1.47E-23	0.48557985	0.491	0.377	2.92E-19	3
Clmn	3.50E-23	0.47981687	0.127	0.059	6.93E-19	3
Arl4a	6.37E-23	0.57952117	0.167	0.088	1.26E-18	3
Palmd1	2.85E-22	0.43463526	0.193	0.106	5.65E-18	3
Sdc4	6.71E-22	0.43689872	0.59	0.497	1.33E-17	3
Scd11	5.35E-21	0.55606776	0.424	0.32	1.06E-16	3
Serpinb5	6.08E-21	0.59393815	0.264	0.17	1.20E-16	3
Tm4sf11	1.57E-20	0.25091074	0.865	0.826	3.11E-16	3
Ldha	6.85E-20	0.4964179	0.572	0.495	1.36E-15	3
Krt14	2.02E-19	0.83255579	0.332	0.234	4.00E-15	3
Nfib	5.82E-19	0.37685232	0.634	0.548	1.15E-14	3
BC0069651	7.35E-19	0.49401661	0.156	0.086	1.46E-14	3
Apod1	8.70E-19	0.56148609	0.277	0.184	1.72E-14	3
Rb1	9.07E-18	0.52273406	0.119	0.06	1.80E-13	3
Pgf	1.78E-17	0.55913607	0.181	0.109	3.53E-13	3
Basp11	2.11E-17	0.38159716	0.548	0.456	4.18E-13	3
Wnt5b	2.14E-17	0.47061122	0.114	0.057	4.24E-13	3
Ppp1r21	1.29E-16	0.47802162	0.327	0.235	2.55E-12	3
Myo6	1.42E-16	0.41149435	0.122	0.064	2.81E-12	3
Krt23	1.45E-16	0.40942516	0.102	0.05	2.87E-12	3
Cd811	7.01E-16	0.31808609	0.641	0.547	1.39E-11	3
Cited21	9.21E-16	0.47868323	0.384	0.292	1.82E-11	3
Rhou	1.05E-15	0.46349946	0.128	0.07	2.08E-11	3
Cebpd	1.48E-15	0.57615004	0.224	0.147	2.94E-11	3
Nipal2	2.27E-15	0.42250701	0.145	0.083	4.51E-11	3
Coro2a	4.79E-15	0.44155152	0.192	0.122	9.49E-11	3
Tcf7l2	7.76E-15	0.44952226	0.153	0.091	1.54E-10	3
Egln31	7.86E-15	0.50531965	0.19	0.121	1.56E-10	3

Eif1	8.91E-15	0.26304384	0.85	0.826	1.76E-10	3
Myl12a	2.85E-14	0.40879422	0.471	0.383	5.65E-10	3
Ctsh1	6.23E-14	0.45528718	0.266	0.188	1.23E-09	3
Gas6	6.69E-14	0.50120134	0.154	0.094	1.32E-09	3
Irx1	2.38E-13	0.38539997	0.368	0.284	4.72E-09	3
Hebp2	2.50E-13	0.41842052	0.135	0.08	4.95E-09	3
Trim47	4.25E-13	0.43877628	0.141	0.085	8.41E-09	3
Sorbs21	4.52E-13	0.40965887	0.249	0.175	8.94E-09	3
Id2	4.98E-13	0.4445289	0.312	0.233	9.86E-09	3
Celf21	2.16E-12	0.41004179	0.122	0.072	4.29E-08	3
Map3k1	2.63E-12	0.35237658	0.108	0.061	5.21E-08	3
Lurap1l	3.22E-12	0.41367882	0.161	0.102	6.37E-08	3
Thbs1	6.50E-12	0.43198244	0.229	0.161	1.29E-07	3
Tln2	6.78E-12	0.3826658	0.142	0.088	1.34E-07	3
Bsg	2.85E-11	0.53147267	0.68	0.641	5.64E-07	3
Far1	4.04E-11	0.37043813	0.152	0.097	7.99E-07	3
Tubb2a	8.56E-11	0.37297614	0.101	0.058	1.69E-06	3
Reep5	9.18E-11	0.30764585	0.548	0.479	1.82E-06	3
Ier21	9.86E-11	0.28999087	0.586	0.53	1.95E-06	3
Pde4d1	1.01E-10	0.37299272	0.129	0.08	2.01E-06	3
Tgfb31	1.14E-10	0.40126273	0.156	0.101	2.26E-06	3
Nfkbia1	3.64E-10	0.3536623	0.184	0.126	7.20E-06	3
Pik3r1	3.65E-10	0.34543718	0.361	0.288	7.23E-06	3
Nupr1l	3.68E-10	0.35508587	0.405	0.335	7.30E-06	3
Pgk1	3.71E-10	0.47142603	0.375	0.313	7.35E-06	3
Ier31	4.47E-10	0.31244982	0.6	0.535	8.85E-06	3
Pbx1	5.10E-10	0.34298487	0.219	0.158	1.01E-05	3
Zfp36l1	5.65E-10	0.34856956	0.364	0.292	1.12E-05	3
2200002D01Rik	8.18E-10	0.32972145	0.133	0.084	1.62E-05	3
Apobec31	1.11E-09	0.31779577	0.391	0.321	2.20E-05	3
Ugp2	2.14E-09	0.34259567	0.124	0.079	4.24E-05	3
Trp53bp2	3.54E-09	0.34810522	0.126	0.081	7.02E-05	3
Cracr2b	3.65E-09	0.32764706	0.185	0.13	7.23E-05	3
Notch1	6.42E-09	0.31214553	0.153	0.104	0.00012705	3
Tpi1l	1.45E-08	0.28904869	0.409	0.345	0.00028637	3
Psmd8	2.12E-08	0.28283056	0.392	0.326	0.00041923	3
Atp6v1e1l	2.82E-08	0.33194129	0.388	0.324	0.00055796	3
Bzw2	3.55E-08	0.31355451	0.282	0.223	0.00070304	3
Josd2	4.03E-08	0.30773423	0.25	0.193	0.0007982	3
Txndc12	4.10E-08	0.32010804	0.1	0.063	0.00081228	3
Csrp1	4.26E-08	0.30960549	0.291	0.234	0.00084327	3
Gls	6.03E-08	0.36793144	0.126	0.085	0.00119496	3

Efhd2	7.03E-08	0.36308112	0.126	0.086	0.00139285	3
Shisa5	8.00E-08	0.30126784	0.164	0.116	0.00158454	3
Map1lc3a	1.14E-07	0.30418291	0.393	0.329	0.00226459	3
Rhoj	1.43E-07	0.25073954	0.124	0.082	0.00283104	3
Atp6v1a1	1.45E-07	0.2994866	0.194	0.144	0.00287776	3
Anxa3	2.88E-07	0.31033748	0.334	0.276	0.00569482	3
Aldoa1	3.44E-07	0.34639861	0.678	0.651	0.00680547	3
Rhoq	3.76E-07	0.28502792	0.13	0.09	0.00744532	3
Tnfrsf12a1	4.70E-07	0.34642298	0.234	0.183	0.00931167	3
Rab25l	4.88E-07	0.28397296	0.429	0.373	0.00965982	3
Dbndd2	5.41E-07	0.3712375	0.151	0.109	0.01072317	3
St14	6.37E-07	0.33021412	0.171	0.127	0.0126247	3
Litaf	8.09E-07	0.32834106	0.183	0.138	0.016012	3
B4galnt1	8.17E-07	0.30244082	0.143	0.102	0.0161889	3
Spint1	1.01E-06	0.26468949	0.14	0.099	0.02007277	3
Camk2n1l	1.07E-06	0.30114186	0.205	0.158	0.02115774	3
Ltbp3	1.18E-06	0.27108113	0.299	0.242	0.02326994	3
Irx2	1.36E-06	0.33555727	0.262	0.211	0.02698306	3
Plekhb1	1.40E-06	0.32102457	0.133	0.095	0.02780103	3
Actn4l	1.52E-06	0.25072112	0.463	0.411	0.03013043	3
Tjp2	1.54E-06	0.26547634	0.129	0.091	0.03058825	3
AY036118	1.66E-06	0.30505033	0.509	0.463	0.03289409	3
Pkp1	1.83E-06	0.30972485	0.15	0.11	0.03630915	3

Table S 2. Top DEGs in cluster MO5

Gene	p_val	avg_log2FC	pct.1	pct.2	p_val_adj	cluster
Hmgb2	0	2.49405492	0.806	0.152	0	5
Hist1h1b	0	2.27126034	0.417	0.05	0	5
Top2a	0	2.04238811	0.46	0.039	0	5
Mki67	0	1.97894889	0.462	0.034	0	5
Pclaf	0	1.96761958	0.498	0.03	0	5
H2afz	0	1.92961322	0.973	0.463	0	5
Stmn1	0	1.92953585	0.863	0.26	0	5
Hist1h2ap	0	1.85185011	0.359	0.032	0	5
Cenpf	0	1.6187645	0.352	0.029	0	5
Birc5	0	1.53165123	0.385	0.031	0	5
Prc1	0	1.49641628	0.332	0.029	0	5
Cenpa	0	1.36808293	0.325	0.027	0	5
Cdca8	0	1.3653409	0.351	0.029	0	5
Spc24	0	1.33491422	0.342	0.027	0	5
Tpx2	0	1.25026868	0.281	0.019	0	5
Ube2c	9.35E-306	1.53736687	0.33	0.032	1.85E-301	5
Hmmr	9.69E-301	1.18344493	0.247	0.014	1.92E-296	5
Cdk1	1.61E-295	1.18316105	0.306	0.027	3.19E-291	5
Ccnb2	1.44E-281	1.23764694	0.271	0.021	2.86E-277	5
Tuba1b	1.27E-270	1.43250596	0.587	0.132	2.52E-266	5
Cdca3	6.20E-269	1.15425156	0.264	0.021	1.23E-264	5
Nusap1	5.89E-268	1.0150787	0.204	0.01	1.17E-263	5
Cdc20	9.95E-267	1.16307576	0.244	0.018	1.97E-262	5
Pbk	1.90E-262	0.97019744	0.216	0.012	3.76E-258	5
Lmnb1	2.98E-259	1.1857001	0.337	0.041	5.90E-255	5
Cenpe	1.32E-258	1.05725607	0.232	0.016	2.60E-254	5
Ccna2	3.08E-254	0.8709304	0.194	0.009	6.10E-250	5
Racgap1	3.12E-254	0.97784884	0.24	0.018	6.17E-250	5
Ccnb1	7.36E-245	1.0429025	0.215	0.014	1.46E-240	5
Smc2	3.06E-241	1.12056609	0.33	0.043	6.05E-237	5
Cks2	1.82E-231	1.12510808	0.35	0.051	3.61E-227	5
Knl1	9.23E-228	0.81263677	0.178	0.009	1.83E-223	5
Rrm2	7.57E-227	0.8537311	0.185	0.01	1.50E-222	5
Tyms	3.92E-226	1.11544481	0.324	0.044	7.76E-222	5
Cenpm	1.39E-220	0.88631243	0.22	0.018	2.76E-216	5
Ran	8.42E-219	1.34840912	0.829	0.341	1.67E-214	5
Kif11	1.68E-218	0.83673924	0.188	0.012	3.33E-214	5
Cdkn3	6.74E-211	0.91498163	0.183	0.012	1.34E-206	5
Tubb4b	1.01E-209	1.44272716	0.8	0.341	2.00E-205	5

Hist1h2ae	4.00E-207	0.90293225	0.176	0.011	7.91E-203	5
Dut	2.36E-205	1.12920901	0.409	0.079	4.68E-201	5
Mcm3	1.67E-202	1.01576525	0.246	0.028	3.31E-198	5
Rrm1	2.21E-199	0.96862161	0.282	0.038	4.37E-195	5
Tk1	1.57E-198	0.95198155	0.244	0.027	3.10E-194	5
Anp32b	7.77E-198	1.25031595	0.828	0.361	1.54E-193	5
Incenp	8.99E-198	0.90044919	0.212	0.02	1.78E-193	5
Ptma1	4.17E-189	0.91054721	0.991	0.837	8.26E-185	5
Ndc80	4.19E-188	0.69228656	0.147	0.008	8.29E-184	5
Smc4	2.92E-185	1.19674752	0.389	0.08	5.79E-181	5
Gmnn	2.03E-184	0.88287528	0.243	0.03	4.03E-180	5
Clspn	2.26E-182	0.73026356	0.152	0.009	4.48E-178	5
Knstrn	1.30E-176	0.79889459	0.172	0.014	2.57E-172	5
Uhrf1	2.04E-176	0.79683541	0.184	0.016	4.04E-172	5
Spc25	1.49E-175	0.6833648	0.156	0.01	2.96E-171	5
Hmgn2	1.12E-173	1.12813999	0.521	0.144	2.21E-169	5
Tmpo	4.34E-172	1.07098825	0.352	0.07	8.60E-168	5
H2afx	3.66E-171	1.08782519	0.365	0.075	7.26E-167	5
Mcm5	2.28E-170	0.84164578	0.182	0.017	4.52E-166	5
Esco2	1.74E-169	0.65042049	0.134	0.007	3.44E-165	5
Ckap2	2.20E-167	0.78589633	0.164	0.013	4.36E-163	5
Nucks1	4.45E-167	1.12619312	0.616	0.206	8.81E-163	5
Hmgb1	5.26E-167	1.07951446	0.86	0.439	1.04E-162	5
Tubb5	4.23E-166	1.23965162	0.762	0.349	8.39E-162	5
Ube2s	7.78E-163	1.21467363	0.729	0.301	1.54E-158	5
Kif20b	1.21E-161	0.67228812	0.153	0.012	2.39E-157	5
Aurkb	6.19E-161	0.62269573	0.127	0.007	1.23E-156	5
Pcna	2.16E-158	1.03292235	0.33	0.067	4.28E-154	5
Sgo2a	3.13E-157	0.66236106	0.155	0.012	6.20E-153	5
Tacc3	5.86E-157	0.72215569	0.16	0.014	1.16E-152	5
Melk	1.16E-155	0.59311744	0.129	0.007	2.29E-151	5
Tubb6	3.84E-154	0.8411219	0.229	0.032	7.60E-150	5
Bub1b	5.24E-154	0.68082575	0.157	0.013	1.04E-149	5
Ckap2l	1.73E-153	0.5891373	0.136	0.009	3.43E-149	5
Dek	2.79E-153	1.04427223	0.497	0.145	5.52E-149	5
Mcm6	1.28E-150	0.87607073	0.257	0.042	2.53E-146	5
Mis18bp1	6.87E-149	0.61221734	0.135	0.009	1.36E-144	5
Ranbp1	4.79E-148	1.01961601	0.653	0.242	9.49E-144	5
Nasp	9.23E-147	0.92996497	0.328	0.069	1.83E-142	5
Kif4	1.27E-146	0.57999627	0.124	0.007	2.51E-142	5
Fbxo5	1.88E-146	0.61710485	0.133	0.009	3.72E-142	5
Lig1	4.35E-142	0.83712231	0.223	0.033	8.62E-138	5

Rpa2	1.88E-141	0.75780165	0.187	0.023	3.72E-137	5
Cenpk	3.62E-141	0.62142666	0.141	0.012	7.16E-137	5
Prim1	5.78E-141	0.69994972	0.151	0.014	1.15E-136	5
Rbp71	2.72E-140	1.49259018	0.449	0.135	5.39E-136	5
Ncapg2	1.81E-138	0.54552976	0.116	0.007	3.58E-134	5
Dnajc9	4.54E-137	0.76127833	0.227	0.036	9.00E-133	5
Snrpd1	3.94E-135	0.97712905	0.536	0.177	7.80E-131	5
Kif23	2.10E-134	0.60950023	0.144	0.013	4.17E-130	5
Ncapg	8.74E-134	0.48652116	0.108	0.006	1.73E-129	5
Mcm7	3.85E-129	0.88219684	0.276	0.056	7.62E-125	5
Atad2	5.71E-128	0.87723364	0.254	0.048	1.13E-123	5
Anln	6.19E-128	0.65595038	0.177	0.023	1.23E-123	5
Shcbp1	1.33E-127	0.52816385	0.101	0.005	2.63E-123	5
Nap1l1	6.18E-126	0.94418782	0.62	0.238	1.22E-121	5
Kif20a	3.70E-125	0.45591612	0.105	0.006	7.33E-121	5
Cenpw	1.13E-124	0.64482348	0.152	0.017	2.24E-120	5
Rangap1	1.54E-123	0.7618561	0.292	0.064	3.06E-119	5
Dhfr	1.33E-122	0.65257155	0.15	0.017	2.63E-118	5
Ncl	7.68E-122	0.95947231	0.852	0.516	1.52E-117	5
Kif15	7.87E-122	0.55841543	0.121	0.01	1.56E-117	5
Rfc4	1.25E-121	0.70556239	0.196	0.03	2.48E-117	5
Plk1	1.99E-121	0.55088211	0.128	0.011	3.95E-117	5
Rfc5	2.18E-121	0.68377023	0.167	0.021	4.31E-117	5
Hirip3	5.41E-121	0.71868045	0.185	0.027	1.07E-116	5
Diaph3	9.24E-119	0.57647883	0.134	0.013	1.83E-114	5
Dlgap5	8.91E-118	0.48114143	0.104	0.007	1.76E-113	5
Hsp90aa1	1.81E-117	0.88804855	0.851	0.488	3.59E-113	5
Mns1	2.42E-117	0.51084783	0.111	0.008	4.79E-113	5
Eif5a	3.19E-114	0.87650322	0.882	0.537	6.33E-110	5
Rad51	2.21E-113	0.46960308	0.101	0.007	4.37E-109	5
Dnmt1	3.89E-113	0.84269818	0.298	0.072	7.71E-109	5
Srsf3	6.57E-113	0.88645434	0.72	0.334	1.30E-108	5
Hspd1	2.05E-109	0.89452075	0.678	0.307	4.06E-105	5
Slfn9	3.36E-108	0.61233794	0.117	0.011	6.65E-104	5
Hells	1.60E-105	0.63777255	0.148	0.02	3.18E-101	5
Cenph	1.44E-104	0.55471724	0.118	0.012	2.85E-100	5
Lockd	3.29E-104	0.53197249	0.111	0.01	6.52E-100	5
Cks1b	1.06E-103	0.82530561	0.402	0.127	2.11E-99	5
Fabp51	3.02E-102	0.84139157	0.687	0.311	5.98E-98	5
Ddx39	7.72E-102	0.71774199	0.256	0.059	1.53E-97	5
Dtymk	3.37E-101	0.77655461	0.384	0.119	6.67E-97	5
Usp1	5.24E-101	0.70276942	0.251	0.057	1.04E-96	5

Aspm	6.12E-101	0.56664546	0.106	0.01	1.21E-96	5
Plk4	5.81E-99	0.48500309	0.119	0.013	1.15E-94	5
Hint1l	8.33E-99	0.76266389	0.774	0.39	1.65E-94	5
Alyref	1.52E-98	0.70279665	0.281	0.071	3.01E-94	5
Srsf2	2.21E-98	0.81141903	0.515	0.196	4.38E-94	5
Tipin	1.25E-97	0.65265646	0.215	0.044	2.48E-93	5
Ccdc34	1.58E-97	0.74517526	0.345	0.101	3.12E-93	5
Exosc8	1.10E-96	0.72228795	0.246	0.057	2.19E-92	5
Ssrp1	4.51E-96	0.73189638	0.395	0.128	8.93E-92	5
Nop56	5.51E-96	0.72782427	0.329	0.095	1.09E-91	5
Hnrnpa3	4.59E-95	0.83381421	0.643	0.293	9.09E-91	5
Cenps	2.09E-94	0.56272391	0.136	0.018	4.15E-90	5
Hmgn5	2.34E-93	0.64366555	0.21	0.044	4.63E-89	5
Selenoh	2.85E-93	0.79034096	0.371	0.119	5.64E-89	5
Topbp1	4.17E-93	0.63117886	0.192	0.037	8.26E-89	5
Pa2g4	1.13E-92	0.77793655	0.5	0.192	2.23E-88	5
Mad2l1	3.08E-92	0.48618	0.103	0.01	6.10E-88	5
Chaf1b	3.83E-92	0.4950592	0.118	0.014	7.59E-88	5
Spdl1	8.34E-92	0.52040567	0.135	0.019	1.65E-87	5
Nhp2	1.46E-91	0.77936255	0.5	0.193	2.90E-87	5
Lsm2	6.57E-91	0.70227688	0.312	0.09	1.30E-86	5
Cdkn2d	1.91E-89	0.53434206	0.139	0.02	3.79E-85	5
Anp32e	1.43E-88	0.6863225	0.321	0.095	2.83E-84	5
Ybx1	2.09E-88	0.72988841	0.868	0.547	4.14E-84	5
Rad21	1.98E-87	0.65638741	0.285	0.079	3.92E-83	5
Aarsd1	2.46E-87	0.65765449	0.259	0.067	4.88E-83	5
Pmf1	8.84E-87	0.68858601	0.206	0.045	1.75E-82	5
Fen1	9.88E-87	0.49864964	0.122	0.016	1.96E-82	5
Ncapd2	1.15E-86	0.46541877	0.109	0.013	2.28E-82	5
Ppia	1.35E-85	0.4593376	0.996	0.926	2.68E-81	5
Chaf1a	5.93E-85	0.50430168	0.129	0.018	1.18E-80	5
Nme1	6.34E-85	0.78438718	0.706	0.36	1.26E-80	5
Ezh2	1.45E-84	0.65907716	0.278	0.078	2.87E-80	5
Lyar	2.78E-83	0.625501	0.273	0.076	5.50E-79	5
Hnrnpd	1.22E-82	0.75331669	0.399	0.143	2.41E-78	5
Siva1l	2.99E-82	0.65932467	0.388	0.134	5.92E-78	5
H1fx	1.89E-80	0.58906011	0.164	0.031	3.73E-76	5
Cenpp	2.99E-79	0.49321031	0.11	0.014	5.91E-75	5
U2af1	3.90E-78	0.68881733	0.476	0.192	7.72E-74	5
Ppa1	1.28E-77	0.62934815	0.297	0.09	2.53E-73	5
Gins2	1.95E-77	0.57145129	0.158	0.031	3.86E-73	5
Dctpp1	4.08E-77	0.65401083	0.291	0.089	8.08E-73	5

Hpf1	4.47E-76	0.59416541	0.264	0.076	8.85E-72	5
Hspe1	1.19E-75	0.65939412	0.645	0.305	2.35E-71	5
Mrpl18	9.99E-75	0.64043816	0.459	0.183	1.98E-70	5
Pola1	1.03E-74	0.46409722	0.104	0.014	2.04E-70	5
Dbf4	1.50E-74	0.46177567	0.119	0.018	2.97E-70	5
Hat1	1.37E-73	0.55270401	0.206	0.051	2.72E-69	5
Hnrnpab	4.96E-73	0.72303305	0.634	0.315	9.82E-69	5
Srsf7	6.19E-73	0.69716087	0.542	0.243	1.23E-68	5
Cycs	7.38E-73	0.57516882	0.317	0.104	1.46E-68	5
Lsm4	3.23E-72	0.69832811	0.555	0.253	6.39E-68	5
AI506816	4.99E-72	0.57940764	0.215	0.056	9.89E-68	5
Slc25a5	8.34E-72	0.64552514	0.689	0.345	1.65E-67	5
Banf1	5.77E-71	0.59996207	0.352	0.125	1.14E-66	5
Ak2	6.96E-71	0.57287848	0.318	0.107	1.38E-66	5
Orc6	2.02E-70	0.58396091	0.183	0.043	4.01E-66	5
Timm50	3.60E-70	0.58689787	0.252	0.074	7.12E-66	5
Oxct1l	4.02E-69	0.61200703	0.403	0.157	7.95E-65	5
Rbm3	4.58E-69	0.64065502	0.779	0.454	9.07E-65	5
Lbr	6.17E-69	0.49588029	0.131	0.024	1.22E-64	5
Hist1h1e	1.60E-68	0.73269001	0.294	0.099	3.17E-64	5
Tomm40	2.20E-68	0.58480513	0.356	0.129	4.35E-64	5
Nsmce4a	7.80E-68	0.52296897	0.281	0.089	1.54E-63	5
Aldh1a31	8.78E-68	0.73204258	0.34	0.125	1.74E-63	5
Srm	3.01E-67	0.5731042	0.249	0.075	5.97E-63	5
Snrpa1	1.46E-66	0.5581174	0.318	0.11	2.90E-62	5
Rbbp7	2.22E-66	0.59061557	0.381	0.146	4.39E-62	5
Set	7.08E-66	0.64016891	0.649	0.337	1.40E-61	5
H2afv	7.56E-66	0.68292147	0.572	0.276	1.50E-61	5
Cmc2	8.67E-66	0.5659688	0.201	0.054	1.72E-61	5
Cacybp	2.48E-65	0.57790287	0.393	0.154	4.91E-61	5
Npm1	2.97E-65	0.55629902	0.936	0.758	5.88E-61	5
Nop58	4.25E-65	0.60604754	0.305	0.105	8.42E-61	5
Mthfd1	5.41E-65	0.51654306	0.145	0.03	1.07E-60	5
Mcm4	5.60E-65	0.53417064	0.138	0.028	1.11E-60	5
Ptges3	9.59E-65	0.62524451	0.483	0.214	1.90E-60	5
Hist1h4d	2.09E-64	0.40528877	0.119	0.021	4.14E-60	5
Sae1	2.28E-64	0.51099898	0.263	0.083	4.52E-60	5
Lsm3	3.89E-64	0.48642248	0.209	0.057	7.71E-60	5
G3bp1	5.32E-64	0.58243849	0.382	0.15	1.05E-59	5
Tmem97	5.38E-64	0.50963778	0.171	0.041	1.07E-59	5
Prdx4	1.82E-63	0.57253904	0.45	0.19	3.60E-59	5
Gemin6	2.98E-63	0.42513032	0.115	0.02	5.91E-59	5

Hsp90b11	6.81E-62	0.64893359	0.848	0.578	1.35E-57	5
Hdgf	8.94E-62	0.5708695	0.461	0.199	1.77E-57	5
Lsm5	3.99E-61	0.48129162	0.207	0.058	7.90E-57	5
Kpnb1	1.56E-60	0.49687792	0.237	0.074	3.10E-56	5
Wfdc181	1.65E-60	0.61602442	0.802	0.511	3.26E-56	5
Kcnn41	3.30E-60	0.58880955	0.529	0.247	6.53E-56	5
Snrpb	5.43E-60	0.57091381	0.513	0.237	1.08E-55	5
Erh	7.08E-60	0.53222096	0.356	0.138	1.40E-55	5
Ybx3	7.39E-60	0.6019172	0.452	0.201	1.46E-55	5
Lsm6	8.33E-60	0.50352777	0.334	0.125	1.65E-55	5
Nme2	1.40E-59	0.527369	0.903	0.681	2.78E-55	5
Slbp	5.67E-59	0.57283679	0.211	0.062	1.12E-54	5
Fbl	8.93E-59	0.52417883	0.379	0.152	1.77E-54	5
Ywhah	1.19E-58	0.5262077	0.362	0.142	2.35E-54	5
Fkbp3	2.08E-58	0.55058055	0.473	0.211	4.12E-54	5
Phf5a	2.57E-57	0.54963978	0.384	0.158	5.08E-53	5
Nsd2	5.42E-57	0.51054513	0.219	0.067	1.07E-52	5
Tmem54	5.78E-57	0.43600766	0.131	0.028	1.14E-52	5
Uchl5	5.92E-57	0.51766834	0.219	0.067	1.17E-52	5
Dkc1	9.90E-57	0.47495795	0.191	0.054	1.96E-52	5
Hjurp	1.04E-56	0.48296725	0.242	0.079	2.05E-52	5
Nolc1	4.51E-56	0.51681909	0.233	0.075	8.93E-52	5
Ddx39b	4.55E-56	0.53818929	0.504	0.235	9.01E-52	5
Naa50	6.29E-56	0.58814846	0.307	0.116	1.25E-51	5
Id21	7.23E-56	0.55834197	0.48	0.22	1.43E-51	5
Timm8a1	7.70E-56	0.5126765	0.203	0.061	1.52E-51	5
Psat1	7.84E-56	0.49457582	0.135	0.03	1.55E-51	5
Idi1	2.64E-55	0.58563684	0.278	0.101	5.22E-51	5
Fdps	7.03E-55	0.61589843	0.581	0.304	1.39E-50	5
Hnrnpu	1.75E-54	0.58295426	0.654	0.365	3.46E-50	5
Rnaseh2c	1.79E-54	0.52571478	0.367	0.15	3.55E-50	5
Rpsa	1.83E-54	0.29156294	0.999	0.986	3.61E-50	5
Psip1	2.71E-54	0.51434578	0.251	0.086	5.36E-50	5
Sfpq	3.20E-54	0.56517914	0.471	0.219	6.33E-50	5
Nudcd2	3.39E-54	0.53162015	0.299	0.112	6.71E-50	5
Smc1a	1.33E-53	0.53444084	0.403	0.176	2.64E-49	5
Hnrnpa2b1	2.17E-53	0.58029268	0.688	0.389	4.31E-49	5
Rad18	4.03E-53	0.36602681	0.101	0.018	7.98E-49	5
Rfc2	4.99E-53	0.45983961	0.209	0.065	9.88E-49	5
Srrt	5.78E-52	0.56151729	0.27	0.1	1.14E-47	5
Cbx1	6.74E-52	0.47543411	0.412	0.18	1.33E-47	5
Mrpl12	9.82E-52	0.51487097	0.501	0.238	1.94E-47	5

Gspt1	1.02E-51	0.4963798	0.451	0.206	2.01E-47	5
Impdh2	1.06E-51	0.45633929	0.369	0.154	2.10E-47	5
Elf52	1.09E-51	0.53160889	0.271	0.099	2.16E-47	5
Phgdh	1.69E-51	0.52694431	0.171	0.048	3.34E-47	5
Wee1	8.74E-51	0.38105921	0.158	0.042	1.73E-46	5
Dpy30	1.25E-50	0.4133408	0.331	0.132	2.47E-46	5
Idh2	1.31E-50	0.47600694	0.232	0.079	2.59E-46	5
Mat2a	1.82E-50	0.51933139	0.346	0.144	3.61E-46	5
Nudc	2.09E-50	0.49770959	0.526	0.26	4.14E-46	5
Bcl7c	2.12E-50	0.45870518	0.468	0.218	4.19E-46	5
Jpt11	2.34E-50	0.56538504	0.592	0.318	4.64E-46	5
Ndufaf2	4.45E-50	0.42504112	0.22	0.073	8.81E-46	5
Dynlt1f	5.07E-50	0.39992348	0.151	0.04	1.00E-45	5
Manf1	8.79E-50	0.53972182	0.675	0.38	1.74E-45	5
Hnrnpdl	9.77E-50	0.46672905	0.266	0.098	1.93E-45	5
Smc3	1.03E-49	0.44669837	0.378	0.162	2.05E-45	5
Ckap5	1.30E-49	0.43751915	0.172	0.049	2.58E-45	5
Syncrip	1.40E-49	0.48992411	0.352	0.149	2.77E-45	5
Pbdc1	2.25E-49	0.40834843	0.219	0.072	4.46E-45	5
Snrnp40	3.74E-49	0.46402408	0.202	0.065	7.40E-45	5
Mpp6	3.96E-49	0.4242147	0.252	0.09	7.84E-45	5
Atp2b11	6.65E-49	0.46434843	0.429	0.197	1.32E-44	5
Ppih	7.03E-49	0.43376645	0.146	0.038	1.39E-44	5
Nubp1	1.02E-48	0.40729876	0.226	0.077	2.03E-44	5
Rfc3	1.33E-48	0.44909374	0.172	0.05	2.64E-44	5
Hspa14	1.34E-48	0.39977923	0.166	0.047	2.66E-44	5
Supt16	1.94E-48	0.45742604	0.345	0.145	3.84E-44	5
Cct6a	3.65E-48	0.51891314	0.56	0.292	7.22E-44	5
Anapc5	4.37E-48	0.45435775	0.374	0.162	8.66E-44	5
Tmem14c1	4.42E-48	0.46222354	0.508	0.249	8.74E-44	5
Fkbp2	1.27E-47	0.45802562	0.354	0.151	2.51E-43	5
Snu13	1.41E-47	0.49129227	0.485	0.238	2.80E-43	5
Smc6	1.72E-47	0.4746834	0.298	0.119	3.41E-43	5
Hmgb3	4.26E-47	0.44974011	0.222	0.076	8.45E-43	5
Sumo2	4.42E-47	0.50497805	0.758	0.457	8.76E-43	5
Ppil1	9.79E-47	0.41930582	0.161	0.046	1.94E-42	5
Nol7	1.68E-46	0.440268	0.443	0.206	3.34E-42	5
Tsen34	3.15E-45	0.426361	0.231	0.083	6.24E-41	5
Hspa51	5.08E-45	0.49029558	0.767	0.48	1.01E-40	5
Arl6ip1	2.09E-44	0.5663999	0.442	0.22	4.14E-40	5
Gar1	3.25E-44	0.46191182	0.185	0.06	6.44E-40	5
Hnrnpf	3.78E-44	0.49020235	0.62	0.349	7.48E-40	5

Aimp2	4.31E-44	0.39385314	0.178	0.056	8.53E-40	5
Hmgcs1	6.64E-44	0.49402073	0.243	0.092	1.32E-39	5
Tcp1	1.13E-43	0.45465643	0.529	0.272	2.24E-39	5
C1qbp	1.89E-43	0.43306019	0.412	0.193	3.75E-39	5
Eif4a1	2.14E-43	0.47291911	0.82	0.546	4.23E-39	5
Mrpl51	2.58E-43	0.45030197	0.487	0.241	5.10E-39	5
Smarca5	2.72E-43	0.40387942	0.411	0.192	5.39E-39	5
Magoh	4.05E-43	0.44947564	0.285	0.116	8.02E-39	5
Snrpg	6.29E-43	0.42585789	0.562	0.293	1.25E-38	5
Cbx3	6.61E-43	0.42385086	0.319	0.136	1.31E-38	5
Ppm1g	8.29E-43	0.40458536	0.208	0.073	1.64E-38	5
Raly	8.45E-43	0.45075272	0.437	0.21	1.67E-38	5
Pradc1	1.49E-42	0.4660719	0.168	0.053	2.96E-38	5
Pfdn6	1.56E-42	0.43334167	0.325	0.141	3.09E-38	5
Tuba1c	1.59E-42	0.40938126	0.255	0.099	3.15E-38	5
Lsm8	1.94E-42	0.41813478	0.217	0.078	3.84E-38	5
Ehf1	1.95E-42	0.46083878	0.312	0.134	3.86E-38	5
Haus1	2.03E-42	0.37454394	0.13	0.035	4.02E-38	5
Hspa9	3.24E-42	0.41596437	0.339	0.149	6.42E-38	5
Pdap1	4.02E-42	0.47350919	0.538	0.284	7.96E-38	5
Cinp	4.71E-42	0.42197951	0.141	0.04	9.33E-38	5
Cnbp	4.83E-42	0.46334734	0.453	0.228	9.57E-38	5
Pop5	6.06E-42	0.39039768	0.391	0.179	1.20E-37	5
Gins4	6.74E-42	0.35750653	0.16	0.049	1.34E-37	5
Arl4a1	7.79E-42	0.3780497	0.231	0.086	1.54E-37	5
Ndufab1	1.10E-41	0.44221192	0.555	0.294	2.17E-37	5
Car2	1.14E-41	0.45109475	0.121	0.031	2.26E-37	5
Rps2	1.59E-41	0.28777666	0.995	0.962	3.14E-37	5
Cbx5	1.68E-41	0.36137644	0.215	0.077	3.33E-37	5
Ppp1r22	2.60E-41	0.50010952	0.451	0.228	5.15E-37	5
Cenpx	3.03E-41	0.4075631	0.273	0.111	5.99E-37	5
Gmps	3.12E-41	0.3988391	0.235	0.089	6.19E-37	5
Snrpf	3.40E-41	0.41556018	0.3	0.127	6.74E-37	5
Rpl7l1	3.88E-41	0.40800535	0.281	0.116	7.69E-37	5
Ebna1bp2	5.99E-41	0.40748974	0.296	0.125	1.19E-36	5
Baz1b	6.15E-41	0.39903718	0.258	0.103	1.22E-36	5
Trim59	6.97E-41	0.32378156	0.106	0.025	1.38E-36	5
Prmt1	8.53E-41	0.41407804	0.513	0.264	1.69E-36	5
Mrto4	8.95E-41	0.40671275	0.317	0.138	1.77E-36	5
Ube2m	1.22E-40	0.44762802	0.496	0.255	2.41E-36	5
Nelfe	1.38E-40	0.40857178	0.212	0.077	2.73E-36	5
Parp1	1.41E-40	0.44681285	0.221	0.083	2.80E-36	5

Immt	2.08E-40	0.44006931	0.374	0.175	4.11E-36	5
Tfdp1	2.21E-40	0.36876714	0.147	0.044	4.39E-36	5
Mthfd2	2.22E-40	0.3819205	0.119	0.031	4.40E-36	5
Ccnd11	2.65E-40	0.45437287	0.628	0.366	5.24E-36	5
Eif2s1	3.50E-40	0.41038175	0.303	0.129	6.94E-36	5
Sdf2l11	4.28E-40	0.47187799	0.239	0.094	8.48E-36	5
Atp5g1	4.93E-40	0.455969	0.608	0.341	9.76E-36	5
Anapc11	5.08E-40	0.39130926	0.337	0.151	1.01E-35	5
Anapc15	6.01E-40	0.37776515	0.14	0.041	1.19E-35	5
Pold2	6.67E-40	0.33112691	0.107	0.026	1.32E-35	5
Pmvk1	8.30E-40	0.45642848	0.388	0.185	1.64E-35	5
Mrpl42	8.35E-40	0.45517226	0.328	0.148	1.65E-35	5
Snrnp25	8.73E-40	0.39503516	0.137	0.04	1.73E-35	5
Bub3	1.23E-39	0.35943414	0.234	0.09	2.44E-35	5
Xpo1	1.42E-39	0.33651266	0.158	0.05	2.82E-35	5
Tmem238	1.45E-39	0.44361883	0.405	0.197	2.88E-35	5
Rnaseh2b	1.53E-39	0.38024244	0.134	0.038	3.03E-35	5
Acp1	1.58E-39	0.41074961	0.452	0.227	3.13E-35	5
Snorc1	1.88E-39	0.51929965	0.307	0.137	3.73E-35	5
Txnrd1	2.09E-39	0.3883843	0.355	0.162	4.14E-35	5
Ssna1	4.40E-39	0.38875634	0.324	0.144	8.71E-35	5
Tra2b	6.57E-39	0.37955274	0.302	0.131	1.30E-34	5
Mbd3	7.05E-39	0.42010621	0.397	0.191	1.40E-34	5
Ppp1ca	8.15E-39	0.41268069	0.655	0.375	1.62E-34	5
Gm47283	8.33E-39	0.38788865	0.338	0.154	1.65E-34	5
Idh3a	1.05E-38	0.35426136	0.23	0.089	2.08E-34	5
Ruvbl2	1.16E-38	0.35726251	0.199	0.072	2.30E-34	5
Eri1	1.60E-38	0.27944402	0.117	0.031	3.17E-34	5
Rif1	1.88E-38	0.38201253	0.183	0.064	3.71E-34	5
Ruvbl1	2.80E-38	0.35648291	0.226	0.087	5.55E-34	5
Pold3	2.86E-38	0.30649385	0.152	0.048	5.66E-34	5
Mrpl13	3.31E-38	0.36149611	0.339	0.154	6.56E-34	5
Rpp30	4.11E-38	0.31180684	0.119	0.032	8.15E-34	5
Stub1	4.16E-38	0.33529415	0.462	0.229	8.24E-34	5
Mybbp1a	5.31E-38	0.40685864	0.244	0.099	1.05E-33	5
Lrrc59	7.08E-38	0.43614665	0.226	0.089	1.40E-33	5
Chmp6	8.84E-38	0.35924507	0.218	0.083	1.75E-33	5
Eif4a3	9.14E-38	0.39030665	0.313	0.139	1.81E-33	5
Srsf1	2.53E-37	0.3650973	0.241	0.097	5.00E-33	5
Calr1	2.75E-37	0.41463049	0.843	0.602	5.44E-33	5
Psmd13	3.19E-37	0.35156367	0.362	0.17	6.32E-33	5
Cyc1	3.77E-37	0.37403391	0.392	0.189	7.47E-33	5

Anp32a	4.93E-37	0.41958729	0.505	0.269	9.76E-33	5
Dynll2	5.83E-37	0.39707203	0.409	0.204	1.15E-32	5
Nxt1	5.99E-37	0.29275676	0.128	0.037	1.19E-32	5
Pgp1	6.52E-37	0.42433867	0.58	0.32	1.29E-32	5
Eif1ax	6.73E-37	0.37725248	0.475	0.245	1.33E-32	5
Cdk4	8.30E-37	0.34591574	0.469	0.241	1.64E-32	5
Arhgdia	8.45E-37	0.32881172	0.419	0.206	1.67E-32	5
Cdv3	1.04E-36	0.39476972	0.347	0.163	2.06E-32	5
Zfp91	1.21E-36	0.37595522	0.374	0.18	2.39E-32	5
Mrps25	1.21E-36	0.3492811	0.253	0.104	2.40E-32	5
Cldn72	1.23E-36	0.43170183	0.672	0.403	2.43E-32	5
Npm3	1.40E-36	0.3445219	0.377	0.181	2.77E-32	5
Umps	1.58E-36	0.34187034	0.119	0.033	3.13E-32	5
Bzw21	1.82E-36	0.39443979	0.421	0.212	3.61E-32	5
Casp8ap2	2.16E-36	0.31057354	0.141	0.044	4.28E-32	5
Snrpe	2.27E-36	0.37909019	0.551	0.3	4.50E-32	5
A430005L14Rik	2.43E-36	0.35455881	0.185	0.067	4.81E-32	5
H2afy	2.76E-36	0.38364443	0.491	0.257	5.47E-32	5
Cct8	2.94E-36	0.35439367	0.474	0.244	5.83E-32	5
Hnrnpm	3.25E-36	0.39161007	0.367	0.176	6.43E-32	5
Uba2	4.06E-36	0.33794083	0.2	0.075	8.04E-32	5
Vdac3	4.08E-36	0.38530856	0.476	0.25	8.07E-32	5
Prpf40a	4.41E-36	0.33649569	0.425	0.211	8.74E-32	5
Stip1	5.73E-36	0.34644321	0.254	0.106	1.13E-31	5
Smchd1	1.21E-35	0.36712049	0.259	0.11	2.40E-31	5
Rpa1	1.33E-35	0.37018781	0.111	0.03	2.64E-31	5
Ncaph2	1.65E-35	0.38782775	0.21	0.082	3.26E-31	5
Pole3	1.85E-35	0.36331237	0.17	0.059	3.67E-31	5
Dazap1	1.96E-35	0.3522406	0.229	0.092	3.88E-31	5
Ctcf	2.54E-35	0.32366214	0.316	0.144	5.04E-31	5
G2e3	2.56E-35	0.31071991	0.136	0.042	5.06E-31	5
Serbp1	2.94E-35	0.43842889	0.82	0.571	5.81E-31	5
Hnrnpa1	3.59E-35	0.42136055	0.625	0.368	7.10E-31	5
Rnaseh2a	6.67E-35	0.3513829	0.143	0.046	1.32E-30	5
Mrpl20	7.58E-35	0.33251497	0.413	0.205	1.50E-30	5
Coq7	8.00E-35	0.36663635	0.249	0.105	1.58E-30	5
Ogfrl12	9.98E-35	0.36830004	0.334	0.158	1.98E-30	5
Elof1	1.19E-34	0.3497311	0.405	0.204	2.35E-30	5
Rwdd1	1.65E-34	0.35364226	0.334	0.157	3.26E-30	5
Calm3	1.96E-34	0.35036424	0.302	0.137	3.88E-30	5
Tln21	2.15E-34	0.36819131	0.212	0.084	4.26E-30	5
Acat1	2.21E-34	0.35961695	0.287	0.129	4.37E-30	5

Pcbp1	2.21E-34	0.34473053	0.467	0.242	4.38E-30	5
Coro2a1	3.50E-34	0.37198798	0.269	0.118	6.94E-30	5
Ppp1r14b1	3.72E-34	0.4152475	0.666	0.412	7.37E-30	5
Eif6	3.87E-34	0.37702193	0.37	0.182	7.67E-30	5
Ak6	3.89E-34	0.28984683	0.182	0.067	7.70E-30	5
Fxn	5.90E-34	0.29747891	0.122	0.036	1.17E-29	5
Txnl1	6.30E-34	0.34740636	0.512	0.277	1.25E-29	5
Fkbp41	7.17E-34	0.36797727	0.522	0.282	1.42E-29	5
Larp7	7.51E-34	0.33756059	0.169	0.06	1.49E-29	5
Psma6	7.68E-34	0.31972098	0.454	0.235	1.52E-29	5
Tnfaip2	8.34E-34	0.38265215	0.101	0.027	1.65E-29	5
Wdr18	1.10E-33	0.33289477	0.223	0.091	2.18E-29	5
Actl6a	1.35E-33	0.34675396	0.225	0.093	2.67E-29	5
Psmd7	1.41E-33	0.36550756	0.513	0.279	2.79E-29	5
Sf3b5	1.71E-33	0.32020447	0.427	0.219	3.39E-29	5
Ptbp1	1.85E-33	0.34037748	0.234	0.098	3.66E-29	5
Dnajc2	1.85E-33	0.29406757	0.196	0.076	3.67E-29	5
Mrpl28	2.47E-33	0.34737896	0.413	0.209	4.90E-29	5
Tubg1	4.37E-33	0.30876204	0.129	0.04	8.66E-29	5
Thoc7	5.04E-33	0.32401403	0.418	0.214	9.98E-29	5
Rnf187	5.05E-33	0.32420875	0.287	0.13	1.00E-28	5
Ssb	5.12E-33	0.33470543	0.552	0.303	1.01E-28	5
Cox5a1	5.25E-33	0.37565014	0.691	0.418	1.04E-28	5
Mrfap1	5.40E-33	0.37857283	0.581	0.331	1.07E-28	5
Hars	6.53E-33	0.26527309	0.157	0.055	1.29E-28	5
Mrps61	6.58E-33	0.31811276	0.396	0.199	1.30E-28	5
Mrpl21	7.51E-33	0.35707433	0.304	0.142	1.49E-28	5
Dclk1	9.05E-33	0.29984236	0.112	0.032	1.79E-28	5
Timm23	9.94E-33	0.33714789	0.382	0.191	1.97E-28	5
Srsf10	1.04E-32	0.30812161	0.279	0.125	2.07E-28	5
Ifrd2	1.16E-32	0.2830442	0.116	0.034	2.30E-28	5
Pabpn11	1.24E-32	0.36161591	0.468	0.25	2.46E-28	5
Tagln21	1.38E-32	0.42841119	0.489	0.275	2.74E-28	5
Bcas2	1.38E-32	0.33326737	0.397	0.2	2.74E-28	5
Vars	1.72E-32	0.35638914	0.346	0.168	3.40E-28	5
Rsl1d1	1.86E-32	0.34825054	0.368	0.183	3.68E-28	5
Cst32	2.66E-32	0.69189911	0.626	0.384	5.27E-28	5
Cdk5rap2	2.83E-32	0.31459509	0.149	0.052	5.60E-28	5
Snx5	3.00E-32	0.31321793	0.201	0.08	5.95E-28	5
Zfp593	3.22E-32	0.33440037	0.21	0.085	6.38E-28	5
Txn1	3.38E-32	0.37070471	0.688	0.424	6.70E-28	5
Hmgn3	3.78E-32	0.28281513	0.261	0.114	7.50E-28	5

Atp5b	4.02E-32	0.39776687	0.844	0.599	7.95E-28	5
Hcfc1	4.49E-32	0.30177241	0.156	0.055	8.90E-28	5
Rnps1	4.54E-32	0.32095253	0.22	0.091	9.00E-28	5
Hspa8	4.59E-32	0.32450647	0.963	0.829	9.09E-28	5
Commd1	4.84E-32	0.30565532	0.342	0.163	9.59E-28	5
Rrp1b	4.91E-32	0.30901971	0.112	0.033	9.72E-28	5
Arpp19	5.28E-32	0.28824083	0.348	0.169	1.05E-27	5
Ldha1	6.06E-32	0.38719376	0.749	0.482	1.20E-27	5
Lmna1	6.55E-32	0.39384554	0.622	0.371	1.30E-27	5
Uqcc2	6.81E-32	0.33487772	0.405	0.208	1.35E-27	5
Gtf2a2	1.02E-31	0.32789041	0.257	0.114	2.02E-27	5
Eif1ad	1.05E-31	0.30003809	0.128	0.041	2.07E-27	5
Gabrp	1.08E-31	0.28204038	0.108	0.031	2.13E-27	5
Slc9a3r1	1.13E-31	0.32728171	0.27	0.122	2.23E-27	5
Psma1	1.24E-31	0.31440556	0.411	0.211	2.46E-27	5
Fzr1	1.42E-31	0.30085205	0.126	0.04	2.81E-27	5
Emc8	1.43E-31	0.35321402	0.225	0.095	2.82E-27	5
Dhx9	1.47E-31	0.36724312	0.297	0.141	2.92E-27	5
Cdc123	1.57E-31	0.3394743	0.274	0.125	3.11E-27	5
Thyn1	1.62E-31	0.33868348	0.175	0.066	3.20E-27	5
Nudt5	1.98E-31	0.32525405	0.189	0.074	3.92E-27	5
Ebp	2.00E-31	0.34660239	0.356	0.177	3.97E-27	5
Tardbp	2.42E-31	0.31074772	0.254	0.112	4.80E-27	5
Rbmxl1	3.58E-31	0.33363467	0.149	0.052	7.10E-27	5
Pcnt	4.55E-31	0.28508351	0.118	0.036	9.02E-27	5
Pih1d1	4.61E-31	0.34962576	0.185	0.073	9.14E-27	5
Atp5k	5.57E-31	0.31712898	0.491	0.267	1.10E-26	5
Dbi2	6.48E-31	0.33674245	0.923	0.69	1.28E-26	5
Snrpd3	6.66E-31	0.33663482	0.38	0.194	1.32E-26	5
Sptssa	6.91E-31	0.34276811	0.246	0.109	1.37E-26	5
Gnl3	7.58E-31	0.30110423	0.21	0.086	1.50E-26	5
Cops3	7.64E-31	0.32707684	0.223	0.095	1.51E-26	5
Gars	9.22E-31	0.34014199	0.209	0.087	1.83E-26	5
Pdia6l	9.62E-31	0.37989438	0.557	0.329	1.90E-26	5
Mrpl17	9.69E-31	0.33364888	0.4	0.208	1.92E-26	5
Cytip1	9.87E-31	0.33270397	0.155	0.056	1.96E-26	5
Gps1	1.18E-30	0.29575945	0.239	0.104	2.33E-26	5
Bzw1	1.29E-30	0.32688909	0.419	0.222	2.55E-26	5
Gtf3a	1.31E-30	0.25129617	0.245	0.107	2.59E-26	5
Uchl3	1.80E-30	0.31009075	0.268	0.122	3.57E-26	5
Bola3	2.21E-30	0.32407106	0.177	0.068	4.38E-26	5
Tmem109	2.84E-30	0.32749832	0.13	0.043	5.63E-26	5

Tsn	4.03E-30	0.32218757	0.478	0.262	7.98E-26	5
Eif3b	4.16E-30	0.34991068	0.304	0.147	8.23E-26	5
Tex261	5.44E-30	0.30598094	0.307	0.148	1.08E-25	5
Nsmce1	5.96E-30	0.26183617	0.263	0.119	1.18E-25	5
Erg28	6.49E-30	0.30534782	0.27	0.124	1.29E-25	5
Ube2i	6.74E-30	0.31679455	0.489	0.27	1.33E-25	5
Fubp1	6.87E-30	0.30759351	0.37	0.19	1.36E-25	5
Hmgn11	7.03E-30	0.36743133	0.836	0.595	1.39E-25	5
Phb2	7.39E-30	0.29711826	0.492	0.27	1.46E-25	5
Sfxn1	7.84E-30	0.3108302	0.29	0.137	1.55E-25	5
Psph	1.07E-29	0.29659521	0.125	0.041	2.12E-25	5
Cct7	1.20E-29	0.3670041	0.56	0.324	2.38E-25	5
Mrps7	1.39E-29	0.27203534	0.285	0.133	2.74E-25	5
Taf1d	1.51E-29	0.32961272	0.27	0.126	2.99E-25	5
Prpf19	1.58E-29	0.26697336	0.267	0.123	3.14E-25	5
Phb	1.62E-29	0.31245466	0.229	0.1	3.20E-25	5
Itpa	1.82E-29	0.33618127	0.167	0.064	3.61E-25	5
Nsmce2	2.05E-29	0.2997082	0.185	0.074	4.06E-25	5
Vim1	2.14E-29	0.28765873	0.279	0.131	4.24E-25	5
Utp3	2.28E-29	0.27069268	0.294	0.14	4.52E-25	5
Cyp51	2.61E-29	0.31891386	0.194	0.08	5.17E-25	5
Atad3a	2.72E-29	0.27090211	0.137	0.047	5.39E-25	5
Eif4h	3.00E-29	0.28734359	0.373	0.191	5.95E-25	5
Tomm5	3.87E-29	0.31038273	0.349	0.176	7.67E-25	5
Thoc3	4.39E-29	0.25625952	0.173	0.067	8.69E-25	5
Mrps24	5.34E-29	0.33342455	0.472	0.262	1.06E-24	5
Ube2l3	5.98E-29	0.26472729	0.45	0.242	1.18E-24	5
Arl6ip4	6.23E-29	0.27416278	0.319	0.156	1.23E-24	5
Asf1a	6.49E-29	0.32915559	0.15	0.055	1.29E-24	5
Ubl4a	9.74E-29	0.30087323	0.237	0.106	1.93E-24	5
Ddx21	9.90E-29	0.30758728	0.172	0.067	1.96E-24	5
Mphosph10	1.18E-28	0.27302673	0.163	0.062	2.33E-24	5
Nfic	1.46E-28	0.29341777	0.348	0.176	2.88E-24	5
Fus	2.18E-28	0.30884931	0.407	0.216	4.32E-24	5
Spp1	2.44E-28	0.25925918	0.106	0.033	4.84E-24	5
Ahsa1	2.49E-28	0.27953793	0.218	0.094	4.93E-24	5
Mrps26	3.09E-28	0.27846644	0.306	0.149	6.11E-24	5
Lzic	3.60E-28	0.27923514	0.146	0.053	7.13E-24	5
Acat2	3.75E-28	0.32013415	0.134	0.047	7.42E-24	5
Psmb7	3.81E-28	0.28839067	0.372	0.193	7.55E-24	5
Smarcc1	4.23E-28	0.3033988	0.37	0.193	8.38E-24	5
Eif3a	4.70E-28	0.3529136	0.596	0.36	9.31E-24	5

Nudt21	5.09E-28	0.30734194	0.293	0.142	1.01E-23	5
Ndufb8	5.37E-28	0.35111981	0.527	0.308	1.06E-23	5
Eif4ebp1	6.29E-28	0.32188039	0.303	0.15	1.25E-23	5
Mrpl35	6.82E-28	0.25711727	0.239	0.108	1.35E-23	5
Sdhd	7.11E-28	0.29568411	0.204	0.087	1.41E-23	5
Pnn1	7.24E-28	0.27827629	0.378	0.197	1.43E-23	5
Rpn1	8.25E-28	0.27435494	0.258	0.12	1.63E-23	5
Emd	1.09E-27	0.30276076	0.179	0.073	2.15E-23	5
Impa2	1.12E-27	0.29005027	0.128	0.044	2.21E-23	5
Shisa8	1.98E-27	0.37179909	0.133	0.047	3.91E-23	5
Ndufa12	2.18E-27	0.28034434	0.45	0.247	4.31E-23	5
Sf1	2.47E-27	0.25357104	0.201	0.086	4.88E-23	5
Shmt2	2.61E-27	0.27915672	0.122	0.041	5.17E-23	5
Ube2n	3.04E-27	0.25883849	0.257	0.12	6.03E-23	5
Snx3	3.09E-27	0.30125947	0.387	0.206	6.11E-23	5
Mrpl49	3.63E-27	0.27935966	0.162	0.063	7.18E-23	5
Ndufa10	3.74E-27	0.26531257	0.364	0.19	7.40E-23	5
Pgam1	3.86E-27	0.27813899	0.466	0.258	7.65E-23	5
Cisd2	5.32E-27	0.29417667	0.214	0.095	1.05E-22	5
Abce1	5.42E-27	0.26953339	0.174	0.07	1.07E-22	5
Nudt1	5.57E-27	0.27496791	0.191	0.081	1.10E-22	5
Carnmt1	5.99E-27	0.27846029	0.164	0.065	1.19E-22	5
Psmd1	7.33E-27	0.28411054	0.256	0.12	1.45E-22	5
Hsd17b12	7.38E-27	0.28593044	0.255	0.12	1.46E-22	5
Fam92a	8.37E-27	0.258598	0.203	0.088	1.66E-22	5
Psmb51	9.57E-27	0.31286959	0.685	0.432	1.90E-22	5
Mrps15	9.61E-27	0.2756572	0.288	0.141	1.90E-22	5
Uqcr10	1.06E-26	0.31113104	0.491	0.281	2.10E-22	5
Gcsh	1.15E-26	0.35610735	0.164	0.066	2.27E-22	5
Wdr77	1.39E-26	0.27395829	0.101	0.031	2.75E-22	5
Timm9	1.48E-26	0.33381149	0.19	0.081	2.94E-22	5
Hprt	1.60E-26	0.26687366	0.162	0.064	3.16E-22	5
Ddx1	2.19E-26	0.29311522	0.256	0.122	4.33E-22	5
Calm11	2.49E-26	0.2741466	0.819	0.55	4.93E-22	5
Exosc5	2.69E-26	0.26517567	0.248	0.116	5.32E-22	5
Ipo5	4.01E-26	0.29142911	0.158	0.063	7.94E-22	5
Mapre1	4.55E-26	0.26689033	0.269	0.13	9.00E-22	5
Mrpl55	4.85E-26	0.26812719	0.189	0.081	9.61E-22	5
Pam161	4.96E-26	0.35157839	0.261	0.127	9.83E-22	5
Ndufa5	5.06E-26	0.30764201	0.298	0.15	1.00E-21	5
Thop1	5.30E-26	0.25758806	0.125	0.044	1.05E-21	5
Ppp1cc	6.13E-26	0.25411448	0.346	0.18	1.21E-21	5

Ewsr1	6.16E-26	0.32707587	0.265	0.129	1.22E-21	5
Agpat5	6.94E-26	0.29748535	0.129	0.047	1.37E-21	5
Psmc5	7.14E-26	0.26432233	0.447	0.249	1.41E-21	5
7-Sep	8.22E-26	0.28044259	0.441	0.244	1.63E-21	5
Hnrnpk	9.21E-26	0.28616379	0.615	0.369	1.82E-21	5
Tpr	1.16E-25	0.29837505	0.537	0.317	2.30E-21	5
Psmb31	1.21E-25	0.26321094	0.519	0.301	2.40E-21	5
Pelp1	1.30E-25	0.26500624	0.12	0.042	2.58E-21	5
Cct3	1.31E-25	0.30355984	0.51	0.301	2.59E-21	5
Pitpnb	1.41E-25	0.25825366	0.194	0.084	2.80E-21	5
Atp5f1	1.47E-25	0.32412488	0.724	0.472	2.92E-21	5
Tcerg1	1.79E-25	0.25174145	0.179	0.075	3.54E-21	5
Psmd14	1.83E-25	0.25123765	0.249	0.118	3.63E-21	5
Eprs	2.03E-25	0.29580696	0.433	0.242	4.02E-21	5
Tomm22	2.06E-25	0.28054929	0.395	0.215	4.08E-21	5
Nol12	2.34E-25	0.2505256	0.211	0.095	4.63E-21	5
Cryab2	2.37E-25	0.28400574	0.358	0.193	4.69E-21	5
Noc2l	2.48E-25	0.26105408	0.173	0.072	4.90E-21	5
Snrpa	2.98E-25	0.27337337	0.26	0.126	5.89E-21	5
Fads2	3.10E-25	0.27366918	0.246	0.118	6.14E-21	5
Odc1	3.20E-25	0.28109283	0.187	0.081	6.33E-21	5
G0s21	3.38E-25	0.39964498	0.218	0.101	6.69E-21	5
Atp5g3	5.13E-25	0.28031896	0.515	0.301	1.02E-20	5
Pcmt1	5.18E-25	0.26014921	0.229	0.107	1.03E-20	5
Ctnnbip1	6.46E-25	0.28525954	0.323	0.168	1.28E-20	5
Taf10	6.63E-25	0.27431715	0.512	0.298	1.31E-20	5
Ctps	7.22E-25	0.25166352	0.103	0.034	1.43E-20	5
Farsb	7.42E-25	0.26675159	0.16	0.065	1.47E-20	5
Ndufv1	1.04E-24	0.25719832	0.335	0.176	2.06E-20	5
Eif2s2	1.06E-24	0.28169624	0.604	0.367	2.09E-20	5
Vdac1	1.30E-24	0.30682112	0.408	0.229	2.58E-20	5
Eif1a	1.82E-24	0.28618355	0.26	0.128	3.60E-20	5
Eif3d	1.98E-24	0.2716053	0.359	0.194	3.91E-20	5
Ndufb6	2.19E-24	0.26983672	0.277	0.139	4.33E-20	5
Psmb2	2.26E-24	0.26904925	0.458	0.262	4.48E-20	5
Ilf2	2.86E-24	0.26731154	0.209	0.095	5.67E-20	5
Calm2	3.52E-24	0.3231821	0.834	0.628	6.96E-20	5
Ddt	5.71E-24	0.25441845	0.272	0.136	1.13E-19	5
Cct2	6.91E-24	0.26086891	0.597	0.365	1.37E-19	5
Naa10	7.45E-24	0.27305632	0.249	0.122	1.48E-19	5
Suz12	8.19E-24	0.25652645	0.178	0.077	1.62E-19	5
Far11	8.59E-24	0.28793614	0.207	0.095	1.70E-19	5

Tars	1.12E-23	0.27395723	0.193	0.087	2.22E-19	5
Atp6v1b12	1.33E-23	0.29142399	0.239	0.116	2.63E-19	5
Gmds	1.41E-23	0.28478319	0.189	0.084	2.79E-19	5
Pusl1	1.63E-23	0.27256324	0.1	0.033	3.22E-19	5
Ppan	1.70E-23	0.25604666	0.14	0.055	3.36E-19	5
Ywhae	1.72E-23	0.28391612	0.718	0.467	3.41E-19	5
Psmc4	1.74E-23	0.26078771	0.343	0.184	3.45E-19	5
Ube2a	2.53E-23	0.29637941	0.269	0.136	5.02E-19	5
Sem1	2.56E-23	0.29621842	0.588	0.365	5.06E-19	5
Txn2	2.96E-23	0.26540915	0.269	0.136	5.86E-19	5
Ndufb7	3.13E-23	0.26548886	0.44	0.252	6.20E-19	5
Rrp15	3.44E-23	0.26535361	0.139	0.055	6.81E-19	5
Serpinb51	3.49E-23	0.28582124	0.318	0.171	6.91E-19	5
Tssc4	5.99E-23	0.26926573	0.139	0.055	1.19E-18	5
Muc152	7.76E-23	0.2770908	0.247	0.124	1.54E-18	5
Znrd2	9.11E-23	0.28448618	0.227	0.11	1.80E-18	5
Asns	1.08E-22	0.27839961	0.156	0.066	2.13E-18	5
Got2	1.35E-22	0.25146776	0.243	0.12	2.67E-18	5
Rfc1	1.48E-22	0.26593165	0.194	0.089	2.92E-18	5
Ssr2	1.52E-22	0.26186214	0.508	0.305	3.01E-18	5
Ostc1	1.97E-22	0.3039362	0.385	0.218	3.91E-18	5
Mettl1	2.11E-22	0.25313825	0.177	0.078	4.18E-18	5
Txnl4a	2.14E-22	0.25391963	0.362	0.2	4.25E-18	5
Snrpd2	2.30E-22	0.29592163	0.486	0.29	4.55E-18	5
Bag11	2.48E-22	0.25458957	0.561	0.344	4.91E-18	5
Rdx	2.53E-22	0.26775489	0.356	0.197	5.02E-18	5
Ap2m1	3.04E-22	0.25760825	0.269	0.138	6.02E-18	5
Psma31	3.29E-22	0.26082234	0.633	0.398	6.51E-18	5
Alpl1	3.41E-22	0.31234963	0.186	0.085	6.76E-18	5
Cdk2ap2	4.02E-22	0.2502422	0.258	0.131	7.96E-18	5
Sub1	4.89E-22	0.27741707	0.594	0.367	9.69E-18	5
Atp5o	5.58E-22	0.2908773	0.655	0.424	1.11E-17	5
Rnf168	5.87E-22	0.28262915	0.109	0.04	1.16E-17	5
Nars	6.89E-22	0.25757905	0.322	0.174	1.36E-17	5
Timm13	1.05E-21	0.25144553	0.598	0.372	2.07E-17	5
Apip	1.35E-21	0.25320544	0.164	0.072	2.67E-17	5
D8Ertd738e	1.44E-21	0.27646917	0.586	0.364	2.86E-17	5
Atic	1.51E-21	0.28541322	0.16	0.07	3.00E-17	5
Phlda12	1.81E-21	0.25082807	0.539	0.333	3.58E-17	5
Psma7	4.49E-21	0.29639396	0.709	0.475	8.90E-17	5
Sec11c1	5.86E-21	0.28703789	0.355	0.2	1.16E-16	5
Ppid	7.53E-21	0.25589159	0.184	0.086	1.49E-16	5

Atp5a1	7.74E-21	0.27415931	0.733	0.495	1.53E-16	5
Psmb6	9.83E-21	0.27941709	0.637	0.411	1.95E-16	5
Plet12	2.91E-20	0.25104284	0.356	0.201	5.77E-16	5
Elovl6	4.76E-20	0.25225092	0.136	0.057	9.42E-16	5
Eef1g	6.53E-20	0.28254322	0.835	0.629	1.29E-15	5
Fasn1	6.70E-20	0.28524953	0.297	0.163	1.33E-15	5
Slc25a3	9.03E-20	0.26614557	0.765	0.533	1.79E-15	5
Aprt	1.15E-18	0.25071544	0.446	0.273	2.28E-14	5
Mettl16	1.48E-18	0.26431166	0.136	0.06	2.93E-14	5
Tomm20	2.96E-17	0.2505236	0.617	0.409	5.87E-13	5
Anxa12	1.64E-10	0.31571881	0.416	0.287	3.25E-06	5

Table S 3. Genes associated with hallmark terms in MO clusters

HALLMARK TERM	CLUSTER	GENE	RUNNING ES	RANK IN GENE LIST	RANK METRIC SCORE
HYPOXIA	MO1	LALBA	0.1767235	0	2.702094793
		ALDOC	0.314538	1	2.107177734
		AKAP12	0.3647591	13	1.38170886
		CITED2	0.38943002	26	1.046850681
		HSPA5	0.39816093	40	0.858931601
		ERRFI1	0.3969774	55	0.763142109
		IER3	0.39405325	69	0.680725873
		ALDOA	0.4308381	72	0.674044549
		TGFB3	0.43979836	82	0.639226735
		PLIN2	0.4464105	92	0.603324473
		HK1	0.47339243	96	0.579960883
		HS3ST1	0.5072853	98	0.574023366
		PFKL	0.5060215	109	0.538704038
		ZFP36	0.51427794	117	0.516859949
		ENO1	0.47632548	137	0.479961067
		BCL2	0.45748258	151	0.437328964
		CCN1	0.40651336	173	0.392540962
		FOS	0.27737224	215	0.313350797
COAGULATION	MO6	FN1	0.19547978	0	3.089641333
		SPARC	0.30534342	11	2.065721273
		KLK8	0.34564635	33	1.328492403
		PRSS23	0.4036415	42	1.180061698
		BMP1	0.41370735	66	0.916438878
		HTRA1	0.44462416	78	0.850861132
		PDGFB	0.49842855	79	0.850401461
		CSRP1	0.5167443	95	0.783407629
		THBS1	0.5432527	106	0.748256207
		ANXA1	0.5701388	116	0.721297979
		TIMP3	0.58145714	132	0.672811389
		LRP1	0.4589744	208	0.533705413
		TIMP1	0.46154517	223	0.501624227
		MMP14	0.32360157	302	0.388124615
		ITGB3	0.337482	308	0.384025753
		WDR1	0.07166303	445	0.27682212
		CAPN2	0.01946802	479	0.261658788

		KLF7	0.004166544	495	0.252073228

Table S 4. Genes associated with Androgen response in MHP clusters

Cluster	Genes associated with Androgen response	RANK IN GENE LIST	RANK METRIC SCORE	RUNNING ES
MHP1	SAT1	17	3.50563908	0.14306386
	SCD	27	2.9367485	0.26740655
	HMGCS1	59	2.01307821	0.3313452
	B2M	63	1.97779787	0.41771108
	INSIG1	85	1.64285374	0.4735776
	NDRG1	102	1.45260787	0.5251772
	KRT19	119	1.35001183	0.57216316
	XRCC6	259	0.86825162	0.49199623
	XRCC5	305	0.78954124	0.48890728
	ACSL3	358	0.71199983	0.476328
	TMEM50A	433	0.63848436	0.4415749
	DHCR24	490	0.57138246	0.4192417
	AZGP1	569	0.51841843	0.37565887
	IDI1	572	0.51561081	0.3971299
	SMS	743	0.41978291	0.27020934
	HMGCR	781	0.40266013	0.25658396
	FKBP5	861	0.37380776	0.20564057
	SLC38A2	929	0.34585294	0.16373168
	TSC22D1	943	0.34081241	0.1679083
	ELOVL5	1080	0.29303432	0.06444755
	CDK6	1094	0.28719792	0.06621321
	ADRM1	1115	0.28217432	0.06174953
MHP4	SCD	34	2.24072194	0.09932218
	SAT1	51	2.02361608	0.19820052
	B2M	93	1.525895	0.2546971
	HMGCS1	106	1.42939889	0.32410482
	INSIG1	126	1.37214637	0.38606295
	XRCC6	159	1.23731577	0.43265265
	XRCC5	172	1.19526458	0.48946446
	AZGP1	271	0.92840481	0.47823697
	LMAN1	276	0.91960758	0.5252128
	TMEM50A	285	0.88993752	0.5680957
	FADS1	339	0.80690944	0.5784219
	CDK6	534	0.63193762	0.49132004
	KRT19	609	0.565036	0.4755254

	PGM3	647	0.54529804	0.48176503
	NDRG1	786	0.46913263	0.42086098
	HMGCR	876	0.43382019	0.38864392
	SMS	1051	0.38280889	0.30062392
	DHCR24	1079	0.36911538	0.30362755
	PA2G4	1141	0.34942731	0.28434852
	ELOVL5	1492	0.27236876	0.08052445
MHP5	SCD	20	3.30092478	0.1380107
	SAT1	25	2.89816141	0.26794147
	HMGCS1	38	2.37652373	0.36885306
	INSIG1	59	1.99523211	0.44716263
	B2M	64	1.92094588	0.53241146
	NDRG1	200	1.05865693	0.49360788
	XRCC5	251	0.936584	0.5041323
	XRCC6	293	0.85793865	0.5168746
	HMGCR	362	0.75876933	0.5076407
	LMAN1	375	0.74037856	0.53374165
	ACSL3	389	0.72374147	0.5584359
	PGM3	423	0.69353169	0.56882894
	ELOVL5	484	0.63052261	0.55889904
	AZGP1	524	0.60588384	0.5614085
	CDK6	653	0.51551414	0.50229245
	FADS1	669	0.50075555	0.51549894
	FKBP5	1010	0.36883125	0.312725
	DHCR24	1033	0.36280033	0.3151017
	IDI1	1135	0.33584395	0.26521227
	SLC38A2	1345	0.28894156	0.14341083